THE ACCURACY

OF

NUMERICALLY CONTROLLED MACHINE TOOLS

To my wife and parents

THE ACCURACY

OF

NUMERICALLY CONTROLLED MACHINE TOOLS

by

GORDON FREDERICK MUTCH, M.Sc. (TECH)

A Thesis

Submitted to the Faculty of Graduate Studies

in Partial Fulfilment of the Requirements

for the Degree

Doctor of Philosophy

McMaster University

February, 1975

DOCTOR OF PHILOSOPHY (1975)   McMASTER UNIVERSITY

(Mechanical Engineering)   Hamilton, Ontario.

TITLE: The Accuracy of Numerically Controlled
                        Machine Tools

AUTHOR: Gordon F. Mutch, M.Sc. (Tech)
                        (University of Manchester
                         Institute of Science and
                         Technology)

SUPERVISOR: Dr. J. Tlusty

NUMBER OF PAGES: XXVIII, 388

ABSTRACT

The accuracy of work on N.C. machine tools is much more affected by weight, clamping and thermal deformations as well as by variations in accuracy throughout the entire working zone than that of machine tools using other modes of operation.

It is therefore very important to precisely define the concept of accuracy and the methods of testing and evaluating it.

In this thesis the shortcomings and even possible fallacies of the classic form of accuracy evaluation procedure are discussed, together with an appreciation of recent significant contributions to the field which utilise modern instrumentation and high frequency response transducers in sound and informative experimental procedures.

A new system is developed where the problem of formulating a comprehensive and meaningful machine tool accuracy capability statement is practically solved by directly relating the accuracy of the machine tool to the accuracy of a workpiece machined on it. This is achieved by deriving a tolerance law applicable to the evaluation of machine tool translative deviations where the law relates to the practical system of tolerancing a part dimension as

well as to the usual mode of use of an N.C. machine.

An extension of the basic tolerance law provides for a comprehensive statement of accuracy achievable throughout any defined two-or three-dimensional working zone of a machine tool. For every type of machine tool configuration there is a finite (minimum) number of translative deviation measurements that is required to be evaluated only along well defined lines located at extreme offsets of the tool with respect to each moving member of the machine.

Additionally the procedure for including in the machine tool capability statement the adverse "further" effects of weight, clamping and thermal deformations is outlined.

While it is comparatively straight-forward to formulate tests such that the effect of weight and clamping deformations may be defined, the problem of correctly specifying a thermal test cycle warranted a rather more extended study.

It is shown how the correct identification and classification of the type of heat source affecting a machine tool's structural components leads to a rather precise knowledge of the particularly affected translative deviation measurements. The design of the test cycle, the general laws governing the specification of the tests and

the test procedure, are developed by reference to many practically obtained measurements complemented by computational studies of simplified and simulated machine tool structures.

Two computational procedures are developed for the calculation of steady-state and transient temperature fields together with the resulting thermal deformations: a lumped-mass/time-continuous technique the solution of which leads to an eigenvalue problem, and the finite-element approach to the problem. In each case a step by step solution technique is outlined, and a Fortran IV computer program listing is included in the Appendix for the finite-element analysis of two-dimensional structures using tri-angular elements.

Finally, an investigation is made of new concepts of errors of an axis of rotation. The experimental technique results in the generation of a polar trace on an oscilloscope screen, the form of which relates directly to a Talyrond gram which could be obtained from a machine specimen if there were no unwanted disturbances of the cutting process. In this way, an exact picture of the influences of spindle rotation errors on the workpiece accuracy is obtained by an idle run test at normal spindle speeds without machining. The design of a comprehensive electronic instrument is included in the Appendix together with details of associated instrumentation.

ACKNOWLEDGEMENTS

TABLE OF CONTENTS

<u>List of Figures</u>

PLATES

NOMENCLATURE

A	=	surface area
$A^{(e)}$	=	element surface area
A	=	positioning accuracy
$\bar{A}$	=	mean position variation
$A_{i,i+1}$	=	cross sectional area of structure joining nodes (i) and (i+1)
$A_{i,j}$	=	matrix element of i-th row and j-th column
A_{mn}	=	parameter of an evaluation template
a	=	an offset
a_o, a_n	=	constant coefficients
B	=	a constant
B	=	width
B_1, B_2, B_n	=	constants
Bi	=	Biot modulus
b	=	an offset
$b^{(e)}$	=	element thickness
b_{nk}	=	a constant
C	=	a constant
C_i	=	the thermal capacitance of the i-th lumped mass
C_1, C_2, C_n	=	constants
c	=	an offset
c_p	=	specific heat

D = a constant

D_o, D_n = constants

d = an offset

d = thickness

E = total number of elements

E = Young's modulus

e = element number

e = eccentricity

f = frequency

g''' = rate of internal heat generation/unit volume

h = coefficient of convection

$h^{(e)}$ = coefficient of convection of element (e)

I = an integral

i = an integer

i = element node point

j = element node point

K_{mn} = parameter of an evaluation template

$K_{i,i+1}$ = conductivity of section between (i) and (i+1) lumped masses

k = element node point

k = coefficient of conduction

$k^{(e)}$ = coefficient of conduction of element (e)

L = length, depth

l = width

$l_{i,i+1}$ = length of section joining (i) and (i+1) lumped masses

M	=	number of target points
M_i	=	mass of i-th lumped section
m	=	$\sqrt{(hp/kA)}$
N	=	number of trials
n	=	number of revolutions
n	=	an integer
P	=	periphery
q	=	rate of heat transfer
q''	=	rate of heat transfer / unit area
$q_{ex,i}$	=	external heat input to i-th node
R_i	=	variation width at target i
$\bar{R}$	=	position scatter width
S_i	=	surface area of i-th section
S_{mn}	=	length of element edge between nodes m and n, where m/n = i, j, k
T_E	=	positioning tolerance
T_i	=	temperature of i-th node point
t	=	time
t	=	column matrix of nodal temperatures
t_e	=	element mean temperature
t_i, t_j, t_k	=	node temperature
u	=	radial error motion at time t
V_i	=	volume of i-th section
v	=	time
v_a	=	random motion in measurement of axis of rotation axial error polar chart

v_r = random motion in a measurement of axis of rotation radial error polar chart

W   = axis nomenclature

w   = co-ordinate position

X   = actual attained value

X   = axis nomenclature

X_{in} = eigenvector

X_j = deviation from a given target

$\bar{X}$ = mean attained value

x   = co-ordinate position

x_{mn} = $x_n - x_m$ where n = i, j, k and m = i, j, k

Y   = axis nomenclature

y   = co-ordinate position

Y_{mn} = $y_n - y_m$ where n = i, j, k and m = i, j, k

Z   = axis nomenclature

z   = co-ordinate position

Greek Symbols

α = phase angle

α = thermal diffusity

α_s = coefficient of thermal expansion

β = phase angle

β_n = eigenvalue

γ = shear strain

Δ = time increment

Δ_s = steady-state deformation

Δ_t = transient deformation

$\Delta_{m,n}$ = deformation between point m and point n

Δ_r = radial error motion

Δ_{fa} = fundamental axial motion

δ = thickness

δ_{sa} = superimposed axial motion

$\delta_m(n)$ = a translative deviation, where m=x,y,z,w and n=x,y,z,w. Interpreted as: a deviation in the direction "m" while traversing in direction "n"

$\delta_m(n)_X$ = a translative deviation (defined above) - made along line X, where X=A,B,C....

δ_m = a "drift", where m=x,y,z,w

ε = strain

$\varepsilon_m(n)$ = an angular deviation, where m=x,y,z,w and n=x,y,z,w. Interpreted as: an angular deviation occuring around axis "m" while traversing in direction "n"

$\varepsilon_m(n)_{Ex+}, \varepsilon_m(n)_{Ex-}$ = the maximum and minimum values of the angular deviation $\varepsilon_m(n)$

r_k = eigenvalue

θ = a temperature change $(T-T_\infty)$

θ = time

λ_n = eigenvalue

μ_n = eigenvalue

ν = Poisson's ratio

ρ = density

σ = a standard deviation

σ = stress

τ = shear stress

τ = time constant

Φ = a steady-state temperature solution

ϕ = a phase angle

ψ = a transient temperature solution

ω = angular frequency

Matrices

$\{a_n\}$ = column matrix of coefficients

$[B]$ = strain - displacement matrix

$[C]$ = capacitance matrix

$[D]$ = stress-strain matrix

$\{F\}$ = column vector of nodal forces

$\{f\}$ = element column vector of nodal forces

$[H]$ = thermal stiffness matrix

$[\bar{H}]$ = modified thermal stiffness matrix

$[K]$ = overall stiffness matrix

$\{Q\}$ = column matrix of heat flux input

$\{Q_i\}$ = modified column matrix of heat flux input

$\{T_i\}_{st}$ = column matrix of steady-state temperature

$\{T_i\}_{trans}$ = column matrix of transient temperatures

$[X_{in}]$ = matrix of eigenvectors

$\{\varepsilon\}_O$ = initial (thermal) strain vector

$\{\delta\}$ = column matrix of nodal displacements

ABBREVIATIONS

ANSI	=	American National Standards Institution
BAS	=	Bofors - Alpha Laval - Scania Vabis
BSI	=	British Standards Institution
CIRP	=	College International Researches Production
DIN	=	Deutscher Normenauschuss (German Standards Institution)
GOST	=	Russian Standards Institution
HP	=	Hewlett-Packard
IER	=	Inner Envelope Reading
ISO	=	International Organization for Standardization
IT	=	ISO Standard Tolerance
LSC	=	Least Squares Center
LVDT	=	Linear Variable-Displacement Transformer
LRL	=	Lawrence Radiation Laboratory, Livermore, California
MCC	=	Minimum Circumscribed Circle
MIC	=	Maximum Inscribed Circle
MRS	=	Minimum Radial Separation
MWZ	=	Mean Working Zone
NC	=	Numerically Controlled
NMTBA	=	National Machine Tool Builders Association

OER	=	Outer Envelope Reading
PERA	=	Production Engineering Research Association of Great Britain, Melton Mowbray, England
PC	=	Polar Center
TIR	=	Total Indicator Reading
TR	=	Total Reading
UER	=	Upper Envelope Reading
UMIST	=	University of Manchester Institute of Science and Technology, Manchester, England
VDI	=	Verein Deutscher Ingenieur
VUOSO	=	Machine Tool Research Institute, Prague, Czechoslovakia

CHAPTER 1

INTRODUCTION

1.1. The Need for Specifications

The only internationally accepted procedure for
measuring the accuracy of machine tools is that provided by
sets of static alignment tests based on the original concept
as published by Schlesinger in 1927. Despite, however, the
general opinion of the inadequacy of these tests as a proced-
ure for fully expressing the capabilities of modern machine
tools, especially numerically controlled (N.C.) machine tools,
no alternative set of procedures has yet been proposed which
is sufficiently comprehensive to be acceptable internationally.
In other words, machine tool makers and users have no commonly
understood and accepted means of measuring a machine tool's
ability to meet todays demands of accuracy.

1.2 The Accuracy of N.C. Machine Tools

While generally thought of as the most accurate form
of machine tool, it could be justifiably put that in fact,
N.C. machine tools may be rather the most inaccurate.

Let us compare the method of operation of an N.C.
machine tool with that of a manual (or conventionally auto-
matic) machine.

The standard mode of operation of the latter class of
machine is to pre-machine the surface concerned and to make

the finishing cut after a corrective displacement of the tool, or mechanical stop, is made according to some hand inspection measurement at that particular part of the working zone concerned, in a given thermal state of the machine and including applicable weight and clamping deformations.

In N.C. machines, however, generally more complicated shapes have to be machined, having a greater number of dimensions, while the number of operator interferences for measuring and correcting co-ordinates should be kept to a minimum. The position measuring transducer may be remote from the machining area of the machine yet is the only reference for dimensions throughout the entire working zone of the machine.

It is for these reasons that the accuracy of an N.C. machine is much more susceptible to weight, clamping and thermal deformations than other types of machine tools and it is much more important for them to maintain consistent high accuracy in the whole working zone of the machine in order to obtain precise work.

Let us look quantitatively at the industrial requirements for workpiece accuracy as established for British industry by two surveys [1][2].

In these surveys, a statistical analysis, performed with reference to the dimensional tolerances as specified on engineering component drawings from a cross sector of

-----

† Numbers in parentheses [ ] refer to the appended refer-

industry, produced results which have been summarised in Figure 1.1 for various types of machine tools. The tolerances are expressed in terms of I.T. classes of accuracy (the I.S.O. system [3]), and the numbers in circles indicate the required classes of workpiece accuracy to be obtained on the individual classes of machines, the number underlined being the most important one.

Take for example lathes: lathes capable of producing accuracy class IT6 are required though the most common type should give IT8.

There is no reason to expect that these accuracy requirements will differ greatly among modern industrialised countries.

However, the results of a survey [4] on the accuracy actually attained on various types of N.C. machine tools installed in the plants of a group of Swedish companies including Bofors, Alfa Laval and Scania Vabis produced some interesting data, a summary of which is shown in Figure 1.2.

In a single test, a series of six standard test workpieces, specified according to machine tool type, is machined throughout a twenty-four hour period during which the machine undergoes a thermal cycle. The tests were specified and performed in such a way as to reflect the working accuracy of the machine tools including thermal effects.

If Figure 1.2 is compared with Figure 1.1, a discrepancy is seen to exist.

It may be realised that while the requirements of workpiece accuracy are obviously being met, they are, equally obviously, not being met by N.C. machine tools, which lack the presence of the self-adaptive operator of a manual machine who, by constantly making measurements before finish machining, effectively compensates for such errors as thermal, weight, clamping deformation or Abbé offset errors on alignment and positioning accuracy or tool wear.

Therefore, in dealing with the problem of defining and testing accuracy of N.C. machine tools we are looking for such a concept of testing procedure where accuracy in the whole working zone of the machine is established and that the procedure be practical enough so as to enable the inclusion of thermal, weight and clamping deformations in the test cycle.

This having been done, the next stage would be to introduce special design features to limit the occurrence of these further effects.

1.3 Machine Tool Accuracy - what the user wants

Many specifications already exist having been compiled by individual machine tool makers and national machine

tool advisory bodies and, although each one is not
comprehensive, each one can contribute to the development
of some internationally acceptable set of specifications.

It was the aim of a project[5] at The University of
Manchester Institute of Science and Technology (U.M.I.S.T.)
to assemble and analyse these various specifications,
together with tests and experimental procedures developed
by universities and research institutes, in order to form a
sound basis from which the eventual formulation of compre-
hensive rules may be derived.

The project was established in the face of a grow-
ing demand, e.g. [6][7], from both machine tool makers and,
often disenchanted, machine tool users for not only commonly
accepted but scientifically supported procedures of testing
on which an unambiguous understanding of a machine tool's
capability could be based.

Company interest in Canada has likewise been
stimulated, by increasing demands on accuracy and the rapid
growth of N.C. installations in Canada. From only seven
installations in the early sixties, there were 500 in 1970
[8] and at the latest count, approximately 1200 diversified
machine types in early 1974 [9] located mainly in Quebec and
Ontario.

A survey investigation [10] was performed at the out-
set of this project to establish the significance of any

problem associated with the accuracy of N.C. machine tools.
It was found that while in many instances N.C. machine tools
were used mainly because of their capability of flexibly
automating complex operations in small lot production where
no special degree of accuracy was required, an important
group of companies existed where accuracy requirements were
at the very limit of the capabilities of their machines.

In the last group of companies considerable effort
and time was expended in regular accuracy checks and accuracy
maintenance of the machines, using the best techniques
commonly available - though usually limited to checking
straightness and positioning accuracy along single lines in
each axis. The specifications of accuracy as obtained from
the machine supplier are taken for granted and regarded as
valid for actual workpiece accuracy.

It was established that a genuine interest in the
development of advanced and reasoned techniques of specify-
ing N.C. machine tool accuracy exists.

1.4 Scope of the Investigation

The scope of the present investigation is limited
to those problems associated with the geometric accuracy of
machine tools, excluding however, dynamic errors for which
a generally acceptable solution has been proposed elsewhere
[11].

Here, the aims may be listed as follows;

1)   To formulate some definition and concept of accuracy for the whole working zone of a machine (two or three dimensional).

The accuracy concept should be able to accommodate the possibility of being able to quote some definitive statement of machine accuracy inclusive of the effects of thermal, weight and clamping deformations.

On application, the accuracy assessment tests, specified in accord with the concept as developed, should be practical in nature and the whole test procedure should be open to an accelerated and automated means of data acquisition.

2)   To investigate in some detail, the most complicated of the further effects, thermal effects, in the interest of formulating precise rules for specifying the thermal test cycle.

3)   To investigate new concepts of spindle rotation accuracy and to develop instrumentation capable of measuring all errors associated with spindle rotation.

4)   To generally develop practical methods of application of the techniques, as specified in accord with the formulated laws, and apply these to various practical situations.

CHAPTER 2

ACCURACY SPECIFICATIONS - THE STATE OF THE ART

2.1 The Current System

2.1.1 The Accuracy of the Workpiece

The accuracy of the workpiece may be expressed in purely geometric terms i.e. in terms of form (including surface waviness and roughness) and dimensions, the accuracy being determined in relation to tolerances on these dimensions. The tolerances are chosen and applied in turn with respect to the functional requirements of the workpiece and with reference to some system of tolerancing.

Examples of this approach are shown in Figure 2.1 and 2.2 for the errors of rectangular and cylindrical workpieces respectively. In these Figures, the idealized forms are shown by the thick lines and the plus tolerances used by the thin lines. Possible actual forms of acceptable workpieces are shown by the dashed lines.

Taking for example the workpiece depicted in Figure 2.1a, of sole interest are sides 1,2,3 and 4 and the machining of flat, parallel and mutually square surfaces, the dimensions A and B and respective tolerances δ_1 and δ_2 applying, as shown in Figure 2.1b.

An acceptable form of produced workpiece may there-

fore be as shown in Figure 2.1c which satisfies the given
limited requirements. The actual surfaces are not flat,
parallel or square, but they are located within the specified
limits. The form may however, be improved without modifying
the basic tolerances, by imposing special restrictions on the
form of the surfaces. In Figure 2.1d for example, additional
tolerance δ_3 places limits on the parallelism of opposite sur-
faces 2 and 4, and tolerance δ_4 places a squareness tolerance
on planes 3 and 2.

An analogous example is given in Figure 2.2 for a
cylindrical workpiece which has a tolerance δ_1 imposed on
the diameter D. Possible acceptable forms of the workpiece
are shown in Figures 2.2b and 2.2c while a further possible
restriction, in the form of additional tolerance δ_2, may be
introduced on the error of circularity of any cross-section.

Both of these examples necessarily imply the
capability of the producing machine to perform within the
acceptable error deviations as imposed, involving the re-
quirements of straightness of motion and positioning
capabilities to be embodied in the machine.

The requirements of accuracy of workpieces may be
based on the ISO system [3] of limits and fits which relates
to tolerances on components and to fits corresponding to
their assembly. Here, tolerances on workpiece dimensions
are quantitatively classed in eighteen IT standard tolerance

grades ITO1, ITO, IT1 to 16, the limiting numerical values being linked to dimensional size by empirical formulae calculated on the basis of former national standards.

With the exception of the three finest classes ITO1, ITO and IT1, for which a basic relationship between tolerance and dimension is assumed, a general formula exists for the other standard grades which takes into account that the relationship between the values of manufacturing errors and the workpiece dimension is approximately parabolic in nature. Figure 2.3, reprinted from [3] shows the numerical values of the standard tolerances.

This ISO recommendation was the basis for the recently introduced British Standard of Limits and Fits [12] from which Figure 2.4 is reprinted. It includes an adequate illustration of the increasing significance of temperature effects for steel workpieces via the attainment of accuracy grades for increasing sizes of parts.

2.1.2   The Accuracy of the Machine Tool

The metrological definition of geometric accuracy and the basic measuring methods remain the same now as in the classic geometric accuracy concept generally attributed to Schlesinger [13] and first published in 1927. The work of establishing acceptance standards had commenced in 1901 and, in a German machine tool industry trying to establish

itself in a competitive world market the need for a comprehensive series of acceptance test specifications became very real. Since the original German publication, the procedures have become generally adopted the world over, being translated into many languages and periodically updated.

The original recommendations were used as a basis for German (DIN) and Russian (GOST) standards.

Figure 2.5 is a single example of the typical form of Schlesinger test chart, extracted from the latest edition in English of his recommendations [14] where a collection of seventy test charts for diversified machine tool types is given.

The measurements depicted are basically measurements of parts of the machine tool e.g. guideways, tables, etc., and the tolerances are those derived from practical achievability..

The system however, does not show any direct relation to the accuracy of the workpiece. (However, the tests were and still are of great value to the plant engineer in connection with the initial installation, maintenance and overhaul of machine tools in his care).

Schlesinger was aware of this limitation, reasoning however that the direct test consisting of actual machining tests would often not be practical because of high costs and

that it would be difficult to cover the full range capacity of a machine tool.

Salmon [15] on the other hand provided for the application of direct tests by proposing a series of practical tests (épreuves pratiques) for each machine tool type, backed up by a series of geometric inspection procedures (vérifications géométriques). The change in emphasis is significant for in the Machine Tool Test Code ISO R230[16], which is probably the ultimate refinement of the classic approach to geometric accuracy testing, it is stated that if geometric tests and practical tests having the same objective are applied to a machine and the results differ, then the results obtained by making practical (i.e. direct) tests should be accepted.

The classic geometric accuracy tests have great drawbacks and in some cases the procedures lead to incorrect conclusions.

Figure 2.6 will serve to show how the incorrect interpretation of data may result:

Figure 2.6a refers to the basic procedure of measuring the angular deviations occuring in a machine tool slide motion i.e. pitch, roll and yaw (analogous to the motions of a ship), a test which is commonly misrepresented as a check of straightness of motion. Sometimes even pitch alone is taken to be indicative of straightness while it is seen in

Figure 2.6b that even if no pitch is indicated on the level, a roll motion could occur about some point O resulting in an up and down motion of the table and causing a great error of straightness of motion.

Figures 2.6c,d show that even if no roll,pitch or yaw motion is indicated, up and downwards motion or sideways motion may occur and the motion certainly is not straight.

However, it should be said that measurements of angular deviations are very valuable in evaluating the motion of some point P located above the table surface, once the error of straightness motion in the plane of the table is known.

The next series of diagrams in Figure 2.6 refer to the correct measurement of straightness of a motion.

The straight-edge should be located on the stationary portion of the machine while the gauge is fixed to the moving member as shown in Figure 2.6e. Thus the measurement of straightness of motion in a lathe is a correct one, the mandrel held between centres and the gauge being held in the traversing carriage.

However, for some types of machine, the configuration of the machine prevents this ideal set up and the straight-edge has to be located on the moving member. In this case, in order to avoid the occurrence of the situation shown in Figure 2.6f where the gauge indicates no error, the

measurement has to be complemented by the measurement of the pitch motion, this test corresponding to Figure 2.6g. In a similar way for horizontal measurements of straightness, a combination of measurements of straightness and yaw motion should be made using for example an autocollimeter for the angular deviation measurement. These are correct procedures limited however in their validity only to the plane in which the straightness measurement is made.

While the utilisation of two straight-edges A, B as in Figure 2.6j would identify the presence of roll, pitch and yaw motions having instantaneous centres of rotation in the points of either gauge will remain undiscovered. Adding the additional straight-edge C does not help much, the only conclusion being that straight lines in the X direction may be generated all over the working zone if the tool works in the plane of the gauges as for example would be the case for a horizontal boring machine.

Again, measurements of pitch and yaw are additionaly required.

Now, since the measurement of a moving straight-edge with a gauge in a fixed position in the place of a tool gives proof of generating straight lines in the plane concerned, the common method used in grinding machines (see Figure 2.6k) is correct for confirming the cylindricity of ground work pieces, although the longitudinal movement of the table need not be straight.

The table may perform both roll and yaw motion with instantaneous centres of rotation at the point of contact of the grinding wheel with the workpiece and it may also pitch without affecting the cylindricity of the workpiece. By this concept of straightness of motion as opposed to straightness of a guideway the classic approach has been refined, as previously mentioned, and a useful guide to the correct application of geometric tests as well as to the choice of conventional test equipment is given in ISO R230.

The same principles are embodied in their final form in the more recent ISO recommendations particular to specific machine tool groupings [17] [18] for which ISO R230 is a hand in hand reference manual.

However, in the final analysis of shortcomings of the present system, while the accuracy of the workpiece is expressed in solely geometric terms, the accuracy of the machine tool is covered not only by geometric aspects but by kinematic and functional ones related to the machining movements and affected by the machining process.

So for example, if thermal effects are taken into consideration, the deviations from a prescribed geometric form should be considered in a predetermined range of thermal states of the machine. Also, especially for N.C. machines, displacement accuracy should be considered taking into

account the kinematic errors of the machine and the dynamic errors of the control system. Additionally, such effects as weight and clamping deformations should be considered. The accuracy of spindle rotation requires a precise definition also, as will be seen in a later chapter.

2.2 Significant Attempts tò Solve the Problems

Summarising the preceding paragraph we can see that the fundamental limitation of the classic concept of geometric accuracy as created by Schlesinger and further developed by national and international authorities is the fact that it is based on a "steady and balanced" thermal state of a machine. Such a state actually never exists in a working machine. Besides the fact that it does not provide a definition of machine accuracy throughout the entire working zone, it does not allow for dynamic errors, thermal, weight or clamping deformations or for spindle rotation errors, each of which may have a decisïve influence on the geometric accuracy and quality of a machined surface.

A number of recent significant developments have contributed to the developing concept of what constitutes a modern comprehensive approach to the formulation of machine tool accuracy specifications.

2.2.1 Three Dimensional Accuracy Specifications

(a)   First, consider the practical approach of the
Dixi company in the test charts for a Jig Boring machine
[19].

An extract is shown in Figure 2.7 where it is
apparent that their approach is much different from the
classical approach of clear separate definitions of
straightness and squareness errors.

Here, a cylindrical square is moved into three
positions longitudinally and three positions transversely.
In each position the dial indicators attached to the spindle
slide up and down with the headstock along the master
cylinder.

In case 7, dial indicators fixed to the table at
three different heights slide along the extended spindle in
two places during the longitudinal motion of the table.

On realising that the main function of the machine
is primarily to bore holes, having straight axes parallel
to each other, all over the working zone, the practical
aspects of the tests become apparent. That is, the test is
not too time consuming and the result bears an integrated
direct relationship to the errors of a machined workpiece
since anyway, the errors of the workpiece will be the non-
separable tolerance combinations of the effects of straight-
ness and parallelism.

(b)   A further significant development is the working zone

concept which has been well formulated by Erikson [20],
and applied by the Sundstrand Corporation [21] in the
evaluation of accuracy of their range of Omnimill Machining
Centers. The philosophy is ultimately passed on to their
customers [22].

Erikson states quite correctly that the current
procedure of concentrating on checking the alignment of
guideways has no significance for the customer and mis-
directs the attention of the manufacturer away from the real
problems.

Figure 2.8a is a partial example of how the magnifi-
cation of errors can occur in the working zone because of
Abbé offsets and this applies in fact not only to the posi-
tioning errors as depicted, but also to errors of straight-
ness of motion if other angular deviations are considered.

The dimensions of the working zone, as shown in
Figure 2.8b, are defined by Sundstrand in each application
and this is subdivided into primary and secondary work zones,
the primary zone being established on a basis of where most
of the machining work would be accomplished.Having predeter-
mined the dimensions of the primary zone, measurements of
straightness deviations and the displacement accuracy, as
experienced at the tip of some mean length of tool, are made
by locating straight-edges or lug bars along each of the
three mutually perpendicular lines passing through the center

of the working zone (i.e. the Mean Work Zone) and tracing

these reference surfaces using a gauge located in the

spindle nose.

In order to extrapolate these results to other

parts of the work zone, the angular motions of pitch and

yaw are simultaneously measured.

2.2.2 Master Part Trace Testing

A further trend is in the use of automatic record-

ing and integrated testing techniques and in the development

also of techniques for automating and accelerating procedures

and the computer evaluation of test results.

(a) The master part trace test of Bryan [23] from which

Figure 2.9 is reproduced is an example of an automated,

accelerated and integrated test procedure, the expression

"integrated" being used because instead of any component

errors, only their resulting effect on the accuracy of the

workpiece is measured.

Choosing a shape and size of workpiece representa-

tive of the work to be carried out on a particular machine

tool is the first step in the production of a master work-

piece of known accuracy. This master component is clamped

in the place of the workpiece and the tool is replaced by a

displacement transducer. The transducer is moved under con-

trol of a tape program and its signals, representing the

resulting effect of the machine tool and the control system,

are recorded for subsequent computerised analysis. It is obvious that in an ideally accurate machine the signal of the transducer would stay constant throughout the tests.

(b) Kirkham [24] has described an integrated procedure not only for assessing the accuracy of a machine tool but also for determining, from the test, the individual components of the geometric errors of the machine.

Considering two-dimensional positioning accuracy only, the master part consisted of a rugged plate having holes of one inch diameter randomly placed in it. It is not necessary to accurately machine the holes in precise locations as long as the coordinate locations of the holes have been carefully calibrated using the best possible measuring techniques. The plate is mounted on the machine table perpendicular to the spindle axis and a tape, made·in accord with the calibrated locations of the holes, is used to move a gauging probe into each hole in random sequence, the probe consisting of a tool holder carrying two gauging heads at right angles.

. The indicated deviations, in two coordinate directions, from the calibrated positions are recorded and processed. The final computational analysis gives data on positioning accuracy as well as the out-of-squareness and parallelism errors of component motions.

The accelerated and automated techniques involved in

the master part trace test are also especially suitable for geometric accuracy tests where functional effects are to be included, for the technique is fast. For example, the tests may be repeated at various stages in a thermal duty cycle, each set of data being represented as that specific to one instant in time.

2.2.3 Positioning Accuracy

Displacing a body along a line to a target involves in all cases several characteristic types of errors, the basic components of which are;

(1) Cumulative error - a systematic error over a certain length of travel or over the full length of travel. A portion of this error may be indentified as a cyclic error.

(2) Scatter - a random error characterizing the accuracy of repeated positioning to the target.

(3) Dead zone - defined as a difference in final position attained when approaching the target from two different directions.

(4) Least possible displacement.

Two major specifications for evaluating the positioning accuracy of N.C. machine tools have been issued, by Verein Deutscher Ingenieur (V.D.I.) in Germany [25] [26] and the National Machine Tool Builders Association (N.M.T.B.A.) in America [27].

(a) N.M.T.B.A. [27]

A definition of N.C. machine tool accuracy has been proposed by N.M.T.B.A. as follows:

"Numerical control system accuracy at a point is defined as the sum of the signed value of the difference between the mean and the target at any point plus the value of the dispersion at that same point which gives the largest absolute sum".

The following example will illustrate the technique adopted. A machine slide is commanded to move from its zero position to a target through a prescribed displacement. The actual position attained by the slide will generally differ from the target position and if the command is repeated a number of times, the difference between the target position and the mean of the attained positions ΔX may be evaluated.

The repeatability of the positioning system has been additionally defined by N.M.T.B.A. as "the expected diversion on each side of the mean resulting from a series of trials when approaching any given point under the same conditions".

Adopting standard statistical practice, the expected deviation is 3σ where,

$$3\sigma = 3\sqrt{\frac{\sum(X-\bar{X})^2}{(N-1)}}$$

where $\bar{X}$ = mean attained value

X = actual attained value

N = number of trials

The accuracy is then defined as

$$A = \Delta X \pm 3 \sigma$$

The procedure is illustrated in Figure 2.10 where the accuracy of a linear measuring system has been determined at a number of points along its traverse.

The value ΔX has been evaluated at every target position and a mean line constructed through the calculated points. At each point also the dispersion $\pm 3\sigma$ has been calculated enabling the construction of an envelope containing the $\Delta X \pm 3\sigma$ values to be formed.

The system accuracy may be quoted as a plus or minus figure having equal values, the symmetry of the graph being achieved by shifting the zero on the ordinate as required.

As a consequence of dead zone, recognition has been given by N.M.T.B.A. to the evaluation of bidirectional as opposed to unidirectional positioning accuracy where, while in the former the accuracy evaluation is based on approaching the target from only one direction, the latter includes approaching the target from two directions.

(b) <u>V.D.I. 3254 [25]</u>

The experimental procedure is virtually identical to that of N.M.T.B.A. though the terminology differs. V.D.I. have dispensed with the term positioning "accuracy" in connection with any quantitative statement, replacing it by positioning "tolerance".

The mean position attained at each point is determined and compared with the commanded position and the errors plotted as shown in Figure 2.11, giving the "mean position deviation" similar to the theoretically perfect target of the N.M.T.B.A. specification

$$\text{i.e.} \quad \bar{A} = \frac{\bar{X}_{max} + \bar{X}_{min}}{2}$$

The position scatter width R_p is defined as $\pm 3\sigma$ but in this case, σ is calculated taking into account the entire set of results and is thus constant over the whole traverse range.

For 5 samples at the target point, as in Figure 2.11,

$$\sigma = \frac{\bar{R}}{2.326}$$

where
$$\bar{R} = \frac{1}{M} \sum_{i=1}^{M} R_i$$

M = number of target points

R_i = variation width at target i = $X_{jmax} - X_{jmin}$

X_j = the deviation from a given target.

Finally, the positioning tolerance T_E is given by,

$$T_E = \bar{X}_{max} - \bar{X}_{min} + 6\sigma.$$

Recently a revision of V.D.I.3254 [26] was issued which brings it much more into line with the N.M.T.B.A. proposal in that

the influence of dead zone and hence the specification of
bidirectional and unidirectional accuracy is now included,
as well as finally expressing the tolerance in an identical
manner.

2.2.4 Spindle Rotation Accuracy

In the standard machine tool testing procedure,
spindle rotation accuracy is assessed with a dial gauge
clocking on to a precision mandrel, fixed in the taper in
spindle nose, and positioned close to the nose. The limita-
tion of this method is that any eccentricity in the
location of the mandrel is included in the reading. Also,
no recording facility is available and the method is limited
to low speeds of spindle rotation.

Alternative methods of measurement have been proposed
recently utilising electronic displacement transducers with
associated recording facilities.

Because these new procedures are the subject of
analysis in a later chapter in the course of designing an
instrument capable of measuring all spindle rotation related
errors, a detailed analysis of the various proposals is de-
layed until then.

Suffice to say for the time being, that a common
feature of all these methods is the display of the measure-
ments in the form of a polar diagram, the significance of
which is the same as that of a standard Talyrond diagram,

the shape of which is directly analogous to the shape
of a machined workpiece.

CHAPTER 3

THE NEW SYSTEM

3.1 The Conceptual Approach to a New System

The problem of formulating a comprehensive and meaningful machine tool accuracy capability statement may be reasonably put as how best to define and test the accuracy of a machine in such a way that it directly relates to the accuracy of a workpiece machined on it.

3.2 Geometric Accuracy : the inter-relationship of factors affecting it

Figure 3.1 is a generalized diagram showing the inter-relationship of factors affecting the machined workpiece accuracy.

The accuracy is directly influenced by the environmental conditions, tool wear, workpiece clamping and temperature changes in the workpiece due to the machining operation and by the geometric accuracy of the machine tool. It is however, indirectly influenced by the further effects of weight deformations, clamping deformations and thermal distortions which affect the finished product accuracy only through their influence on the geometric accuracy of the machine tool which is itself related to the accuracy of its

27

component parts.

The significance of the influence of the further effects is determined then by built-in design factors.

The errors generated in the machine tool may be subdivided into three groups:

(a) <u>Reference surface accuracy</u> This accounts for the geometric errors of the reference surfaces of the machine tool to which the workpiece or tool may be clamped.

(b) <u>Spindle rotation accuracy</u> This covers errors of roundness of surfaces (either internal or external).

(c) <u>Displacement accuracy</u> This is affected by errors of straightness, positioning and (control originated) dynamic errors.

In this chapter attention is directed solely to group (c), this being especially important to N.C. machine tools, though excluding the effects of dynamic errors, additional checks being necessary to determine them. This latter group of errors are those occuring in servomechanisms controlling the co-ordinate motions e.g. those caused by different velocity gain in the individual axes, overshoot and undercut.

The various errors inherent in spindle rotation are explained in Chapter 5 together with the associated measuring techniques and procedures for analysis and definition of these errors.

With reference again to Figure 3.1 we see that the geometric accuracy of a machine tool may be isolated, and hence defined as follows.

The geometric accuracy of a machine tool is that accuracy which is determined by the errors of a general workpiece which would be obtained if all other influences but that of the machine tool are excluded.

This definition justifies the adoption of the "master part trace technique" introduced by Bryan [23], since it is a technique which permits the required isolation.

3.3   Basic Translative Deviations

Figure 3.2 illustrates the measurement of the three basic translative errors, associated with the movement of a machine table, along some defined line in the plane of the table.

The measurements are associated with the X co-ordinate movement of the table and are made along a line parallel with the motion X. They consist of two measurements of straightness and one of positioning, the former made by gauges tracing an accurate master part consisting of a straight-edge, Figure 3.2a, and the latter by utilising one of three possible means, a line standard and telescope, a laser and target or an accurate lug bar as shown respectively in Figure 3.2b1, 3.2b2, 3.2b3.

These three measurements can be interpreted as checking the accuracy of position of points situated on the chosen line, the position of which is fixed in Y and W directions. The position of each of these points is identified by a corresponding X co-ordinate.

The three readings represent deviations in the three co-ordinate directions of the individual points and for example, during the motion X, these readings become functions of X.

Let us choose to refer to these deviations as

$$(a) \quad \delta_w(x) \qquad (b) \quad \delta_y(x) \qquad (c) \quad \delta_x(x) \qquad (3.1)$$

It is understood that three analogous deviations will occur, for the appropriate machine tool slide motion, in the other co-ordinate directions. A generalised nomenclature for translative error deviations can then be derived as:

$\delta_m(n)$ A translational deviation, where m=x,y,z and n=x,y,z. The form is interpreted as a deviation measured in direction "m" while traversing in axis "n".

When m=n, $\delta_m(n)$ is a measurement of positioning accuracy while if m≠n, $\delta_m(n)$ is an error of straightness.

3.4   Comparison of No-load Test with a Machining Test

While having justified previously the adoption of the

master part trace test as a valid procedure in order to isolate and identify the geometric accuracy of the machine tool, it is necessary to further justify it in the absence of a cutting force as is present in the direct test.

There are a number of reasons for avoiding the machining test because,

(a) it is more expensive and time consuming since for statistical reasons, several test workpieces have to be made and subsequently measured, and,

(b) the effects of tool wear and workpiece distortion cannot be separated from those of machine inaccuracy.

Therefore, if the indirect (non-machining) test may be arranged so as to give results for the whole working zone and include thermal, weight and clamping effects, it is un-doubtedly preferable.

The question of the influence of cutting force (or lack of it) could however arise. Firstly, no one should expect good workpiece accuracy to be achievable during a heavy roughing cut, when significant deformation of the workpiece may occur, finished accuracy only being achievable after a light finishing cut.

The only possible significant influence of even a very light cutting force may be to cause some transverse motion of the slide, limited by the motion available within the slide gib adjustment, during the longitudinal motion of

the slide.

However, the same effect may occur naturally through a combination of the weight of the sliding body with the friction forces and it follows then that the master part trace technique is still a valid approach if the measurements of straightness and parallelism of motions are made in both directions.

3.5   The Tolerance Laws

3.5.1   Rules Expressing the Relationship between Error and Distance

With manually operated machines it may be assumed for example that the tolerance Δ_2 on a workpiece of diameter D_2, Figure 3.3b, will increase with its size, being small for a small diameter D_1, the reason being that the error is determined solely by the error of measuring the diameter before taking the final cut, and the measuring gauge error will increase with the size measured. This same principle will apply to an N.C. machine tool if the tool position is corrected on the spindle axis.

However, in an N.C. machine tool the tool position may in fact be corrected to an intermediate diameter D_4. Neglecting the error of the correction, now, while diameter D_4 will be machined without error, both the larger and smaller diameters, D_5 and D_3, will have errors Δ_5 and Δ_3 respectively.

These errors will increase or decrease then with the differences, $(D_5 - D_4)$ and $(D_4 - D_3)$.

Additionally it is shown in Figure 3.3d how the error in a diameter (dimension in X) depends not only on the size of the diameter, but also on the length of that diameter (dimension in Z). Consequently, if it was desired to machine diameter D_6 which has the same nominal diameter as D_5 a larger tolerance Δ_6, larger than Δ_5, would have to be allowed for.

3.5.2   The N.M.T.B.A. Tolerance Template

The foregoing principles governing the concept of N.C. machine tool displacement accuracy are inherent in the form of tolerance template, Figure 3.4, (the so called bow tie template) as proposed by N.M.T.B.A. [27], and adopted also now by V.D.I. [26], for evaluating the positioning accuracy of N.C. machine tools.

The template T is illustrated in its application to a typical graph of positioning accuracy, the error δ_X being a function of distance travelled X. The thick full line depicts the mean positioning error achieved during a series of passes, the hatched area showing the positioning error field including scatter.

The design of this template permits a constant error Δf_X to exist along some basic distance b and it allows also for an additional error increasing in proportion to the

distance additional to b.

The template is applied to the graph in such a way
that the whole figure of the error field must always be
enclosed in the template while the template is shifted in
the direction of the X axis and at the same time is freely
moveable parallel to the direction of the δ_x axis. (It may
not be rotated however).

Its significance is as follows:
The relativity of the error is expressed. That is, in
relation to both distance travelled X and the error δ_x, the
error is taken as relative only between any two points.

3.5.3 A Modified Form of Tolerance Template

A simplification of the N.M.T.B.A. template form is
proposed, as shown in Figure 3.5, where the basic distance b
is diminished to zero. In fact, it is difficult to appre-
ciate the reason for this basic distance anyway.

The use and significance of this modified form of
template as regards the relativity of error and distance
remains.

Let us examine this form of template in relation to
the ISO system of tolerancing. In Figure 3.6 the values of
permissible tolerances are plotted against dimension for the
IT5 class of accuracy.

It is seen that the relationship given by the result-
ing curve a is non linear and that for dimensions approaching

zero the tolerance approaches a certain minimum value.
Except for the three finest classes IT01, IT0 and IT1
where the relationship is linear, the same formula exists
for all other IT tolerance classes but for the scale of δ.

It is proposed to linearize the ISO curve, and the
least squares fit straight line is given by line b which in
fact does not differ from curve a by more than 2 μm except
for small dimensions.

The characteristic features of this modified
(linearized) IT curve are embodied in the proposed template
form of Figure 3.5 if the tolerances and dimensions are
taken as being relative.

A mathematical expression for this template can be
formulated:

$$\left| \delta_x(x_1) - \delta_x(x_2) \right| \leqslant A_{xx} + K_{xx} \left| x_2 - x_1 \right| \qquad (3.2)$$

where x_1 and x_2 are the co-ordinates of any two points along
an axis X and $\delta_x(x)$ is the error in the direction X of the
points x.

The expression (1) may be translated as:
The absolute value of the error of the distance of two points
(whether the error is positive or negative, i.e., whether the
actual distance is greater or smaller, is not relevant) may be
equal to or less than some constant value A_{xx} plus an addi-
tional value proportional by K_{xx} to the distance (while it is

irrelevant which direction is taken as positive).

3.5.4 Extension of the Tolerance Laws to a Three Dimensional Working Zone

The next step will be the consideration of positions of points in a three-dimensional zone depicted in Figure 3.7. Basically, the dimensions of workpieces are distances of two points and this being so, let us consider two generally located points 1 and 2.

The accuracy of the position of a single point is determined by the deviations δ_x, δ_y and δ_w from its ideal position.

The distance between the two points may be determined by means of the three coordinates by,

$$(x_2 - x_1), \quad (y_2 - y_1), \quad (w_2 - w_1) \tag{3.3}$$

and the component errors of the distance as,

$$(\delta_{x_2} - \delta_{x_1}), \quad (\delta_{y_2} - \delta_{y_1}), \quad (\delta_{w_2} - \delta_{w_1}) \tag{3.4}$$

It is proposed to consider the component errors (3.4) as dependent each on the total distance of the two points as expressed by the components (3.3).

This approach is justified if the generation of errors is considered as the tool moves from point 1 to point 2 in the work zone. Section 1 to 1' comprises motion in the X co-ordinate motion, 1' to 1" in the direction W and 1" to 2 in direction Y.

If we consider only one of the component errors δ_x, this is generated in parts as: the positioning error over the distance $(x_2 - x_1)$, a straightness of motion error in direction X in moving in W over the distance $(w_2 - w_1)$ and a further straightness of motion error in direction X is moving in Y over the distance $(y_2 - y_1)$.

In an analogous way, the errors δ_y and δ_w are generated in all the component motions.

An expression for the error in X may then be derived as:

$$\left| \delta_{x_2} - \delta_{x_1} \right| \leq A_{xx} + K_{xx} \left| x_2 - x_1 \right| + A_{xy} + K_{xy} \left| y_2 - y_1 \right|$$

$$+ A_{xw} + K_{xw} \left| w_2 - w_1 \right| \qquad (3.5)$$

In order to generalise this formula we may derive the following:

$$\left| \delta_{m_2} - \delta_{m_1} \right| \leq A_{mx} + K_{mx} \left| x_2 - x_1 \right| + A_{my} + K_{my} \left| y_2 - y_1 \right|$$

$$+ A_{mw} + K_{mw} \left| w_2 - w_1 \right| , \qquad (3.6)$$

where $m = x, y, w$

Hence, the relative component errors of any two points are permitted to be equal to a constant value plus a sum of values proportional to the component co-ordinate distances of the two points.

The error is seen to consist of three parts

$$A_{mn} + K_{mn} \left| n_2 - n_1 \right| \qquad (3.7)$$

where $m = x,y,z$ and $n = x,y,z$, and the constants A_{mn} and K_{mn} are chosen with respect to the significance of the motions in the individual directions.

These components all have the same form as (3.2) meaning that we accept the same form for the errors of straightness of motion as has been proposed for the positioning error.

This is justifiable since as far as lateral deviations of a moving body are concerned (i.e. deviations of straightness of motion) there will always be a basic error A_{mn} due mainly to backlash in the guideways and repeatability of measurement, as well as a deviation K_{mn} that will increase with distance travelled due mainly to the error of squareness of the basic co-ordinate motions.

The forms of the relationships (3.6), (3.7) signify that in this way, tolerances may be expressed for the three basic translative measurements depicted in Figure 3.2, wherever in the working zone and along whatever line in that zone the measurements are made.

It is of course unrealistic to make an infinite number of measurements along an infinite number of lines in the working zone. There is however a minimum necessary number of measurements which may be specified according to

the application of the rules in the following paragraph.

3.6   The Primary Effects of Angular Deviations

Considering the motion in X of the table of a
horizontal boring machine as in Figure 3.8, there are
three unwanted angular deviations associated with this
motion besides the three basic translative error deviations.
These are the angular deviations of roll, pitch and yaw, the
terminology being analogous to the motion of a ship as
previously noted.

Denoting an angular deviation by ε, the angular
deviation being a function of the distance travelled in X;
we have,

$$\varepsilon_x(x) \quad - \quad \text{roll}$$

$$\varepsilon_y(x) \quad - \quad \text{yaw}$$

$$\varepsilon_z(x) \quad - \quad \text{pitch} \qquad (3.8)$$

or, generally, the nomenclature for angular deviations may
be established as;

$\varepsilon_m(n)$:   An angular deviation, where $m=x,y,w$ and
$n=x,y,w$, the form being interpreted as the
angular deviation occuring around axis "m"
while traversing in axis "n".

Now let us consider the Primary Effects of Angular Deviations
occuring during a co-ordinate motion, these being defined as

the effects of angular deviations on translative deviations measured during the same co-ordinate motion.

This type of effect is illustrated in Figure 3.8 where the angular motion of the table of a horizontal boring machine is considered. So that the illustration be as general as possible, the existence of two spindles is assumed. The basic translative error deviations $\delta_x(x)$, $\delta_y(x)$ and $\delta_w(x)$ are measured along some line P, the gauge being fixed in spindle number 1.

Now, if machining takes place, or if the measurement be made, along some line other than P, offset with respect to the moving body, e.g. line Q offset in W, or if the measurement is made along the same line P but from the other spindle, i.e. spindle number 2, the translative error deviations obtained will be different.

In Figure 3.8c the error deviations $\delta_w(x)$ and $\delta_y(x)$ are affected by the roll $\varepsilon_x(x)$ and the offsets b and c respectively according to;

$$\delta_y(x)_Q = \delta_y(x)_P + \varepsilon_x(x).c$$

$$\delta_w(x)_R = \delta_w(x)_P + \varepsilon_x(x).b \qquad (3.9)$$

In Figure 3.8d, the pitch $\varepsilon_w(x)$ affects the deviations $\delta_x(x)$ and $\delta_y(x)$ by offsets b and a respectively.

$$\delta_x(x)_R = \delta_x(x)_P + \varepsilon_w(x).b \tag{3.10}$$

$$\delta_y(x)_{P\,(\text{spindle}\ 2)} = \delta_y(x)_{P\,(\text{spindle}\ 1)} + \varepsilon_w(x).a$$

Finally, in Figure 3.8e, the yaw $\varepsilon_y(x)$ affects the deviations $\delta_w(x)$ and $\delta_x(x)$ by offsets a and c respectively.

$$\delta_x(x)_Q = \delta_x(x)_P + \varepsilon_y(x).c \tag{3.11}$$

$$\delta_w(x)_{P\,(\text{spindle}\ 2)} = \delta_w(x)_{P\,(\text{spindle}\ 1)} + \varepsilon_y(x).a$$

From the foregoing formulae it may be realised that the differences between two translative deviation measurements made at different offsets are caused by angular deviations.

These differences will increase as the offset increases and will be extreme for extreme offsets. Measurements made at offsets smaller than the extreme one may be found by a linear interpolation between the two extreme measurements.

Therefore, if measurements of translative deviations made along two lines extremely offset to each other both satisfy a given tolerance, then the measurements along all intermediate lines between the two offsets will also satisfy the tolerance.

This has great significance for it enables a quantitative and comprehensive evaluation of accuracy in a

two or three dimensional zone to be arrived at by checking only the tolerance of measurements of translative deviations made along those lines, extremely offset to each other, which define the specified working zone.

3.7 Specification of a Basic Minimum Number of Required Translative Deviation Measurements

Let us now utilize the principles of the preceding paragraph in specifying the required measurements for describing the accuracy of a horizontal floor-type boring machine (plate I, pg.43) equipped with a bed plate and a rotary table attachment.

Consider separately two modes of operations with this machine corresponding to:

Model A - machine used with bed-plate, and,

Model B - machine used with rotary table attachment.

The first step in the procedure is the determination of the extreme offsets along which the basic translative error deviations will be measured.

We may proceed by remembering the definition of an offset.

An offset is a variation of the distance of the tool point taking place with respect to the moving body.

The detailed procedure may be followed by reference to Figure 3.9.

A. Model A: Boring machine used with the bed-plate
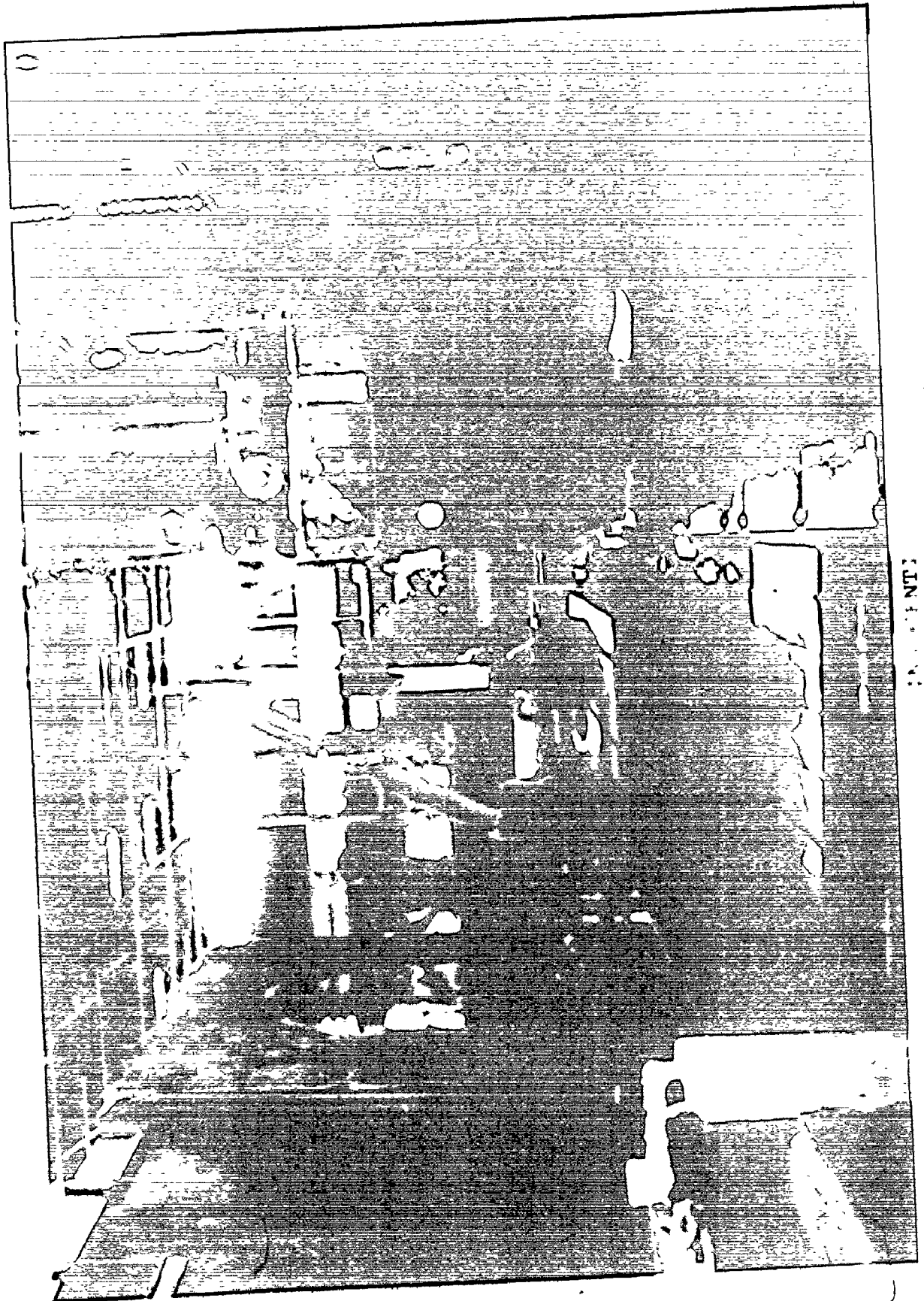
Each co-ordinate motion is taken in turn.

(a) X motion: Considering the X traverse of the column along the bed, the maximum offsets of the tool with respect to the moving body (i.e. column) are given by lines A,B (maximum offset in Y), D (maximum offset in Z) and C (maximum offset in Z and Y).

The necessary error function measurements are therefore;

(1) Straightness errors: $\delta_y(x)$, $\delta_z(x)$ along line A, and for the effect of roll $\epsilon_x(x)$, $\delta_y(x)$ also along line D and $\delta_z(x)$ along line B.

(2) Positioning errors: $\delta_x(x)$ along line A and, for the effect of pitch $\epsilon_z(x)$, $\delta_x(x)$ also along line B, for the effect of yaw $\epsilon_y(x)$, $\delta_x(x)$ along line D. Additionally being affected by both pitch and yaw motions, $\delta_x(x)$ along line C.

(b) Y motion: With respect to the moving body, here the vertical movement of the headstock, an offset may only occur in the Z direction according to extension of the spindle carrying ram or the spindle itself. (An additional offset may be the varying length of the tool but we may normally assume some constant mean length).

Accordingly lines E and F correspond to the extreme offsets of the tool point and extensions of the ram, Z_{min} and Z_{max} respectively.

The required error functions then are;

(1) Straightness errors: $\delta_z(y)$ and $\delta_x(y)$ along line E, and for the effect of "vertical pitch" $\tau_y(y)$, $\delta_x(y)$ also along line F.

(2) Positioning errors: $\delta_y(y)$ along line E and for the effect of "vertical yaw" $\epsilon_x(y)$, $\delta_y(y)$ also along line F.

(c) Z motion (i.e. spindle extension)

There is no offset of the tool with respect to the moving body since the tool moves with it (again assuming a constant mean tool length). Therefore, the basic measurements of translative error deviations need only be performed along any single line, say G.

The required error functions are;

(1) Straightness errors: $\delta_x(z)$, $\delta_y(z)$ along line G

(2) Positioning errors: $\delta_z(z)$ along line G

(d) W motion (i.e. ram extension)

Derived in an identical manner as for spindle extension, the error measurements for the ram extension are;

(1) Straightness errors: $\delta_x(w)$ and $\delta_y(w)$ along the same line G

(2) Positioning errors: $\delta_w(w)$ along line G also

B. <u>Model B: Boring machine used with the rotary table/attachment</u>

All of the previously determined offsets and basic

measurements apply, lines A,B,C and D being extended so as to include the working zone over the rotary table.

$\bar{W}$ motion: The maximum offsets of the tool with respect to the motion of the table are lines H,J (maximum offset in X, L (maximum offset - Y) and K (maximum offset - X and Y).

Thus, the additional tests specific to $\bar{W}$ motion are;

(1) Straightness errors: $\delta_x(\bar{w})$, $\delta_y(\bar{w})$ along line H and, for the effect of roll $\varepsilon_{\bar{w}}(\bar{w})$, $\delta_x(\bar{w})$ along line L and $\delta_y(\bar{w})$ along line J.

(2) Positioning errors: $\delta_{\bar{w}}(\bar{w})$ along line H and, for the effect of yaw $\varepsilon_y(\bar{w})$, $\delta_{\bar{w}}(\bar{w})$ along line J, for the effect of pitch $\varepsilon_x(\bar{w})$, $\delta_{\bar{w}}(\bar{w})$ along line L. Additionally, affected by both pitch and yaw motions $\delta_{\bar{w}}(\bar{w})$ along line K.

This set of measurements will be performed for some constant extension of the spindle.

3.8 The Secondary Effects of Angular Deviation

These may be defined as the effects of angular motions occuring during a co-ordinate motion on translative deviations measured during another co-ordinate motion.

These effects are secondary in name only and not necessarily in magnitude. Also, it may be shown that these

effects do not affect measurements of positioning accuracy.

Now, in the preceding section 3.7, the minimum number of measurements has been defined as a series of translative error deviation measurements. However a common procedure is to measure the basic translative error deviations along only a single line in each axis, complementing these measurements with measurements of pitch, roll and yaw in each axis.

In this way, the other required translative deviation measurements may be derived, according to the principles of section 3.6, as a sum of the basic measurement and an additional component due to the angular error motion as magnified by the appropriate offset into an error of translation.

This is a useful procedure avoiding problems of fixturing especially with the type of large machine we consider here, depicted in Figure 3.9, as an example of the application of the rules. It also provides directly however the angular motion data required to compensate the translative motion errors for the secondary effects of angular motion, the occurrence of which we consider next.

It is important to remember that the straightness measurements are made for example by a gauge tracing a master square which is aligned as far as possible to the co-ordinate motion of the machine by typically locating it against provided reference surfaces.

The measurements therefore will be composed of two parts which are;

(a) the deviation of straightness proper, and,

(b) the deviation of the direction

Now, the contribution of the latter will vary according to the relative position of the moving bodies. Consider for example Figure 3.10 where the measurement of straightness $\delta_y(z)$ has been made by tracing, with a gauge located in the spindle nose, a master square located on our rotary table at position x_F.

Suppose however, the measurement is repeated with the square at position x_F', the column having been moved to x_F'' to bring the gauge opposite the spindle again.

The two measurements, let us call them $\delta_y(z)_F$ and $\delta_y(z)_F''$, will vary by virtue of a changed direction deviation caused by the roll of the column $\varepsilon_x(x)$ (also possibly by poor reference surface accuracy and by location of the table in the $\bar{w}$ direction and the pitch motion $\varepsilon_x(\bar{w})$).

This change in angular deviation given by ε_F between F'' and F would be;

$$\varepsilon_F = \varepsilon_x(x)_F - \varepsilon_x(x)_F'' \tag{3.12}$$

Let us now determine those measurements which are affected as a consequence of the secondary effects limiting ourselves to those measurements which measure deviations in

the X and Y co-ordinate directions, the primary purpose
with this type of machine being accurate positioning in
these directions.

Model A: Square located on the bed-plate

$$\delta_x(y) \text{ affected by } \epsilon_z(x)$$

$$\delta_y(z) \quad " \quad " \quad \epsilon_x(x)$$

$$\delta_x(z) \quad " \quad " \quad \epsilon_y(x)$$ (3.13)

Model B: Square located on the rotary table

$$\delta_y(z) \text{ affected by } \epsilon_x(x)$$

$$\delta_y(z) \quad " \quad " \quad \epsilon_x(\bar{w})$$

$$\delta_x(z) \quad " \quad " \quad \epsilon_y(x)$$

$$\delta_x(z) \quad " \quad " \quad \epsilon_y(\bar{w})$$

$$\delta_y(x) \quad " \quad " \quad \epsilon_{\bar{w}}(\bar{w})$$

$$\delta_x(y) \quad " \quad " \quad \epsilon_z(x)$$ (3.14)

$$\delta_x(y) \quad " \quad " \quad \epsilon_{\bar{w}}(\bar{w})$$

It may be realised that there will be two extremes
of this directional deviation corresponding to the maximum
and minimum angular deviation from that corresponding to the
recorded position of the master square in the initial mea-
surement.

These extremes will be found at some position of the

moving member not normally known in advance.

Returning to the measurement $\delta_y(z)_F$ made in accord with the required tests for Model B, it is seen from the above table, that it is affected both by $\epsilon_x(x)$ and $\epsilon_x(\bar{w})$.

Having made the measurement of the two angular deviations involved, we may determine the position at which $\epsilon_x(x)$ and $\epsilon_x(\bar{w})$ reach their maximum and minimum values.

i.e. for $\epsilon_x(x)$ the maximum and minimum will be given by

$$\epsilon_x(x)_{Ex+} \quad \text{and} \quad \epsilon_x(x)_{Ex-} \tag{3.15}$$

Correspondingly, for the motion $\epsilon_x(\bar{w})$ we have for the maximum and minimum

$$\epsilon_x(\bar{w})_{Ex+} \quad \text{and} \quad \epsilon_x(\bar{w})_{Ex-} \tag{3.16}$$

The two extreme error functions will therefore be given by

$$\delta_y(z)_{Ex+} = \delta_y(z)_F + \left[(\epsilon_x(x)_{Ex+} - \epsilon_x(x)_F) + (\epsilon_x(\bar{w})_{Ex+} \right.$$
$$\left. - \epsilon_x(\bar{w})_F) \right] \cdot z \tag{3.17}$$

and,

$$\delta_y(z)_{Ex-} = \delta_y(z)_F + \left[(\epsilon_x(x)_{Ex-} - \epsilon_x(x)_F) + (\epsilon_x(\bar{w})_{Ex-} \right.$$
$$\left. - \epsilon_x(\bar{w})_F) \right] \cdot z \tag{3.18}$$

N.B. the deviation δ_y being a function of the distance z, the contribution to the basic translative error of the added angular deviation is also a function of z.

Accordingly, by analogous means, upper and lower bounds for each of the similarly affected measurements may be calculated. Thus, the parameters of the template describing the accuracy of the individual error motions may be correctly derived so as to reflect the worst situation occuring in the working zone.

Using this approach, i.e. combining measurements of translative error deviations and angular deviations, it is comparatively easy to calculate the minimum number of translative error deviations required for a definition of machine accuracy. Referring again to Figure 3.9 and the measurements specific to Model A and Model B mode of utilisation of the machine.

A.   <u>Model A: use of the machine with the bed-plate</u>

(a)   X motion:

$$\delta_x(x)_B = \delta_x(x)_A + \varepsilon_z(x).a$$

$$\delta_x(x)_D = \delta_x(x)_A + \varepsilon_{\dot{y}}(x).b$$

$$\delta_x(x)_C = \delta_x(x)_A + \varepsilon_z(x).a + \varepsilon_y(x).b$$

$$\delta_z(x)_B = \delta_z(x)_A + \varepsilon_x(x).a$$

$$\delta_y(x)_D = \delta_y(x)_A + \varepsilon_x(x).b$$

(3.19)

(b)   Y motion:

$$\delta_y(y)_F = \delta_y(y)_E + \epsilon_x(y).b$$

$$\delta_x(y)_F = \delta_x(y)_E + \epsilon_y(y).b \qquad (3.20)$$

(c)   Z motion, W motion require no derived measurements

B.   Model B: use of machine with the rotary table

$\bar{W}$ motion:

$$\delta_{\bar{w}}(\bar{w})_L = \delta_{\bar{w}}(\bar{w})_H + \epsilon_x(\bar{w}).a$$

$$\delta_{\bar{w}}(\bar{w})_J = \delta_{\bar{w}}(\bar{w})_H + \epsilon_y(\bar{w}).c$$

$$\delta_{\bar{w}}(\bar{w})_K = \delta_{\bar{w}}(\bar{w})_H + \epsilon_x(\bar{w}).a + \epsilon_y(\bar{w}).c$$

$$\delta_x(\bar{w})_L = \delta_x(\bar{w})_H + \epsilon_{\bar{w}}(\bar{w}).a \qquad (3.21)$$

$$\delta_y(\bar{w})_J = \delta_y(\bar{w})_H + \epsilon_{\bar{w}}(\bar{w}).c$$

In a similar way as previously demonstrated, those
measurements affected, according to (3.14), will have to be
modified for the secondary effects of angular deviations.

3.9   Design of a Master/Part - the integrated test procedure

It is possible to incorporate all the desired measure-
ments in some form of master part. In this way all the
specified translative error deviation measurements can be
obtained taking into account the primary error motions.

Figure 3.11 shows a master workpiece designed for
checking a horizontal boring machine. Typically it consists
of a combination of straight-edges and stepped bars (or a.

series of accurately spaced holes).

The data obtained from tracing such a master part is of course integrated data and the angular deviations will have to be calculated by comparing pairs of measurements, this procedure being necessary in order to calculate the secondary effects of angular deviations.

Another master part [28] designed for an N.C. lathe is shown in Figure 3.12. It consists of a base plate attached to the end of the spindle of the tested machine.

Attached to the plate are the X step bar and the X straight-edge and, in a plane perpendicular to this one, the Z step bar.

The Z straight-edge is materialised by the mandrel clamped in the spindle nose.

The fixture is swiveled during the test cycle subsequently into the A,B,C and D positions so that positioning and straightness measurements can be made at the appropriate offsets.

In order to take into account the extreme possible tool positions, the master workpiece is traced subsequently by gauges attached to the tool post in positions corresponding to the minimum and maximum extreme tool lengths.

For large machines however, such a master part is not practical and the "flexible" master which is the laser beam is much preferred.

3.10   Extension of the Tolerance Laws to include further effects

Whichever method is used, i.e. the direct measurement of translative error deviations or the combination of translative and angular error deviations to give the desired translative error motion at other offsets of the tool, the various measurements may be checked directly against the prescribed tolerance rules using the method illustrated in Figure 3.5.

The results however, show only the accuracy of the machine in its state during the measurement. The accuracy is affected by what we choose to call "further effects", i.e. clamping, weight and thermal deformations.

The influence of these further effects may be accommodated in the design of the tolerance template Figure 3.13 in accord with the following principles;

(1) Clamping deformations As clamping deformations are those displacements of the moveable bodies (i.e. slides, tables, etc.) which occur as such a body is clamped to the guideway.

The presence of this effect is naturally only applicable to those machines and to those operating modes of the machine in which clamping is used.

Then, the specified measurements which are considered affected must be performed in the appropriate operating mode

e.g. the positioning accuracy of a body would be measured
during a cycle of steps where in each position the body
is clamped to its guideway before readings are taken.

It is conceivable that for some machines there are
two possible modes of operation for a particular motion.
For example, the table of a boring and milling machine may
be moved continuously for milling operations, but moved
intermittently and clamped for positioning in boring
operations.

In such a case, the positioning, and/or straightness
measurements as the case may be, should be made during both
simulated modes of operation.

(2) <u>Weight Deformations</u> These may be, for example, the
deformations of a horizontal boring machine structure caused
by the influence of the weight of the workpiece on the table.

Those error measurements likely to be affected will
have to be carried out at both no-load and at extreme load.
If both results satisfy the specified tolerance, it will be
satisfied for any load between the extremes.

(3) <u>Thermal Effects</u> It may be suggested to carry out those
measurements which are likely to be affected repeatedly
through a range of thermal states of the machine such as
they result from a typical working cycle. This is a recom-
mendation however which is less precise than those related
to clamping and weight deformations.

The specification of this procedure, i.e. which measurements to repeat and through which range of thermal states is the subject of the investigation in Chapter 4.

CHAPTER 4

THERMAL EFFECTS IN MACHINE TOOLS

4.1   General Description of the Problem

Changes in alignment and positioning accuracy of a machine tool due to thermal distortions of the machine are often several times the magnitude of the specified tolerance of the machine.

However, the effects of these phenomena have been largely neglected from quotation of machine tool accuracy.

Some reasons for the greater recognition of the problem at this time are:

1)   the trend towards closer tolerances,

2)   the trend towards numerical control and the elimination of the skilled, self-adaptive man,

3)   the trend towards better measuring techniques and electronic instrumentation, and,

4)   the possibility of breaking down the overall error into the individual components e.g. tool wear, static and dynamic compliance, kinematic accuracy and thermal effects.

Thermal effects may be classified as follows:

1)   Effects of temperature other than 20°C.

2)   Effects of temperature variation.

3)   Effects of temperature gradient.

In order to visualize the thermal error system, Bryan [29] used Figure 4.1 to demonstrate the complexity of the problem.

The six sources of thermal influence shown may be roughly classified into either internal or external heat sources:

a)   Internal Heat Sources

(i)   spindles/power trains - these are often the most troublesome accounting for thermal effect errors of the largest magnitude

(ii)   hydraulic systems - these are often built into the structure and especially if additionally, fixed displacements pumps and relief valves are utilised for feed drives, they may be a significant source of error.

(iii)   lubrication systems - here, the pump's work is dissipated in heat and the heated oil is further heated by the serviced elements of the machine before being recycled to the pump

(iv)   slideways and leadscrews

(v)   electric motors - these are often found buried in the machine structure with no provision for venting heated air away, or the air of external motors is blown onto the structure.

b)   External Heat Sources

1) room environment

2) coolant system

3) heat created by the cutting process - the pro-
   vision of guards is often necessary to shield the
   workpiece from the heated chips. Often to mini-
   mise, the roughing and finishing operations are
   separated

4) people

5) thermal memory from a previous environment

The only influences that can create uniform tempera-
tures are those of the environment and coolant systems (hence
the arrow in Figure 4.1), all other heat sources causing
either steady-state gradients or temperature variations or
both.

All sources affect the basic three element system of
master, part and machine frame, which comprises the structural
loop, through the three possible modes of heat transfer. The
errors introduced may either be of geometry or size.

By geometric errors we mean errors of straightness,
squareness and positioning etc., developed as a consequence
of temperature gradients.

However, while the potential reduction in machine
accuracy is not insignificant, neither is it inevitable.
Various solutions may be found which could be listed under
general approaches to the problem of decreasing thermally

originated errors:

      1)   decrease the rate of heat generation - or remove the heat source

      2)   sensing or predicting unwanted deformations and compensating

      3)   stabilisation of machine component temperatures by cooling

      4)   stabilisation of the entire temperature environment of the machine tool

      5)   designing the structure to be insensitive to temperature

4.2   Identification of Heat Sources and Affected Error Functions

    There are three classes of heat source which will not be considered in this chapter:

1)   The environment

    Even if the effect of the environment is not negligible as is often the case, and if a possible machine shop air conditioning system with high local air flow rates does not solve the problem, it is an effect which may be considered separately from and superimposed on the effects of internal heat sources. These internal heat sources constitute a more complex variety and the concern of this chapter is limited to them.

2)   Coolant

The omission is justified by assuming that in most operations no coolant is used and where it is used and high precision is considered, it should be temperature controlled and this is a special case.

3) Heat generated in cutting

This may be neglected if it is assumed that for the manufacture of highly accurate workpieces, rough machining is carried out first and finish machining is carried out later, the thermal effects of the roughing process having decayed in the intervening period.

The heat generated in the finishing (low power) operation is small and thermal deformation of the workpiece itself and of the machine can become insignificant, especially if the chips, which accept the greater part of the heat generated in the cutting process, are carefully deflected from the machining area.

In other words, while not denying the undoubted influence of these sources of heat, we limit the discussion to those sources which are really an integral part of the no-load work of the machine.

These sources may be roughly divided into two groups:

1) Constant heat sources

     e.g. (a) a hydraulic power supply with a constant delivery pump,

        (b) heat generated in an electric motor and blown onto the machine structure

2) <u>Variable heat sources</u>

      e.g. (a) Typically these include the spindle

              bearings and gear-box (possibly with

              hydraulic clutches) in the spindle

              drive, where the heat generated will be

              dependent on the spindle speed

          (b) friction in feed drives where the heat

              generated will be dependent on the feed

              rate

In fact, it is usually possible to estimate well which are the heat sources of either type that apply in the case of a given machine. Furthermore it is even usually possible to assess which parts of the structure are affected by the identified heat sources. Also, it is possible to identify which of the specified error functions will be affected.

With reference to a number of specific examples, let us try to localize the individual heat sources and their effects, applying first the techniques of the previous chapter in determining the minimum number of translative measurements specific to each machine's function.

<u>MACHINE A</u>: <u>A 5 Axis Machining Center</u> (plate II, pg.63)

The axis nomenclature of this machine is shown in Figure 4.2a. The tools used are all of practically the same length and therefore, as regards X and Y motions, machining is practically performed in a single (X,Y) plane, instead
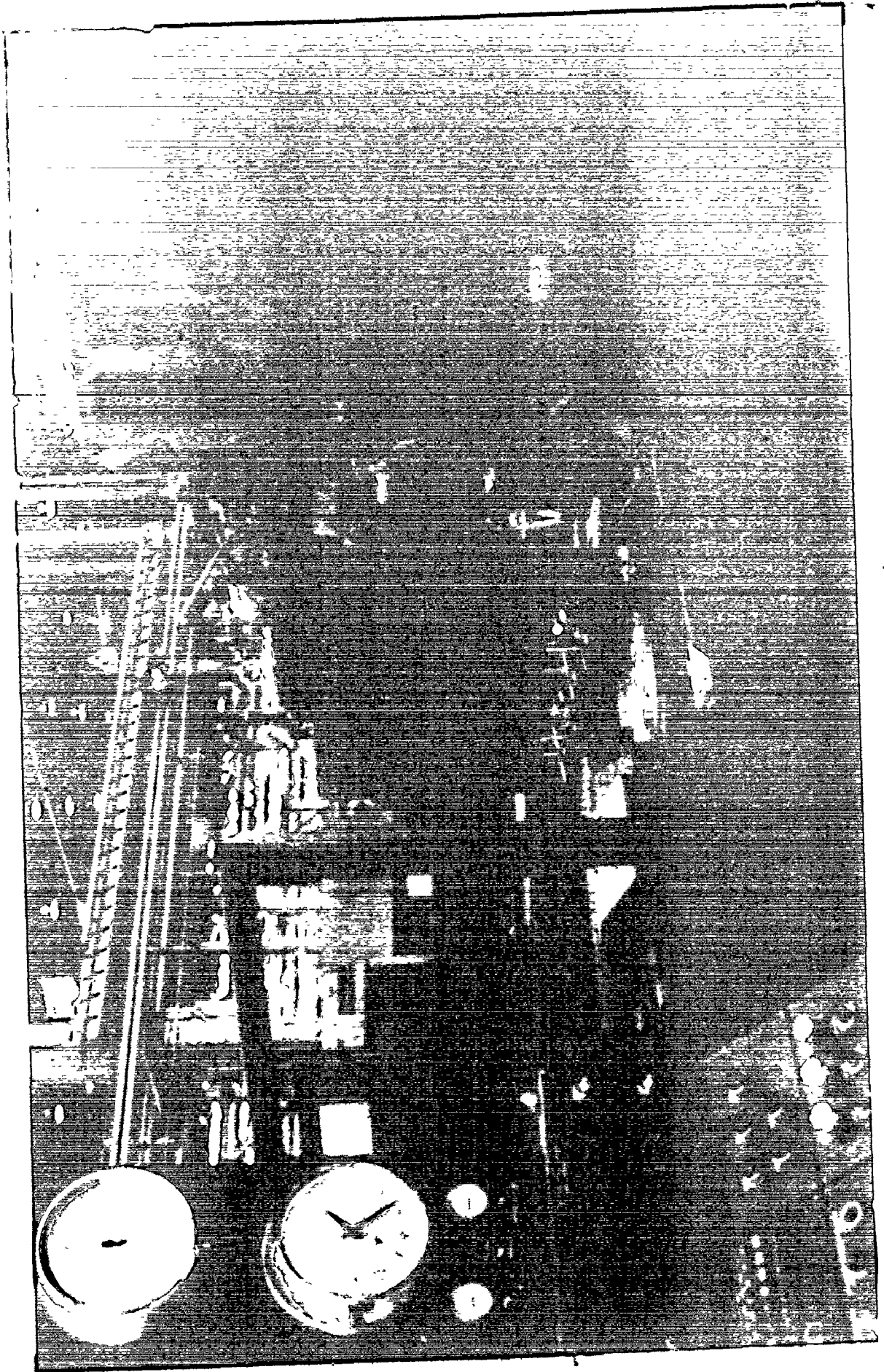
of in a three-dimensional working zone. This does not
however exclude the workpiece from being three-dimensional
with machined surfaces on all sides of the maximum possible
size of cube. The three-dimensional zone is here effective-
ly reduced by one half by machining in that half cube only
which faces the headstock and subsequently bringing the
opposite half into action by indexing the table. In this
respect co-ordinate motions Z,A and B are used as setting
motions and to bring the machined surface into the above
mentioned (X,Y) plane. In other words, Z, A and B motions
are not normally working motions, the exception being for
the boring operation where X and Y motions are the setting
ones and Z the working motion.

A sensible approach to this case is to consider the
errors associated with the individual motions in two separ-
ate groups:

1) X, Y as regards work in one (X,Y) plane only
which passes through the tip of some average length of tool

2) Z,A,B as regards straightness and depth of
bored holes

For the X,Y group, the necessary measurements, hav-
ing first defined the appropriate offsets, are limited to:

(a) X motion

(i) straightness errors $\delta_y(x)$ and $\delta_z(x)$ along line
A and also, for the effect of roll $\epsilon_x(x)$, $\delta_z(x)$ along line B

(ii)   positioning errors $\delta_x(x)$ along line A and,
for the effect of pitch $\epsilon_z(x)$ also along line B

(b)   Y motion

(i)   straightness errors $\delta_x(y)$ and $\delta_z(y)$ along
line C

(ii) positioning error $\delta_y(y)$ along line C

For the Z,A,B. group:

(a)   Z motion

(i)   straightness errors $\delta_x(z)$ and $\delta_y(z)$ along line
D and, for the effect of roll $\epsilon_z(z)$, $\delta_x(z)$ also along line E

(ii) positioning error $\delta_z(z)$ along line D and, for
the effect of pitch $\epsilon_x(z)$, also along line E.

(b)   A,B motions

A tolerance is set for setting motions A and B and
it can be practically limited to $\delta_a(a)$ and $\delta_b(b)$ errors of
angular positioning.

Let us now determine the location of the heat sources
and the affected measurements:

It may be the case that there are no significant heat
sources in the transversal (Z) bed. Heat generated by slid-
ing in the guideways during Z motion is negligible and we
consider one possible effect only. That is, the heat gener-
ated between the nut and the leadscrew, especially d ng
the rapid traverse withdrawals in boring, provided of course
that the positional feedback is derived from the leadscrew.

from the leadscrew, $\delta_z(z)$ and $\delta_x(x)$ must also be repeated through a thermal cycle of the leadscrew.

It is often satisfactory to replace the repeated (continuous) measurements of the error functions by a single measurement of such functions, complemented by reppeated measurement of the corresponding errors at the end points of the corresponding travel. In this way, repeated measurements $\delta_x(y)$, $\delta_z(y)$ and $\delta_y(y)$ may be replaced by measurement of deviations δ_x, δ_y, δ_z in the position y_{min} and y_{max} as shown in Figure 4.2c.

MACHINE B: A Three-spindle Bed-Type Milling Machine
(plate III, pg.68)

The specification of the rather small number of measurements indicated in Figure 4.3 is based on the assumption of using this machine for flat workpieces only i.e. for machining low above the table surface, and for utilising only a single spindle. It will be appreciated that for a truly three-dimensional working zone and especially for the three spindle mode of use of the machine, the number of required error function measurements will increase considerably.

Again, for this machine, there are no significant heat sources in the bed. Heat generated in the motor, the gearbox and the spindle mounting affects the motion of the ram (motion Y) and the headstock (motion Z).
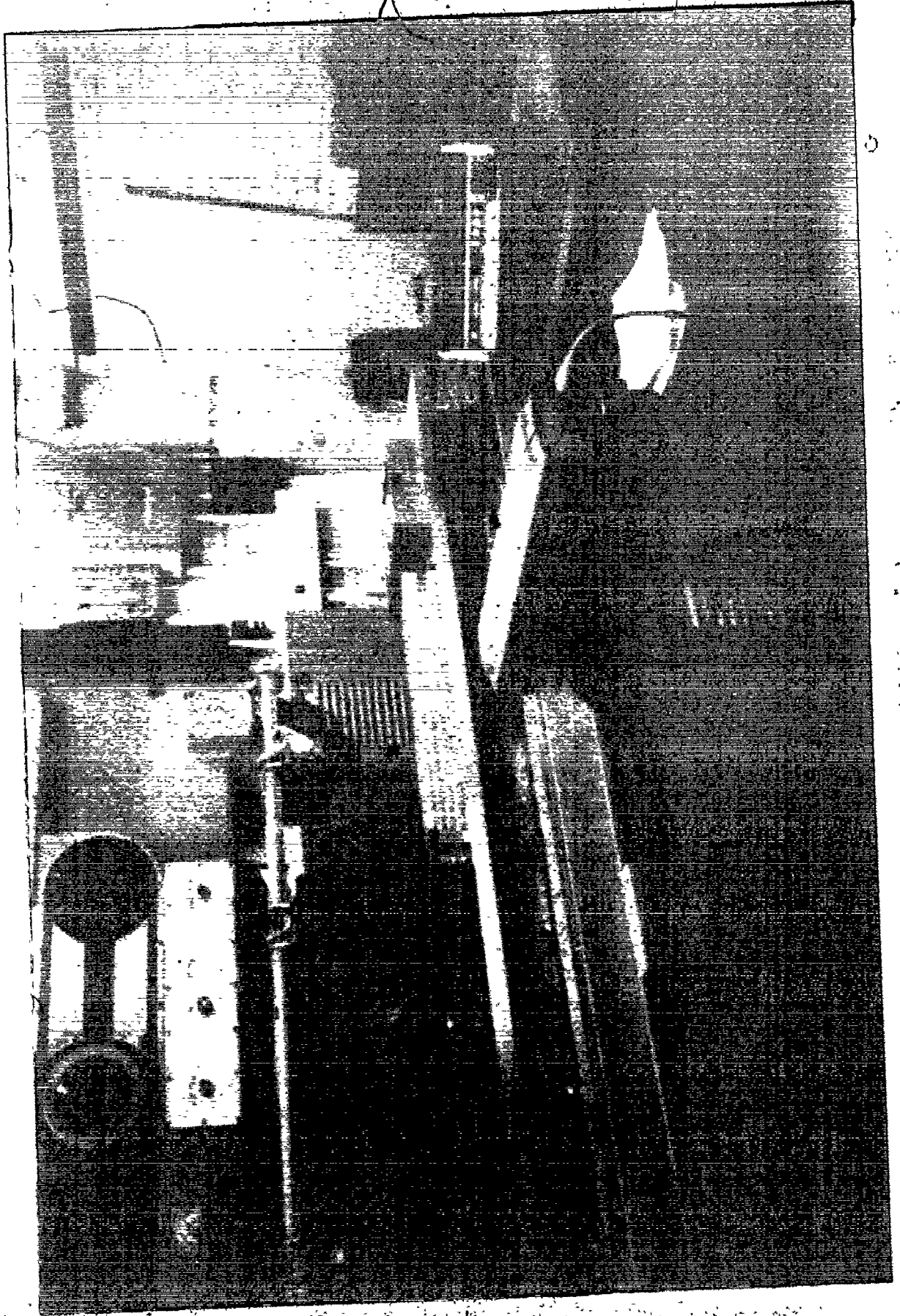
Consequently, measurements $\delta_x(y)$, $\delta_y(y)$ and $\delta_z(y)$ are affected. Of the whole motion Z, with respect to the assumed case of flat workpieces, practically only the bottom end of travel is of interest.

Therefore, error functions associated with the Z motion are reduced to deviations δ_x, δ_y and δ_z to be measured, at the end of a mandrel, the length of which equals some mean tool length, as they vary during the thermal cycle. These variations are often referred to as "drifts".

If on the same machine, the whole Z travel is used for machining, the limitation to flat workpieces not applying, the functions $\delta_x(z)$, $\delta_y(z)$ and $\delta_z(z)$ should be measured instead of the drifts only. In this case, and in analogy to Figure 4.2c instead of $\delta_x(z)$ and $\delta_y(z)$, drifts δ_x and δ_y are measured at both top and bottom end of travel, together with one measurement of δ_z.

The positional signal being derived from the lead-screw, error functions $\delta_x(x)$, $\delta_y(y)$ and $\delta_z(z)$ are affected by the heat generated by friction in the drive nut.

The error measurements affected by the heat sources are denoted by T in Figure 4.3b-d.

MACHINE C: A knee-type (vertical-spindle) Machining Center
(plate IV, pg. 70)

The configuration of the machine is shown in Figure 4.4a and the necessary error functions in Figure 4.4b-e,
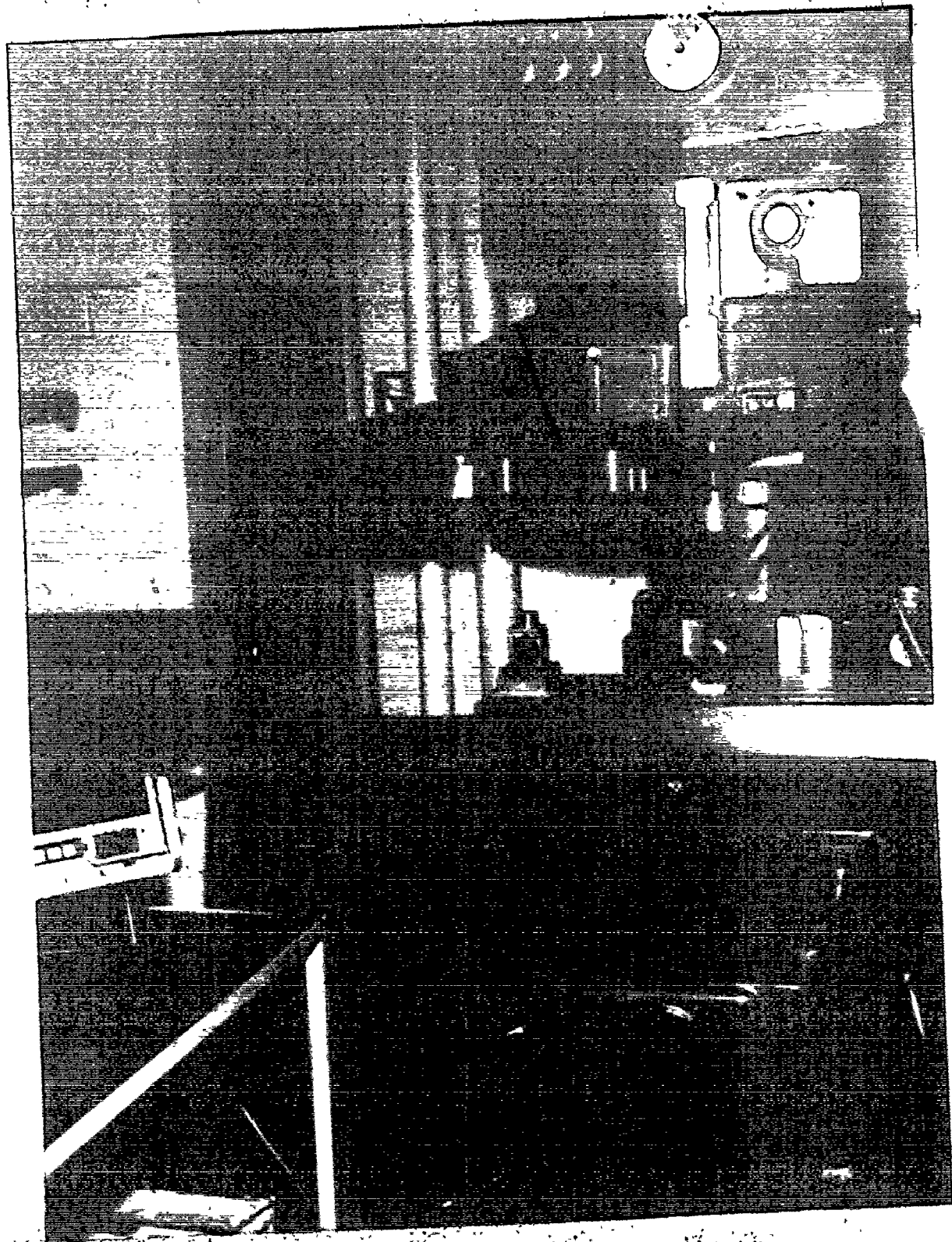
Plate IV   HOOG HYDRAPOINT 83-1000 NC
            MACHINING CENTER

specified for a case where we assume the use of tools of a fairly uniform length.

The case is in some respects similar to the two preceding ones: Heat generated in the headstock affects the errors associated with the Z motion and this effect is accounted for, in Figure 4.4c, by measuring drifts δ_x, δ_y and δ_z at the bottom and also drifts δ_x and δ_y at the top end of a mandrel clamped in the spindle.

In this machine, where feed drives are by means of hydraulic cylinders, the positional feedback is derived from a special gauging system inside the hydraulic cylinders. In this way, the hydraulic oil heated in the power supply affects all the error functions associated with both X and Y motions.

Having illustrated, for the various examples, the measurements to be repeated through a thermal cycle, it is now necessary to discuss and specify the form of the thermal cycle to be used in the tests and, further, how to evaluate the results. These two questions are dealt with in the following sections.

4.3 The Character of Thermal Deformations in Machine Tools

4.3.1 The Analysis of Thermal Deformations of a Simple Structure using a Spacewise lumped/ Timewise continuous approach

The background for the discussion in this section is

presented in the Appendix A, where calculations are given
of transient thermal fields and of transient thermal dis-
placements of a simple but typical structural system. The
diagram of the system is shown in Figure 4.5a and it con-
sists of a six inch long steel cylinder attached to. a 48
inch long cast iron housing with a wall thickness approx-
imately one inch and periphery P=48 inches.

At the root of the cylinder heat q is generated
equivalent to 0.5 hp. This may represent the energy loss
in the bearings of a rotating spindle. Both the housing
and the "spindle" are cooled on the outside by convection
to the surrounding air, though the convection coefficients
are chosen so as to correspond to very slow motion of the
air around the housing and to a fast motion of the air
around the (rotating) spindle.

The housing shown here is straight yet in reality
it could have various forms. The system however simplified
is analogous to a part of a typical machine structure.

It is a single-dimensional system because the tem-
perature variation along axis X only is considered and in
part 1 of Appendix A a calculation is presented justifying
the assumption of a uniform temperature distribution both
across the wall thickness and also across any section per-
pendicular to the X axis. In this way, temperature deform-
ations are considered also along the X axis only, and they

are represented by a translative elongation. This
corresponds to one basic form of temperature deformation
in machine tool structures, another form being where a non-
uniform temperature field causes bending of a part of the
structure such as for example, the column in the case of
Figure 4.5c which will be discussed later on. It will also
be shown later that both these fundamental modes of deform-
ations have common features.

In Appendix A it is shown that in these typical
cases, the internal resistance to heat flow is rather small
compared to that for convection of heat from the surfaces
of the bodies. Therefore, the temperature gradients in
these bodies are low and only a small number of "modes" are
necessary in order to describe the temperature fields with
good accuracy.

It is tempting therefore to try to treat these
bodies as consisting of a small number of lumped masses, for
while the exact solutions of Appendix A become very difficult
for even only slightly more complicated systems or boundary
conditions, it is not so for the lumped mass system where
the facilities of a computer may be utilised. Here we do
not apply the complete finite-difference or finite-element
technique, for the time variable is treated as continuous.
For those cases with constant boundary conditions, this would
seem to be an advantageous approach.

We shall compute the spindle-housing system as a whole and represent it by 11 discrete masses as shown in Figure 4.6. The spindle length of 0.5 feet is divided into four parts and the housing length of four feet into six parts, each part being centered in points one to eleven and extending half way to the neighbouring one. The masses at the ends of the spindle and the housing are half those in between, point five consisting therefore of a half-unit mass of the spindle and a half-unit mass of the housing. Within each mass temperature is assumed constant and each mass has a surface S_i and volume V_i and the masses M_i, M_{i+1} are interconnected by heat conducting channels with section areas $A_{i,i+1}$ and lengths $\ell_{i,i+1}$.

As in the classical solution of Appendix A, we solve both temperature fields and displacements by the super-imposition of the steady-state and transient solutions. There is a single geometric co-ordinate. It is discrete and is replaced by the number i of a point. T_i denotes the temperature of the individual points.

For steady-state, an energy balance on point i gives:

$$\sim \sum q_i - h\, S_i\, T_i = 0$$

expanding,

$$K_{i-1,i}\,(T_{i-1} - T_i) + K_{i,i+1}\,(T_{i+1} - T_i) - h\,S_i T_i = -q_{ex,i}$$

rearranging,

$$-K_{i-1,i}\, T_{i-1} + (hS_i + K_{i-1,i} + K_{i,i+1})\, T_i - K_{i,i+1}\, T_{i+1}$$

$$= q_{ex,i} \tag{4.1}$$

where $i = 1,2,3. \ldots 11$, $K_{i,i+1} = \dfrac{kA_{i,i+1}}{\ell_{i,i+1}}$

and $q_{ex,i}$ is the external heat input

Here,

$$A_{i,i+1} = A_a \text{ and } \ell_{i,i+1} = \ell_a \ , \ i = 1 \text{ to } 4,$$

or

$$A_{i,i+1} = A_b \text{ and } \ell_{i,i+1} = \ell_b \ , \ i = 5 \text{ to } 10,$$

and $q_{ex,i} = 0$ for all values of i except $i = 5$

Solving the steady-state case means solving the system (4.1) for the eleven values T_i. The system has the form:

$$\begin{bmatrix} hS_1 + K_{12}, & -K_{12} & , & 0 & , & \cdots & \cdot \\ -K_{12}, & hS_2 + K_{12} + K_{23}, & -K_{23} & , & \cdots & \cdot \\ 0, & -K_{23} & , & \cdots & \cdots \\ & & & & & \\ & & & & & \\ & & & & & \end{bmatrix} \cdot \begin{Bmatrix} T_1 \\ T_2 \\ T_3 \\ \cdot \\ \cdot \\ \cdot \\ T_{11} \end{Bmatrix}_{st} = \begin{Bmatrix} 0 \\ 0 \\ 0 \\ 0 \\ q_{ex,5} \\ 0 \end{Bmatrix}$$

$$\tag{4.2}$$

where the subscript st stands for steady-state.

For the transient case, we have

$$\sum q_i - hS_i T_i = \rho c_p V_i \frac{dT_i}{dt}$$

or,

$$C_i \frac{dT_i}{dt} = K_{i-1,i} T_{i-1} + (hS_i + K_{i-1,i} + K_{i,i+1}) T_i - K_{i,i+1} T_{i+1}$$

(4.3)

where $C_i = \rho c_p V_i$ (4.4)

For the cases of constant boundary conditions, it is

possible to assume the solution :

$$T_i = X_i e^{-\beta_i t}$$

(4.5)

Therefore, $\frac{dT_i}{dt} = -\beta_i T_i$

Inserting (4.5) into (4.3) and rearranging, we obtain

$$\beta \begin{Bmatrix} X_1 \\ X_2 \\ X_3 \\ \cdot \\ \cdot \\ \cdot \\ X_{11} \end{Bmatrix} = \begin{bmatrix} A_{11} & , & A_{12} & , & 0 & , & 0 & , & \cdots \\ A_{21} & , & A_{22} & , & A_{23} & , & 0 & , & \cdots \\ 0 & , & A_{32} & , & A_{33} & , & A_{34} & , & \cdots \end{bmatrix} \begin{Bmatrix} X_1 \\ X_2 \\ \cdot \\ \cdot \\ \cdot \\ X_{11} \end{Bmatrix}$$

(4.6)

The system (4.6) yields a characteristic equation solving

for eleven eigenvalues β_n and eleven eigenvectors X_{in},

these eigenvectors representing the "mode shapes" of temperature distribution on the individual masses.

Finally, we obtain,

$$
\begin{Bmatrix} T_1 \\ T_2 \\ T_3 \\ \cdot \\ \cdot \\ \cdot \\ T_{11} \end{Bmatrix}_{trans} = \sum_{n=1}^{11} a_n e^{-\beta_n t} \begin{Bmatrix} X_1 \\ X_2 \\ X_3 \\ \cdot \\ \cdot \\ \cdot \\ X_{11} \end{Bmatrix}_n \qquad (4.7)
$$

The coefficients a_n are obtained by means of the initial conditions equating the solution of (4.7) for $t=0$ to the solution of (4.2):

$$
[X_{in}] \{a_n\} = \{T_i\}_{st} \qquad (4.8)
$$

where $[X_{in}]$ is now a square matrix (11 x 11), the columns of which are the obtained eigenvectors X_{in}

To obtain the thermal deformations between points i and j it is necessary to sum the displacements $\Delta \ell_i$ obtained at each point, where

$$
\Delta \ell_i = \alpha_s T_i \; \frac{\ell_{i-1,i} + \ell_{i,i+1}}{2} \qquad (4.9)
$$

Therefore, we obtain the following expression:

$$\Delta_{ij} = \alpha_s \sum_{n=1}^{11} a_n e^{-\beta_n t} \left\{ \begin{matrix} X_i \\ \cdot \\ \cdot \\ \cdot \\ X_j \end{matrix} \right\}_n \left\{ \frac{\ell_{i,i+1}}{2}, \frac{\ell_{i,i+1} + \ell_{i+1,i+2}}{2} \cdots \frac{\ell_{j-1,j}}{2} \right\} \tag{4.10}$$

Solutions have been obtained using the following numerical values for the various parameters:

i	C_i	hS_i	$K_{i,i+1}$
1	0.3	0.25	21
2 to 4	0.6	0.5	21
5	9.6875	4.25	26
6 to 10	18.775	8	26
11	9.3815	4	26

The steady-state temperatures as calculated for the separated systems 1 to 5 and 5 to 11 are plotted for comparison with the exact solutions (as computed in Appendix A) in Figure 4.7. The variation of temperature of a number of points in the "housing" as computed from Appendix A is shown in Figure 4.8.

The time constants are compared below in TABLE I:

TABLE I

Time constants τ hours						
a) Housing						
Mode	0	1	2	3	4	5
System continuous	2.16	1.14	0.474	0.24	0.14	0.093
System lumped	2.35	1.26	0.55	0.31	0.22	0.18
b) Spindle						
Mode	0	1	2	3	4	5
System continuous	1.1	0.04	0.01	0.005	0.003	0.002
System lumped	1.2	0.06	0.04	0.01	0.008	

The whole system as regards eigenvalues β and eigenvectors X_{in} is shown in Figure 4.9.

In Figure 4.10 the variation of the temperature field with time is shown during the heating period at the beginning of which, the heat source q was switched on and maintained at a constant value. The temperature field consists of data computed for sections 1 to 11 distributed at regular distances of 0.125 inches for the spindle and 8 inches for the housing.

In Figure 4.11, the transient temperature field in the system is shown for the cooling-off phase following a

long (infinite) period of heating at the end of which a steady-state was reached and heat source q was switched off.

All these variations are, at every point, composed of variations in individual "modes" with various time constants as they are depicted in Figure 4.9.

These temperature variations produce thermal deformations between the various points of the system. In Figure 4.5a various parts of the system are selected and denoted A,B,C,D and E. The variations of these distances for both the heating-up and cooling-down periods are shown in Figure 4.12.

First of all, curves A and B show how the end points of the spindle and of the housing move with respect to the heating point 5. The directions on the graph are such that motion to the right from point 5 in the Figure 4.5a corresponds to the positive displacement in Figure 4.12. Curve E shows that the deformation of a section distant from the source is delayed in both the heating-up and cooling-down periods.

The sum of deformations A and B representing the variation of the distance between the end points 1 and 11 shows that this distance increases all the time of the heating-up period (with a rate decreasing with time) and it decreases all the time of the cooling-down period.

An arrangement could be imagined such that the relative displacement of two points would result from the difference of changes of two parts of the system. Such a case is depicted in Figure 4.5a1:

There, the distance between points 11 and 1 increases with the expansion of the distance C between points 6 and 11 and it decreases with the expansion of the distance D between points 1 and 6. Because the prevailing time constants in the part D are shorter than those in part C, the difference C-D which expresses variation of the distance between points 1 and 11 first decreases and then increases. This is shown by the broken line curve in Figure 4.12. In the cooling-down period, the distance first increases and then decreases.

The just described case illustrates some very basic characteristics of thermal deformations in machine tools. Our approach has been similar to that of McClure [30] who has stated, in a very general way, that basic feature which is expressed in the Appendix A by equation (A.38) for a very simple part, and in this section by equation (4.10) for the system of Figure 4.5a. It can be formulated as follows:

Assuming a particular structure with a particular configuration of cooling by heat conduction, the variation of a thermal deformation along a particular path (between two particular points) will be obtained as a sum of

particular exponential time functions, each of which being characterised by a time constant. Given a particular location of specific constant heat sources in the structure, each of the time functions is also characterised by an amplitude. The effect of several heat sources is obtained by superimposition of the effects of the individual heat sources.

Our contribution to this statement is in its detailed illustration for a simple typical case. McClure has also shown how the deformation of a structure can be modeled using model constants obtained from simple experiments.

An interesting contribution to the general picture of thermal deformation is presented in [31] and [32] where especially the effect of periodic off and on switching of a heat source is treated. In these same references, one practical example of a milling machine is described with measured deformation curves all of the variety as presented in Figure 4.12. In such a milling machine, depicted in Figure 4.5b, the vertical displacement of the spindle end above the table may have the form of our curve (ΔC-ΔD) in Figure 4.12, both for the reasons explained in relation to Figure 4.5al and as a result of the opposing influences of the expansion of the headstock, due to the heat generated in the spindle mounting 1, and of the expansion of the column,

due to the heat generated in the spindle drive gearbox 2.

4.3.2 The Finite Element Approach to the Analysis of Thermal Deformation of a Structure

A number of case histories that have shown curves similar to those in Figure 4.12 have been described in [5]. Among them is the case represented in Figure 4.5c. The heat generated in the headstock 1 of a horizontal boring machine will first produce the positive displacement of the spindle because the distance a from the spindle to the column grows. Later, the side of the column adjacent to the headstock will also warm. This produces bending of the column and the reversal of the displacement of the spindle into the negative direction. The effect of the hydraulic power source 2 located at the root of the column causes a different bending trend of the column which is opposed to the other bending motion.

In order to study more complex configurations of structures, the procedure of the preceding section suffers from the same drawbacks as the finite-difference method of solution, for the formulation of data is essentially identical, in that difficulties increase when either the arrangement of the nodes or the geometry is irregular. The finite-element method will simplify many of these problems.

Now, while in the finite-difference method approximations of derivatives are used to solve the problem, in the

finite-element method, the problem is put as an integral
to be minimised, and a numerical approximation of the
integral is used to obtain a solution.

Also, the starting point of the finite-element
method is the variational statement of the problem rather
than a governing differential equation.

a)   Temperature distribution in the steady-state problem

The variational statement for two-dimensional
steady-state problems, derived from the governing partial
differential equation and applicable boundary conditions
and the appropriate Euler-Lagrange equation is given by
equation (4.11). For guidance in the procedure, see [34].

$$I = \tfrac{1}{2} \iint_A [k(\tfrac{\partial t}{\partial x})^2 + k(\tfrac{\partial t}{\partial y})^2] \, dxdy - \iint_A g''' t \, dxdy + \tfrac{1}{2} \iint_A$$

$$h(t^2 - 2t_\infty t) \, dxdy + \tfrac{1}{2} \int_{B_h} h(t^2 - 2t_\infty t) ds - \iint_A q'' t \, dxdy - \int_{B_q} q'' t \, ds$$

$$(4.11)$$

Separating the integral into parts,

$$I = I_k - I_g + I_{h(A)} + I_{h(B)} - I_{q(A)} - I_{q(B)} \qquad (4.12)$$

where,

I_k (is associated with) conduction through the element area A

I_g "   heat generation within element area A

$I_{h(A)}$ "   heat convection out of element area A

$I_{h(B)}$ "   heat convection out of element

B

$I_{q(A)}$ (is associated with) heat input into element area A

$I_{q(B)}$ "   heat input into element boundary B

We assume a linear temperature distribution over the element and consequently, the temperature at any point is a linear function of the nodal temperatures. Later, for computing deformations we assume a constant temperature within the element which gives constant thermal strain which is used in determining the thermal nodal forces.

Equation (4.11) is an integral to be minimised which means minimising each term by formulating its derivative with respect to temperatures of nodal points and equating to zero.

Therefore, $\quad \dfrac{dI}{dt} = 0$ (4.13)

or,

$$\frac{dI_k}{dt} - \frac{dI_g}{dt} + \frac{dI_{h(A)}}{dt} + \frac{dI_{h(B)}}{dt} - \frac{dI_{q(A)}}{dt} - \frac{dI_{q(B)}}{dt} = 0 \quad (4.14)$$

Now, each of the terms of equation (4.14) is made up as a sum of terms corresponding to the terms of the individual elements.

$$\sum_{e=1}^{E} \frac{dI_k^{(e)}}{dt} - \sum_{e=1}^{E} \frac{dI_g^{(e)}}{dt} + \sum_{e=1}^{E} \frac{dI_{h(A)}^{(e)}}{dt} + \sum_{e=1}^{E} \frac{dI_{h(B)}^{(e)}}{dt} -$$

$$\sum_{e=1}^{E} \frac{dI_{q(A)}^{(e)}}{dt} - \sum_{e=1}^{E} \frac{dI_{q(B)}^{(e)}}{dt} = 0 \quad (4.15)$$

Denoting the nodes of element (e) by i,j,k, the various element integrals may be derived. For details of the procedure refer to Myers [34].

The generalised expressions, for application to structures whose continuum has been divided into varying sizes of triangular elements, are given by the following equations, (4.16) through (4.21)

$$\frac{dI_k^{(e)}}{dt} = \frac{k^{(e)}A^{(e)}}{(x_{ij}y_{jk}-x_{jk}y_{ij})^2}$$

$$\begin{bmatrix} (x_{jk}^2 + y_{jk}^2), & -(x_{ik}x_{jk} + y_{ik}y_{jk}), & (x_{ij}x_{jk} + y_{ij}y_{jk}) \\ & (x_{ik}^2 + y_{ik}^2), & -(x_{ij}x_{ik} + y_{ij}y_{ik}) \\ (Symmetric) & & (x_{ij}^2 + y_{ij}^2) \end{bmatrix} \cdot \begin{Bmatrix} t_i \\ t_j \\ t_k \end{Bmatrix} \quad (4.16)$$

where x_{mn}, y_{mn} denotes $(x_n - x_m)$ and $(y_n - y_m)$ respectively

and $\quad$ n = i,j,k

$\quad$ m = i,j,k

$$\frac{dI_g^{(e)}}{dt} = g^{'''(e)}\frac{A^{(e)}}{3} \begin{Bmatrix} 1 \\ 1 \\ 1 \end{Bmatrix} \quad (4.17)$$

$$\frac{dI_{h(A)}^{(e)}}{dt} = \frac{h^{(e)}A^{(e)}}{12} \begin{bmatrix} 2 & 1 & 1 \\ & 2 & 1 \\ (sym) & & 2 \end{bmatrix} \cdot \begin{Bmatrix} t_i \\ t_j \\ t_k \end{Bmatrix} \quad (4.18)$$

$$\frac{dI_{h(B)}^{(e)}}{dt} = \frac{h^{(e)}S_{mn}^{(e)}b^{(e)}}{6} \begin{bmatrix} 2 & 1 \\ (sym) & 2 \end{bmatrix} \cdot \begin{Bmatrix} t_m \\ t_n \end{Bmatrix} \quad (4.19)$$

where S_{mn} = the length of the element boundary connecting node points m and n,

b = element thickness

$$\frac{dI_{q(B)}^{(e)}}{dt} = \frac{q''^{(e)}S_{mn}^{(e)}b^{(e)}}{2} \cdot \begin{Bmatrix} 1 \\ 1 \end{Bmatrix} \quad (4.20)$$

$$\frac{dI_{q(A)}^{(e)}}{dt} = \frac{q''^{(e)}A^{(e)}}{3} \cdot \begin{Bmatrix} 1 \\ 1 \\ 1 \end{Bmatrix} \quad (4.21)$$

Noting the independence from temperature of equations (4.17), (4.20), (4.21) equation (4.15) may be rearranged as follows;

$$\sum_{e=1}^{E} \frac{dI_k^{(e)}}{dt} + \sum_{e=1}^{E} \frac{dI_{h(A)}^{(e)}}{dt} + \sum_{e=1}^{E} \frac{dI_{h(B)}^{(e)}}{dt} = \sum_{e=1}^{E} \frac{dI_g^{(e)}}{dt} +$$

$$\sum_{e=1}^{E} \frac{dI_{q(A)}^{(e)}}{dt} + \sum_{e=1}^{E} \frac{dI_{q(B)}^{(e)}}{dt} \quad (4.22)$$

or

$$[H] \ \{t\} \ = \ \{Q\} \qquad . \qquad (4.23)$$

where,   [H] is the overall thermal stiffness matrix

            {t} is the nodal temperature vector

            {Q} is the heat input/generation vector

The equation (4.23) may be solved by some appropriate technique to give the steady-state temperature distribution of the considered structure.

b)   <u>Temperature distribution in the non-steady state problem</u>

For the transient solution, the variational statement is the same as equation (4.11) but with the addition of one more term to the left hand side of the equation - that due to the heat capacity, given as;

$$I_c = \tfrac{1}{2} \iint\limits_{A} \rho c_p \frac{\partial(t^2)}{\partial \theta} \, dxdy \qquad \qquad (4.24)$$

where ρ = density

c_p = specific heat

t = temperature

θ = time

As in the previous approach,

$$\frac{dI_c}{dt} = \sum_{e=1}^{E} \frac{dI_c}{dt}^{(e)} \qquad (4.25)$$

where,

$$\frac{dI_c^{(e)}}{dt} = \frac{\rho^{(e)} c_p^{(e)} A^{(e)} b^{(e)}}{12} \begin{bmatrix} 2 & 1 & 1 \\ & 2 & 1 \\ (\text{Symmetric}) & & 2 \end{bmatrix} \cdot \begin{Bmatrix} \dot{t}_i \\ \dot{t}_j \\ \dot{t}_k \end{Bmatrix}$$

(4.26)

Summing over E elements and substituting in (4.23),

$$[H]\{t\} + [C]\{\dot{t}\} = \{Q\} \tag{4.27}$$

where $[C]$ is the thermal capacitance matrix.

Equation (4.27) may be solved using the Crank-Nicolson method:

Here, the solution is moved ahead in time by the relation

$$t^{(v+1)} = t^{(v)} + \frac{\Delta\theta}{2}(\dot{t}^{(v)} + \dot{t}^{(v+1)}) \tag{4.28}$$

where $\Delta\theta$ is the time increment between time (v) and time (v+1).

Premultiplying equation (4.28) by $[C]$,

$$[C]\{t\}^{(v+1)} = [C]\{t\}^{(v)} + \frac{\Delta\theta}{2}\left[[C]\{\dot{t}\}^{(v)} + [C]\{\dot{t}\}^{(v+1)}\right]$$

(4.29)

Substituting for $[C]$, from (4.27) into (4.29),

$$[C]\{t\}^{(v+1)} = [C]\{t\}^{(v)} + \frac{\Delta\theta}{2}\left[-[H]\{t\}^{(v)} - [H]\{t\}^{(v+1)} \right.$$
$$\left. +\{Q\}^{(v)} + \{Q\}^{(v+1)}\right] \tag{4.30}$$

rearranging,

$$\left[[\overset{v}{C}] + \frac{\Delta\theta}{2} [H] \right] \{t\}^{(v+1)} = \left[[C] - \frac{\Delta\theta}{2} [H] \right] \{t\}^{(v)}$$

$$+ \frac{\Delta\theta}{2} \{Q\}^{(v)} + \frac{\Delta\theta}{2} \{Q\}^{(v+1)} \qquad (4.31)$$

which may be reduced to

$$[\bar{H}] \{t_i\} = \{Q_i\} \qquad (4.32)$$

where $\quad \{t_i\} = \frac{1}{2} \{t\}^{(v+1)} + \frac{1}{2} \{t\}^{(v)}$

$$[\bar{H}] = [H] + \frac{2}{\Delta\theta} [C]$$

$$\{Q_i\} = \frac{1}{2} \{Q\}^{(v+1)} + \frac{1}{2} \{Q\} + \frac{2}{\Delta\theta} [C] \{t\}^{(v)}$$

c)   Calculation of Thermal Deformations

In the following, we follow closely the procedure of Zienkiewicz [35].

For displacements, we assume a linear distribution of displacement over the element, which means constant strain.

Therefore, we simplify the temperature field by assuming a constant average temperature over each and every element.

i.e. $\quad t_e = \dfrac{t_i^{(e)} + t_j^{(e)} + t_k^{(e)}}{3} \qquad (4.33)$

The thermal strain vector is given by equation (4.34)

$$\varepsilon_0 = \left\{ \begin{array}{c} \varepsilon_x \\ \varepsilon_y \\ \gamma_{xy} \end{array} \right\} \qquad (4.34)$$

For plane stress, the shear strain $\gamma_{xy} = 0$ and the thermal strain is then, for an isotropic material with linear coefficient of expansion α and subject to temperature rise t_e, given by equation (4.35)

$$\varepsilon_0^{(e)} = \alpha \left\{ \begin{array}{c} t_e \\ t_e \\ 0 \end{array} \right\} = \frac{\alpha}{3} \left\{ \begin{array}{c} t_i + t_j + t_k \\ t_i + t_j + t_k \\ 0 \end{array} \right\} \qquad (4.35)$$

The stress in the element is given by equation (4.36)

$$\sigma^{(e)} = \left\{ \begin{array}{c} \sigma_x \\ \sigma_y \\ \tau_{xy} \end{array} \right\} = [D] \; \varepsilon_0^{(e)} \qquad (4.36)$$

where [D] is the stress-strain matrix for a plane stress case and an isotropic material given by

$$[D] = \frac{E}{1-\nu^2} \left[\begin{array}{ccc} 1 & \nu & 0 \\ \nu & 1 & 0 \\ 0 & 0 & \dfrac{1-\nu}{2} \end{array} \right] \qquad (4.37)$$

From (4.36), the nodal forces are obtained from

$$\{f\}^{(e)} = [B]^T \sigma^{(e)} b \; A^{(e)} \qquad (4.38)$$

where,

$$[B] = \frac{1}{2A} \begin{bmatrix} y_{kj} & 0 & y_{ik} & 0 & y_{ji} & 0 \\ 0 & x_{jk} & 0 & x_{ki} & 0 & x_{ij} \\ x_{jk} & y_{kj} & x_{ki} & y_{ik} & x_{ij} & y_{ji} \end{bmatrix}$$

(4.39)

and, as before, y_{kj} denotes $(y_j - y_k)$ etc.
The element stiffness matrix is

$$[k]^{(e)} = [B]^T [D] [B] b A^{(e)} \qquad (4.40)$$

The overall nodal forces and stiffness matrices of the whole system, $\{F\}$ and $[K]$, are obtained by assembling the above element force and stiffness matrices to give,

$$[K] \{\delta\} = \{F\} \qquad (4.41)$$

where

$$\delta_i = \begin{Bmatrix} \delta_{x_i} \\ \delta_{y_i} \end{Bmatrix}, \quad F_i = \begin{Bmatrix} F_{x_i} \\ F_{y_i} \end{Bmatrix}$$

Equation (4.41) is solved to give the thermal deformations arising as a consequence of the temperature distribution calculated from the previous sections. A computer program was developed, using the finite-element theory and procedure as outlined previously, to calculate the steady-state and transient temperature fields in two-dimensional structures and the resulting thermal deformations. The program has built-in provision for the presence of various common

boundary conditions: heat input to the face or edge of an element, convection cooling from the face or edge of an element, as well as the provision for geometric boundary constraints.

The theoretical formulation and computer program were verified by the standard technique of comparison of computed results with the results calculated from an exact solution for a selected problem. Also of importance in the transient solution is the relation between the length of the chosen time step and the accuracy of the computed results in relation to the results from the exact solution. This investigation, together with the comparison of steady-state and transient temperature solutions with the exact solution is detailed in Appendix B.

The program listing itself, together with flow-charts of the various subroutines involved and instructions for use etc., is given in Appendix C.

Now let us return to the case of interest, that of the general structural configuration of the machine as shown in Figure 4.5c.

Having chosen some specific dimensions for the horizontal boring machine as depicted in Figure 4.13, the problem remains as how to create a two-dimensional model of the structure representative of the three-dimensional machine.

While it is possible to "unfold" the structure for the analysis of temperature fields, it would not be possible to obtain the thermal deformation.

Therefore it is necessary to analyse the structure as in the two-dimensional representative section of the machine, Figure 4.14. In order to ensure that the thermal capacity of the model is identical to that of the three-dimensional model, when the continuum of the structure is divided into the finite-elements there are two basic types of element:

1)   the "face" element - this has a double wall thickness to allow for the front and rear walls of the column or headstock

2)   the "edge" element - an element of width equal to the thickness of the wall but of a "thickness" equivalent to the total length of the side wall.

For the calculation, the following parameters were chosen: the coefficient of conduction $k = 30$ Btu/hr.ft.$^\circ$F; the coefficients of convection, $h_1 = 3.2$ Btu/hr.ft.$^{2\circ}$F (outside wall), $h_2 = 0.5$ Btu/hr.ft.$^{2\circ}$F (inside wall); density $\rho = 450$ lb$_m$/ft^3; specific heat $c_p = 0.1$ Btu/lb$_m$ $^\circ$F; Poisson's ratio $\nu = 0.25$; coefficient of expansion $\alpha = 6.5$ ppm/$^\circ$F; modulus of elasticity $= 30.0 \times 10^6$ lbs/in^2.

The displacements, in the x and y co-ordinate direction, of the point O, Figure 4.14, which corresponds to

the position of the spindle axis, were computed for the
presence of two different combinations of heat source
locations:

A   (i)   0.75 hp (1908.36 Btu/hr.)- distributed on the
inside walls of the headstock, corresponding
to the influence of the presence of a
lubricating oil sump in the headstock and the
splashing of heated oil on the walls.

     (ii)   1.0 hp (2544.48 Btu/hr.)- at the location of the
spindle bearings, heat being generated here
proportional to the rotating speed of the
spindle.

B   (i)   0.75 hp on the inside walls of the headstock

     (ii)   1 hp at the location of the spindle bearing,
and additionaly,

     (iii)   0.75 hp at the rear of the column and corres-
ponding to the heat generated for example in
a hydraulic power source.

The transient deviations δ_x and δ_y of the point O are plotted
in Figures 4.15, 4.16 for the separate cases A and B. Let
us look at these contrasting situations as regards the effect
of the presence or non-presence of the heat source at the
rear of the column.

In Figure 4.15 (case A) the spindle moves quite
quickly in the positive x direction due mainly to the heat

generated in the spindle bearing. The deviation δ_y in the positive y direction due to the heat generated in the headstock warming the adjacent wall of the column proceeds at a slower rate.

In Figure 4.16 (case B), the effect of the heat source at the rear of the column is seen to be very significant, the deviation δ_x being pronounced due to the bending of the column. The accompanying smaller deviation δ_y in the negative y direction gradually decreases however due to the partially compensating growth of the column wall adjacent to the headstock.

While not as pronounced an effect as in the curves of Figure 4.12, the δ_y deviation of Figure 4.16 shows similar characteristics.

4.4   Rules for Choice of Thermal Test Cycle

Let us now summarize those features of the described phenomena which are relevant for our problem of specifying the thermal test cycle.

a)   In distinction of the effects of the offset in the working zone, or to the weight and clamping effects as they have both been discussed in Chapter 3.9, the thermal effects depend on two parameters: the intensity of the heat source and the time.

The former of these parameters may be a complex one because more than one source could be acting simultaneously.

However, let us first consider those cases only where, apart from constant heat sources, there is only one variable source or where there are two variable sources, the effects of which are separated. This situation has been described, in relation to Figure 4.2, 4.3, 4.4, in section 4.2.

b) The effect of time on any error is such that the error increases or decreases continuously during heating-up and cooling-down respectively - or this variation is reversed after a certain initial period, see Figure 4.12.

c) The effect of a heat source increases with the intensity of this source. For an intermittent source, the average intensity increases with the increase in the ratio of on-time to off-time (provided the periods of change are shorter than the primary time constants of the system).

From these statements, the following conclusions may be drawn:

1) Every error constituent of the whole accuracy formulation (see section 4.2) must be measured over a time period long enough to enable the achievement of a sufficient steady-state or the usual working period whichever is the shorter. The whole range of the error constituent deviation must be established.

2) The effect of every variable heat source should

be tested with two extreme intensities of this source and with the constant sources acting simultaneously. The two extreme intensities of the variable heat source are; source on at a specified maximum intensity, source off. If the range of the error in both these extreme situations satisfies the required tolerance it will be satisfied also during any intermediate action of that source.

3) Summarizing: The test should first be done with all the constant heat sources only and, for the second time with also the variable source running at a specified maximum intensity. The latter test must be done during both the heating-on and the cooling-off periods i.e. as regards to the variable source.

The only measurements to be made are those which may be affected and, if a single error function may be affected by two heat sources, the relevant tests must be made under the extreme combination of these sources.

4.5   Evaluating the Thermally Affected Errors - examples

The tolerance rule as formulated in Chapter 3 is applicable to the evaluation of any of the prescribed error functions - components of the total accuracy check.

Figure 3.13 represents the general form of the re- sult of the measurement of any error function $\delta_m(n)$. The error function has a certain range (the shaded field) due

to dead zone and scatter. This range may be further extended by weight effects or by thermal effects, the whole range of the error function necessarily fitting into the tolerance template TT.

The range of the error function as obtained during the thermal test is determined by the field between the extreme curves of the error function concerned as they have been obtained through both the time and the intensity of the heat source extremes of the thermal test.

There is however, one provision which may reduce the range of the error. In the evaluation, the possibility of "zero-shift" of the co-ordinate system has to be admitted.

Let us now describe some examples, the sample only representing a small selection of many measurements performed. They have not in fact been carried out in strict accord with the recommendations of section 4.4 since these evolved only after the computational studies and measurement program. However the examples serve to illustrate well the evaluation technique.

a) The first example is given in Figure 4.17 and it concerns a particular measurement performed on the machine depicted in Figure 4.3. In the test, the limitation to low workpieces was not applied and therefore error functions $\delta_x(z)$, $\delta_y(z)$ and $\delta_z(z)$ have been measured as well. For the thermal

test, the simplified approach was chosen analogous to
that explained in relation to Figure 4.2c. Displace-
ments δ_x and δ_y were read periodically during the thermal
cycle at both the top and bottom ends of a mandrel in the
spindle. The thermal cycle was an extreme one, all con-
stant heat sources on, plus an extended run of the spindle
at 1800 rpm. Measurements were taken every 30 minutes for
a total period of 6 hours of heating, none however being
taken during the cooling-down period (spindle off, all con-
stant heat sources on) which does not comply with our
present recommendation. Making an allowance for zero-
shift after every two hours, the corresponding tolerance
templates, which include the worst 2 hour (i.e. measuring
intervals) error ranges, are drawn onto the $\delta_x(z)$ and $\delta_y(z)$
fields.

The parameters of the δ_{xz} and δ_{yz} tolerance template
and the values of their respective constants, A_{xz} and K_{xz}
and A_{yz} and K_{yz} are:

1) δ_{xz}

$$\left| \delta_{x_2} - \delta_{x_1} \right| \leq 0.001 \text{ in.} + 0.0008 \text{ in.}/12 \text{ in.} \left| z_2 - z_1 \right|$$

2) δ_{yz}

$$\left| \delta_{y_2} - \delta_{y_1} \right| \leq 0.001 \text{ in.} + 0.0015 \text{ in.}/12 \text{ in.} \left| z_2 - z_1 \right|$$

b)   The second example is the diagram of the position-
ing error $\delta_z(z)$, Figure 4.18, as obtained during a very
severe cycle of continuous rapid traverse (50 in./min.)
of the head (in its Z motion) of the machine depicted in
Figure 4.3. The duration of the test was $3\frac{1}{2}$ hours and on
Figure 4.18 the individual graphs 1 to 8 are records from
the laser interferometer taken every 30 min.

The heat source effective here is the heat gener-
ated between the ball screw and nut and the effect in the
elongation of the leadscrew to which the feedback resolver is
attached.

Again, to be strictly correct, the records should
have been taken after having stopped this motion, but the
machine hydraulic system overheated and shut off near to the
completion of this test. However, probably the same great
change as took place in the first 30 min. would have been
obtained in reverse.

It is observed that in this case, the effect consists,
for the most part, mainly of a zero drift and could be
eliminated in fact by the introduction of a zero-shift. If
a zero-shift is permitted every hour and no warm-up period
is specified, the tolerance template (for unidirectional
positioning) as shown has to be accepted.

$$\left|\delta_{z_2} - \delta_{z_1}\right| \leqslant 0.0006 \text{ in.} + 0.0025 \text{ in.}/12 \text{ in.} \left|z_2 - z_1\right|$$

The specification of the template parameters on a basis of unidirectional positioning corresponds to final position being made always in the downwards direction.)

c) The next example, Figure 4.19, concerns a simplified error concept for the machine depicted in Figure 4.4 and the measurement of "spindle-growth" with respect to the table.

In this case, the whole error function is replaced by a single value δ_z corresponding to the top position of the Z co-ordinate. Correspondingly, instead of a tolerance template δ_{zz}, the constant A_{zz} only is evaluated:

$$A_{zz_a} = 0.0003 \text{ in.}, \quad A_{zz_b} = 0.0005 \text{ in.}, \quad A_{zz_c} = 0.0008 \text{ in.}$$

The test was done by continuously running the spindle at three different speeds subsequently in one hour periods and a continuous record of the deviation δ_z was obtained. A portion of the cooling-down period is shown and it is seen that no such occurrence of the effect of "overshoot" as in curve ΔC-ΔD of Figure 4.12 happens. Thus, there is no real necessity for showing the whole cooling-off period.

d) The final example concerns the positioning error function $\delta_x(x)$ again for the machine of Figure 4.4. As mentioned previously, this machine uses a system of hydraulic

gauges for the derivation of its position feedback signal and these, being mounted on the feed driving hydraulic cylinder, are rather affected by the temperature of the oil. The diagram shown in Figure 4.20 is the record of the positioning error as recorded from a laser interferometer repeatedly in intervals of 15 mins up to curve 9 and then in 30 min. intervals. It may be observed that the variation of the error with the position x preserves its character while the actual distance positioned increases almost uniformly over the whole travel length.

In this case, it is difficult to decide whether or not the first two readings should be disregarded and a half-hour warm-up period permitted. In order to answer this problem correctly, it would have been necessary to interrupt the cycle and observe how the beginning of the variable heat source cooling-down period appeared.

The extreme heating cycle consisted here of continuously moving the slide with a slow feed. It may be assumed that stopping the feed should not start a sudden reverse of the drift with a rate similar to the beginning of the heat-on period.

The usual fast initial reversals of thermal deformations following the shut-off of the heat source makes it impractical to allow for warm-up periods concerning variable heat sources. This is different for the effect of a constant

heat source which is probably the present case. Therefore, in evaluating, we disregard the range between curves 1 and 3 and, assuming a one-hour period for zero-shifting, we obtain the value A_{xx} for the applicable tolerance template from the distance between curves 3 and 6 and the slope K_{xx} from the curve 12 of Figure 4 therefore,

$$\left| \delta_{x_2} - \delta_{x_1} \right| \leq 0.003 \text{ in.} + 0.005 \text{ in.}/12 \text{ in} \left| x_2 - x_1 \right|$$

CHAPTER 5

SPINDLE ROTATION ACCURACY

5.1   Reasons for New Methods of Testing

The standard technique for measuring radial run-
out of a spindle is to use a dial gauge sensing the peri-
phery of a spindle associated reference surface (e.g. the
spindle flange, or a mandrel held in the spindle) while
the spindle is rotated slowly, usually by hand. This pro-
cedure is depicted in Figure 5.1a.

There are however a number of disadvantages asso-
ciated with this classic technique:

1)   A purely eccentric motion of the reference
surface (e.g. a mandrel) does not represent an error of
rotation since it has no harmful effect. Actually a great
part of the gauge reading is due to the eccentricity of
the rotating master part.

2)   The test can only be performed while the
spindle is rotated slowly while in fact, the result may
differ at working speeds.

3)   The slow components of spindle rotation error
(i.e. low harmonic components) are not distinguished from
the fast components (i.e. higher harmonics) although the

two have different significances for the machined surface.

4) No record is obtained.

5) It is not possible to analyse the source of the error.

While all the other points will become clear after the advantages of the new techniques have been detailed, let us clarify the meaning of point 1) above.

One of the main objections to the method is that the method will read an "eccentricity" of motion of the mandrel and, irrespective of how this is caused (e.g. eccentric bearing ring, taper in spindle, etc.), eccentricity (simultaneous harmonic motion in two mutually perpendicular directions with 90° phase shift), or even a harmonic motion along a straight line in the case of a rotating workpiece, will not affect the roundness of a machined surface.

Actually, pure eccentricity does not represent an error of spindle rotation at all.

Thus, truly, the problem of the method is therefore that it does not give a true indication of how out-of-round the machined surface will be.

In fact, in relation to Figure 5.1b we may see how the classic test of total indicator reading (TIR) senses twice the magnitude of the eccentricity of the reference surface. Suppose now that the cone of spindle is eccentric to the axis of spindle rotation O because of the eccentricity

of the race of the inner ring of the roller bearing with respect to its bore. Assume also that the spindle rotation is perfect i.e. axis O does not move, then the motion of the center of the rotating mandrel will trace a circular arc c with an eccentricity e to the axis of rotation O. Therefore the center of the mandrel will pass through points 1 and 2 corresponding to the two extreme positions of the surface of the mandrel, M_1 and M_2, in relation to the sensing gauge. The T.I.R. reading will indicate 2e.

It has been stated that in fact eccentricity has no influence on the error of circularity of the workpiece. This is clarified in relation to Figures 5.1c, d.

In Figure 5.1c a boring bar located in a machine spindle nose is eccentric by e to the axis O of the spindle. The tool will rotate about the point O producing an exactly round bored hole, the only effect of the eccentricity being that the radius of the tool path R_1 will be slightly different from the radius R preset in the tool as the required hole radius. The difference $(R_1 - R)$ will depend on the angular position of the tool with respect to the direction of the eccentricity (both rotating together) and the maximum value will equal e. The influence of this however will not be detected since the tool setting anyway will be altered for small corrections to the hole diameter.

In Figure 5.1d, the effect of eccentricity of the workpiece in turning is examined. Here, the tool point is fixed with respect to the axis of spindle rotation 0. Therefore, since the horizontal distance r between the tool point and the axis 0 does not vary during the rotation of the spindle a perfectly circular workpiece will be produced of diameter D.

The only error that might occur in the diameter D is one of eccentricity with reference surface D_{ref}, which is held in the chuck having been machined in a previous operation, the center of which rotates with an eccentricity e to the axis of rotation 0.

However, if concentricity of the two diameters D_1 and D_{ref} was desired, they would have been machined in the same workpiece setting.

It is also conceivable that in measuring the radial run-out on the outer surface of a spindle flange nothing is revealed about the spindle rotation error. This occurrence is depicted in Figure 5.1e. Suppose the spindle axis moves in an ellipse, denoted 1, and that the spindle flange has been ground using the grinding wheel GW after the spindle mounting has been assembled. Now, the periphery of the flange will have accepted the shape 2 and, if a gauge replaces the grinding wheel GW, no run-out will be indicated.

There is an existing correct method for evaluating spindle rotation accuracy and that is in the direct (i.e. machining) test where departures from roundness of sample workpieces may be evaluated using a roundness measuring instrument e.g. a Talyrond.

The direct test though suffers from the usual disadvantages associated with machining tests in that the results are influenced by the cutting process and, the procedure is time and cost demanding. Also, a number of other influences may interfere, e.g. clamping deformations, tool wear and vibrations, all of which combine to make separation of the spindle rotation errors difficult.

Finally, let us compare quantitatively (on a basis of ISO IT tolerance classes) the best accuracy specifications for machine tool spindles radial run-out with the tolerance classes quoted by manufacturers for high precision roller bearings:

The IT class of accuracy of a rotational surface is a result of an absolute value of spindle run-out and of the size of the workpiece diameter. Now, the best machine tool specifications limit the radial run-out to between 0.0002 in. and 0.0004 in. and, if this should mean out-of-roundness of the workpiece, then without any error at all in setting the dimension, the error of form alone gives nothing better than, for example IT4 to IT6 for a diameter of 0.5 ins. and

IT3 to IT5 on a 2.5 in. diameter.

However, considering the best tolerance classes for high precision bearings of various manufacturers, Figure 5.2, based on the radial run-out of the inner ring, or the TIR reading of the movement of the stationary outer ring of the assembled bearing if the inner ring rotates, then it may be observed that the best guaranteed accuracies give less than 2μm (0.00008 in.) radial run-out <u>for all sizes of bearings practically used in machine tools.</u>

Of course, the accuracy of rotation of a spindle depends not only on the accuracy of the bearing but also on the accuracy of the bearing seatings. These seatings however are often finished by lapping and cylindricities in the order of microinches are commonly achieved. Further, these tolerances are maximum values while better <u>average</u> values will be obtained, and they include the effect of eccentricity which, from our assessment, does not affect cylindricity of a machined surface.

It could be reasonably assumed then that accuracies in the order of 1μm (0.00004 in.) can be readily obtained which gives ITO/ITO1 accuracy class for the large range of diameters of Figure 5.2. Therefore, despite great progress in the development of high precision spindle mountings, the standard machine tool test specification cannot reflect. this because of the inadequacy of the test methods. In

other words, mostly because run-outs apply in a different way than in the current test methods, roundness errors may in fact be expected to be better than the run-outs specified. For certain classes of machine tools and operations e.g. jig-boring, fine turning etc., a high accuracy of spindle rotation is essential and, since the classic methods are inadequate, it has been necessary to develop new techniques where high frequency response transducers and oscilloscopes are used enabling the correct measurement of errors associated with axes of rotation.

5.2 Definition of Errors of Spindle Rotation

The accuracy of spindle rotation is a very important aspect of machine tool performance applicable to all machine tools and not only N.C. machines. · The concept has been completely reformulated and an entirely new concept has been developed due to the contributions over the past fifteen years e.g. [36] [37],[38]. Also, in a draft of a new "Axes of Rotation" standard [39] precise statements defining an axis of rotation and the errors associated with an axis of rotation are given, together with recommended testing and evaluation procedures.

Let us review the popular concept of an axis of rotation, for example of a machine tool spindle. In this case, a line is assumed and proclaimed to be the axis of rotation. This line in the ideal case remains stationary

during spindle rotation so that all points connected to

the spindle would move around the axis in perfect circles.

However, in reality, the axis of rotation moves with respect

to an axis average line passing through the mean position

of the axis of rotation.

Let us formulate an exact definition relating to

radial error motion and consider a plane perpendicular to

the axis of the spindle. The movement of a point on the

spindle could be assumed to be a sum of component motions

with individual frequencies f_i, each of them being the i-th

multiple of the frequency of spindle rotation $f_1 = \frac{\omega}{2\pi}$ where

ω is the angular spindle speed.

$$\text{i.e.} \quad f_i = i\, f_1$$

Each such component could be further considered to

give rise to an elliptical motion i.e. a general harmonic

motion in a plane. An outstanding significance is the first

harmonic component i=1, which may be represented by an

ellipse through which the point repeats its path once per

revolution of the spindle, see Figure 5.3 a. This elliptical

motion may be resolved into a circular motion with radius b

and a harmonic rectilinear motion in the direction of the

major axis of the original ellipse, and with an amplitude

A=a-b, see Figure 5.3b. The center of this circular motion

determines in the chosen plane the axis of rotation Q. In

this way, the axis of rotation performs in the first har-

monic only a rectilinear harmonic motion as shown in Figure 5.3c. In all other harmonics, it moves along ellipses. This is the definition of the axis of rotation.

Consider in conclusion therefore, the general case of harmonic motion in an (X,Y) plane

$$x = \sum_{i=1}^{\infty} X_i \sin (i\omega t + \phi_i)$$

$$y = \sum_{i=1}^{\infty} Y_i \sin (i\omega t + \phi_i)$$

(5.1)

Taking only the first harmonic component, then,

$$x = X_1 \sin \omega t$$

(5.2)

$$y = Y_1 \sin (\omega t + \phi_1)$$

Now $\quad y = Y_1 (\cos \phi_1 \sin \omega t + \sin \phi_1 \cos \omega t)$

$$= Y_1 \cos \phi_1 \sin \omega t + Y_1 \sin \phi_1 \cos \omega t$$

$$= \qquad A_y \qquad + \qquad B_y \qquad (5.3)$$

We may express x as,

$$x = Y_1 \sin \phi_1 \sin \omega t + (X_1 - Y_1 \sin \phi_1) \sin \omega t$$

$$= \qquad A_x \qquad + \qquad B_x \qquad (5.4)$$

If we combine A_x and B_y we obtain a circle and, on combining the remaining two components B_x and A_y, noting that

they are in phase, it is seen that they represent a harmonic motion along a straight line. This leads to the definition of an axis of rotation.

The basic types of error motion may be identified if the relative motion of a line segment of the axis of rotation which is embedded in the workpiece is considered with respect to a line segment of the axis average line which is fixed in relation to the tool, Figure 5.4a.

Figure 5.4b shows the six degrees of freedom, at any given time t, between the axis of rotation and the axis average line, and these comprise of three linear and three angular motions, the last of which θ(t) being the spindle rotation of which the other motions are a function.

Which of the other five motions contributes significantly to the error motion depends on:

1) the direction of greatest sensitivity to the error motion i.e. the sensitive direction, which may be defined as the line perpendicular to the ideal generated surface passing through the instantaneous point of machining, and,

2) the axial and radial location of the gauge and tool at the point of machining.

On examination of machining operations it may be realised that two basic situations arise corresponding to the concepts of rotating and non-rotating sensitive directions.

In accord with these basic principles, the individual components of spindle rotation errors are illustrated in Figure 5.5, the first one, Figure 5.5a, relating to the concept of errors for the case where the tool rotates with respect to the work holding surface e.g. as in boring, and the other, Figure 5.5b, to the concept of errors for the case of the fixed tool and rotating workpiece e.g. as in turning. Figures 5.5a, 5.5b refer then respectively to the situation of rotating and non-rotating sensitive directions as defined above.

Three basic or primary error motions may be identified and these are <u>axial</u>, <u>angular</u> and <u>pure radial</u> error motions. Two secondary motions also exist being formed by the combination of primary ones; <u>face motion</u>, which is a consequence of the combination of axial and angular motions and, <u>radial motion</u>, which is a combination of pure radial and angular motions.

It should be appreciated, because of its conformity to machining conditions, that for a real axis of rotation, the term error motion refers to relative displacements, in the sensitive direction, between the tool or gauge and the workpiece. The total error motion is therefore a sum of spindle rotation errors, relative between the spindle and spindle housing, and structural error motions between the spindle housing and the tool. The cause of the former error

motion may be for example due to non-round bearing components, while the latter might be due to the influence of drive motors or gears.

If the separation of the two error motions is possible, it will facilitate the analysis of the source of the contributory factors to the overall axis of rotation error.

5.3 Significant Attempts in Devising New Methods of Measuring Radial Error Motions

The common feature of all of the following methods is that they all result in a polar record, the significance of which is exactly the same as a Talyrondgram which would be obtained from the surface of a machined specimen workpiece, but unaffected by the disturbing influence of the cutting process. In this way, an exact picture of the influence of errors of spindle rotation on the accuracy of the workpiece may be obtained by an idle-run test and without machining.

The test methods must be arranged so as to correctly represent the errors as machined into the workpiece. Figures 5.6 and 5.7 show, for the separate cases of boring and turning respectively the error actually machined into a workpiece surface at an instant in time. Also shown are the error sensing transducers appropriate to the separate

applications and error components as measured in the various test methods, these being the basis for the derived system theory for each of the described methods that follow:

N.B. Pure radial motion (motion X(t) in Figure 5.4b) may be defined as an error motion where the axis of rotation remains parallel with the axis average line and moves perpendicular to it in a sensitive direction. However, in fact, no attempt is made to measure pure radial motion since it is only used as a concept in conjunction with angular motion to explain the deterioration of radial motion with distance from the main spindle bearing.

In this review the measurement of spindle rotation accuracy will be concerned only with the measurement of radial error motion.

5.3.1 Basic method for boring (i.e. rotating sensitive directions

The pioneering work in the introduction of a new approach to measuring axis of rotation errors took place twenty years ago in Czechoslovakia [36]. The diagram of the experimental set up is shown in Figure 5.8 and its main feature is in the use of an oscilloscope, from the screen of which a photograph is taken of a polar record representing the radial motion of the spindle axis. The generation of the polar record comes from the output voltages, taken to the X and Y plates of the oscilloscope, of two electronic

displacement transducers located at right angles to each
other sensing the circular motion of a highly precise
"master" ball fixed in the machine spindle at some small
eccentricity.

The transducers may be either the non-contacting
type (e.g. capacitative) or contacting type (e.g. linear
differential transformers). In the case of the latter,
usually thin steel strips are fixed so as to slide on the
ball and guide also the shafts of the pick-ups.

Supposing the rotation of the spindle axis is per-
fect, a perfect circle will be traced on the oscilloscope
screen generated by the end point of a rotating vector
created by the sine and cosine signals formed by sensing
the 90° separated components of the radial motion of the
ball. The end point of the vector is shown as a bright
spot which will describe the circumference of the circle
and it will rotate in synchronism with the spindle.

However, the motion of the ball will be affected by
the radial error motions of the spindle itself and these
motions will be superimposed on the perfect circle. The
obtained trace on the oscilloscope screen is entirely
analogous to the well-known Talyrondgram "suppressed zero"
form of trace where, if the trace is compared to the work-
piece, the errors of the machined surface are much more

magnified than the diameter of the workpiece.

<u>System Theory</u> – <u>basic method for boring</u> (Refer to Figure 5.6)

let e = the offset of the master ball

U = the displacement of the axis O from its center position

The spindle rotates at speed ω and at time t, the reference direction is at an angle ϕ to the X axis. The offset direction is at an angle β to this reference direction.

Error components sensed by the pick-ups:

Component in X due to the offset of the test sphere =

$$e \cos (\phi + \beta)$$

Components in Y due to the offset of the test sphere =

$$e \sin (\phi + \beta)$$

Component in X due to the displacement U of the axis =

$$U \cos \alpha$$

Component in Y due to the displacement U of the axis =

$$U \sin \alpha$$

Therefore, the total signal on the X plates of the oscilloscope is

$$e \cos (\phi + \beta) + U \cos \alpha \qquad (5.5)$$

and the total signal on the Y plates is,

$$e \sin (\phi + \beta) + U \sin \alpha \qquad (5.6)$$

The reference circle generating components are the

terms e cos (ϕ + β) and e sin (ϕ + β) and the projections

of the error motion are correctly added as U cos α and

U sin α respectively.

However, for this basic two pick-up method, the

polar trace obtained is only valid for a path traced out

by a tool, the angular position of which, with respect to the

spindle, corresponds to the offset direction of the spherical

master, i.e. β=0.

If this is not the case or if, for example, the

best orientation of the tool is required to be determined,

then the offset of the spherical master has to be readjusted

accurately for each possible orientation of the tool. This

is a difficult operation.

5.3.2 Modified method for boring

For situations where a detailed analysis is required
[41]
Vanek has proposed the technique shown in Figure 5.9 where

the offset of the spherical master is not used to generate

the base circle on which the errors are superimposed. Here

in fact, the eccentricity of the ball should be minimised.

In this modified technique, again requiring a spindle

rotation synchronised base circle, he has employed a synchro

resolver the rotor winding of which is attached to the

rotating spindle. A constant level carrier frequency volt-

age is fed to the rotor as well as to the L.V.D.T. type

pick-ups used. The output signals of the two 90°- separated

stator windings, consisting of the carrier frequency voltage
level modulated by the sine and cosine of the angle of
spindle rotation, are demodulated and fed through summing
amplifiers to the X and Y plates of the oscilloscope, thus
generating the required base circle on which the error
motion is to be superimposed. The demodulated output of
the two pick-ups represent the horizontal and vertical
components of this error motion and these are added to the
base circle generating signals at the previously mentioned
summing amplifiers.

System Theory - modified method for boring (refer to Figure 5.6)

    let e = the residual eccentricity of the master ball

    U = the displacement of the axis O from its center position

    B = the constant amplitude of the carrier
frequency voltage signal supplied to the rotor of the synchro resolver.

The spindle rotates at speed ω and at time t, the reference
direction is at an angle ϕ to the X axis. The eccentric
offset of the master ball is at an angle β to this reference
direction.

Components sensed by the pick-ups:

Component in X due to the eccentricity of the master ball =

$$e \cos (\phi + \beta)$$

Component in Y due to the eccentricity of the master ball =

$$e \sin (\phi + \beta)$$

Component in X due to the displacement U of the axis =

$$U \cos \alpha$$

Component in Y due to the displacement U of the axis =

$$U \sin \alpha$$

The (demodulated) signals from the synchro resolver are:

$$B \cos \phi \text{ (to the X plates of the oscilloscope)}$$

$$B \sin \phi \text{ (" " Y " " " ")}$$

The total signal on the X plates of the oscilloscope is

$$B \cos \phi + e \cos (\phi + \beta) + U \cos \alpha \tag{5.7}$$

and the total signal on the Y plates of the oscilloscope is,

$$B \sin \phi + e \sin (\phi + \beta) + U \sin \alpha \tag{5.8}$$

It is apparent that an out-of-phase component exists in the terms $e \cos (\phi + \beta)$ and $e \sin (\phi + \beta)$ which effect is unwanted and therefore e has to be minimised or alternatively the angle β reduced to zero in order to create an additional in-phase, and hence harmless, component.

In this experimental procedure, the synchro resolver is mounted in such a way that it may be pivoted around the spindle axis. Setting the stator to various angular positions corresponds in the basic method to various orientations of the eccentric offset of the master ball with respect to the spindle, and, analogously to the various angular orientations of the boring tool.

Thus, by varying the settings of the stator of the synchro resolver the worst case may be found and recorded.

5.3.3 Basic method for turning (i.e. fixed sensitive directions)

It was pointed out by Pearson [38] that the basic method of section 5.3.1 does not reflect errors machined into the workpiece for the case where the tool is stationary and the workpiece rotates. This is because the depth of cut of a tool depends on the radial motion of the axis of rotation towards and away from the tool in the sensitive direction, being almost insensitive to transverse motions of the spindle. The correct way to find the effects on the workpiece of radial error motions is to simulate the action of turning which corresponds to using only one pick-up to replace the tool.

This realisation leads however to the necessity of providing some external means of generating the reference circle on which to superimpose the error.

J. Bryan [38] solved the problem by attaching to the spindle two cylindrical cams equally eccentric from the axis of rotation, the eccentricities however being perpendicular to each other. Their test set-up is shown in Figure 5.10. By means of the "wobble" plate the master sphere is centered as accurately as possible.

The signals from the two low-magnification (non-contacting) pick-ups sensing the motion of the cams provide the sine and cosine signals necessary for base circle generation. The radial error motion signal is derived from a highly sensitive pick-up sensing the motion of the master sphere.

System Theory - basic method for turning (refer to Figure 5.7)

let e = the residual eccentricity of the master ball

U_s= the displacement of the axis O from its center position

C = the eccentricity of the circle generating cams

The workpiece rotates at speed ω and, at time t, the reference direction is at an angle ϕ to the X axis. The eccentric offset of the master ball is at an angle β to this reference direction.

Components sensed by the single pick-up in X:

Component due to the eccentricity of the master ball =

$$e \cos (\phi + \beta)$$

Component due to the displacement U of the axis = $U \cos \alpha$

The signals from the circle generating cams are:

$C.\sin \phi$ (to the X plates of the oscilloscope)

$.C \cos \phi$ (" " Y " " · ")

Now, in order that the error motion is correctly superimposed radially it is necessary to create two signals

$\delta.\sin \phi$ and $\delta. \cos \phi$ (where δ = the total component sensed by the pick-up) which are added to the circle generating signals $C \sin \phi$ and $C \cos \phi$. The required multiplication is achieved here by the use of Hall multipliers

The total signal to the X plates of the oscilloscope is,

$$C \sin \phi + (e \cos (\phi + \beta) + U \cos \alpha). C \sin \phi \qquad (5.9)$$

and the total signal to the Y plates of the oscilloscope is,

$$C \cos \phi + (e \cos (\phi + \beta) + U \cos \alpha) . C \cos \phi \qquad (5.10)$$

The effect of the residual eccentricity and the phase angle of the offset with respect to a reference direction will produce a distortion of the polar diagram from that required as representative of the true deviation from roundness of a turned workpiece.

This system also naturally is only as good as the quality of manufacture and setting of the two offset circle generating cams for, if the circle generating signals contain some harmonics then the reference circle will be deformed and this deformation may be interpreted as radial error motion.

Initially, eddy-current type transducers were used which however imposed apparently severe restrictions on the satisfactory attainment of good surface finish on the circle generating cams, any discontinuities or cracks causing

signal errors. The system was improved with the adoption
of capacitance probes, and further by the use of only
one cam and positioning the two pick-ups perpendicular to
each other [40].

5.3.4 Modified method for turning

Vanek [41] in his modification of the technique
to be used when analysing radial error motions in turning,
adopted the same technique as his modified method for
boring (section 5.3.2) in that the difficulties of gener-
ating pure reference signals for base circle generation
are avoided by using sine and cosine signals derived from
a synchro resolver attached to the spindle.

Again, it is necessary to superimpose the error
radially on the base circle and the necessary multiplica-
tion of error signal δ with circle generating signals
sin ωt and cos ωt is achieved by a process of "double de-
modulation". His experimental set-up is shown in Figure
5.11.

Here two LVDT type pick-ups are used and, being
connected in tandem, their spindles move in an identical
manner. When they are fed by a carrier frequency oscill-
ator, they pass an amplitude of voltage proportional to the
displacement of the spindle from the null position. In
other words, the voltage passing through is amplitude
modulated in proportion to the displacement.

Additionally, the carrier frequency voltage level from one of the oscillators is fed to the rotor of the synchro resolver. From the two 90°-separated windings of the stator we obtain voltages amplitude modulated by the sine and cosine of the angle of rotation of the spindle. These two voltages feed the two pick-ups and, in their outputs, sine and cosine functions therefore occur with magnitudes proportional to the displacement of the pick-up.

In this technique, the base circle radius is achieved by an initial DC zero offset of the pick-up signal which represents a certain constant amplitude of the sine and cosine signals. Due to the radial error motion of the machine spindle, the pick-up is moved from the initial setting and the corresponding error signal is superimposed on the reference base circle.

<u>System Theory</u> - <u>modified method for turning</u> (refer to Figure 5.7)

let e = the residual eccentricity of the master ball

U = the displacement of the axis O from its center position

D = the initial transducer offset from its null position

The spindle rotates at speed ω and at time t, the reference direction is at an angle ϕ to the X axis. The eccentric offset of the master ball is at an angle β to this reference

direction.

Components sensed by the tandem pick-up unit located in X:

Components due to the eccentricity of the master ball =

$$e \cos (\phi + \beta)$$

Components due to the displacement U of the axis = U cos α

∴ Total displacement of the pick-up is

$$D + e \cos (\phi + \beta) + U \cos \alpha \qquad (5.9)$$

The total signal to the X plates of the oscilloscope is

$$(D + e \cos (\phi + \beta) + U \cos \alpha) \ . \ \sin \phi \cdot \qquad (5.10)$$

and the total signal to the Y plates of the oscilloscope is

$$(D + e \cos (\phi + \beta) + U \cos \alpha) . \cos \phi \qquad (5.11)$$

The form of these equations is essentially identical to

that derived from the basic method for turning.

A disadvantage of the technique lies in the direct

mechanical contact of the pick-up with the spherical master

or with thin strips of metal sliding on the surface of the

master. This contact is reported as being a source of

noise, especially for high rotational speeds of the spindle.

5.4   A Universal Axis of Rotation Analyser

In accord with the attitude of Vanherk [42] who

deemed necessary the development of a versatile electronic

instrument (in the absence of any commercially available one)

enabling a comprehensive analysis of all errors associated

with an axis of rotation as defined in the proposed "Axes

of Rotation" standard [39], such an instrument has been constructed and calibrated as part of this thesis.(plate V,pg.130)

The instrument contains circuitry (see Appendix D for details) enabling the following measurements to be achieved:

(A)   For turning (and other fixed sensitive direction applications)

1)   Radial error motion

2)   Angular error motion, and

3)   Axial error motion

(B)   For boring (and other rotating sensitive direction applications)

1)   Radial error motion - measured by either of two methods:

a)   Reference circle generated by offset

b)   Reference circle generated by synchro resolver

5.4.1   <u>Measurement of radial error motion in turning</u>

The basic block diagram for group A measurements is shown in Figure 5.12 for sensing the radial error motion of the spindle.

A single non-contacting capacitance transducer senses the motions of a master ball which is centered as far as possible using a wobble plate. There will be some con-

Plate V AXIS OF ROTATION ANALYSER

1 The Analyser
2 The Master Ball and Wobble-plate holder
3 The Capacitance pick-up and Synchro-resolver holder

stant voltage output from the bridge amplifier according
to the width of the gap between the pick-up and the master
ball. This may be effectively zeroed using the offset
voltage P1 so that only the error motion signal is sensed.
This signal may be filtered if necessary, to remove the
lower frequency structural motions, using variable filter
F1.

A 5KHz oscillator feeds the rotor of a synchro
resolver attached to the spindle. If ω is the speed of
spindle rotation then after demodulation and filtering we
derive from the two 90°- separated stator windings two pure
harmonic signals $A \sin \omega t$ and $A \cos \omega t$.

The signal multiplication necessary in this fixed
sensitive direction measurement for correct radial super-
imposition of the error on the polar trace is achieved
here by economical I.C. multipliers.

A complication arises however due to the remaining
eccentricity of the master ball, if it is excessive. (It
should be remembered though that eccentricity of the refer-
ence surface has no effect on the attainment of a perfectly
round machined surface, see section 5.1). The consequence
of this eccentricity is in the generation on the oscilloscope
screen of a deformed reference circle. This occurrence is
analogous to the effect of checking the roundness of a work-
piece mounted on the platen of a roundness testing machine

at some small eccentricity as discussed by Reason [43] in his explanation of the obtained deformed (elliptical) polar chart.

In this instrument an electronic centering circuit was built-in to compensate all harmonic signals with the same period as the rotation itself.

The theory behind this is as follows:

Suppose that the voltage component of the output signal from the pick-up due to the eccentricity of the master ball is given by

$$B \cos (\omega t + \beta) \qquad (5.12)$$

where B is a constant due to the eccentric offset and amplifier gain, and β is the angle between the reference direction of the synchro resolver and the direction of the offset.

This may be decomposed as

$$B \cos (\omega t + \beta) = B \cos \beta \cos \omega t - B \sin \beta \sin \omega t$$

$$= D \cos \omega t - E \sin \omega t \qquad (5.13)$$

This means that if two signals - D cos ωt and + E sin ωt are added to the signal of the pick-up, the effect of the offset of the sphere is completely suppressed.

The provision in Figure 5.9 of the potentiometers P2 and P3 allows the deviation of the two required signals inside the range $\pm$ P cos ωt and $\pm$ P sin ωt, which are then added to the total error motion component before entering

the multipliers.

N.B. For a direct and correct representation of the shape of the polar chart with the shape of some machined workpiece, the vector rotation on the oscilloscope screen is opposite to the direction of the rotating spindle. This corresponds to the workpiece being held stationary while the tool rotates around it.

5.4.2 Measurement of Angular Error Motion

Measurement of angular error motion is achieved by using two pick-ups in the same horizontal plane sensing the motions of two spherical masters which are positioned at some known distance apart. By placing the instrument function selector in the correct position, the signals of the two pick-ups are subtracted and then further processed as in the previous section 5.4.1.

5.4.3 Measurement of Axial Error Motion

For measuring this, a single pick-up is positioned to sense the motions along the axis of rotation. It is processed in exactly the same manner as in section 5.4.1 with the exception that the compensation device is switched off since here we are primarily interested in the fundamental axial motion (i.e. the error motion occuring once per revolution of the spindle) for in this case, the fundamental motion is not caused by offset of the master but by an axial motion of the spindle along the axis average line.

5.4.4 Measurement of radial error motion in boring

a) Reference circle generated by offset

To enable the measurement of radial error motion in not so critical cases, the basic boring circuitry of section 5.3.1 is built into the analyser, Figure 5.13, generating the reference circle by means of an eccentricity of the master ball.

If a perfect axis of rotation is assumed here, then the only effect of the offset is to shift the polar diagram on the oscilloscope away from the center but still we have a perfect reference circle which for convenience may be recentered using potentiometers P1 and P2.

However, it is re-emphasized that the obtained error motion polar trace is only valid for the case where the offset direction of the spherical master coincides with the actual orientation of the tool in boring (i.e. with respect to the boring-bar). If these directions do not coincide then it is not possible to relate to the desired measurement by simply rotating the chart by the angular difference between the offsets since the obtained polar trace is also distorted in relation to that of the desired measurement.

b) Reference circle generated by synchro resolver

The block diagram of the circuit is shown in Figure 5.14 where we see that in a similar procedure to the pre-

vious case, the radial error motions of the master ball
are sensed by two capacitance pick-ups located at right
angles to each other sensing the horizontal and vertical
components of the error motion.

Unlike the previous case however, the offset of
the master ball has to be minimised for reasons given
previously in connection with Equations (5.7), (5.8).
Assume for the time being that perfect centering has been
achieved.

The signals from the pick-up are added to the
pure harmonic signals derived from the stator windings of
the synchro resolver which form the basic reference circle.

Even if the error motion itself is zero, while the
reference circle will be perfect it will not be central on
the oscilloscope screen due to the signals produced by the
gap width between the pick-up and the master ball. The
trace may be centralised using potentiometers P1 and P2.

Since in fact it is practically impossible to per-
fectly center the master ball, what is the effect of the
residual eccentricity?

The effect of the eccentricity is not in the gen-
eration of a limacon as in the case of the one pick-up
method for measuring radial motion for there, the pick-up
signal modulates the synchro resolver signal whereas in
this two pick-up method the vertical and horizontal error

components are <u>added</u> to the circle tracing vector.

Suppose the spot on the oscilloscope screen is the end point of a vector consisting of two components, AB due to the synchro and BC due to the offset as shown in Figure 5.15a. Angle β is the angle between the vector generated by the synchro signal and the offset direction of the spherical master.

A perfect circle is always generated by point C which may be used as a reference circle. However, if the stator is adjusted in phase with the position of the tool point then the tracing point on the screen C will not be in phase with the position of the tool point and a distorted image will result. The amount of the distortion will depend on the magnitude of β and also on the amplification of the error signal which governs the vector length BC.

It is possible to compensate for the phase shift by adjusting the angular position of the stator, the difficulty being in knowing how much adjustment is necessary.

The instrument therefore includes Vanherk's solution to the problem [42] which consists of providing zero - level - crossing detectors in the sine and cosine signal branches controlling a Z axis modulation (i.e. trace intensity) input to the oscilloscope, Figure 5.15 b.

Now, if the stator is adjusted in phase with the horizontal position of the tool point and if low error

amplification factors are used so that the length of
vector BC is small then the tracing spot on the screen
should be suppressed at the intersections with the
horizontal and vertical axes as in Figure 5.15c. As the
error amplification is increased, the spot follows point
C and thus deviates from the AB direction. Here, the
tracing point is suppressed at an angle β' from the ver-
tical and horizontal axes as in Figure 5.15 d. Rotation
of the stator enables the readjustment of the phase of
spot C so as to enable it to cross the horizontal axis at
the same time as does the tool.

5.5   Evaluating spindle rotation errors

In evaluating the error motion value from the
photograph of the polar trace as obtained on the oscillo-
scope screen it is, generally speaking, equal to the differ-
ence in radii of two concentric circles that will just en-
close the error motion polar plot, and the value obtained
depends on the location of the common center of these two
circles.

Four methods are recognised in Ref [39], as in Ref
[44] from which Figure 5.16 is extracted, for locating the
center and these centers and corresponding error motion zone
names are:

(a) Minimum circumscribed circle (MCC) center and
zone

(b)   Maximum inscribed circle (MIC) center and zone

(c)   Minimum radial sepatation (MRS) center and zone

(d)   Least squares circle (LSC) center and zone

It will be appreciated from Figure 16a and Figure 16b that two values of error motion could be obtained from the same trace depending upon whether it represents a shaft or a hole. Also the MCC and MIC centers are not unique and are therefore listed [44] as non-preferred centers.

The radial width of the MRS zone is numerically unique in that a larger value by definition cannot exist and the MRS center is thus generally thought of as unique although its method of location is a trial and error procedure.

The LSC center is unique and this approach to graphical determination provides a unique least squares mean circle from which a mathematically precise statement of error can be obtained. The graphical procedure for determining the LSC center and zone is depicted in Figure 5.17 extracted from Ref[44] and the proof of the formulae used in the determination of the least squares center and circle is given in the same reference.

The MRS and LSC centers are "preferred" centers, but because of non-standardisation in this area, it should always be quoted which method has been utilised in the

evaluation of error zone width since as demonstrated in Figure 5.16 the application of different techniques results in a differing assessment.

The application of the foregoing techniques for locating the center are relevant to the evaluation of radial and angular error motions where there is no significance to the fact that the located center does not coincide with the center of the chart due to an offset of the spherical master causing a pseudo-fundamental (i.e. once per revolution) error. In fact, accepting the concept of Ref [39], no actual fundamental radial or angular error motion exists since the removal of the once per revolution sinusoidal component corresponds to the test ball being perfectly centered.

However, a fundamental axial motion does exist and is not caused by the master ball mounting error but by a once per revolution sliding motion of the axis of rotation along the axis average line caused by, for example, out-of-square thrust bearing components. In this case the required center is the polar chart (PC) center and the error motion is determined by drawing concentric circles from this center.

Now, there are three main characteristics which serve to identify the features of spindle error motion polar charts:

(a) the repeatability of the various spindle motions

(b) the distinction between the lower and higher harmonic component motions, the order of the harmonic being understood as the number of whole undulations per spindle revolution

(c) the change of shape of the whole figure, or the movement of the center of the concentric circumscribing and inscribing circles with, for example, a change of spindle speed, or a change in the magnitude or orientation of an external force. (Another cause may be thermal changes in the structural loop, though in this particular case, the maximum change in the mean position of the spindle axis is included in the appropriate tolerance law as in Chapter 4 having been identified in the spindle "drift" test).

The particular significance of the individual features depends on whether the measurement is of radial or axial error motion and its application e.g. accuracy of rotation of grinding wheel spindles, spindle of a lathe etc. Generally speaking however for b), the distinction lies in the tendency of lower harmonics to lead to errors of form e.g. a lobed machined surface, and that of the higher harmonics to relate more to errors of surface finish.

For c), while it is measured as part of spindle rotation accuracy, the significance is in its relation to the change of displacement of the tool with respect to the workpiece.

Let us look at the concept of repeatability which is the most important and refer to Figure 5.18 where several idealised cases of radial error motion polar charts are presented.

In Figure 5.18a, it is assumed that the trace is repeated exactly in each revolution no matter how long we record. The trace if evaluated by an appropriate method represents the machined internal or external surface. If the MRS center is found, then the MRS zone width will represent the error motion.

In case b), it is assumed that the figure is exactly repeatable every two subsequent revolutions. If we assume turning or boring with a tool having its secondary edge parallel with the feed motion and the width of the edge is greater than the feed per revolution then obviously in this case, only the internal envelope will be significant for internal machining and only the external envelope for external machining. The MRS center of the whole figure no longer applies since the internal and external envelope will have different centers and different zone widths.

The overlap of subsequent cuts may be effective for a number of subsequent revolutions. In Figure 5.18c the figure has been recorded during four revolutions. This figure represents therefore a motion which is not at all

repetitive, however the non-repeatability may be re-stricted to a small number of revolutions. Again, supposing we consider the case of internal machining then the MRS center and zone width of the total figure do not apply, only the MRS center and zone width of the internal envelope of Figure 5.18c being relevant. This internal envelope is reproduced in Figure 5.18d for evaluation.

Figure 5.18e represents a very dense cloud of non-repetitive motion taken over the effective overlapping revolutions assumed. Both the internal and external envelopes are practically perfect circles and with a sufficient overlap, perfectly circular internal and external surfaces will be machined.

In Figure 5.18f the most commonly obtained type of trace is reproduced with clearly distinguishable internal and external envelopes, the area in between being filled by the cloud of varying width. This may be used for adding to the features of the MRS zone width of the internal and external envelopes the feature of maximum "random" motion. (Evaluating this parameter in Ref [39] it is noted that the term random does not require the physical causes of the random error motions to be random in the statistical sense, but simply refers to the appearance of the total error motion polar plot after a number of revolutions).

It has been shown then that when speaking of non-repeatability the number of revolutions must be given to which it is related.

a) <u>For radial motion errors</u> then,

If no overlap is assumed, the total figure must be evaluated as in Figure 5.18 a),b),c) over a sufficient number of revolutions e.g. ten. A shorthand notion could be

$$\Delta_r, \text{ TR, } 10 \text{ revs}$$

where Δ_r denotes the radial error motion, and

TR represents the total reading.

Since it is often useful in practice to make a record of one or two revolutions in order to identify the basic form of error, this record will be evaluated as

$$\Delta_r, \text{ TR, } 1 \text{ rev.}$$

If however a practical overlap is assumed, by choosing the number of spindle revolutions over which it extends, the record will be evaluated with regard to its inner envelope (IE) or its outer envelope (OE). For example, in Figure 5.18d, for the inner envelope of Figure 5.18c, we will evaluate

$$\Delta_r, \text{ IER, } 4 \text{ revs}$$

The concept of using envelopes is entirely analogous with the practice of evaluating direct tests on the Talyrond

roundness testing instrument because the machined surface is in fact an envelope.

When using an envelope it will be additionally necessary to evaluate the random motion which may influence the surface finish and hence the maximum radial distance between the IE and OE will be indicated as

$$v_r \text{ (n revs).,}$$

where v stands for vibration and the suffix r for radial.

This practice of separating the bare envelope error from the random motion corresponds to the use of filters in making Talyrond records.

It is furthermore, necessary to specify the spindle speed and the axial distance from the spindle at which the measurement was obtained.

b) <u>For axial motion errors</u>, the fundamental motion is significant and it should be evaluated as,

$$\Delta_{fa}$$

this being twice the distance between the polar center (PC) and the MRS center of the upper envelope figure, see Figure 5.19.

In this case, the width of the MRS zone - the difference in radii of the circumscribed and inscribed circles of the envelope (upper envelope UE) in this case, represents the superimposed (i.e. on the fundamental) axial

motion error and it can be denoted

$$\Delta_{sa}, \text{ UER, n revs}$$

The random motion is expressed as

$$v_a$$

At other times, when no overlap is considered, the super-imposed error and vibration error may be combined and denoted

$$\Delta_{sa}, \text{ TR, n revs}$$

in an analogous manner to the case of the radial error motion total reading.

5.6   Classifying spindle rotation accuracy

Because of the special significance of spindle rotation errors relating to a specific part of the total error of form and dimension of the workpiece it should not be included in the tolerance laws governing the accuracy of workpieces as a whole, but assessed separately.

A UMIST proposal [5] has classified spindle rotation errors according to the Table A below where the basis for the numerical values accorded each class was derived from the bearing manufactures quoted tolerances (see Figure 5.2) and from best achieved spindle rotation accuracies.

TABLE A

Class	0	1	2	3	4	5	6	7	8
Error μm less than	0.25	0.5	1	2	5	10	15	20	40
Error μin less than	10	20	40	80	200	400	600	800	1600

5.7 Separating the influence of the error of the master ball

Until now, it has been assumed that the master ball is a perfect sphere. If it is not, then naturally the influence will affect the shape of the polar trace. However, a simple procedure devised by Donaldson [45] permits the elimination of the unwanted influence by a procedure analogous to taking the mean of two straightness of motion measurements on a mandrel held in a lathe spindle, rotating the mandrel 180° between measurements to eliminate any error in the setting of the mandrel.

To identify correctly the most accurate classes of spindle rotation, this procedure will be necessary even with the use of the most accurate master ball if we wish to comply with the general "rule-of-ten" applicable to metrological measurements.

e.g. our master ball, provided by J. Bryan of the Lawrence Radiation Laboratory shows a deviation from round-

ness of approximately 4 μin (see Figure 5.20) and there-
fore could not be used to identify Class 0 or 1 of TABLE
A without.separating the roundness error.

CHAPTER 6

MACHINE TOOL CALIBRATION VIA LASER INTERFEROMETRY

6.1 Introduction and Basic Concepts

Before proceeding to introduce some significant measurements in the following chapter (Chapter 7) it is necessary to appreciate the working operation and capabilities of the laser interferometer system used in the large scale machine tool accuracy investigation. The specifications of the system and accessories are detailed in Appendix E.

Interferometric measurement techniques have been in use for well over half a century and have been applied particularly to the measurements of slip gauges and end bars for engineering reference standards.

On the introduction of laser light sources, besides encouraging the production of more simple and robust designs of interferometer so that interferometric measurements are no longer confined to the laboratory, measurements are no longer restricted to short distances and may be used for example to measure the travel of a machine tool slide over distances of many feet.

All modern interferometers are based on the techniques pioneered by A.A. Michelson in the 1890's.

Figure 6.1 shows the basic Michelson interferometer.

Here, a half-silvered mirror splits the beam from the monochromatic light source into two beams, each of which is reflected from a mirror and then recombined at the half-silvered mirror. With the mirrors exactly aligned and motionless, the observer sees a constant intensity of light. However, if one of the mirrors is moved very slowly, the observer sees the beam repeatedly increasing and decreasing in intensity as the light from the paths adds or cancels. Each half-wavelength of mirror travel means a total optical change of one wavelength and one cycle of intensity change.

If the wavelength of light is accurately known therefore, and the number of fringe patterns of alternate light and dark bands is counted, then the travel of the mirror may be accurately known.

It is important to note that only changes of position of the mirror may be measured.

Now, in order to make the device into a practical electronic instrument for modern applications it is basically necessary only to add a photocell to convert the beam intensity variations into a series of pulses and to use an electronic counter to count the cycles of beam intensity variations.

However, the basic components of a modern inter-

ferometric system also include:

a) <u>cube corner reflectors</u> These are preferred over plane mirror reflectors because of the critical alignment requirements of the latter. With cube corner reflectors, the reflected beam is always returned parallel to the incident beam (see Figure 6.2) and hence it may tolerate the deviations encountered in a fairly crude slide motion.

b) <u>the laser as a light source</u> With its high degree of coherence and intensity the laser may be used over distances of many feet. Its short wavelength permits resolution into the microinch range, and its wavelength can be determined to a high degree of accuracy. Now, the primary standard of length since 1960 is measured in terms of the wavelength of radiation of the Kr-86 isotope which can be reproduced to a relative accuracy of one part in a hundred million. The wavelength of the radiation of a He-Ne laser (most often used in commercially available systems for metrological applications) has not yet been internationally adopted as a secondary length standard but its wavelength also may be stabilised to a comparable degree over short periods and can have in the long term a reproducibility of better than one part in ten million.

c) <u>direction sensing electronics</u> Rather obviously, a single photocell is inadequate to sensing changes in the

direction of motion of the measuring mirror or cube corner.

6.2   The Hewlett-Packard Laser Interferometer

The H.P. laser system is the most advanced of its
type in the world and it was selected because of the many
innovations incorporated in the system contributing to its
ease of use, performance and reliability. Plate VI (pg. 152)
shows an assembly of all the accessories to the basic laser
system.

One of its most important features is that it
operates on a two frequency principle. Most other lasers
operate on a d.c. principle which is subject to such inherent
problems as warm-up time and change of intensity of either
light beam or source due to laser tube aging or turbulence
in the shop environment deflecting the beam away from the
preset trigger threshold at which counts are registered.

The H.P. laser, on the other hand, operates on an
a.c. principle [46] using a two frequency system and from
this derives its immunity to turbulence, 95% of signal loss
being tolerated. This is by virtue of the fact that distance
information is carried on a.c. waveforms and a.c. amplifiers
are not sensitive to changes in the d.c. levels of their
inputs.

A simplified schematic of the laser system is shown
in Figure 6.3. A low power Helium-Neon laser emits a
coherent light beam composed of two slightly different
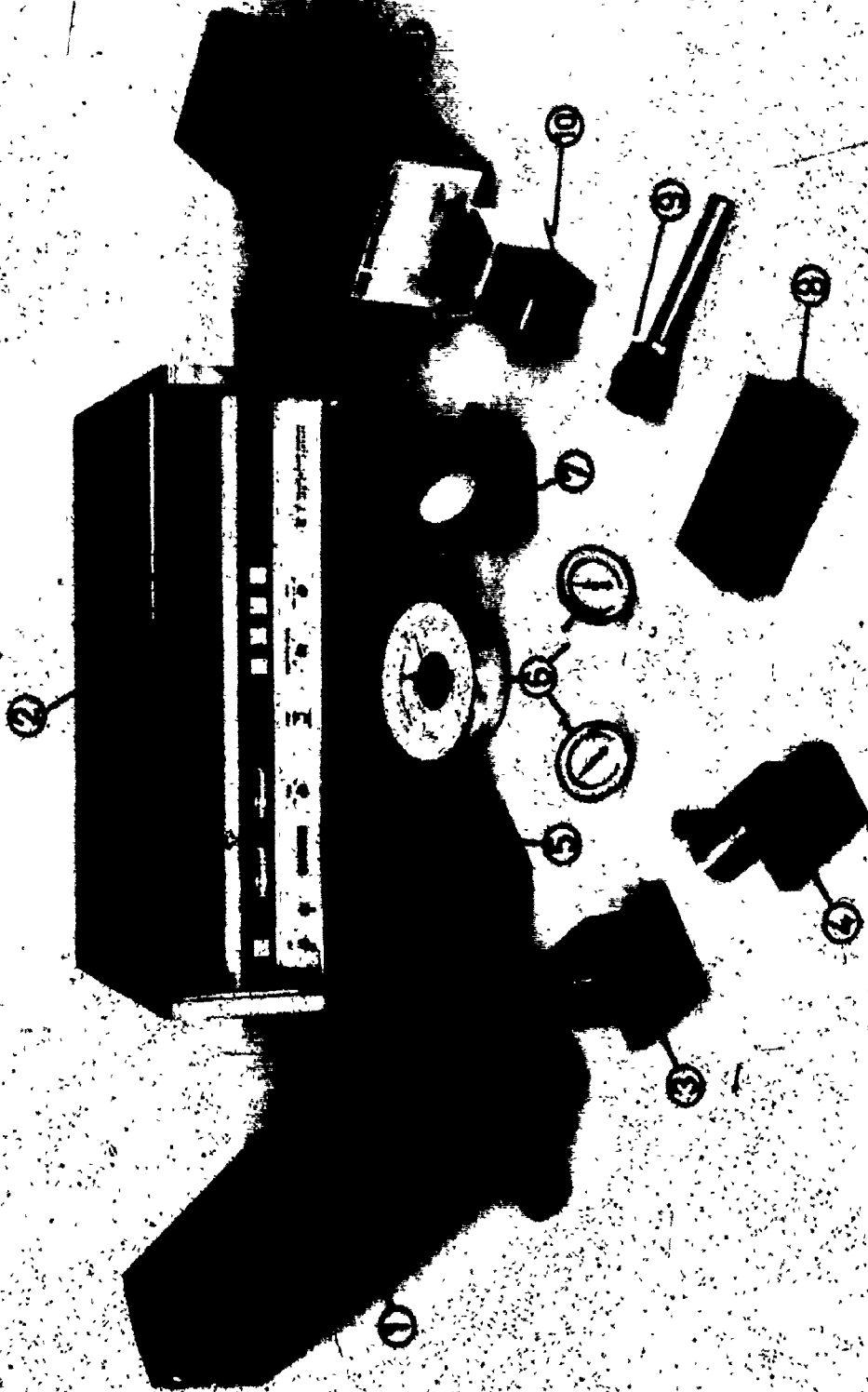
Plate VI   THE HEWLETT-PACKARD 5525B LASER INTERFEROMETER SYSTEM

1. 5500A Laser Head
2. 5505A Laser Display
3. 10565A Remote Interferometer
4. 10550A Retroreflector and mount
5. 10558A Beam Bender

6. 10560A Barometer/Thermometer Kit
7. 10551A Beam Bender/Alignment Mirror
8. Option 30 Straightness Reflector
9. Option 30 Straightness Interferometer
10. Option 30 Straightness Adaptor

11. Option 30   35X Resolution Extender

frequencies f_1 and f_2 of opposite circular polarisations. After conversion to orthogonal linear polarisations, the beam is expanded and collimated then directed to the reference beam splitter where a small portion of the beam is split off to be used both as a reference frequency and to provide an error signal to the laser cavity tuning system. The a.c. component of the difference between f_1 and f_2 (about 2MHz) is used for reference and goes to a counter in the laser display.

The major component of the beam passes on to an interferometer. One of the frequency components f_1 is used as a measuring beam and is reflected from the retroreflector. On its return it is mixed with the second frequency f_2 but the fringe patterns do not appear until the combined beam strikes a demodulating polariser adjacent to the photocell in the laser head.

Now if the measuring reflector is stationary, then the light and dark bands will flicker at a rate of approximately 2MHz, corresponding to the difference in frequencies of the two beams and since the reference and Doppler signals are equal, no net count will be accumulated at the display unit.

On the other hand, if the reflector is moved, the return frequency will be Doppler-shifted up or down slightly (as with a passing train's whistle), a reflector velocity of

1 ft/sec causing a shift of approximately 1 MHz. Accordingly net positive or negative cumulative counts corresponding to the distance traversed in wavelengths of the light will be monitored by the counter for conversion into the chosen units (i.e. in., m.m.) by an in-built integrated circuit calculator.

Other functions of this calculator include smoothing, electronic resolution extension and velocity computation.

6.3   Computation of Velocity of Light Compensation Factors:

6.3.1   For the Refractive Index of the Air

A complication in interferometric measurements is the refractive index of the air through which the laser beam passes. The wavelength of interest is not the vacuum wavelength i.e. the wavelength in a medium of refractive index equal to 1 but the wavelength in air at the time of measurement.

The refractive index depends on the air pressure, temperature and, to a lesser extent, humidity and composition e.g. less dense air with low pressure and high temperature results in a higher velocity of light and a larger wavelength.

Allowance for these factors is straightforward on the H.P. laser system, a series of thumbwheels being provided for insertion of the ratio of air wavelength to vacuum wavelength calculated from tables and used for conversion by the I.C. calculator from the fringe count to distance travelled

according to the formula:

$$\text{Distance} = (\text{wavelengths of motion}) \times \left(\frac{\text{air wavelength}}{\text{vacuum wavelength}}\right) \times$$

$$(\text{vacuum wavelength})$$

where the vacuum wavelength is "hard-wired" into the system

6.3.2   Material Thermal Expansion Compensation

An additional compensation factor must be taken into account due to the temperature of the machine or part being calculated. The "true" size of a part is defined by metrologists as the measured size at a reference temperature of 68°F (20°C).

The adopted procedure for taking this into account is to modify the air wavelength sufficiently to allow for the thermal expansion. This requires knowledge of the thermal expansion of the material being measured and its temperature.

The procedure is best demonstrated with reference to an example: Suppose a steel part that is known to measure 1.000,000 in. at 68°F is being measured at 80°F. The indicated length would be 1.000,078 in. (the coefficient of expansion of steel being taken as 6.5 ppm/°F). The display measurement could be "forced" to indicate the "true" size by reducing by 78 ppm the strict air wavelength calculated for the particular environmental condition.

This modification is simply made via the previously mentioned thumbwheels.

6.4   Remote Laser Interferometry

6.4.1   The Linear Interferometer

Laser interferometers can measure distances up to hundreds of feet with a resolution of a millionth of an inch. They do this by using the wavelength of laser light as a length standard. This wavelength is known precisely enough to make laser interferometers inherently accurate within a few parts in ten million.

In measuring short distances however, this high inherent accuracy is difficult to realise because of the effect of heat generation in the laser unit. This heat generation is minimised already by the use of an ovenless laser in the H.P. system but, for ultraprecise measurements, the accuracy is still affected to a significant extent.

This realisation led to the development of the Remote (linear) Interferometer [47] for which there are a number of very significant advantages.

The principle of operation for this interferometer is shown in Figure 6.4. The beam exiting from the laser head is split at the surface of the polarising beam splitter, one frequency f_2 being reflected to the reference cube-corner mounted on the interferometer housing and the other f_1 transmitted to the measurement retroreflector. Both frequencies are reflected back along a common axis to the photodetector block in the laser head, frequency f_1 contain-

ing a Doppler frequency shift whenever the measurement reflector moves. Because the polarisations of the beams are orthogonal to each other, interference does not occur until the combined beam reaches a demodulating polariser (see Figure 6.3) mounted in front of the photodetector where the fringes form.

Now, the advantages of this system as compared with the basic system of Figure 6.1, where the internal interferometer is used, may be appreciated with reference to a typical measurement set-up of plate IV pg. 70. Here, the measuring reflector is located in the spindle nose and the interferometer is clamped to the machine table while the laser head itself is mounted on a tripod remote from the area of the measurement.

The advantages of this set-up configuration are:

1) The remote interferometer, being an entirely passive device, is an accurate reference point being un-affected by any internal heat source. The improvement in measuring stability over the normal system is demonstrated by the drift measurement of Figure 6.5.[46]

2) The laser head may be positioned at some dis-tance from the machine and, since the relative position only of the reflector and interferometer is measured, the presence of the metrologically undesirable dead path and any fluctua-tion in this distance due to adverse environmental condi-

tions or vibrations of the tripod stand does not affect the measurement accuracy.

However, the concept of remote interferometry having been introduced, its greatest advantage has been in the development of a family of interferometers whose various functions enable the measurement of error functions not normally associated with the capability of laser measuring systems.

6.4.2 The Angular Deviation/Flatness Interferometer

The use of this interferometer, see Figure 6.6, enables measurements of pitch and yaw motions of machine tool sliding elements to be made as well as replacing the autocollimeter in accurate measurements of surface flatness [48].

The reference reflector of the linear interferometer is replaced by a 45° mirror so that f_1 and f_2 are sent out parallel. The system then measures the difference in movement between the two reflectors, the angular displacement causing a differential Doppler-shift in the returned frequencies that is not affected by axial displacements. The dimensions of the beam bender and remote beam splitter were chosen such that 10 μin difference in movement is equivalent to an angular deviation of 1 sec. of arc.

6.4.3 The Straightness Interferometer

Prior to the introduction of this interferometer,

straightness measurements could only be made reliably using straight-edges of limited length. This method is quite adequate for application to machines where the machine slide travel also is of the same order of length.

However, for longer lengths of travel methods such as, for example, the use of a wire and telescope do not have the same accuracy as the short straight-edge.

The use of the straightness interferometer however enables reliable measurements of straightness of motion to be made continuously over distances up to a hundred feet with an accuracy of 5 microinches/ft.

The principle of the interferometer is shown in Figure 6.7. The two frequency beam exiting from the laser head pass through a partially reflecting mirror to a Wollaston prism. The two polarisations are refracted at equal but opposite angles about a centre line causing f_1 and f_2 to exit along slightly divergent paths. They are reflected back by plane mirrors rigidly attached at an included angle precisely matched to that of the interferometer. The f_1 and f_2 beams are reflected normally to recombine within the prism, this combined beam returning along the same path as the exit beam to the partially reflecting mirror where the major portion of the beam is deflected into the return aperture.

Now, whereas axial motions of the Wollaston prism

create equal Doppler-shifts in both f_1 and f_2, any lateral motions with respect to the plane bisecting the two plane mirrors results in a difference in the two path lengths and hence a difference in Doppler-shifts.

For an included angle of ϕ and a lateral translation x, the fringe counts accumulated will be given by $2x \sin \phi/2$. Therefore the reading must be multiplied by the reciprocal of $2 \sin \phi/2$ to give a correct measurement of x. This multiplication factor is built into a resolution extender unit inserted between the laser head and display units.

It has been demonstrated [49] that small pitch, yaw and roll motions do not affect the accuracy of the measurement.

6.5   Further Metrological Considerations

While the accuracy of the interferometer is inherently very high, this does not necessarily indicate an equivalent accuracy of a practical measurement, this being dependent on the metrology of the system.

Particular attention has to be taken to ensure the best alignment of the laser beam and the optical components of the system with the machine slide co-ordinate displacement direction so as to minimise the occurrence of cosine errors in the measurement.

The use of autoreflection techniques and the provision of accurate reference surfaces on all optical devices enables the achievement of insignificant measurement errors.

Care has also to be taken in the measurement of machine temperature for correct compensation factor calculation. Fortunately, it is often adequate to assume the machine is soaked out to the temperature of the environment.

CHAPTER 7

MACHINE TOOL ACCURACY EVALUATION - APPLICATIONS

7.1   Introduction

An extensive program of machine tool accuracy

evaluations, performed in accord with the proposed laws

with respect to the specification of a minimum number of

tests, the identification and evaluation of thermally

affected measurements, the application of the tolerance

laws and subsequent accuracy classification, has been

carried out with the co-operation of a number of important

Canadian manufacturing companies who requested the study

in each case in the interest of:

1)   having a comprehensive knowledge of the

accuracy, throughout the decreed working-zone, of their N.C.

(mostly) machines which represented their major capital

investment, the test specification in each case being

specially designed in accord with the general or particular

mode of use of the machine, as the case may be, determined

by inspection of the requirements of the typical workpiece

configuration.

2)   obtaining a diagnostic report of the precise

source of the machine tool error(s) and a precisely specified

procedure for improving the machine tool accuracy capa-
bility, thus providing a clearly defined maintenance pro-
-cedure.

e.g. for the machine shown in Plate VII pg. 164
it was possible to identify a source of error that had exist-
ed in the machine from its initial erection 5 years prior to
the test, the straightforward elimination of which enabled
the machine to perform inside its original accuracy specifi-
cation and contributed to the confidence of the firm in final-
izing a major contract which called for extreme accuracy.

3) <u>obtaining the necessary information in as short
a time as possible</u>, facilitated by efficient use of the laser
and its accessories with respect to setting-up time and test
performance, in order to reduce to a minimum the machine
down-time necessary, especially on the large N.C. machines
which in order to justify and earn their high initial
capital investment have to be kept running, often on a 3
shift basis.

e.g. it was possible for one machine operator
together with the laser operator to completely evaluate
(though excluding thermal effects testing) in five, eight-
hour shifts <u>two</u> of the giant floor-type horizontal boring
and milling machines shown in Plate VII, pg. 165. It is
further possible, having initially applied a comprehensive
test, to practically reduce the number of measurements to

CINCINNATI
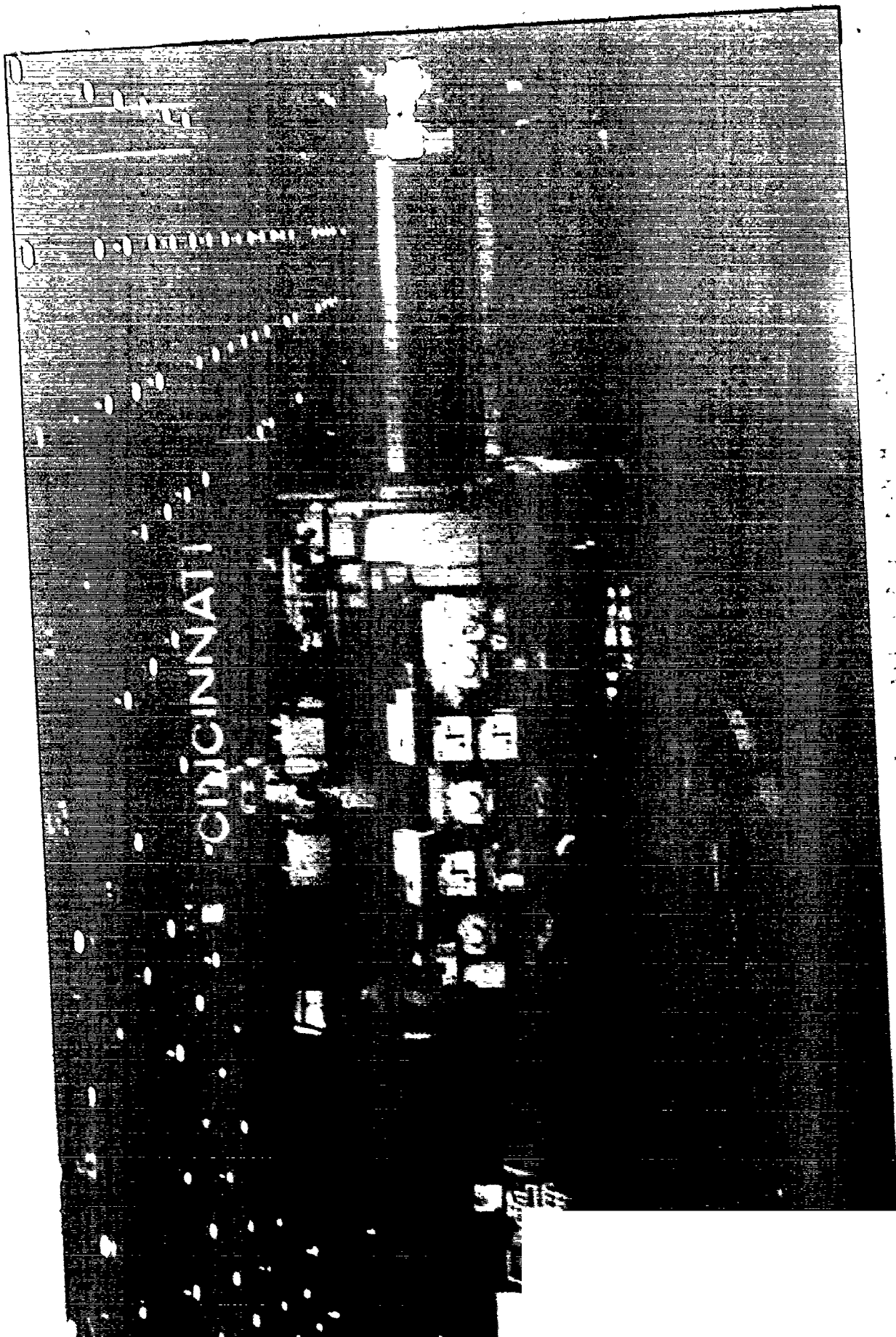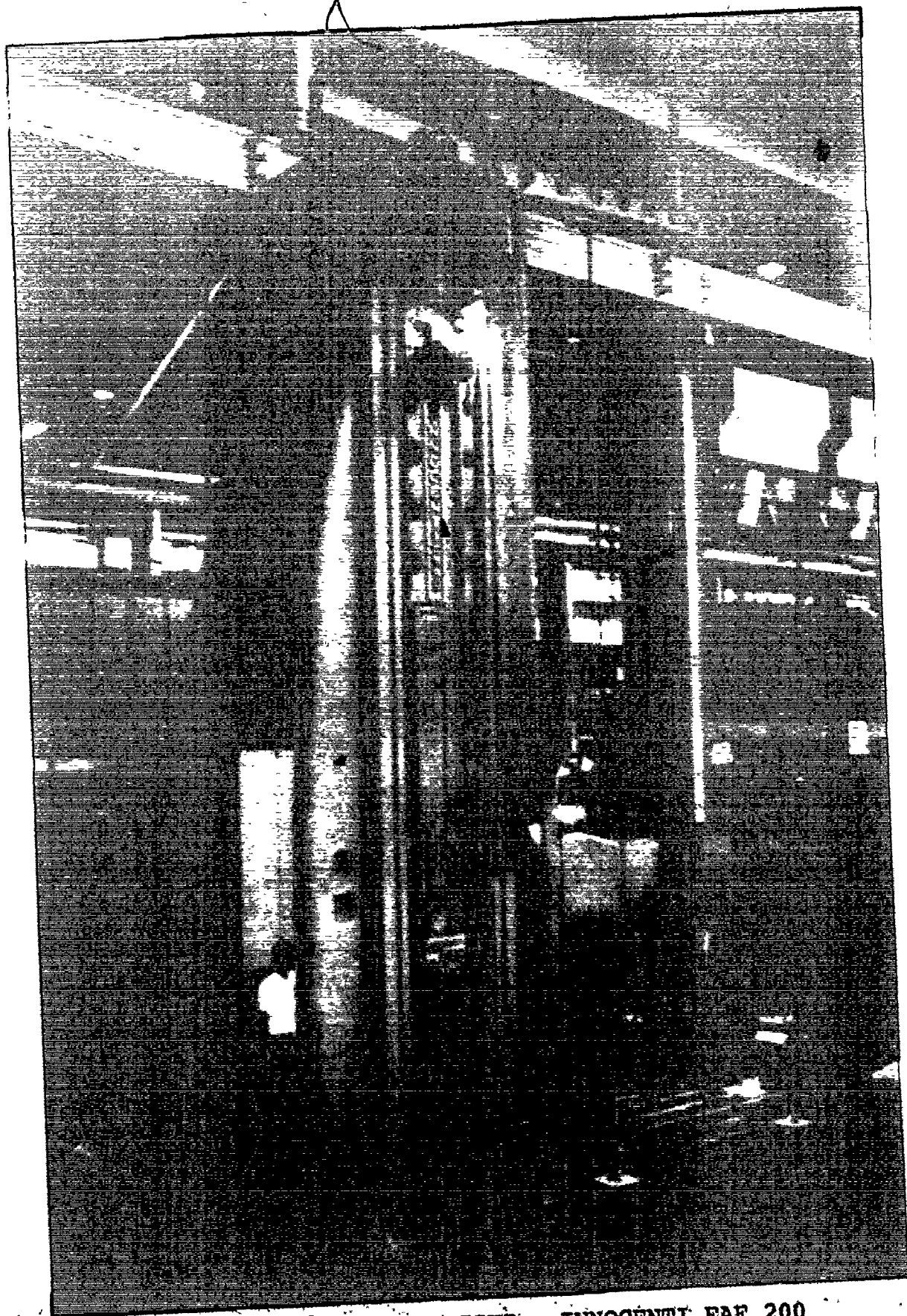
Plate VIII   MITSUBISHI — INNOCENTI FAF 200.
)NTAL BORING AND

only those particular measurements determined to be the most important to a machine's function, and apply the reduced (modified) test procedure periodically in a minimum time.

Complete reports on these applications are available, [50], [51], [52], [53], [54], [55] these containing the detailed procedure involved in computing the accuracy evaluation and the steps recommended (where necessary) for improving the accuracy capability of the machines. Here however, space admits only to the presentation of particular measurements of some significance highlighting or substantiating some of the statements (e.g. similarity in characteristics of positioning accuracy and straightness of motion measurements - their differing interpretation with respect to the common use of nomenclature i.e. DZ, e_p etc.) and procedures (e.g. the value of the master part trace/continuous recording techniques) as formulated in previous chapters, or justifying the approach to the "design" of the positioning accuracy test detailed in the following paragraph.

7.2 Measurements of Positioning Accuracy - determination of test parameters

To enable a thorough, yet fast, evaluation of the positioning capabilities of N.C. machine tools certain procedures may be recommended which differ significantly from

any published procedure e.g. those of the N.M.T.B.A. [27].

Briefly summarising their procedure, they recommend positioning to a number of positions chosen at random but arranged so as to cover the full length of an axis motion. (N.B.this is done by choosing only the least significant figure from a random number table, the most significant number being selected manually to spread over the total traverse length). The test is to be repeated, in forward and reverse directions, seven times for statistical reliability. (N.B. it is conceded that while statistics would demand positioning in random sequence, experimental results have shown the practice of positioning to each point in sequence is adequate)'.

Our objections to this procedure may be enumerated as follows:

(a) Random positioning does not provide a means for analysis of the source of errors present.

. (b) Repeating the measurement in both forward and reverse directions is not necessary since the graph of error is usually exactly the same in the reverse direction, but displaced due to dead-zone (DZ), of which backlash is usually the major component.

(c) Repetition of the tests seven times is an unjustifiable waste of precious machine time. Unjustifiable, since case histories show that the form of error remains the

same but the entire graph of error drifts in a predictable manner in relation to the graph of error obtained in the previous pass i.e. the justification of the NMTBA test in determining repeatability on a basis of it being a random process is lost.

The procedure then to be adopted, necessarily tailored to the features of the particular machine to be tested is as follows:

1) Position at some pre-determined fixed interval over the entire length of axis motion in one direction only, the interval being chosen in relation to the machine design e.g. an integer multiple of some distance over which some cyclic error may exist.

2) Position in fine increments over a short distance in order to determine any possible cyclical errors e.g. resolver or gear train originated.

3) Dead zone may be determined by checking at only one position in the return motion.

4) Repeatability may be checked reliably by positioning repeatedly to any one point.

Checks 3) and 4) above may of course be repeated at more than one position if there is any reason to suppose that the dead zone or repeatability might vary along the axis travel.

Let us now look at some applications of the above

principles in some extracts of case histories.

7.3 'Case A: The Accuracy of a 5-Axis Aerospace Skin
Milling Machine

The axis nomenclature of the machine pictured in
Plate VII pg.164 is shown in Figure 7.1. The apparent three-
dimensional working zone is reduced to one of two dimensions
on consideration that all machined workpieces consisted
initially of thin slabs of material,of which approximately
95% is machined away to leave the desired "skins" - hence
the name of the machine. 'The minimum number of tests
specified in accordance with this modified approach is shown
in Figure 7.2. The steps in the specification of the desired
measurements are:

1) Determination of maximum offsets (taking each co-
ordinate motion in turn)

a) X motion of the gantry along the bed: lines
A and B are the maximum offsets in Y with
respect to the motion in X, and there is no
offset in Z because of the limitation to two-
dimensional workpieces and the assumption of
a constant mean length of tool.

b) Y motion of the spindle carrier: there is no
offset in X, or in Z for the same reason as
above.

c) $\underline{Z \cdot \text{(vertical motion of the spindle carrier:}}$ there is no offset in X, and the maximum offsets in Y are given by lines D and E.

2) Specification of tests

   a) X motion: straightness of motion - $\delta_y(x)$ and $\delta_z(x)$ along line A and, for the effect of roll $\epsilon_x(x)$, $\delta_z(x)$ also along line B

   positioning accuracy - $\delta_x(x)$ along line A and, for the effect of yaw $\epsilon_z(x)$, $\delta_x(x)$ also along line B

   b) Y motion: straightness of motion - $\delta_x(y)$ and $\delta_z(y)$ along line C

   positioning accuracy - $\delta_y(y)$ along line C

   c) Z motion: straightness of motion - $\delta_x(z)$ and $\delta_y(z)$ along line D and, for the effect of roll $\epsilon_z(z)$, $\delta_x(z)$ also along line E.

   positioning accuracy - $\delta_z(z)$ along line D and, for the effect of yaw $\epsilon_x(z)$, $\delta_z(z)$ also along line E.

Let us look now at the design of the machine in determining the relevant parameters governing the correct specification of the positioning accuracy test denoted $\delta_x(x)$:

The X motion of the gantry along the bed is achieved utilising a rack and pinion drive on either side of the wide bed. The fine positioning feedback is derived from a

resolver geared directly to the driving pinion. Other relevant information is that one revolution of the driving pinion occurs every 10.5 ins of X traverse, one revolution of the resolver every 0.200 in. of X traverse and that each of the racks is 3 feet in length, supposedly mounted along the bed in such a way as to avoid cumulative error build-up in the maximum 100 feet of traverse available to the gantry.

The correct evaluation of positioning accuracy capability will depend on the correct application of the appropriately designed tolerance template to the obtained graph of positioning error. This is demonstrated by reference to Figure 7.3.

Here, our "linearized" template is shown in Figure 7.3a applied to the evaluation of the positioning error $\delta_x(x)$ measured in the X direction along a line in our defined working zone, say line A of Figure 7.2. In this example of Figure 7.3a, the error measured in one direction is shown by the full line and the error in the reverse direction by the dashed line. There is a difference DZ (dead zone) between the two errors.

The meaning of the graph is apparent: e.g. when moving from co-ordinate x_1 to co-ordinate x_2 an error of distance $|\delta_{x_2} - \delta_{x_1}|$ is committed.

The error, as shown by the $\delta_x(x)$ line, consists of

short distance errors, which may be partly periodic, and

these are superimposed on the longer distance trend, line

LD in Figure 7.3a. For an illustration of short distance

errors, see Figure 7.3b. In this example, we may see that

during motion indicated between points 1 and 2 an error

$\delta_{r_{1,2}}$ is generated due to that particular rack being longer.

Similarly, the rack between 3 and 4 is accurate, between 5

and 6 it is longer and between 7 and 8 it is shorter. There

may be also discontinuities between the individual racks,

i.e. between points 2 and 3, 4 and 5, 6 and 7, etc., which

represent sudden errors in positioning and they are due to

maladjustment of racks. In addition to these errors there

is perhaps a periodic error once per revolution of the pinion

(10.5 ins) due to for example the run-out of the pinion as

manufactured. There might also be other errors not shown in

this example, like those due to irregularities in the racks,

or errors per tooth of the pinion due to the non-ideal mesh

of the pinion with the rack, or an error per revolution of

the sychro resolver (0.200 in.) due to its inaccuracy.

All these mentioned errors act over rather short

distances of motion, i.e.: 0 (zero) in. for the maladjust-

ment of the racks, 10.5 ins. for the error of the pinion,

0.200 in. for the error of the resolver. These are all

superimposed on the long distance error.

The tolerance template T is shown in Figure 7.3a by

the two shaded angular segments which leave a gap A_{xx} between themselves which recede with a slope K_{xx} from the graph of error. Let us remind ourselves of the mode of use of this template: The template is used in such a way that it is moved along the graph in direction X and simultaneously freely moved up and down so as to clear the graph of $\delta_x(x)$. If this is possible, i.e. if the template does not cover any part of the error graph it is said that the error is within the required tolerance as expressed by this template. Thus, the meaning is: an error of size A_{xx} is permitted for positioning over any distance, however short it is. In addition, an error is permitted which increases with the length of positioning at a rate of K_{xx} per unit travel, e.g. per foot of travel. All errors are considered as relative i.e. they are taken as errors of distance between any two points (not as errors of distance from some fixed datum).

Of importance is that the two components of error, A_{xx} and K_{xx} correspond to two different error sources: short distance and long distance ones. However, they also correspond to the basic approach to the tolerancing of parts (see section 3.4).

Care therefore has to be taken, in the evaluation of positioning accuracy graphs and the recommendation of possible procedures for improvement, that first, the short distance errors should be minimised.

Let us now look at some practically obtained measurements of the $\delta_x(x)$ positioning accuracy deviation on the Skin Mill.

(1) The graph of Figure 7.4 is the long distance trend independent of the sources of cyclic error, the basic increment of 21 ins. being an integer multiple of both 10.5 ins. and 0.200 ins. The periodic nature of the graph is probably a consequence of the cumulative error defeating arrangement of the rack segments. From the graph we obtain the descriptive template K_{xx} value governing the long distance trend. Selecting the value with reference to the worse slope we determine:

$$K_{xx} = 0.002 \text{ in}/ 12 \text{ in.}$$

(ii) The graph of Figure 7.5 examines the positioning accuracy inside one revolution of the driving pinion (10.5 ins) the fine steps of 0.200 in. chosen to eliminate the possible effect of the resolver. It is observed that while no cyclic error exists, there is an error per tooth of the 14 tooth pinion, subsequently determined to be due to a bad involute form and incorrect meshing of the pinion and rack. This is a bad error causing errors of up to 0.003 in. to occur over a short distance of only 0.200 in. The same error existed to varying degrees on both driving pinions on each of six gantries and had been present for the five year working life prior to testing.

The graph also provides an excellent example of the way that the entire form of error drifts with respect to the measurement made on the initial pass, maintaining the same general shape. The initial zero could be recovered by a zero-shift procedure made in accordance with the position of the tool with respect to some provided reference on the bed.

(iii) Finally, the positioning error inside one revolution of the resolver is shown in Figure 7.6. A cyclic error is apparent having a period equal to one revolution of the resolver and its peak to peak amplitude is approximately 0.001 in. which is satisfactory. There is no significance to the "progressive" error on this graph as it simply represents an error superimposed on a longer distance trend.

The A_{xx} specification of the governing tolerance template is formed by summing the amplitudes of the various short distance errors (i.e. e_{p_1}, e_{p_2}, etc.), the repeatability band width (R) - and also the dead-zone (DZ), if a template describing bidirectional positioning capabilities is required. Here, we shall ignore DZ since for accurate positioning it is common practice to position in a unidirectional manner. Therefore we have;

$$e_{p_1} = 0.003 \text{ in., from Figure 7.5}$$

$$e_{p_2} = 0.001 \text{ in., from Figure 7.6}$$

$$R = 0.0004 \text{ in., from Figure 7.6}$$

$$\therefore \; A_{xx} = 0.0044 \text{ in. (maximum)}$$

The mathematical description of the template now added to the long distance error trend of Figure 7.4 is

$$\left| \delta_{x_1} - \delta_{x_1} \right| = A_{xx} + K_{xx} \left| x_2 - x_1 \right| \qquad (7.1)$$

$$= 0.0044 \text{ in.} + 0.002 \text{ in./ft} \left| x_2 - x_1 \right|$$

This of course is only descriptive of the positioning accuracy along the single line A along which the measurement is made.

The two-dimensional positioning accuracy of the machine in the XY plane will be given by the following expressions derived in accord with the principles of Chapter 3,

$$\left| \delta_{x_2} - \delta_{x_1} \right| = A_{xx} + K_{xx} \left| x_2 - x_1 \right| + A_{xy} + K_{xy} \left| x_2 - x_1 \right|$$

$$(7.2)$$

$$\left| \delta_{y_2} - \delta_{y_1} \right| = A_{yy} + K_{yy} \left| y_2 - y_1 \right| + A_{yx} + K_{yx} \left| y_2 - y_1 \right|$$

and where the parameters are evaluated after taking into account the applicable primary and secondary effects of angular deviations.

Returning to the descriptive statement that is equation (7.1) it is readily apparent that the value of the A_{xx} parameter is excessive and should be reduced. This would be achieved by changing the defective pinions.

For a quantitative comparison of the measured accuracy with the requirements of certain IT accuracy classes, classes IT5 and IT7 may be approximately expressed as:

for IT5 : $\delta = 0.00025$ in. $+ 0.001$ in/ft

for IT7 : $\delta = 0.0005$ in. $+ 0.0025$ in/ft

On a basis of the long distance trend descriptive parameter K_{xx}, the positioning capability falls between these and approximates IT6 class.

There is a practical method of eliminating this error, since the trend shows rather a regular form, and that is by a procedure of corrective programming of the machine. This would, however, mean zeroing the machine to a fixed datum at a specific location in the traverse.

7.4   Case B: The Accuracy of an N.C. Lathe - calibration and set-up of position feed back transducers.

The axis nomenclature of the machine pictured in Plate IX, pg.178 is shown in Figure 7.7 together with the minimum required number of tests the evaluation of which is necessary in order to assess the performance of the machine. The limited number of tests indicated is a consequence of the two-dimensional zone in which cutting and positioning always takes place.

Following again the established procedure:

1)   Determine the offsets with respect to each co-

ordinate motion:
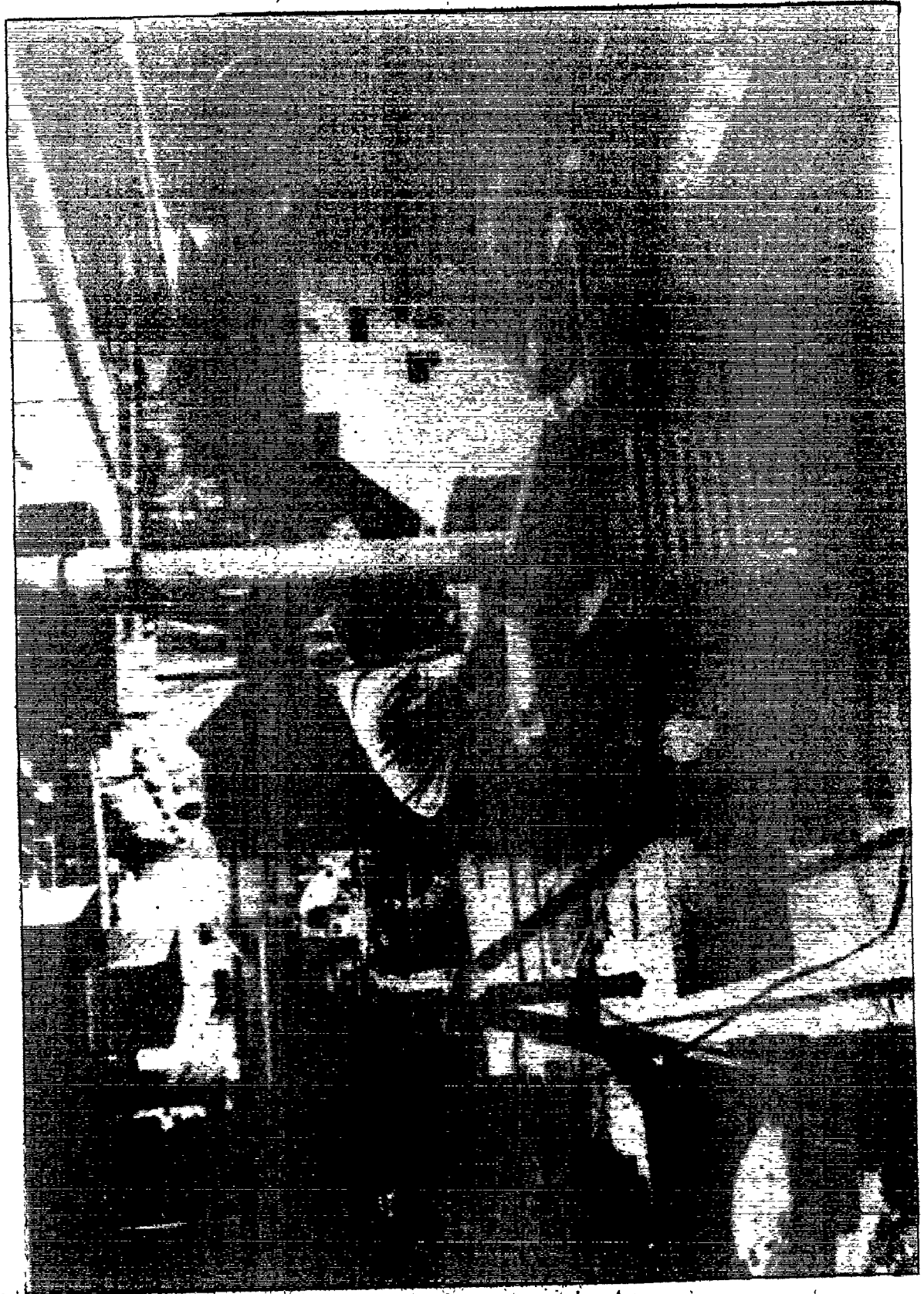
Z longitudinal traverse of the carriage:
lines A and B represent extreme offsets in X.

X transverse traverse of the cross-slide:
there is no offset in Z (unless boring with a
long tool located in the tool post) if we assume
a constant mean length of tool.

2) Specification of tests:

Z motion: straightness of motion - $\delta_x(z)$

along line A

positioning accuracy - $\delta_z(z)$

along line A and, for the effect

of yaw $\epsilon_w(z)$, $\delta_z(z)$ also along line B

X motion: straightness of motion - $\delta_z(x)$

along line C (say)

positioning accuracy - $\delta_x(x)$

also along line C

The primary purpose of this investigation was to set
up the positioning accuracy feedback transducers which con-
sist of a series of precision racks, each 10 in. in length,
spaced along the total length of travel in both axes.

Unlike the previous case, the carriage and cross-
slide drive is quite separate involving a fixed lead screw
and revolving nut. The kinematics of the drive therefore
do not enter the consideration since the position feedback

is derived elsewhere.

As always it is necessary to ideally perform all measurements directly in the working zone of the machine so in this case, the remote interferometer was fixed in the actual position of the tool and the reflector clamped to the chuck between lines A and B.

The initial measurement of positioning accuracy made in 10 in. increments, revealed the errors as shown in Figure 7.8 which exceeded the specified tolerance of $\pm$ 0.001 in. over full length. This was the result of the initial factory set-up of the racks having been made with reference to the displacement readings of a laser system, at the level of the guideway and, as we see in Plate IX, pg. 178 , the tool point in the working zone is considerably higher and more remote from the feedback transducers which are attached to the side of the bed underneath the guideway. i.e. there is a large Abbé offset.

It was a practical operation to adjust the position of the racks with reference to the displacements recorded by the laser in the working zone, care being taken to continuously monitor the environmental changes and the temperature of the machine bed for correct compensation factors, since the duration of the calibration was an entire 8 hour shift. The excellent result is shown in Figure 7.9 where in the working zone over a distance of 25 feet a

maximum error of $\pm$ 0.0002 in. exists.

Unfortunately, spoiling the subsequent accuracy specification was the presence of a rather large cyclic error, superimposed on the graph of Figure 7.9, having a peak to peak amplitude of 0.002 ins. and a period equal to one revolution of the pinion. This was due to an eccentric pinion and it was subsequently replaced.

A similar adjustment procedure was used to accurately space at 10 in. pitch increments the three racks which govern the positioning accuracy of the 30 in. motion available to the cross slide in X. However a very large pitch motion, $\epsilon_z(x)$ shown in Figure 7.11, possibly caused by a weight deformation due to the heavy tool post traversing on an inadequately supported carriage, had the effect of creating a cumulative error in the positioning, accuracy; an effect however periodically corrected due to the finite length of accurately spaced rack segments, Figure 7.10.

Again, the magnitude of this unexpected error was highlighted due to testing the positioning accuracy in the working zone where it should be essentially evaluated for correct specification of machine positioning capability. In the X axis also, a periodic error occuring once per revolution of the pinion existed with an amplitude of approximately 0.002 in. This is identified in Figure 7.12 where it is superimposed on the cumulative error created by

the pitch motion inside the length of 1 rack.

7.5   Case C: Accuracy of a Floor-type Horizontal Boring
        and Milling Machine - an assessment of necessary
        corrective procedures

A picture of the very large type of machine to
which the accuracy evaluation procedures are now applied
is given as Plate VII, pg. 164. Its configuration is
identical to that of Plate I, pg. 43, for which the
minimum number of tests relevant to the working accuracy
of the machine was derived in Chapter 3.7·by reference to
Figure 3.9.

Here, we specify a reduced number of tests, accord-
ing to Figure 7.13, relevant to the usual mode of use of the
machine where positioning and machining always takes place
in practically the same (X,Y) plane when the workpiece is
on the bed-plate, and, for use of the machine with the rotary
table, two groups of measurements are specified according
to whether the (X,Y) group or the $\bar{W}$ group form the setting
motion (see Chapter 4.2).

Again, with this machine the rack and pinion drive
is a separate system from the accurate rack and pinion from
which the positioning feedback signal is derived.

Now, mainly because the positions of each rack seg-
ment are to be determined, the positioning increment of 8 ins.

is chosen as the basic increment, this being the length of
one rack. Ideally however, the chosen basic increment for
the full axis travel positioning test should be an integer
multiple of the distance over which any other error may
occur, so as to be independent. Here, since one revolution
of the resolver occurs in 1.5 ins. of travel, the first un-
affected increment will be 24 ins. Therefore the measure-
ment of $\delta_x(x)$ along line A of Figure 13 made at 8 in. inter-
vals was replotted to eliminate the resolver error only
taking those points at 24 in. intervals, see Figure 7.14.
From this graph the evaluation of positioning accuracy is
made.

In this application an alternative method of pro-
cedure for evaluating the machine tool positioning accuracy
is adopted.

Here, prior to the evaluation, the parameters of the
template form were chosen so as to represent two classes of
accuracy which were thought to be achievable on the machine.
We have seen previously that an approximation to the IT5
and IT7 classes is given by:

for IT5 : $\delta = 0.00025$ in. $+ 0.001$ in/ft

for IT7 : $\delta = 0.0005$ in. $+ 0.0025$ in/ft

However, many measurements have revealed that the proportion
of the short distance errors (i.e. tolerance template con-
stant A) to long distance errors (i.e. tolerance template

constant K) is rather greater than the corresponding ratio

of the two components of errors in the IT system. In order

to be realistic the following accuracy classes of the machine,

chosen with respect to the basic capabilities of the machine

were assumed:

Class A: A = 0.001 ins., K = $\pm$ 0.001 in/ft,
                              DZ = 0.0005 in.

Class B: A = 0.0015 ins., K = $\pm$ 0.0015 in/ft,
                              DZ = 0.001 in.

The graphs of positioning accuracy are then evaluated

and expressed as satisfying one of these classes, or are

better than A or worse than B. The separate tolerance for

dead zone means that when high accuracy is required, posi-

tioning will be made in one direction only thus eliminating

the effect of dead zone. This method of evaluation is

applicable to positioning measurements taken along all the

lines located at all extreme offsets.

e.g. the measurement of $\delta_x(x)$ along line A of

Figure 7.13 plotted at 24 in. intervals is shown in Figure

7.14. Subsequent evaluation shows that mainly the require-

ments of class B are satisfied, the areas where it is not

being indicated by circles.

For angular deviations, normally no separate tolerance

is established and their effects are included in the trans-

lative errors as measured at extreme offsets or as calculated

from other translative measurements and combined with angular measurements.

However, if applying a partial test it is possible to evaluate angular measurements separately, if for instance we are purely interested in the contribution of angular deviations on the positioning accuracy at an extreme offset.

The approach is explained with the example of the pitch motion $\epsilon_z(x)$ of the column while moving in the X direction. The record of this motion as recorded by the laser error-plotting output is shown in Figure 7.15.

This pitch motion affects the positioning error $\delta_x(x)$ as measured along line B at the top of the working zone, Figure 7.13. The error $\delta_x(x)_B$ is a sum of the positioning error $\delta_x(x)_A$ as measured at the bottom of the working zone and of the angular motion $\epsilon_z(x)$ multiplied by the offset y_{max}, this being the vertical distance between lines A and B.

i.e. $\delta_x(x)_B = \delta_x(x)_A + \epsilon_z(x)y_{max}.$

Instead of working according to this formula we will stipulate that the term $\epsilon_z(x) \cdot y_{max}$, which represents an additional error $\delta_x(x)_{add}$ to $\delta_x(x)_A$, be itself within a certain tolerance and that here, these tolerances be given by:

Class A: $\delta_x(x)_{add} \leq 0.0005$ in. $\pm$ 0.0005 in/ft

Class B: $\delta_x(x)_{add} \leq 0.0005$ in. $\pm$ 0.00075 in/ft

which is much less than the primary positioning error.

The graph of $\delta_x(x)_{add}$ is added to Figure 7.15 where it is seen that it satisfies Class A accuracy.

All angular deviations of the column and headstock, were shown to be perfectly satisfactory, contributing only a small additional error to those affected positioning measurements where machining with an offset from the line of the test measurement takes place.

Returning to the positioning accuracy measurement of Figure 7.14 which was typical of the graphs obtained on the machine it may be realised that the machine is very good in the "long distance" errors though relatively bad in the "short distance" errors, mainly due to periodic errors in the pinion (not identified here) and to mismatch of the racks.

Given that it is required to minimise the basic error in any distance (i.e. the 'A' template specification) and this effectively includes the contribution of dead-zone, repeatability and cyclic error amplitudes only, the 'K' template specification is forced on us by the possible short distance errors that exist due to the poor relative positioning of the rack segments.

As we have shown however in section 7.4 the poor relative positioning of the rack segments may be practically

improved using the laser interferometer.

Figures 7.8 and 7.9 are the measurements of positioning made on the N.C. lathe of the previous section before and after a rack adjustment program. The improvement there is marked and a measure of the improvement is given by the template design in each case:

Figure 7.8 K_{zz} = 0.0025 in./12 in.

Figure 7.9 K_{zz} = 0.00025 in./12 in.

This indicates a ten-fold improvement in accuracy, approximating to an improvement in accuracy class from IT7-IT8 to IT1 if the other short distance errors also are minimised.

7.6   Case D: Measurements of Straightness of Motion: similarity of features to measurements of positioning accuracy, interpretation and examples.

It has been previously stated in Chapter 3.5.4, with respect to Equation 3.7, that we assume the same form for the errors of straightness of motion as was proposed for the positioning error since these basic measurements will exhibit similar trends.

However, depending on whether the measurement considered is of positioning accuracy or straightness, the interpretation of the cause of the identified errors e.g. e_p, DZ, etc., will be different.

Let us examine then and briefly explain the relevance of these parameters in each case.

(a) Positioning accuracy measurements

(i) DZ will be identified as the dead zone due primarily to the backlash existing in the drive transmission.

(ii) e_p will be a direct measurement of the periodicity occuring in an element or elements of the drive transmission to a moving machine member, or a measurement as transmitted by the drive of the periodicity of, or present in, the element from which the positioning feed-back signal is derived e.g. servo-resolver or linear grating.

(b) Straightness of motion measurements

(i) DZ will be caused typically by some slackness existing in the guideways of a moving machine member and will therefore be a consequence of some unwanted angular motion within the slackness, occuring on slide reversal.

(ii) e_p.Under certain circumstances periodic errors may similarly be identified in straightness measurements - again as a consequence of some unwanted angular motion.

e.g. returning to the machine of section 7.3, the measurement of $\delta_y(x)$ as indicated in Figure 7.2 was per-

formed by tracing a master granite square with an electronic pick-up and continuously recording the signal on a chart recorder which had the useful facility of a drive reversal for recording the error motion in the return direction on the same portion of graph as the forward motion. We have already seen in Figure 7.5 how errors occur once-per-tooth of the fourteen tooth driving pinion and it was stated that this error existed in the matching pinion on the other side of the gantry. With reference to Figure 7.16, it may be realised how an interaction of the errors existing in both the pinions, combined with the effect of the offset in X of the machine spindle nose (with respect to the line passing through the axis of the driving pinions) where the measuring probe was correctly located, had the effect of producing a straightness deviation $\delta_y(x)$ as shown in Figure 7.17. Here, we may clearly identify twenty-eight peaks over a 10.5 in. interval of traverse which is one revolution of a pinion and which corresponds to a slight crab-wise motion of the gantry on the bed as each pinion alternately drives and is driven.

The amplitude of the motion, 0.001 in. is probably not too significant in practical terms for its effect in machining, the effect being smoothed by overlap cutting of a comparatively large diameter of milling cutter. However, especially in machining at high traverse rates, the effect

would tend to affect the possible surface finish.

The feature of Figure 7.17 is rare though and normally some extremely good straightness of error motions have been recorded:

e.g. the $\delta_x(y)$ and $\delta_y(x)$ measurements on the machine shown in Plate II pg. 63 and as specified in Figure 4.2b. These are complementary measurements from which we may also assess (X,Y) orthogonality as well as the straightness of motion proper. Both the recorded motions as shown in Figures 7.18 and 7.19 are really incredibly straight, for over a traverse of three feet an error of straightness of not even 0.0001 in. exists.

N.B. there is no significance in the "progressive error" of these graphs this being due to misalignment of the square with axis motion. Taken together however, the out-of-squareness of X, Y motions can be assessed as 0.0002 in./3 ft.

CHAPTER 8

CONCLUSIONS

Because of the magnitude of the capital investments being made in increasingly sophisticated machine tools it is becoming increasingly important to base the relationship between the manufacturer and the buyer of machine tools on as accurate specifications as possible.

A basis for the development of a new system of geometric accuracy testing suitable for high precision machine tools, especially numerically controlled machine tools, has been created. The system includes the concept of defining the attainable accuracy throughout the determined working zone of the machine and as affected by the further effects of thermal, weight and clamping deformations. Basic rules have been established concerning the correct specification of a thermal duty cycle.

Spindle rotation accuracy is formulated as a separate test and suitable measuring and test methods are described together with a system of evaluation.

Utilisation of the procedures as documented in this thesis would, it is felt, provide a sound basis for the quotation of a meaningful machine tool accuracy capability statement.

FIGURES
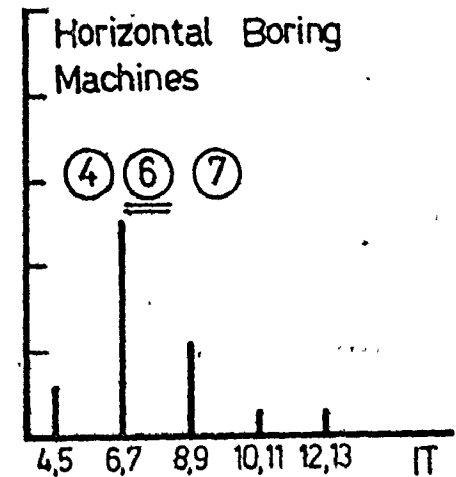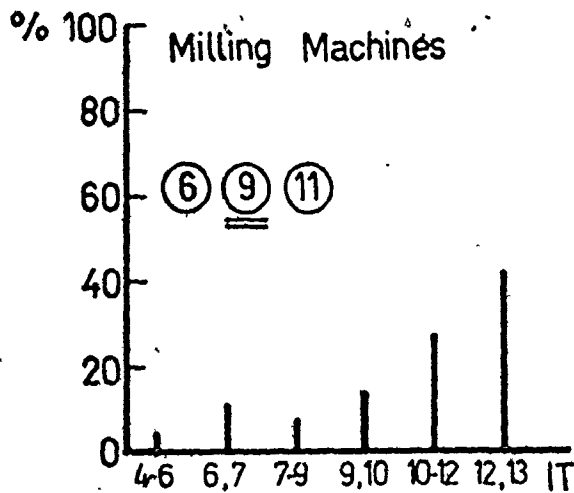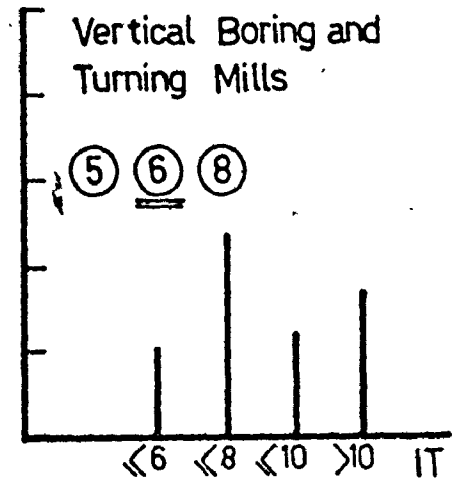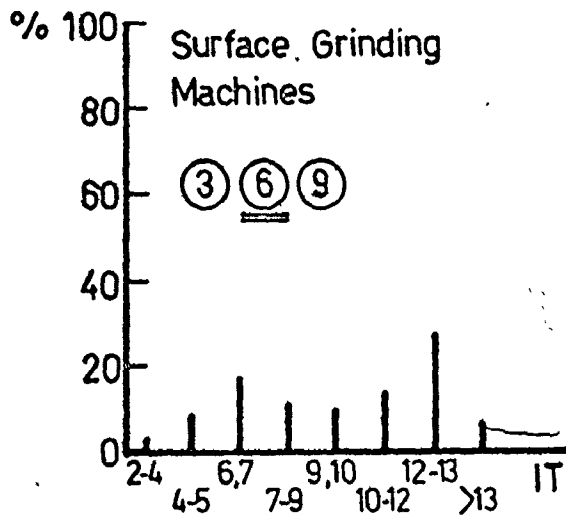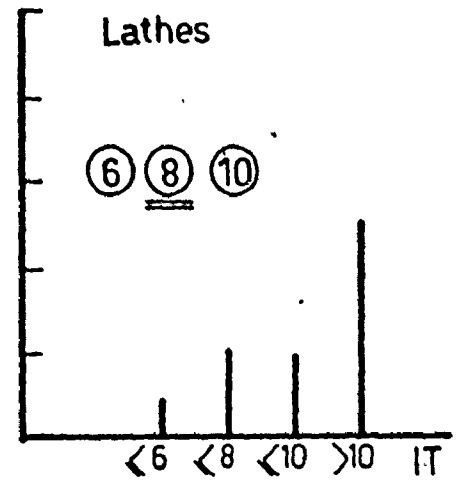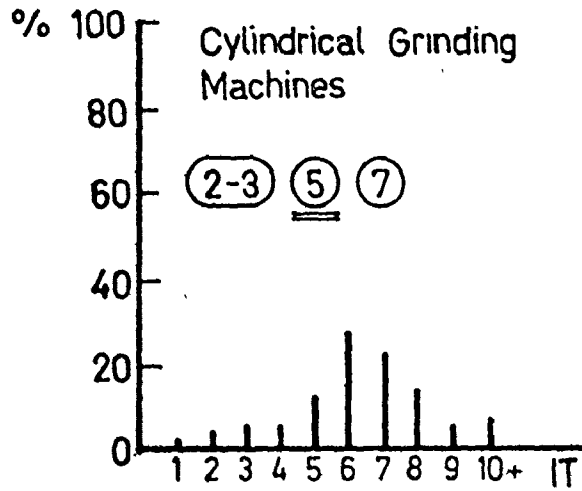
Figure 1.1   Pera Survey, IT Grades Required for
work on Various Machine Tool Types [1] [2]
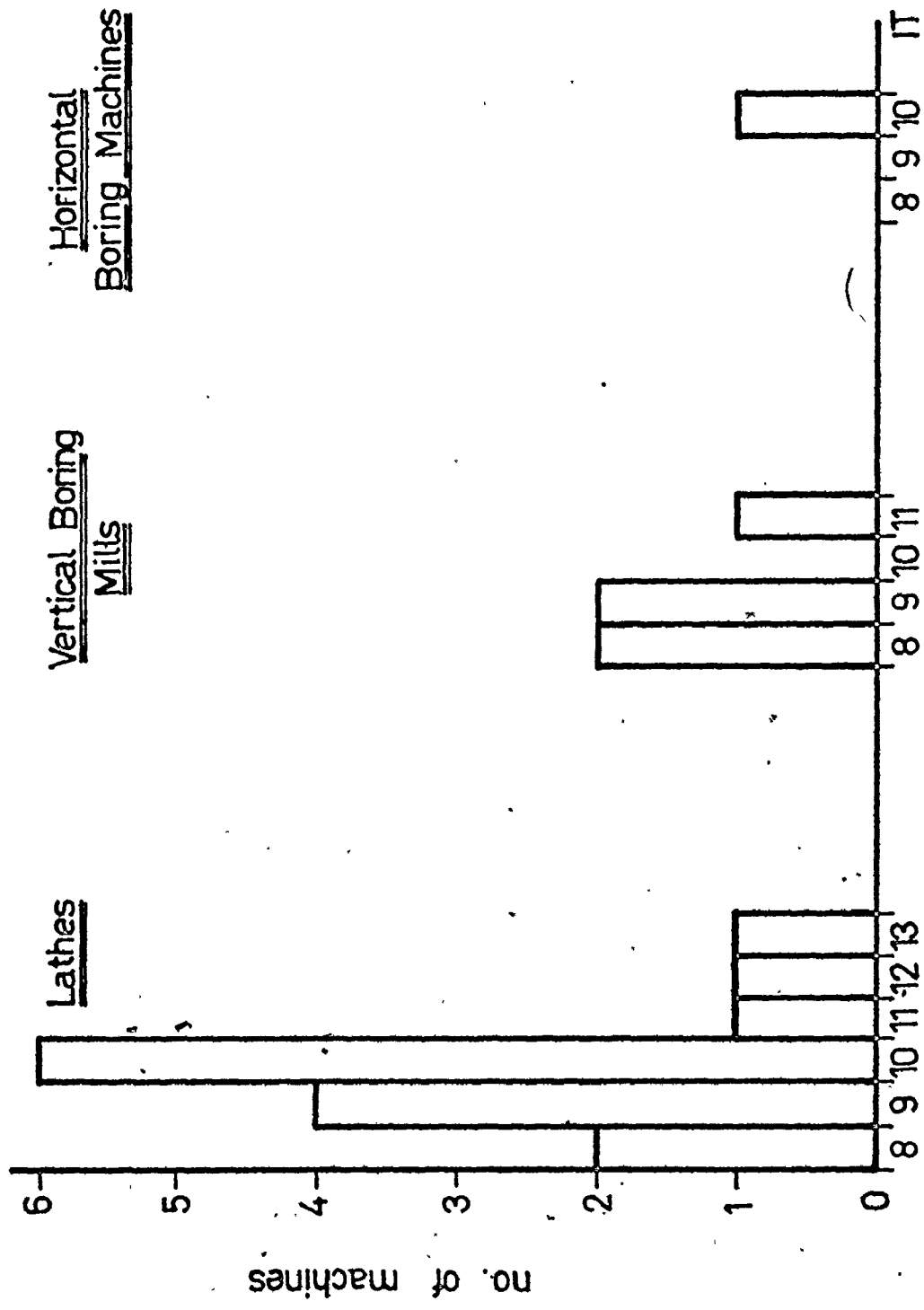
Figure 1.2   IT Accuracy Grades of BAS Test Workpieces [4].
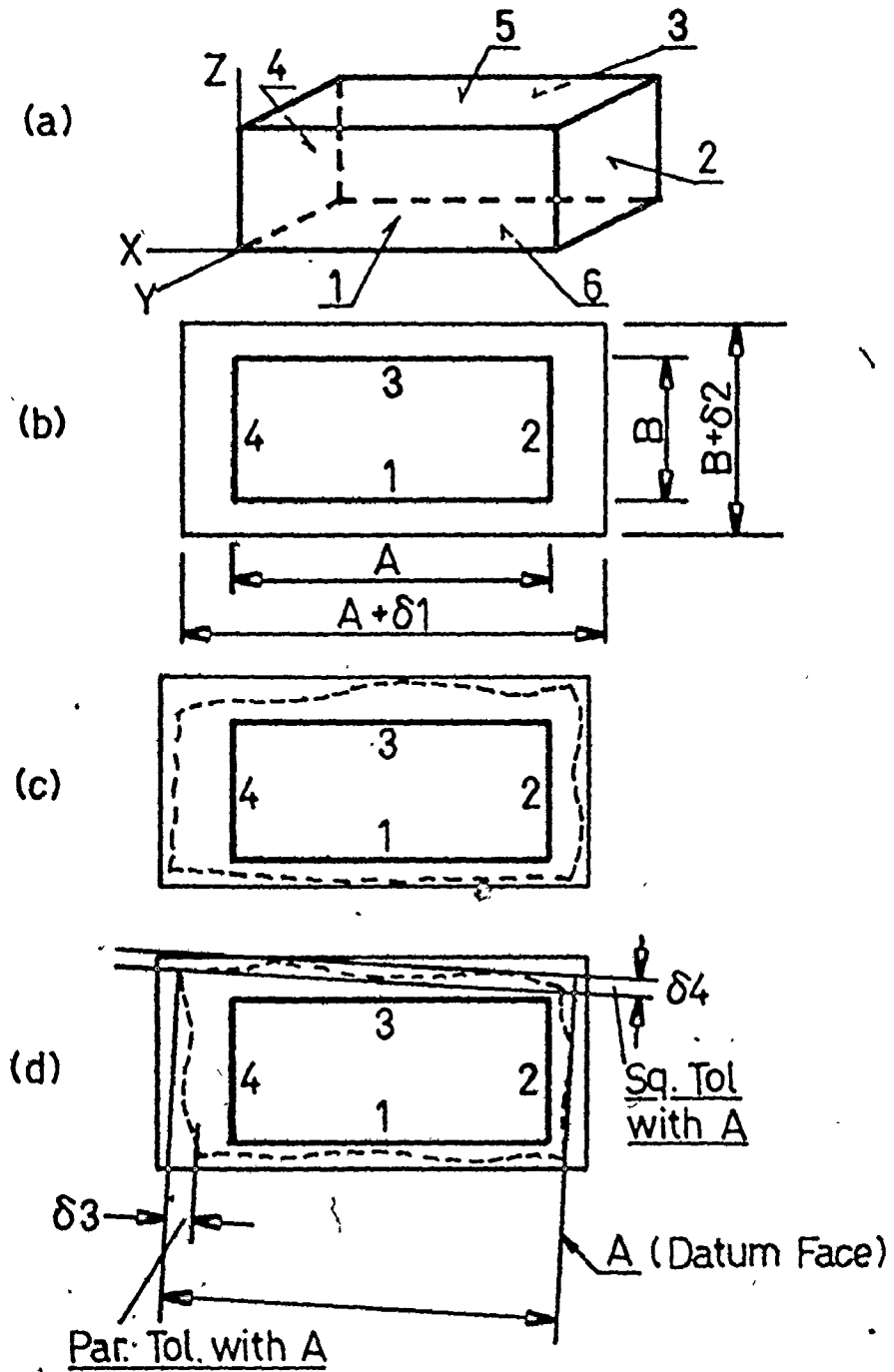
Figure 2.1   Errors of a Box-Type Workpiece
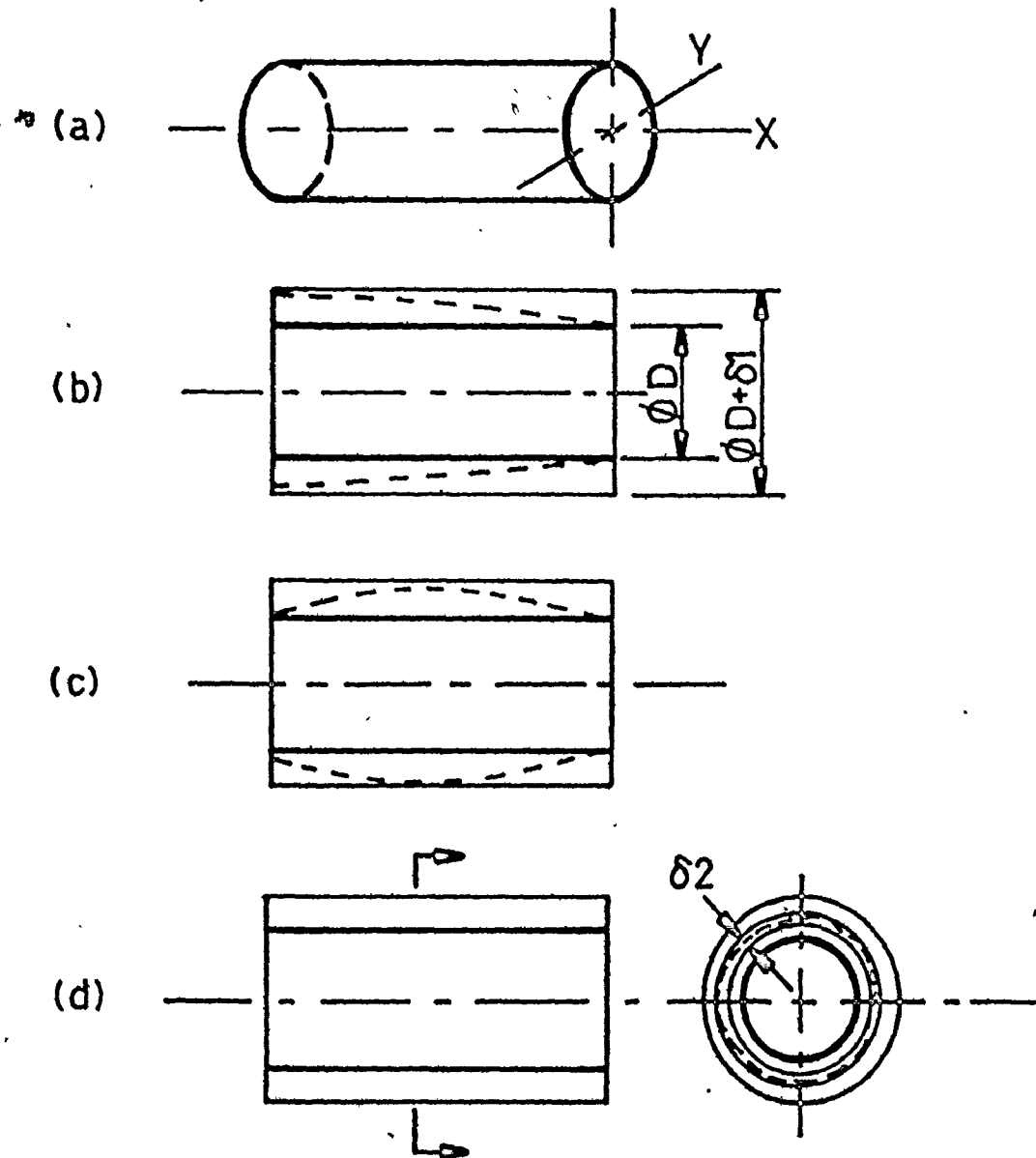
Figure 2.2   Errors of a Cylindrical Workpiece

TABLE 7. — Numerical values of standard tolerances

1. Metric values

Grade	01	0	1	2	3	4	5	6	7	8	9	10	11	12	13	14*	15*	16*
<3	0.3	0.5	0.8	1.2	2	3	4	6	10	14	25	40	60	100	140	250	400	600
>3 to 6	0.4	0.6	1	1.5	2.5	4	5	8	12	18	30	48	75	120	180	300	480	750
>6 to 10	0.4	0.6	1	1.5	2.5	4	6	9	15	22	36	58	90	150	220	360	580	900
>10 to 18	0.5	0.8	1.2	2	3	5	8	11	18	27	43	70	110	180	270	430	700	1100
>18 to 30	0.6	1	1.5	2.5	4	6	9	13	21	33	52	84	130	210	330	520	840	1300
>30 to 50	0.6	1	1.5	2.5	4	7	11	16	25	39	62	100	160	250	390	620	1000	1600
>50 to 80	0.8	1.2	2	3	5	8	13	19	30	46	74	120	190	300	460	740	1200	1900
>80 to 120	1	1.5	2.5	4	6	10	15	22	35	54	87	140	220	350	540	870	1400	2200
>120 to 180	1.2	2	3.5	5	8	12	18	25	40	63	100	160	250	400	630	1000	1600	2500
>180 to 250	2	3	4.5	7	10	14	20	29	46	72	115	185	290	460	720	1150	1850	2900
>250 to 315	2.5	4	6	8	12	16	23	32	52	81	130	210	320	520	810	1300	2100	3200
>315 to 400	3	5	7	9	13	18	25	36	57	89	140	230	360	570	890	1400	2300	3600
>400 to 500	4	6	8	10	15	20	27	40	63	97	155	250	400	630	970	1550	2500	4000

(Standard tolerances in microns (1 μ = 0.001 mm) for diameter steps in millimetres)

* Up to 1 mm, grades 14 to 16 are not provided.

NOTE. — Numerical values amended from the former ISA System are framed in a bold line.

2. Inch values

Grade	01	0	1	2	3	4	5	6	7	8	9	10	11	12	13	14*	15*	16*
<0.12	0.012	0.02	0.03	0.05	0.08	0.12	0.15	0.25	0.4	0.6	1.0	1.6	2.5	4.0	6.0	10.0	16.0	25.0
>0.12 to 0.24	0.015	0.025	0.04	0.06	0.10	0.15	0.2	0.3	0.5	0.7	1.2	1.8	3.0	5.0	7.0	12.0	18.0	30.0
>0.24 to 0.40	0.015	0.025	0.04	0.06	0.10	0.15	0.25	0.4	0.6	0.9	1.4	2.2	3.5	6.0	9.0	14.0	22.0	35.0
>0.40 to 0.71	0.02	0.03	0.05	0.08	0.12	0.2	0.3	0.4	0.7	1.0	1.6	2.8	4.0	7.0	10.0	16.0	28.0	40.0
>0.71 to 1.19	0.025	0.04	0.06	0.10	0.15	0.25	0.4	0.5	0.8	1.2	2.0	3.5	5.0	8.0	12.0	20.0	35.0	50.0
>1.19 to 1.97	0.025	0.04	0.06	0.10	0.15	0.3	0.4	0.6	1.0	1.6	2.5	4.0	6.0	10.0	16.0	25.0	40.0	60.0
>1.97 to 3.15	0.03	0.05	0.08	0.12	0.2	0.3	0.5	0.7	1.2	1.8	3.0	4.5	7.0	12.0	18.0	30.0	45.0	70.0
>3.15 to 4.73	0.04	0.06	0.1	0.15	0.25	0.4	0.6	0.9	1.4	2.2	3.5	5.0	9.0	14.0	22.0	35.0	50.0	90.0
>4.73 to 7.09	0.05	0.08	0.12	0.2	0.3	0.5	0.7	1.0	1.6	2.5	4.0	6.0	10.0	16.0	25.0	40.0	60.0	100.0
>7.09 to 9.85	0.08	0.12	0.2	0.3	0.4	0.6	0.8	1.2	1.8	2.8	4.5	7.0	12.0	18.0	28.0	45.0	70.0	120.0
>9.85 to 12.41	0.10	0.15	0.25	0.3	0.5	0.6	0.9	1.2	2.0	3.0	5.0	8.0	12.0	20.0	30.0	50.0	80.0	120.0
>12.41 to 15.75	0.12	0.2	0.3	0.4	0.5	0.7	1.0	1.4	2.2	3.5	6.0	9.0	14.0	22.0	35.0	60.0	90.0	140.0
>15.75 to 19.69	0.15	0.25	0.3	0.4	0.6	0.8	1.0	1.6	2.5	4.0	6.0	10.0	16.0	25.0	40.0	60.0	100.0	160.0

(Standard tolerances in 0.001 in for diameter steps in inches)

Dimensions in millimetres
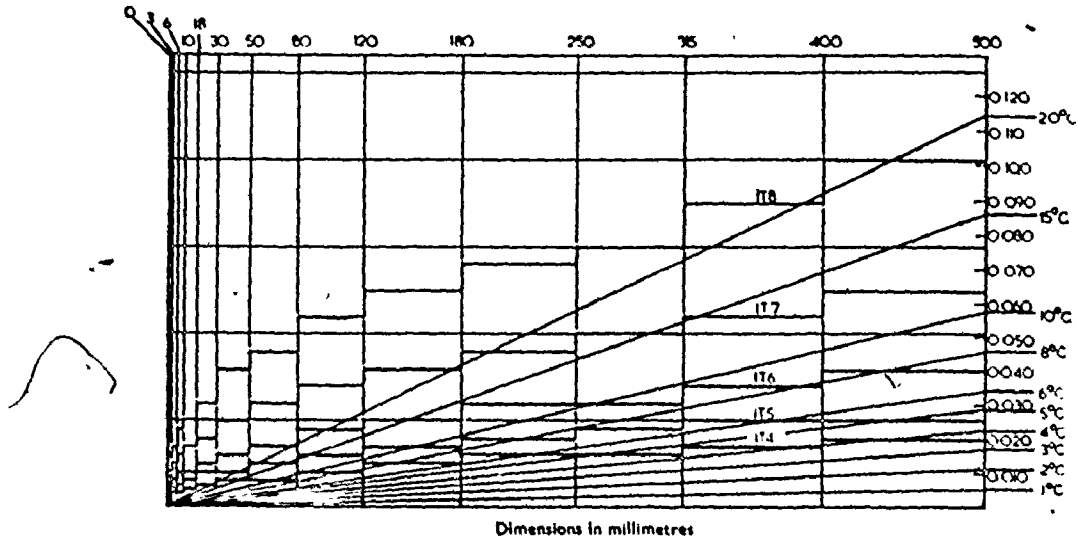
Effects of temperature as related to tolerance grades IT 4 to IT 8 for sizes up to 500 mm

Dimensions in millimetres
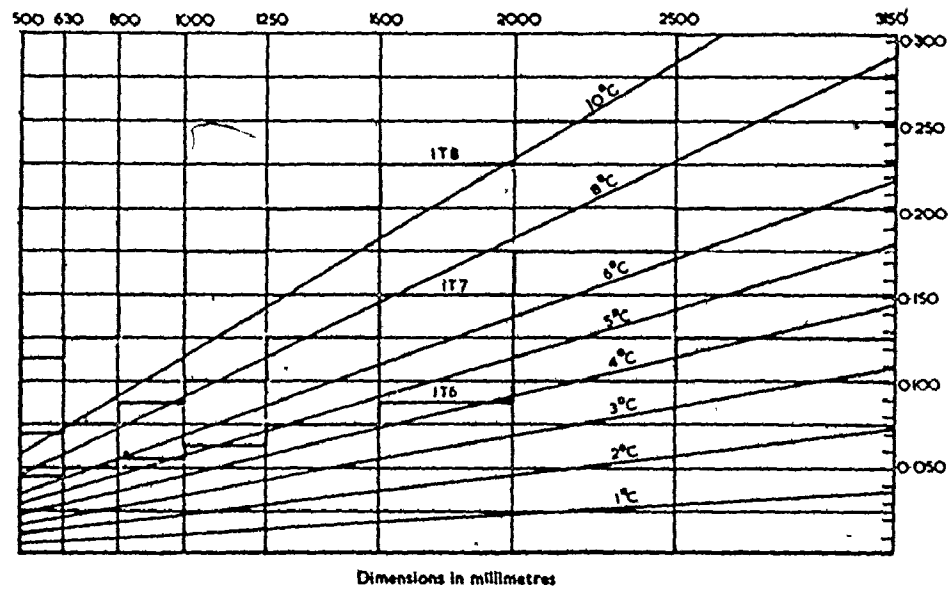
Effects of temperature as related to tolerance grades IT 6 to IT 8 for sizes above 500 mm up to 3150 mm

Figure 2.4   IT Tolerance Grades - Including Effects of.
ire [12]

Testing Vertical Milling Machines — 3

Fig. 1 · Fig. 2 · Fig. 3 · Fig. 4 · Fig. 5 · Fig. 6 · Fig. 7 · Fig. 8 · Fig. 9 · Fig. 10 · Fig. 11 · Fig. 12
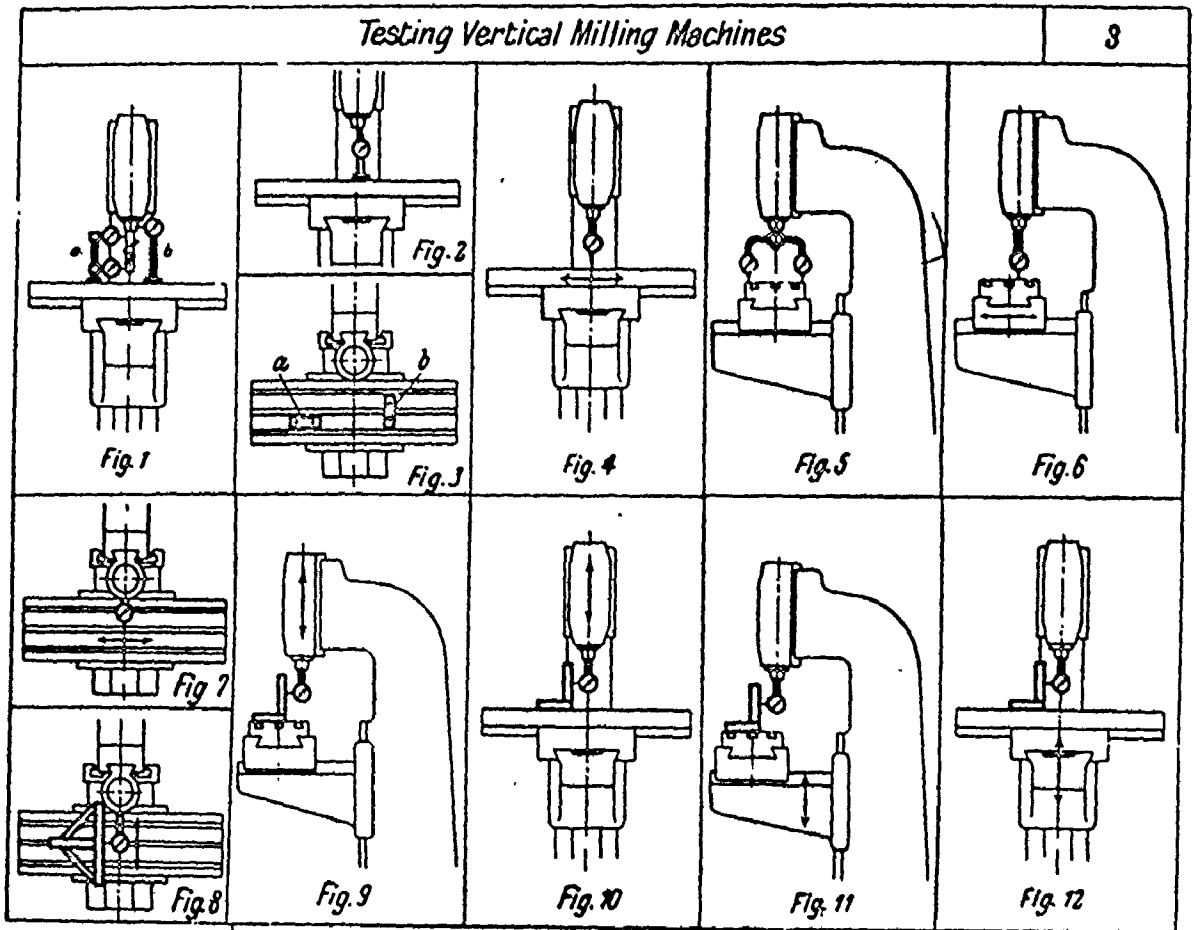
Test Chart for Vertical Milling Machines		No. 3 Chart 1
Test to be Applied	Fig. No.	Permissible Error
Levelling of work table: Work table flat or level in longitudinal direction	3a	mm. ±0·04 per 1,000 mm.
Ditto, in transverse direction ..	3b	±0·04 per 1,000 mm.
Cutter spindle: Internal taper of cutter spindle runs true: (1) Nearest to spindle nose .. (2) At a distance of 300 mm. (12 in.).	1a	0·01 0·02
External taper runs out of truth ..	1b	0·01
Cutter spindle for axial slip in machines with up to 50 mm. (2 in.) dia. of front bearing Over 50 mm. (2 in.) dia. of front bearing	2	0·01 0·02
Work table: Rise and fall of table, in its longitudinal movement Addition, over 500 mm. movement 0·01 per 500 mm.	4	0·02 per 500 mm. 0·01 per 500 mm.
Work table square with cutter spindle in plane through longitudinal axis of machine (turn round method; table rising towards the front side only)	5	0 to 0·02 per 300 mm.
Work table square with cutter spindle in plane perpendicular to that through longitudinal axis (turn round method)	5	0·02 per 300 mm.

Test Chart for Vertical Milling Machines		No. 3 Chart 2
Test to be Applied	Fig. No.	Permissible Error
Surface of work table parallel with its transverse movement	6	mm. 0·02 per 300 mm.
Centre T-slot parallel with longitudinal table movement	7	0·02 per 300 mm.
Centre T-slot square with transverse table movement	8	0·02 per 300 mm.
Width of T-slots: From 10 to 12 mm. (⅜ to ½ in.) .. From 14 to 18 mm. (? to ? in.) .. Over 18 mm. (? in.)		0 to +0·015 0 to +0·02 0 to +0·025
Column: Vertical adjustment of cutter slide square with work table in plane through longitudinal axis of machine (table rising towards the front side)	9	0 to 0·02 per 300 mm.
Ditto, in plane perpendicular to that through longitudinal axis	10	0·02 per 300 mm.
Column ways for knee square with work table, incline towards front and rear side, respectively	11	0·02 per 300 mm.
Ditto, lateral incline	12	0·02 per 300 mm.

a)

pitch

P

yaw

roll

b)

O

c)

d)

e)

S

f)

S

g)

h)

S   M   A

j)

C

A   B

k)

Me   for   s of Motion
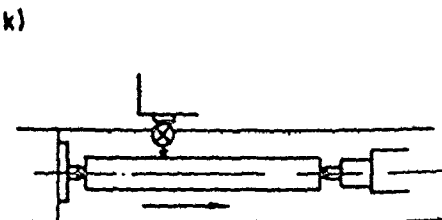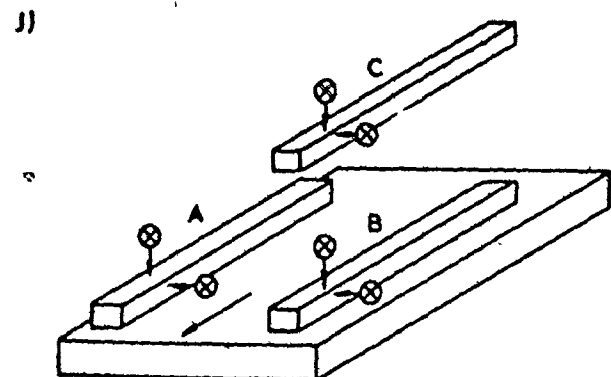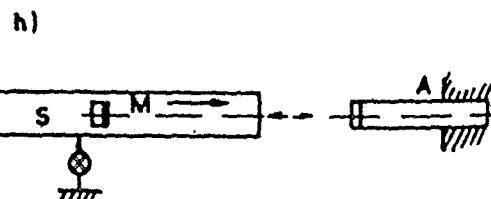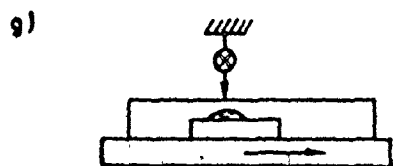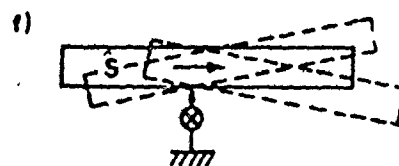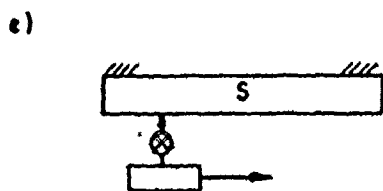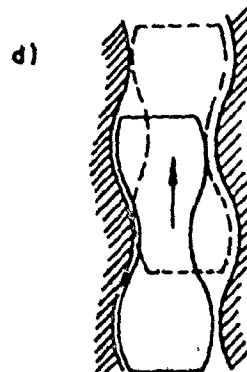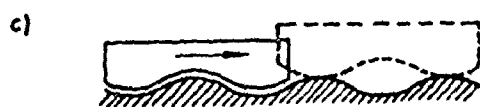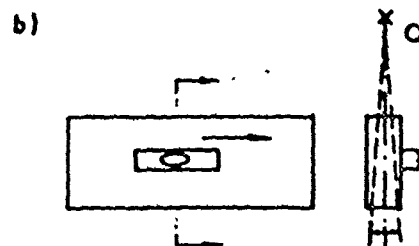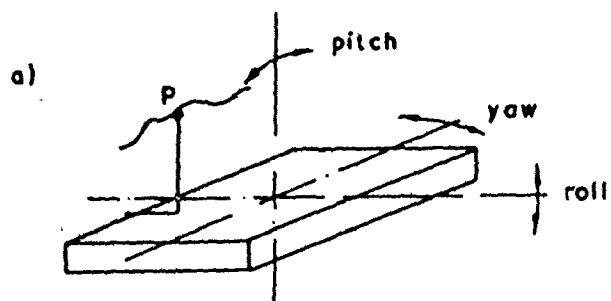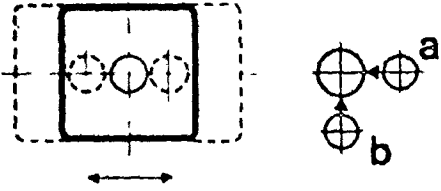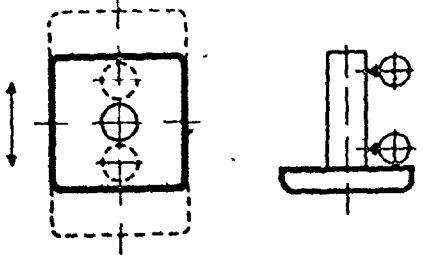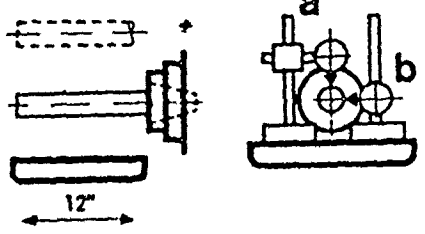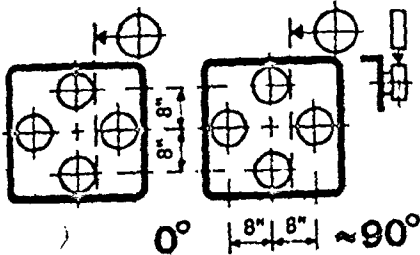
No Measurements	Methods and conditions of testing Testing-appliances	Differences in .00001"		
		permitted	before / after delivery	measured

5 Truth of longitudinal guide ways

Dial indicator in spindle against a precision cylinder
Angular position of table: 0°
Transverse position: 12"
Longitudinal position: 0"
12"
24"

a) longitudinal plane — 24
b) transverse plane — 24

6 Truth of transverse guide ways

As under 5, except:
Longitudinal position: 24"
Transverse position: 2"
12"
22"

a) longitudinal plane — 32
b) transverse plane — 32

7 Truth of vertical guide ways

Measured with dial indicator against measuring-arbor in spindle, using longitudinal motion
Transverse position: 12"
Position of headstock: 22"
12"
2"

a) vertical plane — 20
b) horizontal plane — 20

8 Perpendicularity of transverse to longitudinal guide ways

Measured from spindle: Adjust lines tangential to measuring-discs according to transverse and longitudinal motions. Rotation of table (≈ 90°) Align parallel to longitudinal motion, and measure the deviation on the transverse motion

Error = 1/2 of deviation measured

Errors — 14

0° |8"|8"| ≈90°

Figure 2.7 The DIXI Test of Motions in the Working Zone [19]
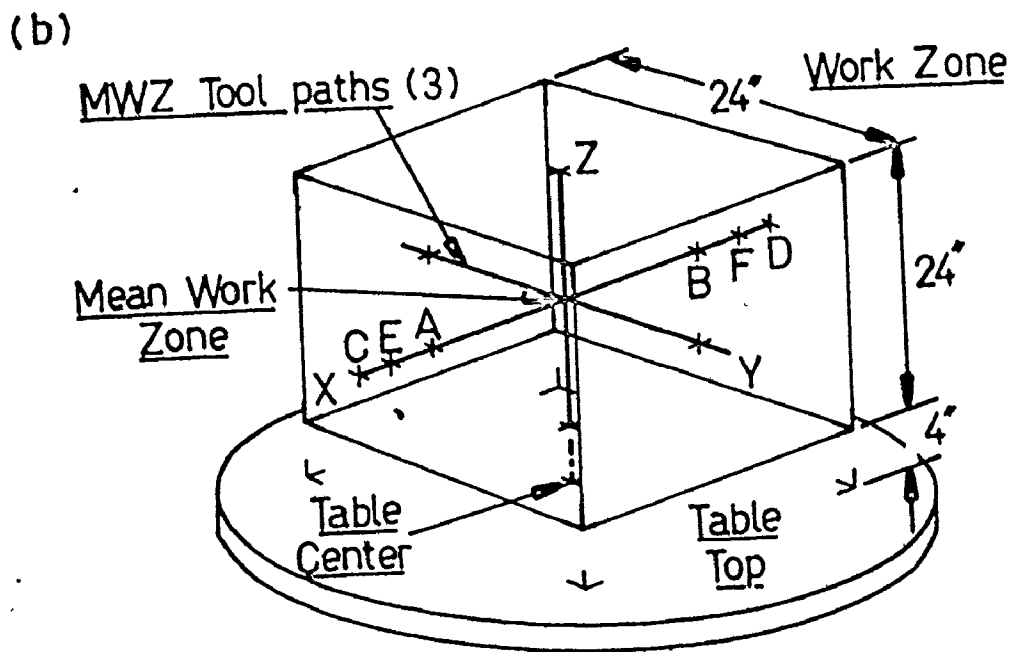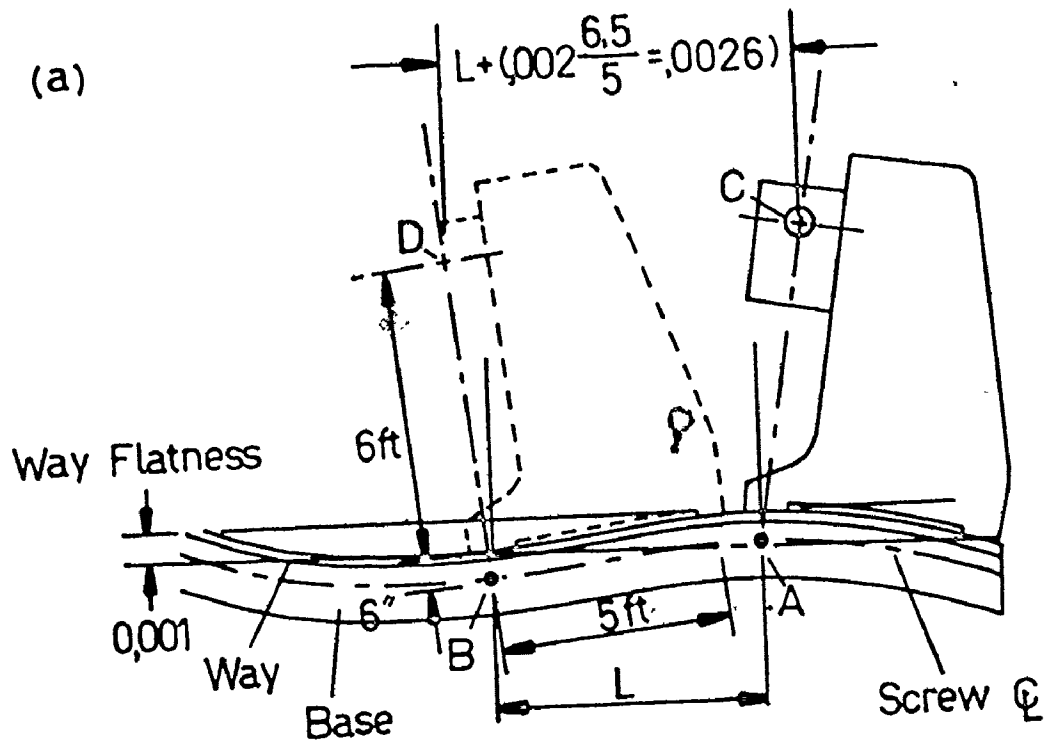
Figure 2.8 The Sundstrand Mean Working Zone Procedure [22]
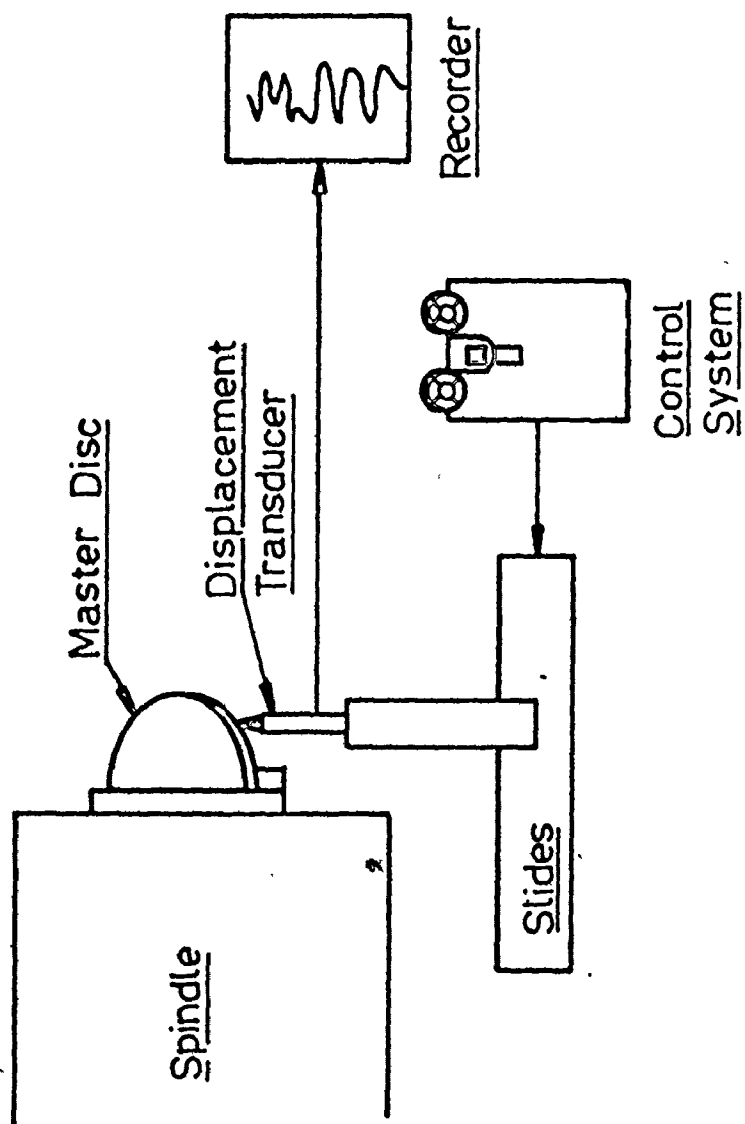
Figure 2.9 The LRL set-up of a Master Part Trace Test [23]
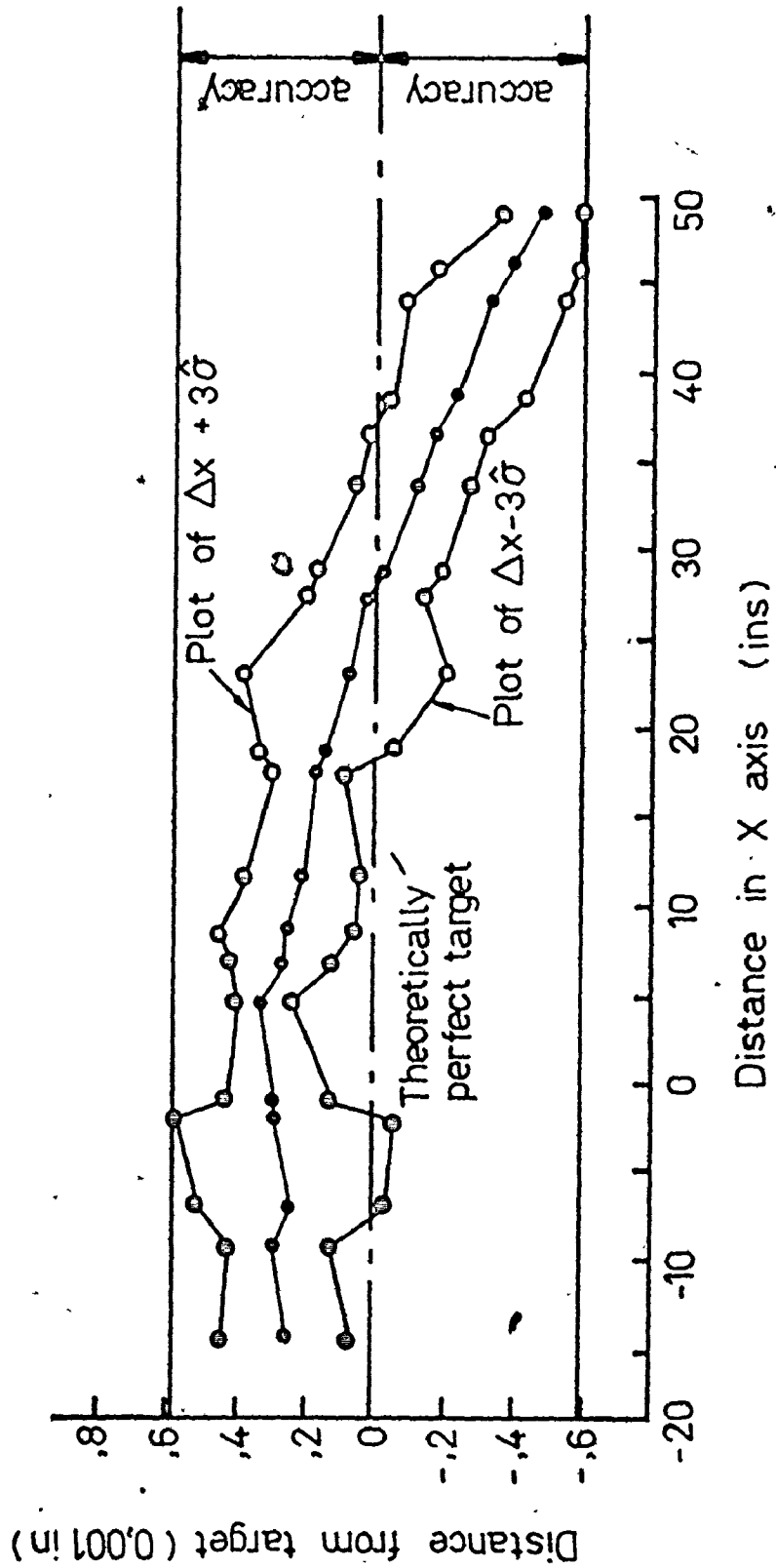
Figure 2.10 Positioning Accuracy Evaluation according to NMTBA [27]
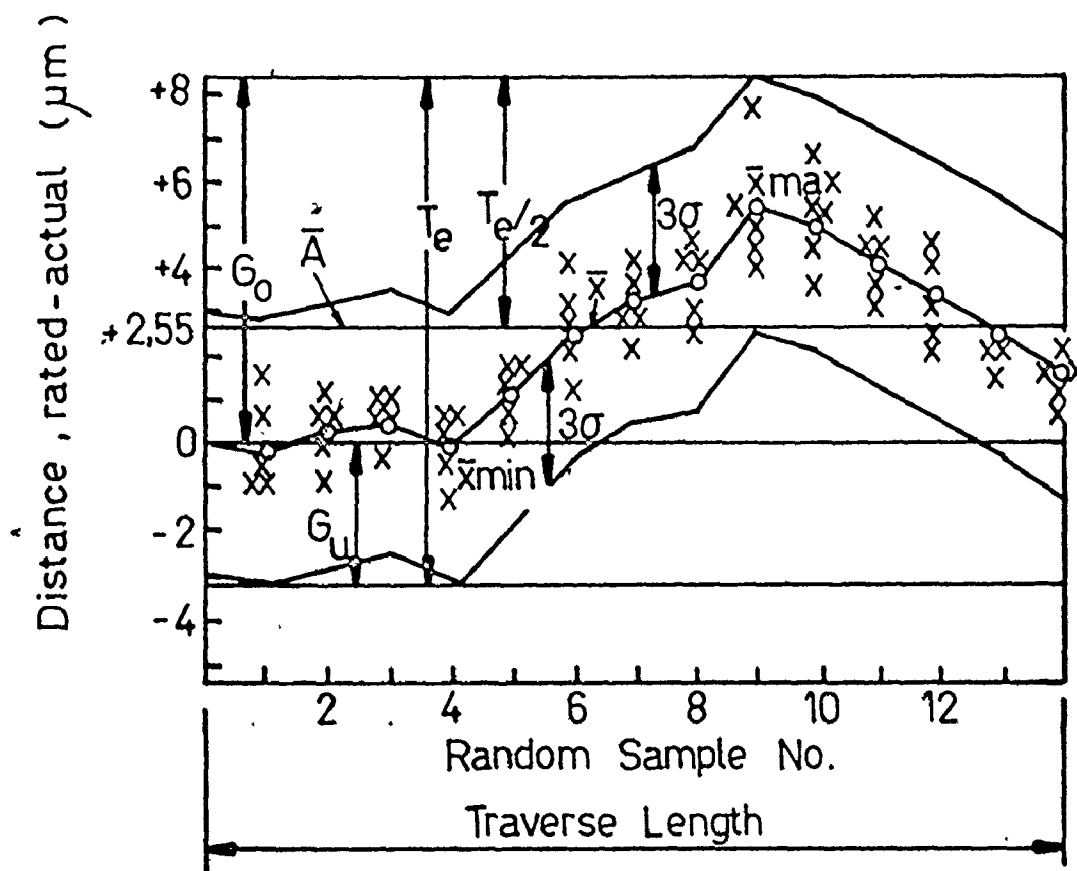
Mean Position Deviation $\bar{A} = \dfrac{\bar{x}max + \bar{x}min}{2} = \dfrac{5{,}3 - 0{,}2}{2}\,\mu m$

$$= 2{,}55\,\mu m$$

Tolerance Limits $G_{o,u} = \bar{A} \pm (\dfrac{\bar{x}max - \bar{x}min}{2} + 3\sigma) = 2{,}55 \pm 5{,}648\,\mu m$

Positioning Tolerance $T_e = \bar{x}max - \bar{x}min + 6\sigma = 11{,}3\,\mu m$

Position Scatter Width $R_p = 6\sigma = 5{,}8\,\mu m$

Figure 2.11 Positioning Accuracy Evaluation according to VDI 3254 [26]
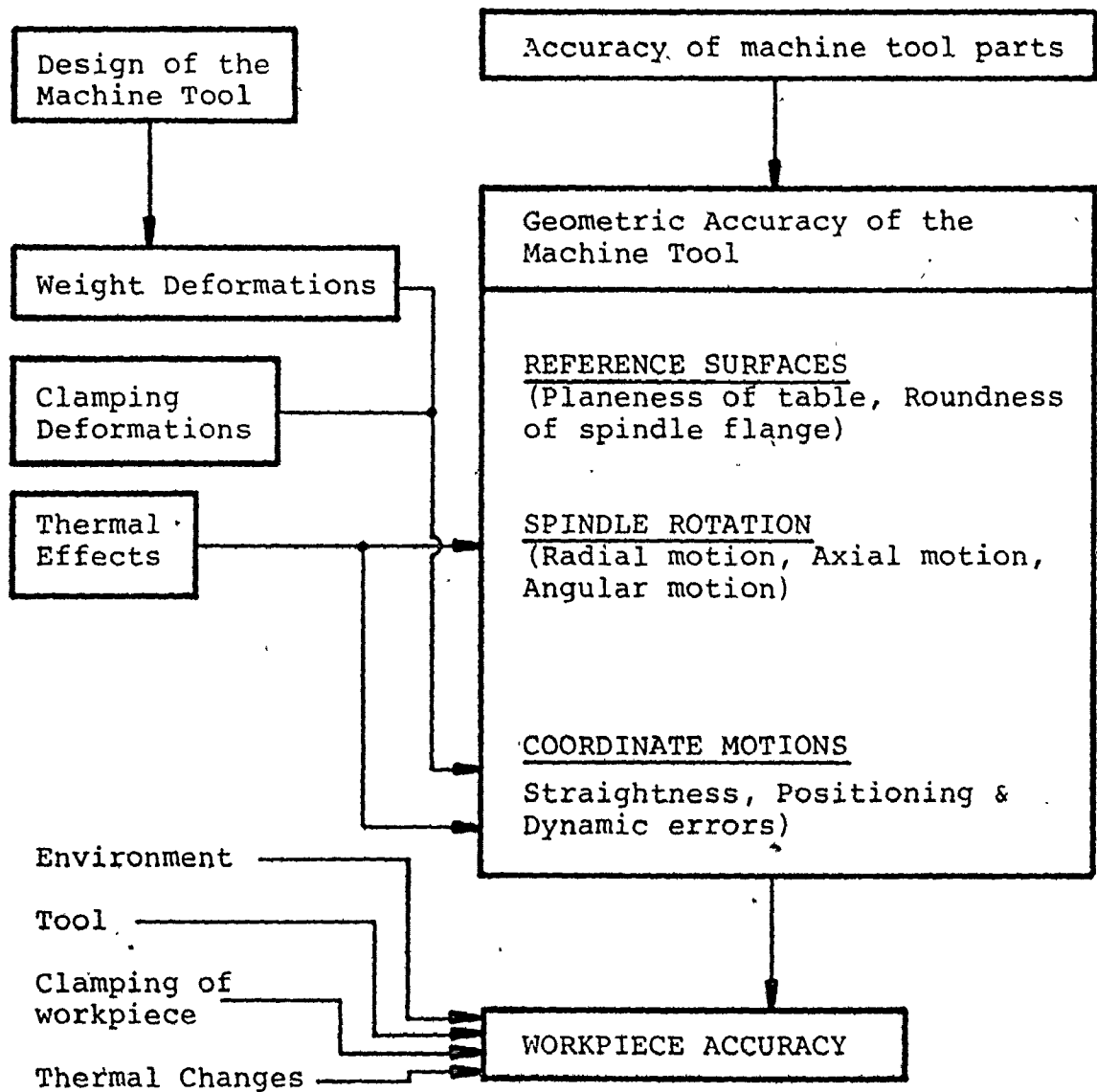
Figure 3.1   The Inter-relationship of Factors Influencing
              Workpiece Accuracy
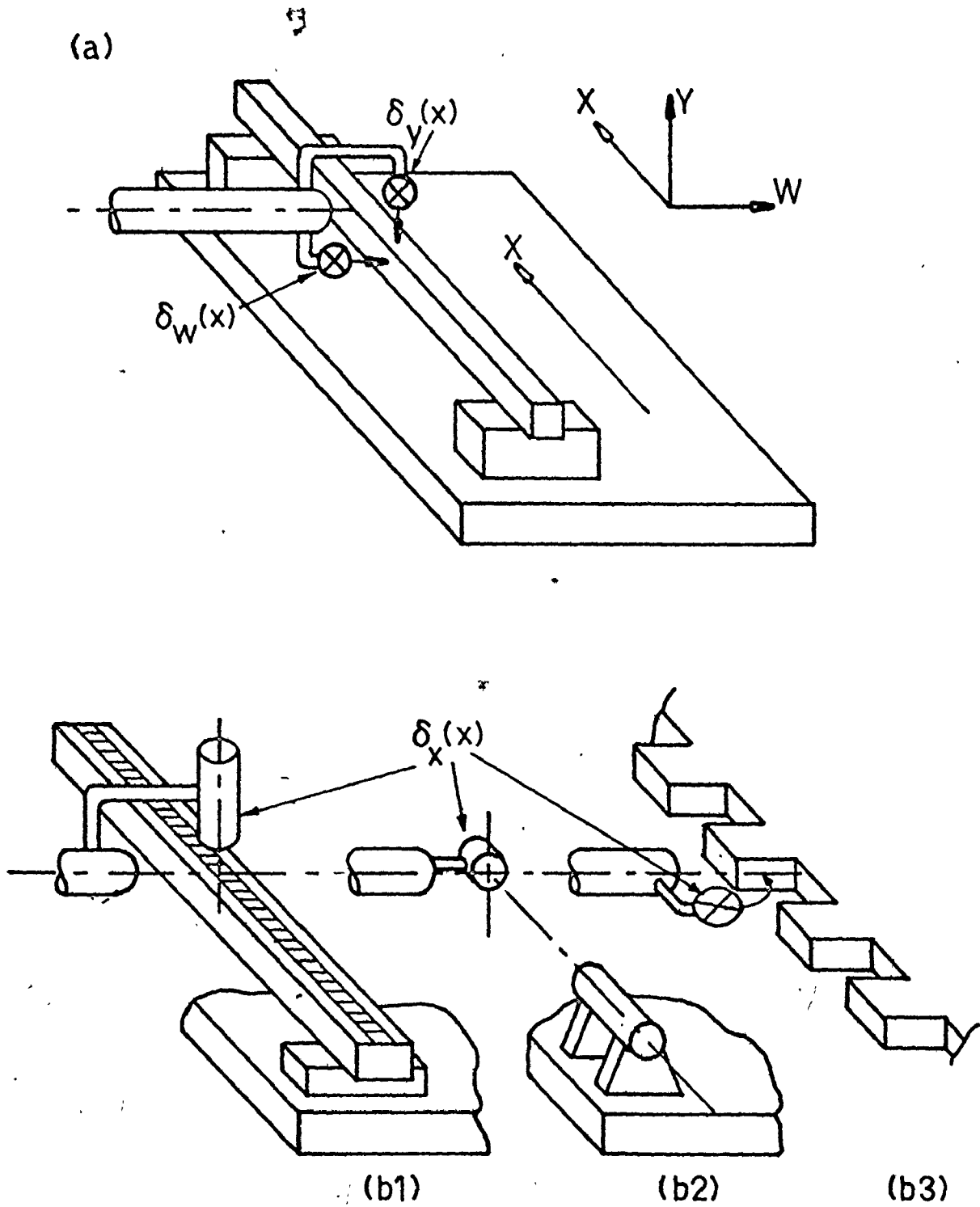
Figure 3.2   The Three Basic Translative Error Measurements
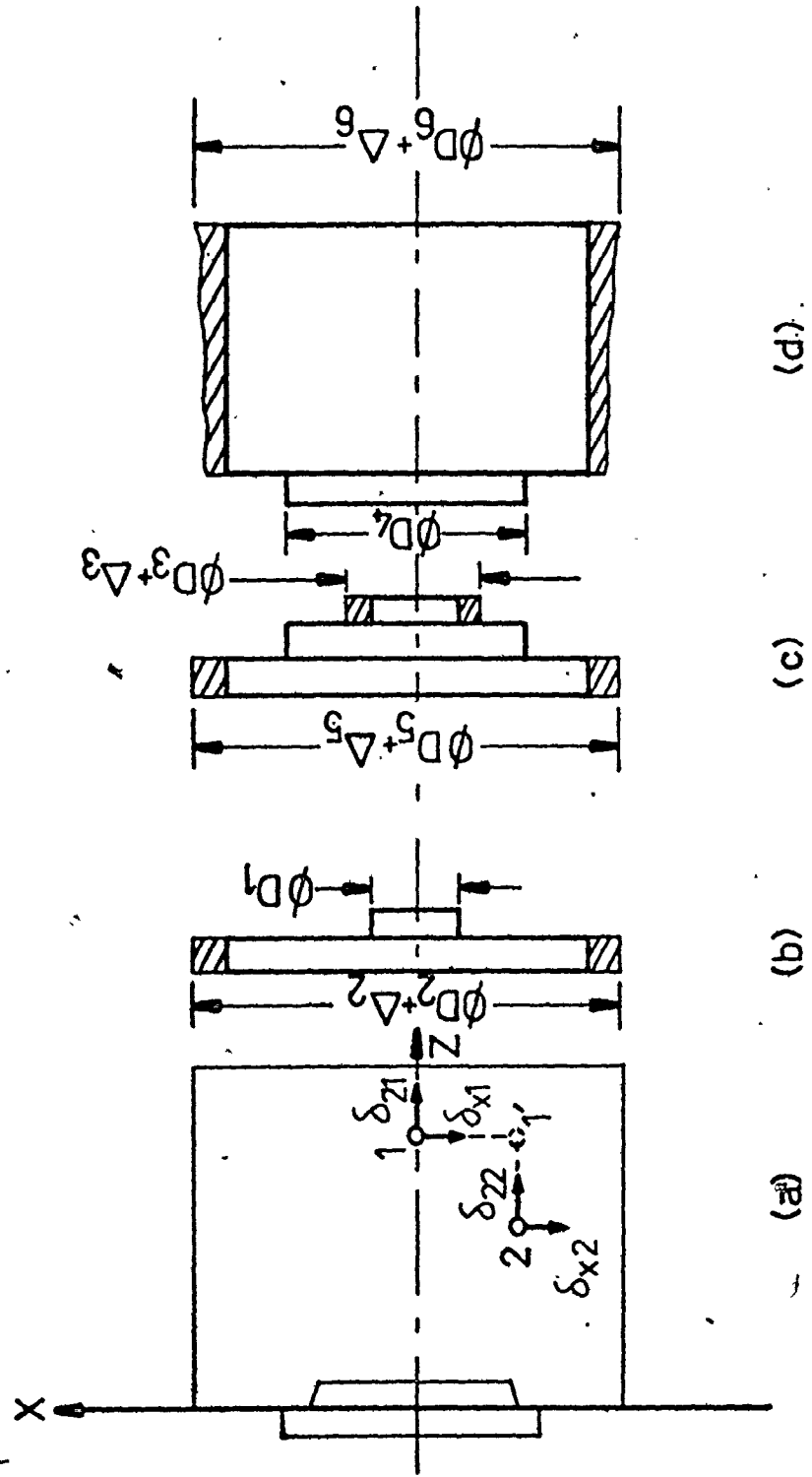
Figure 3.3   Tolerancing Principles in a Two Dimensional Zone
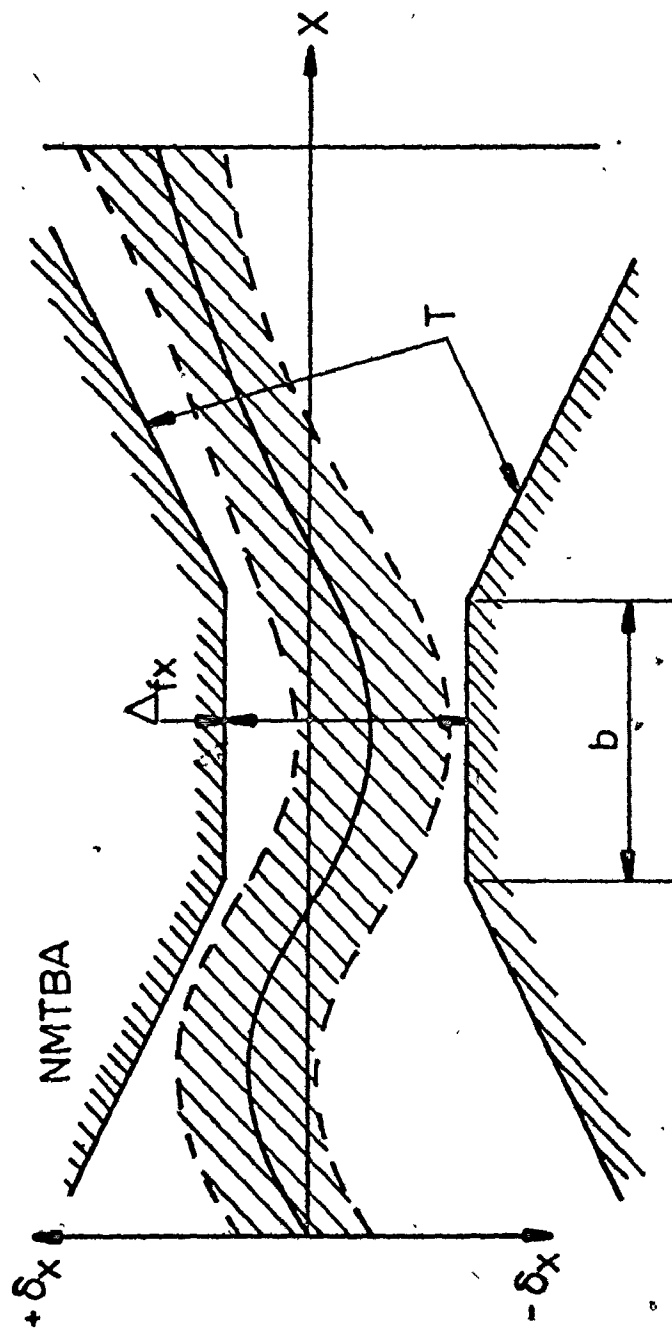
Figure 3.4 The NMTBA Positioning Accuracy Evaluation Template
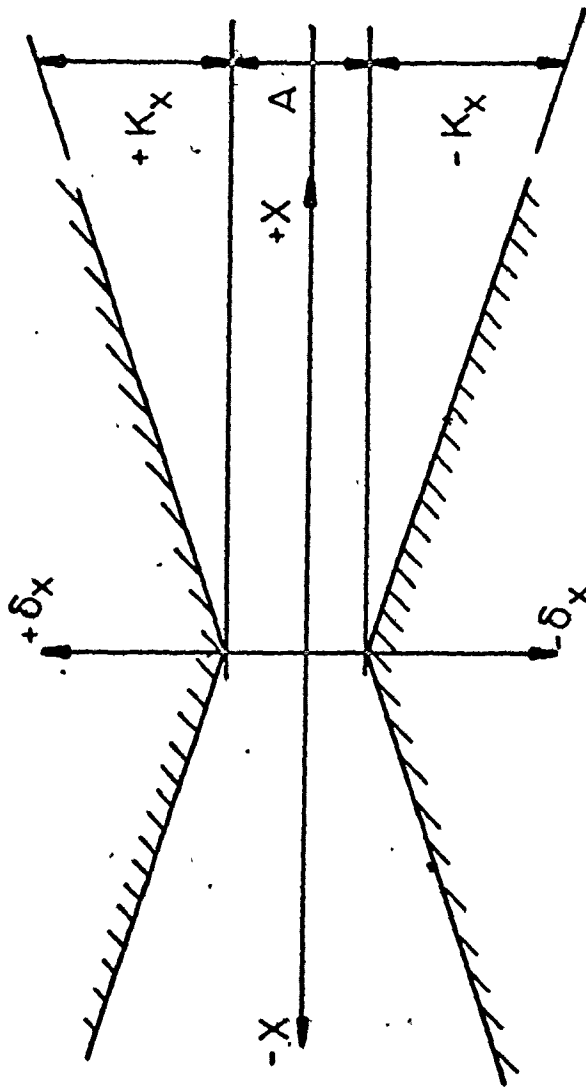
Figure 3.5   A Proposed Modified Form of Template
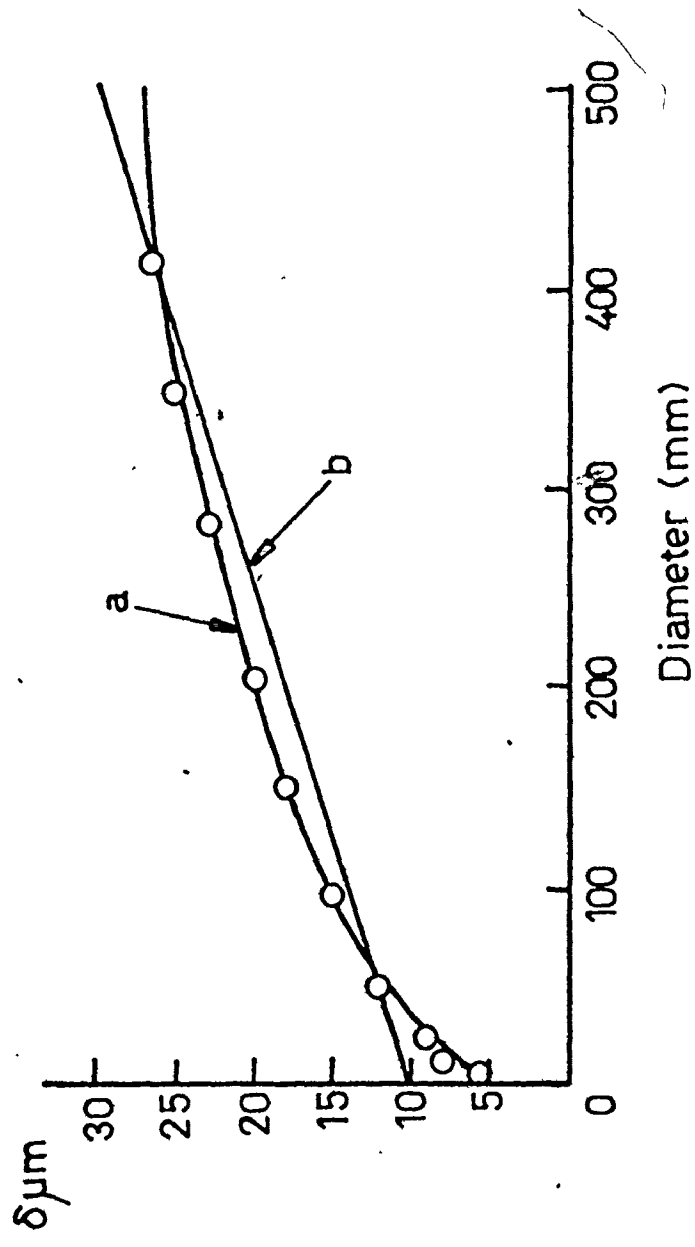
Figure 3.6 A Linearised IT Tolerance Curve
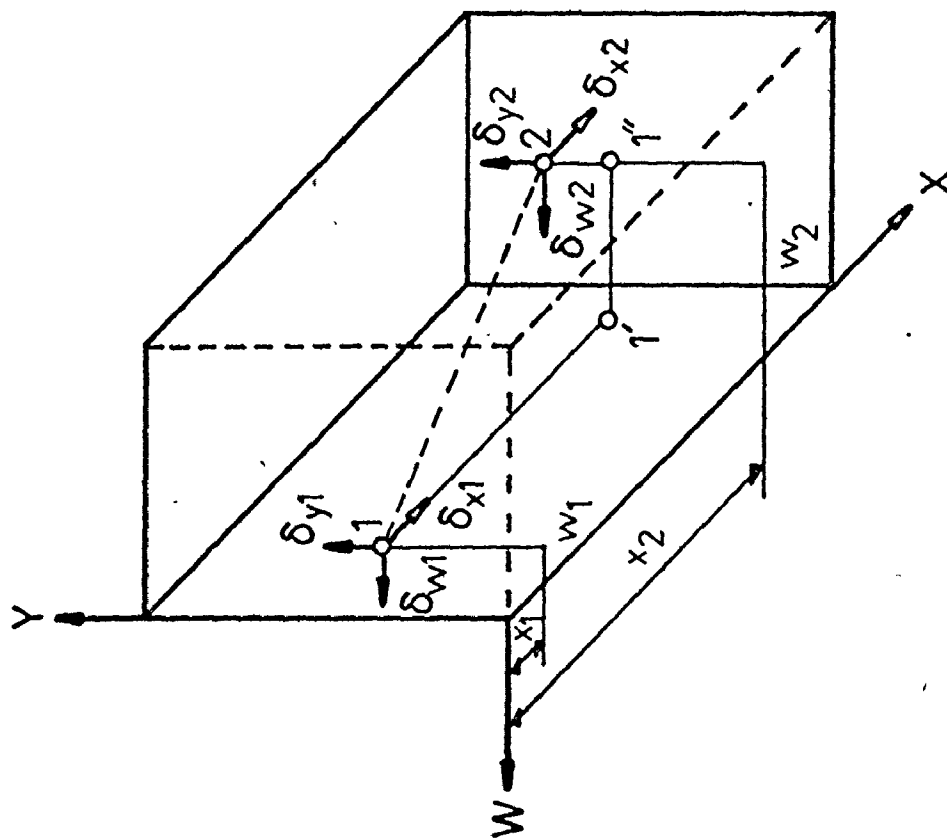
Figure 3.7   Tolerances in a Three Dimensional Zone
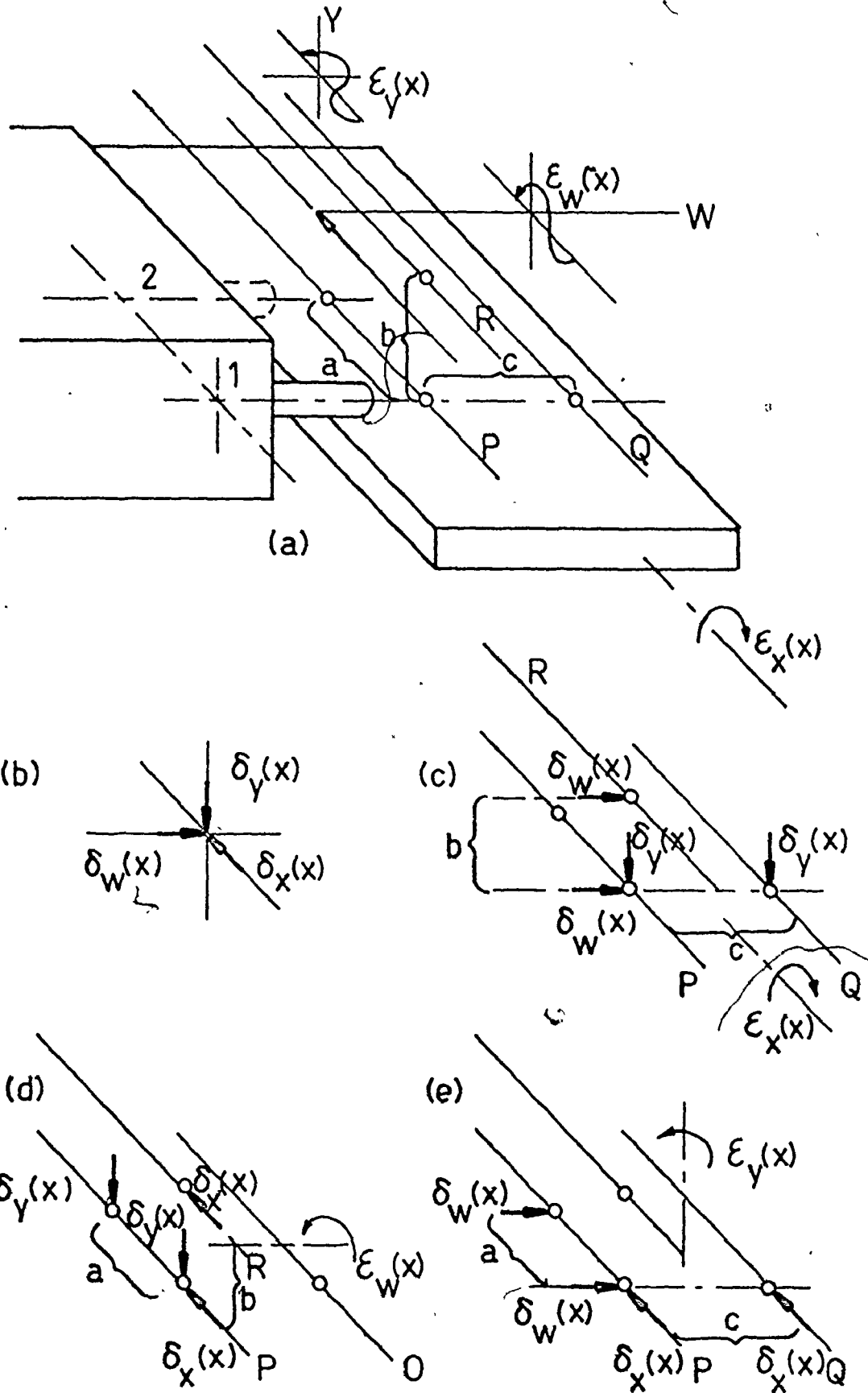
Figure 3.8 The Primary Effects of Angular Deviations
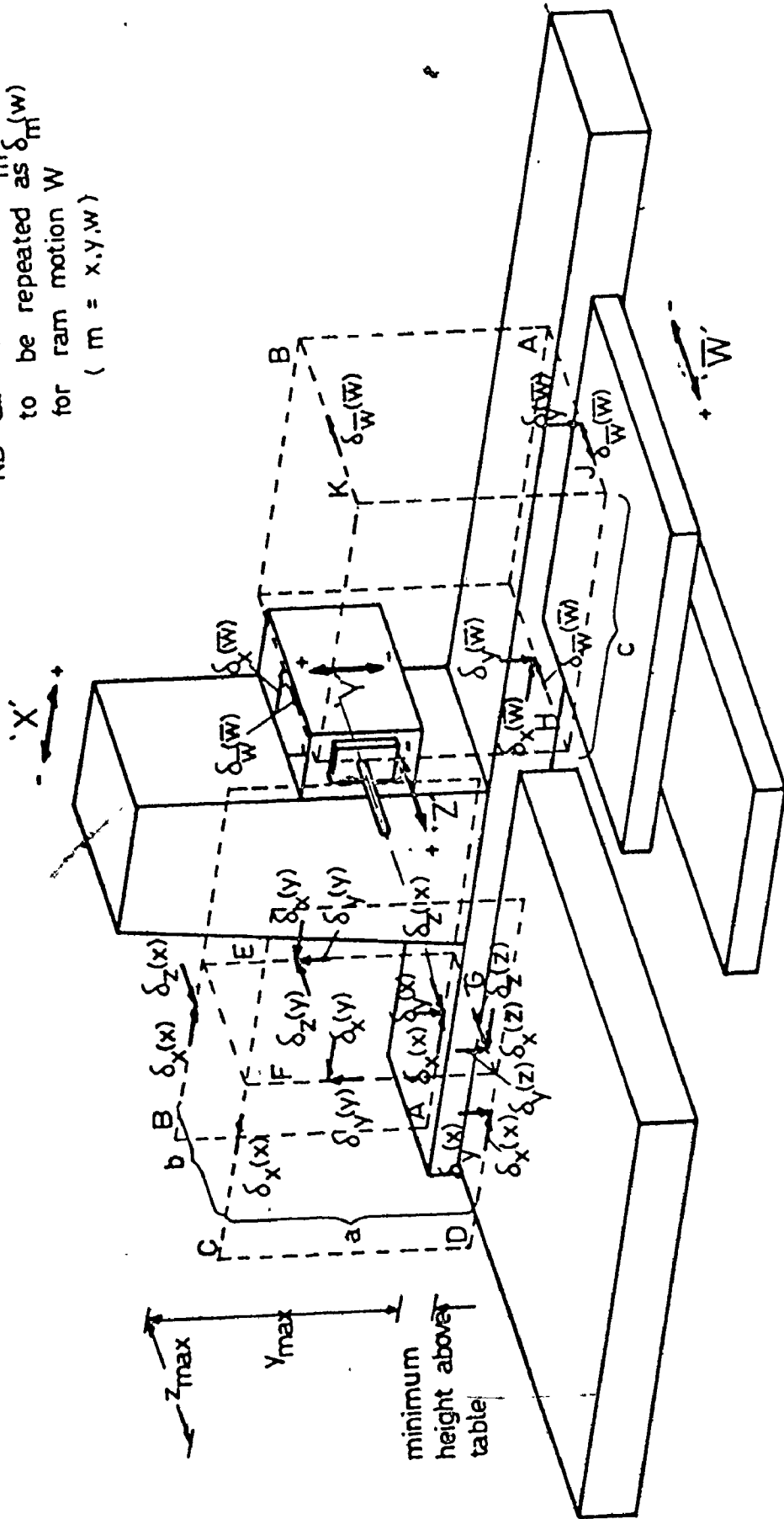
Figure 3.9   The Minimum Number of Translative Deviation Measurements for a Three Dimensional Working Zone.
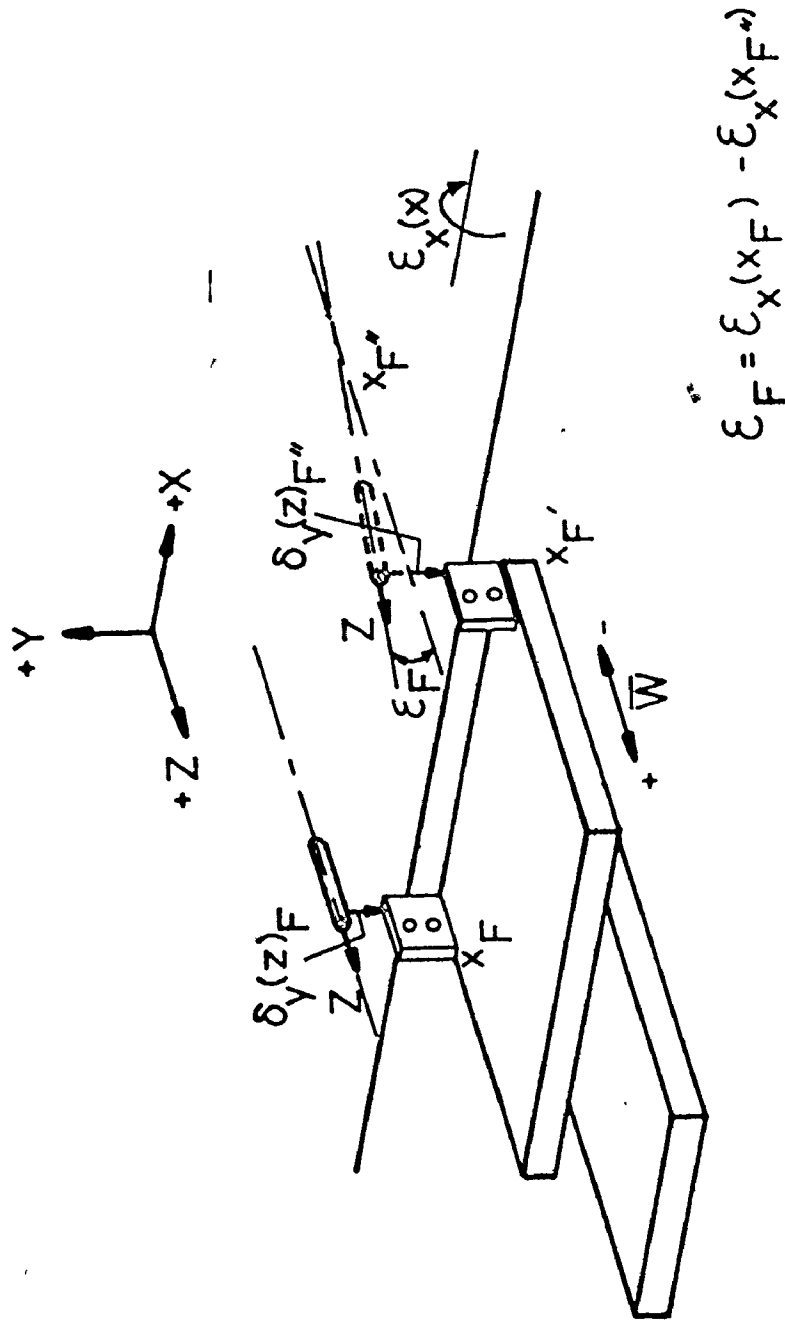
Figure 3.10 The Secondary Effect of Angular Deviations
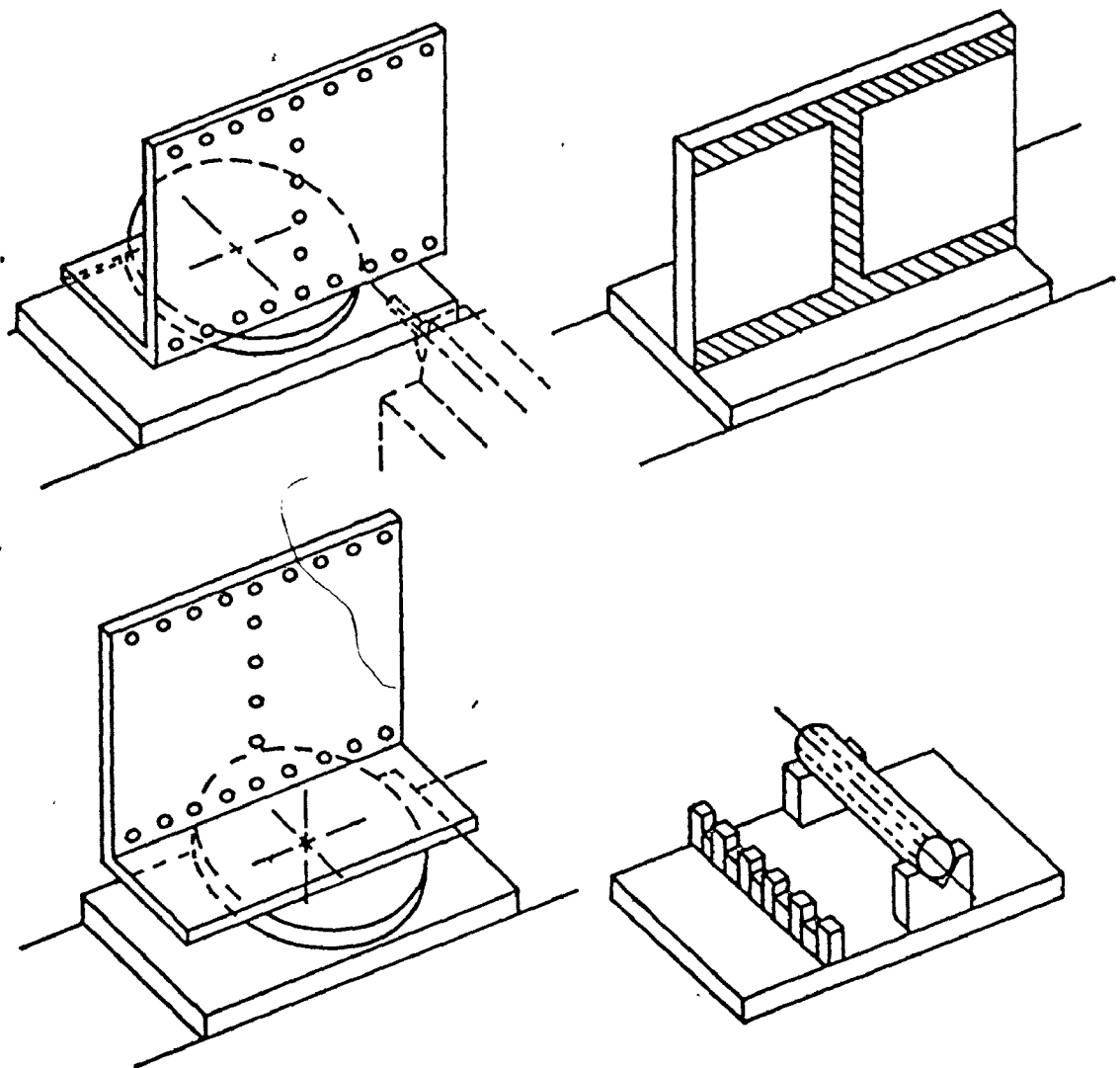
Figure 3.11   Design of a Master Part for a Type of
                 Machining Center.
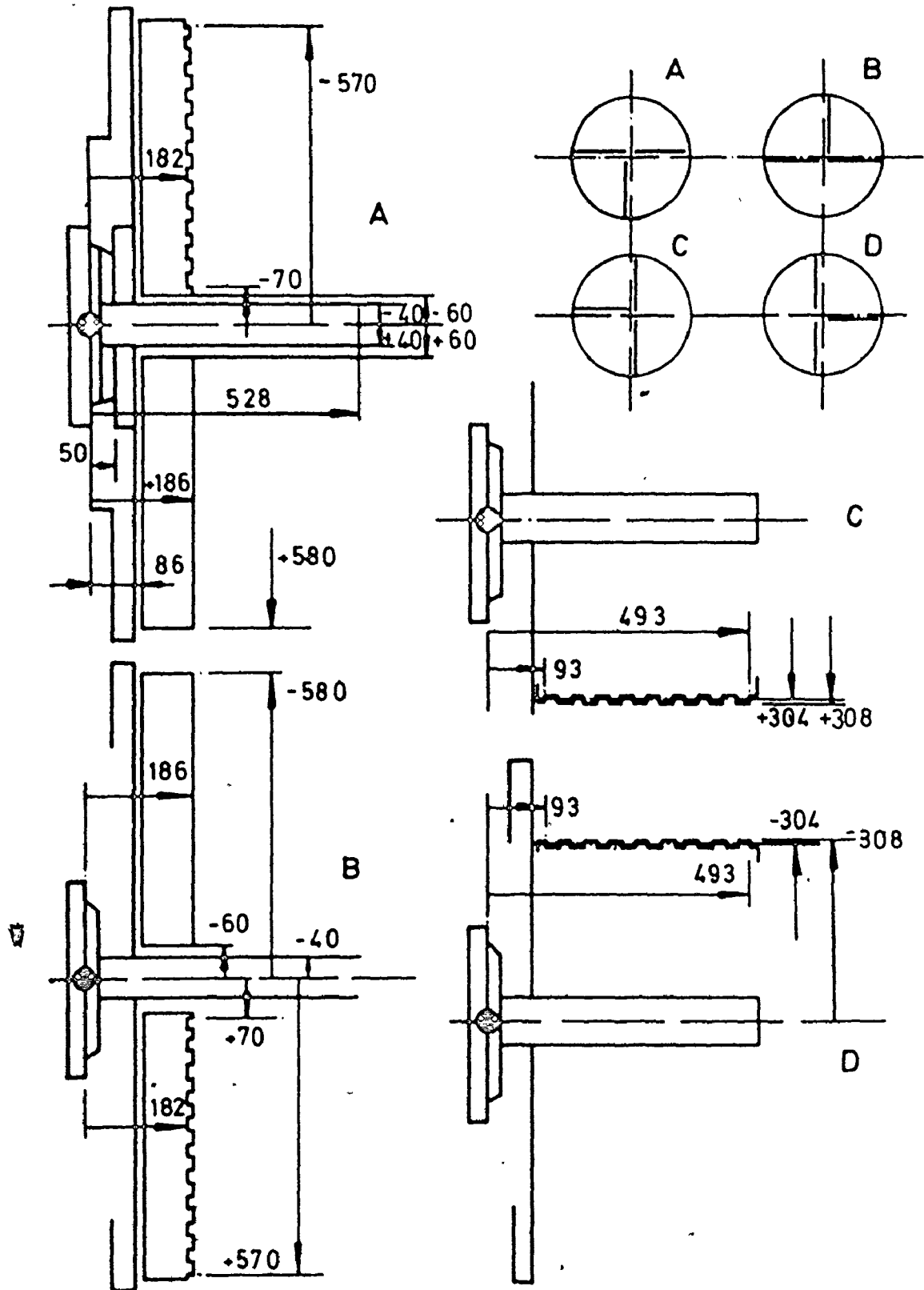
Figure 3.12   Design of a Master Part for an N.C. Lathe.
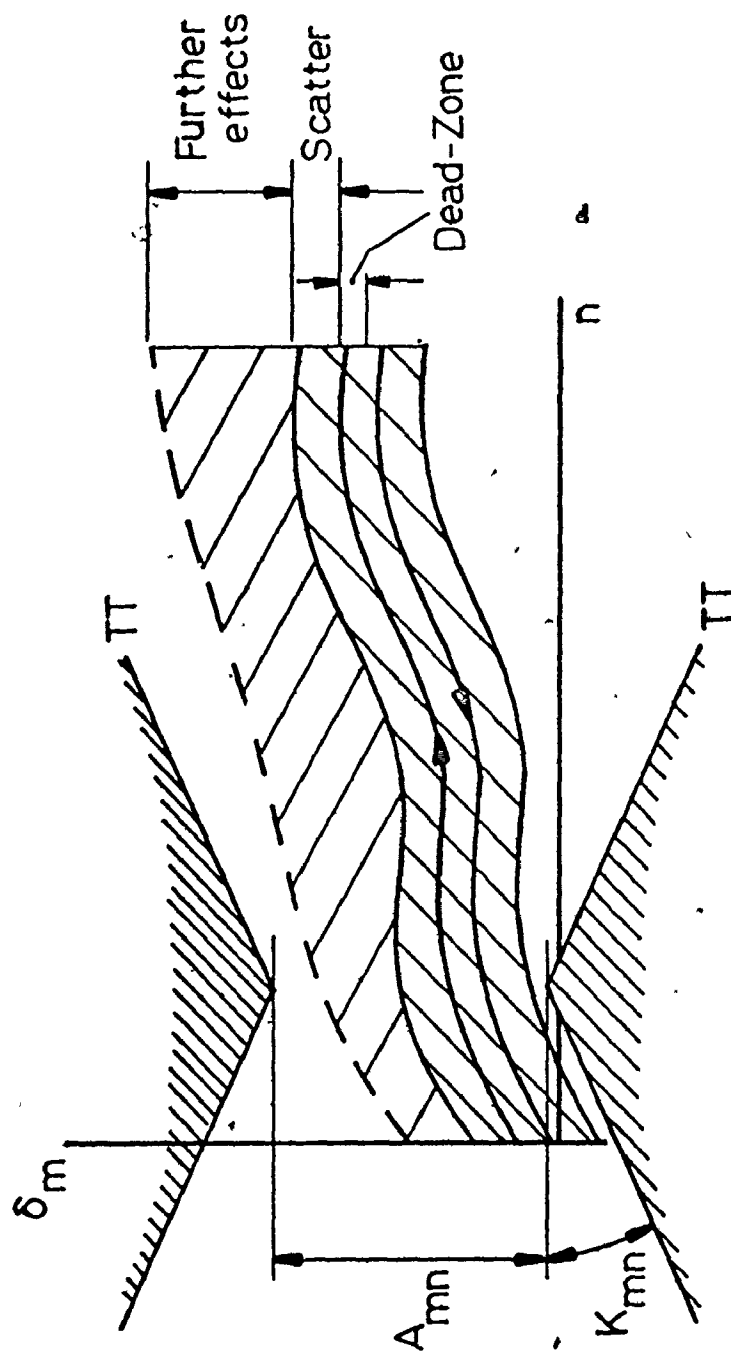
Figure 3.13   The Modified Tolerance Template - the Accommodation of Further Effects.
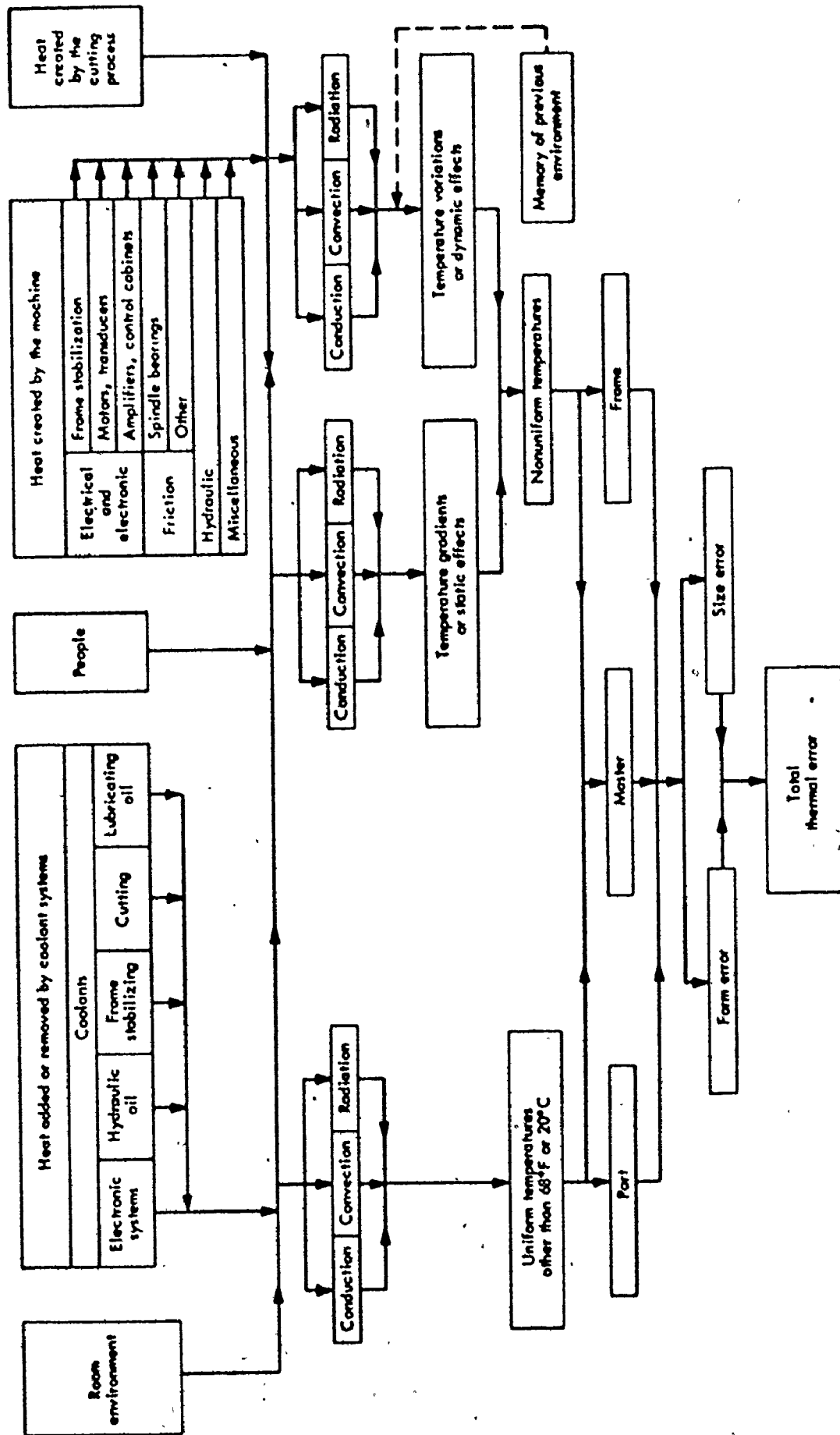
Figure 4.1   Inter-relationship of Elements of the General Thermal Effects
Problem [28].

(a)

(b)

(c)

(a)

(b)

(c)

(d)
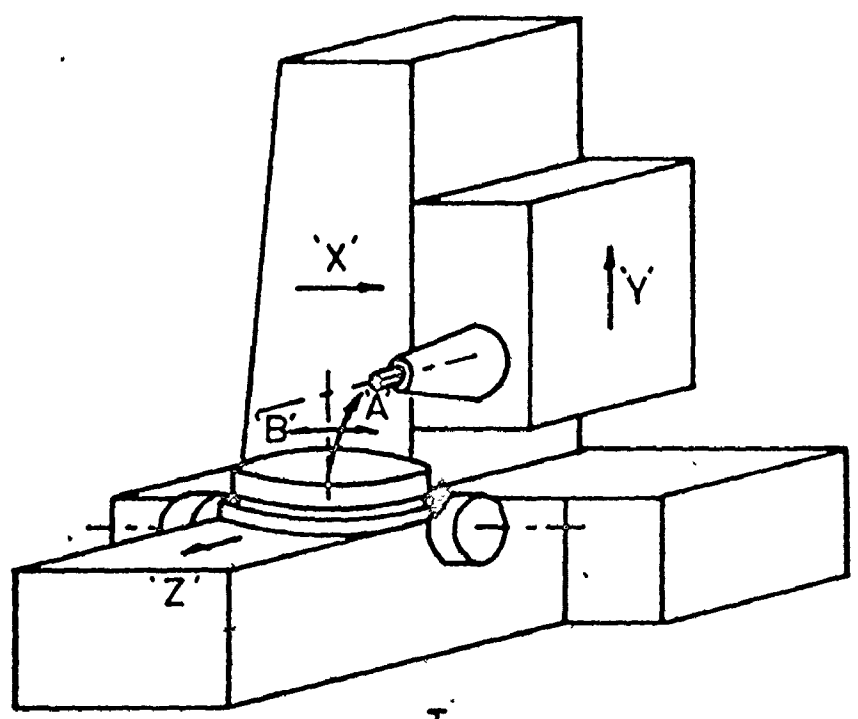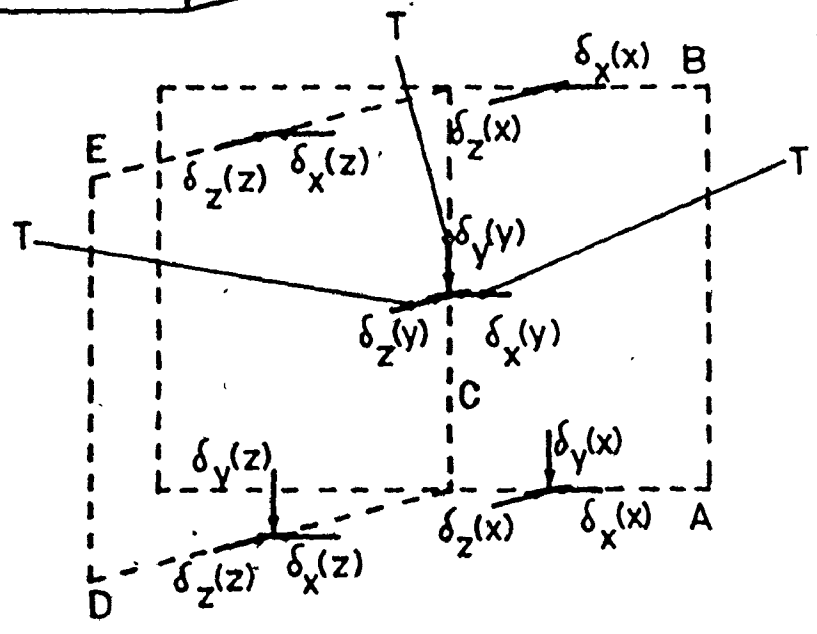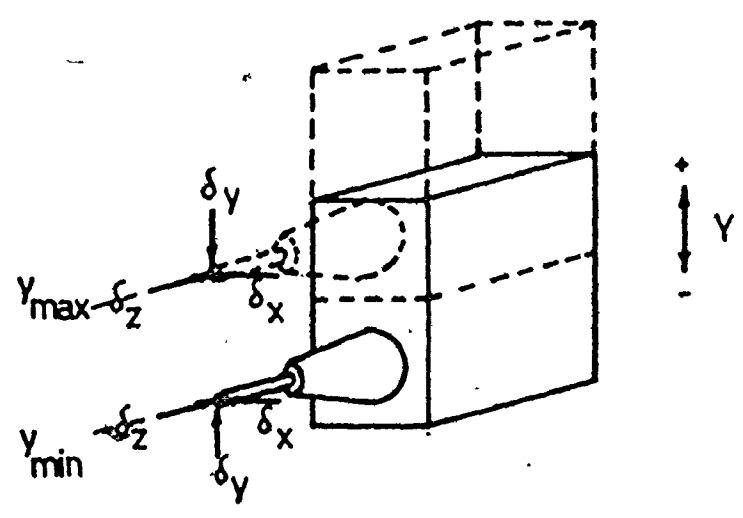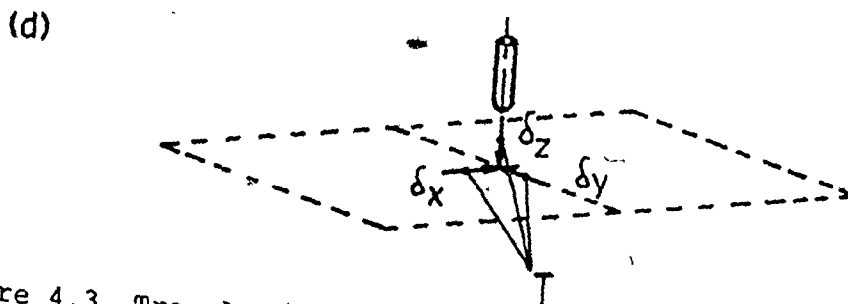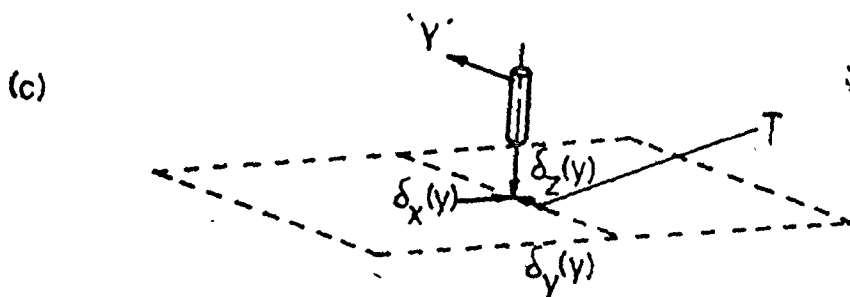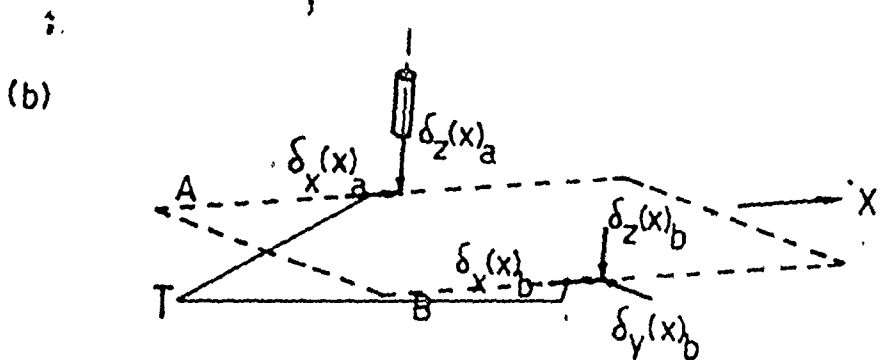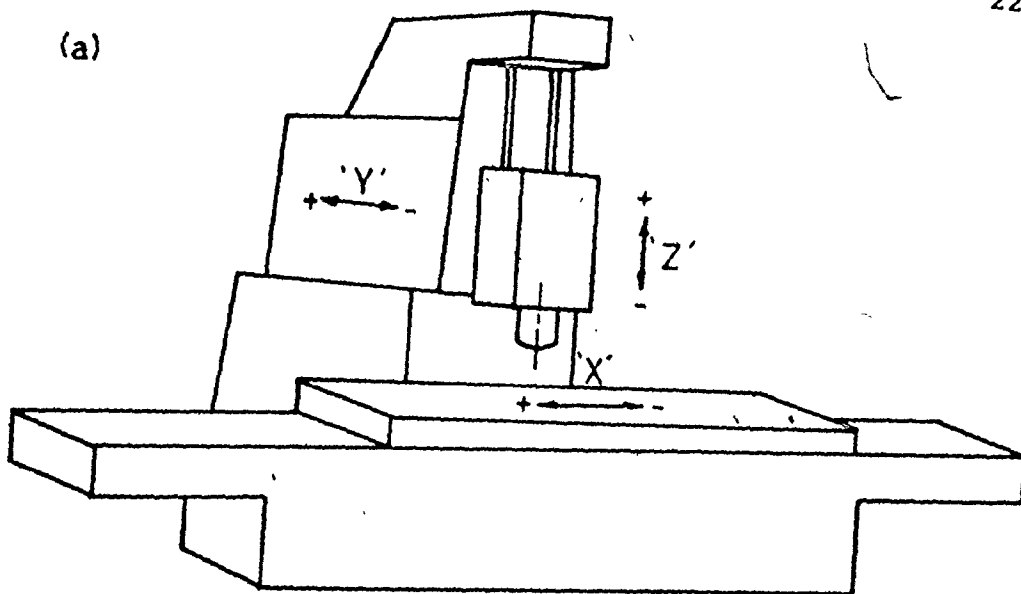
Figure 4.3 Translative Deviations to be Measured on a bed-type Milling Machine with a Limitation to
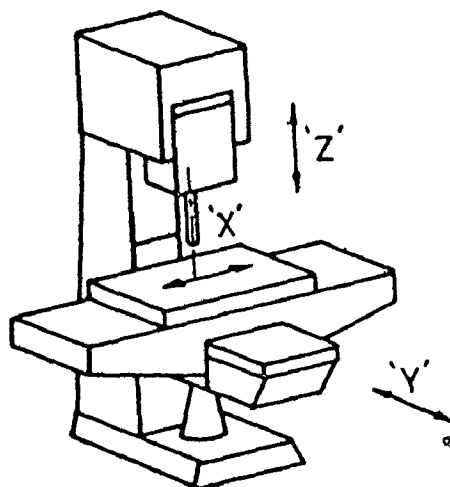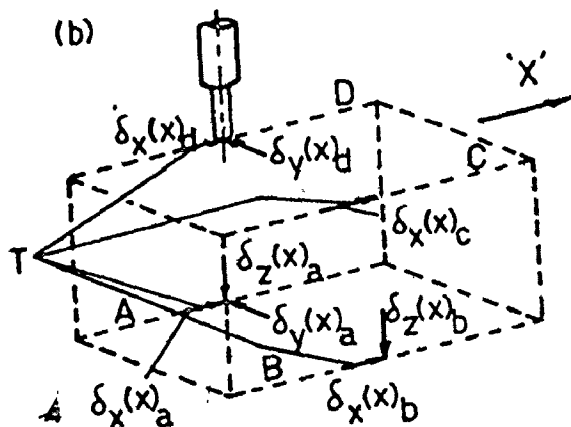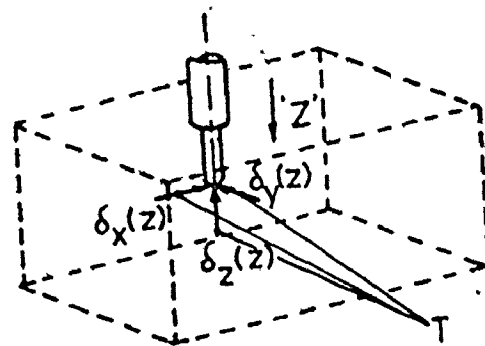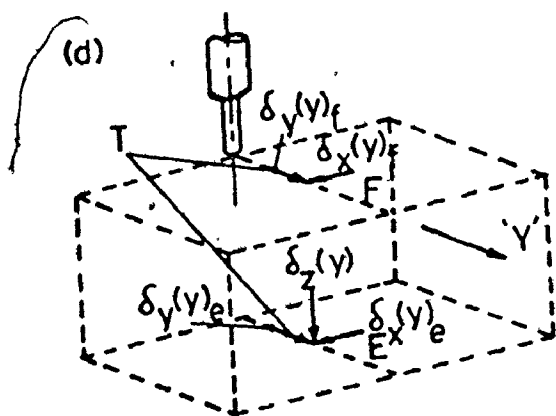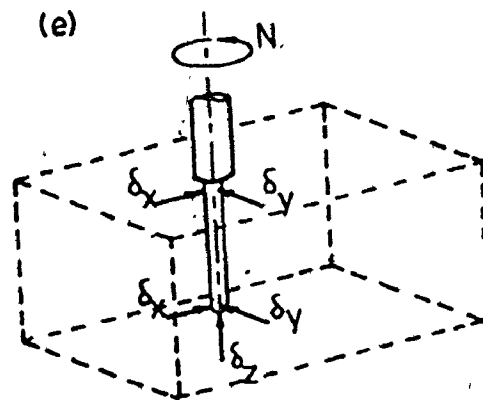
Figure 4.4 Translative Deviations to be Measured on a Small Knee-type Machining Center.
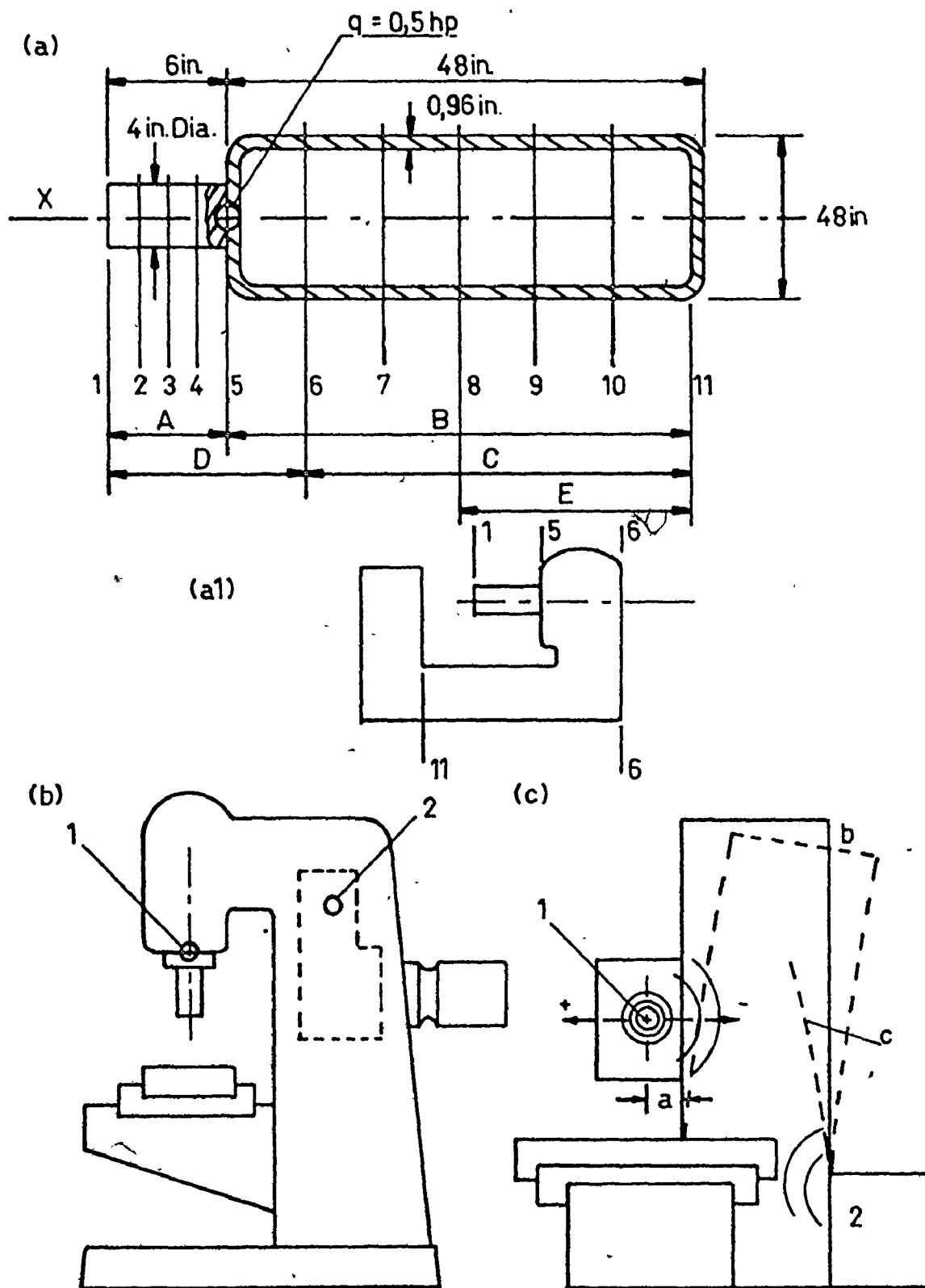
Figure 4.5 Diagrams for the Discussion of Main Features of Thermal Deformations.
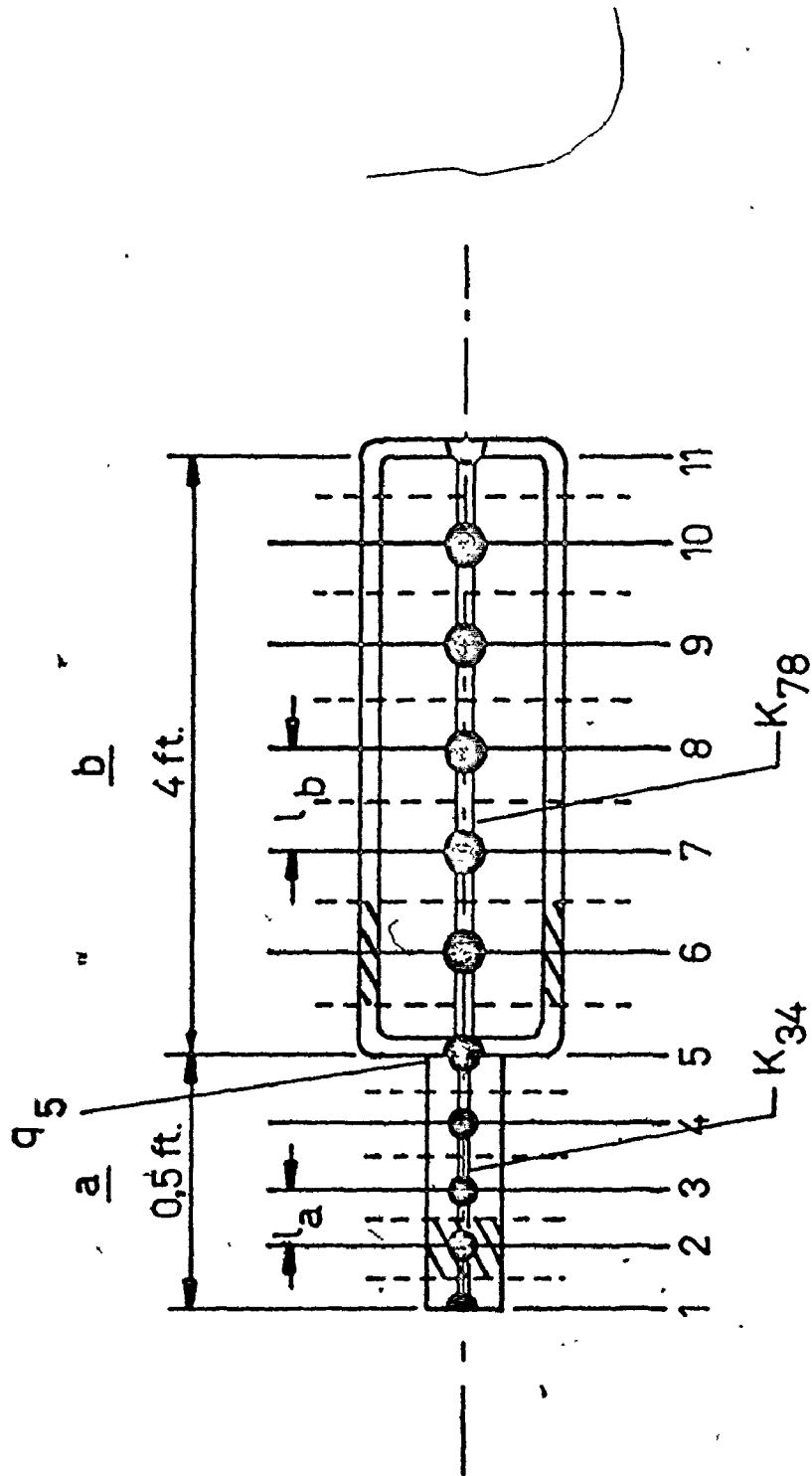
Figure 4.6   The Diagram of the Lumped-mass System
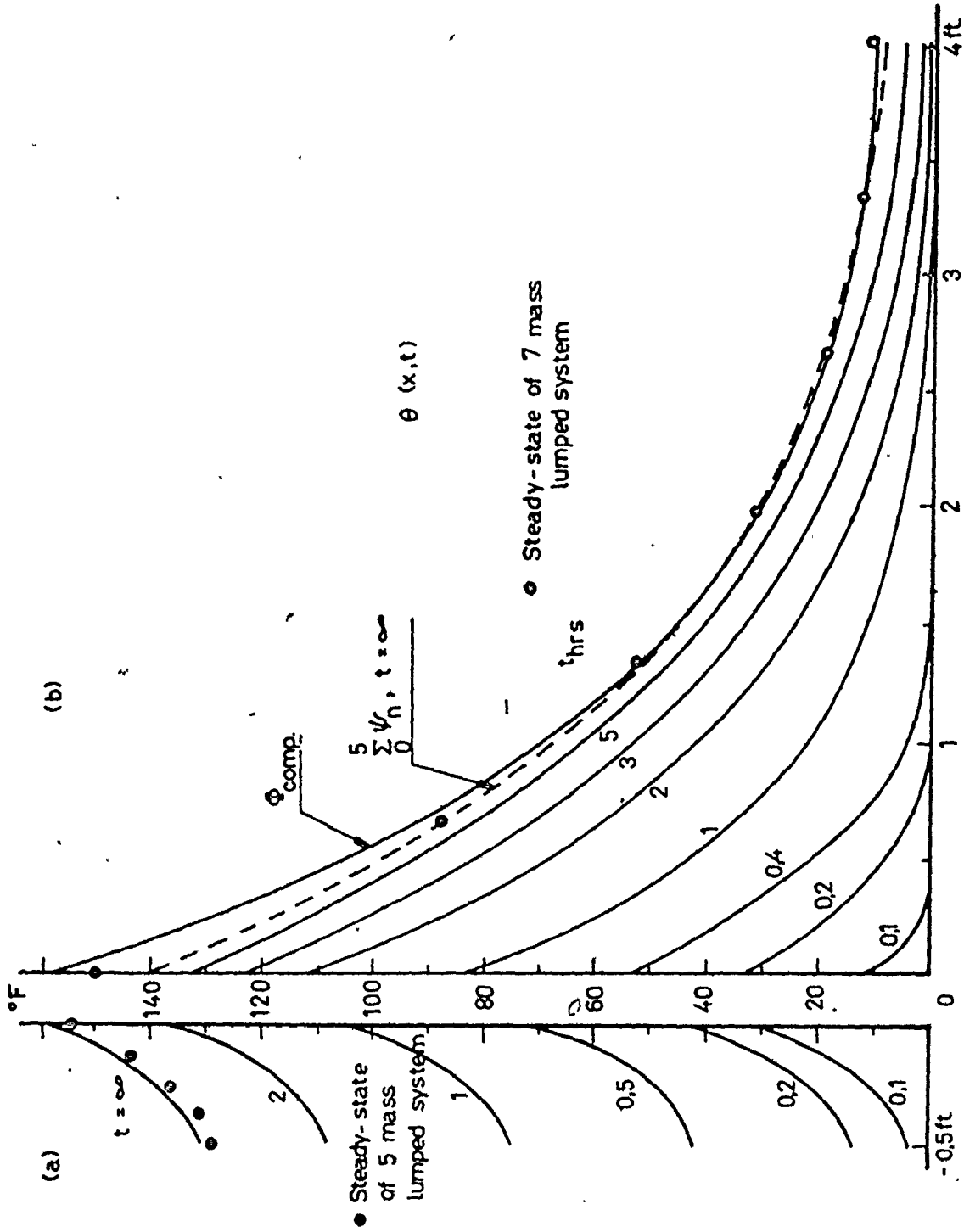
Figure 4.7 Temperature fields during the Heating period in the "Housing" and in the "Spindle".
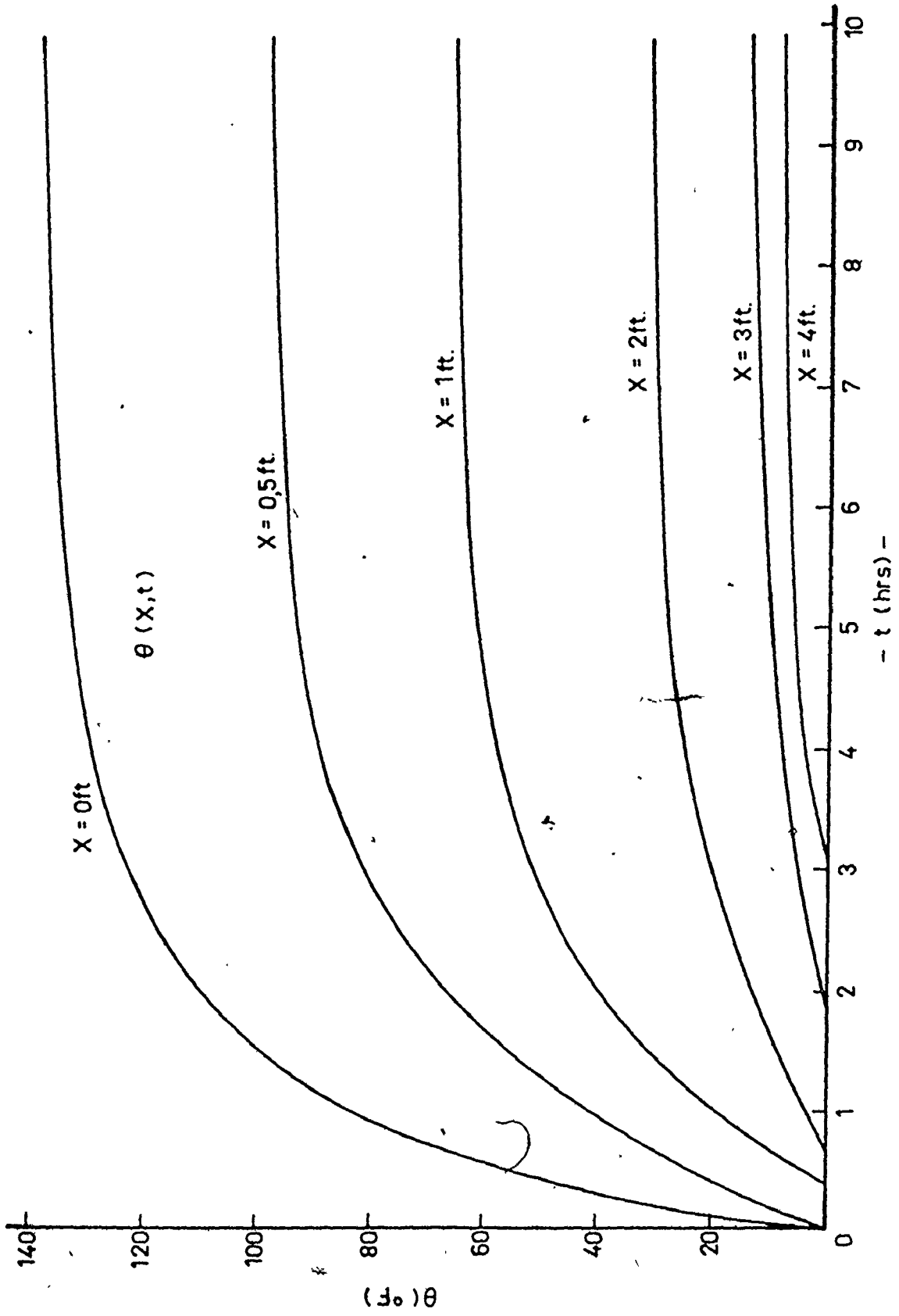
Figure 4.8   Temperature Variation of Various Sections of the "Housing".
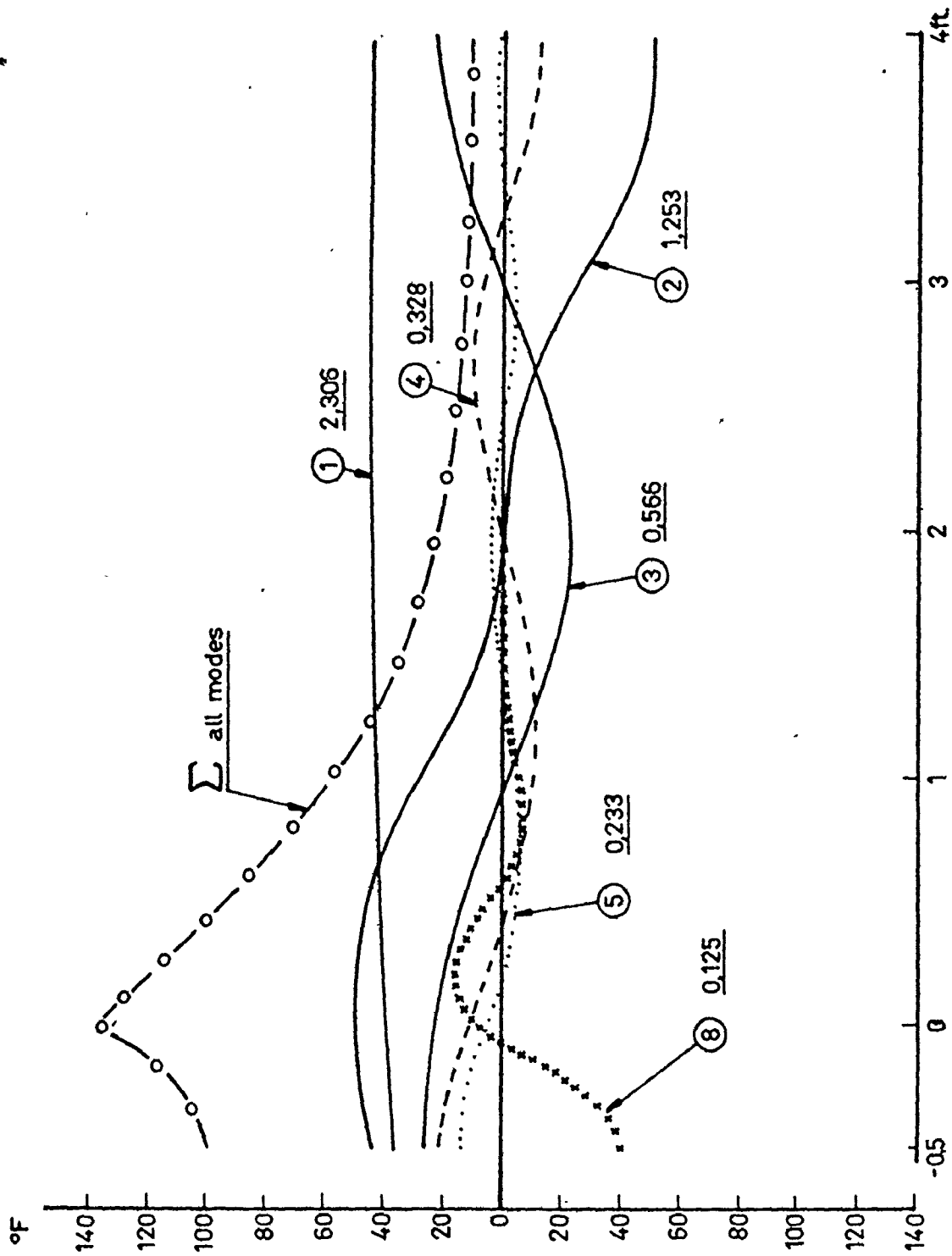
Figure 4.9 The "Mode Shapes" and Time Constants of main components of the Temperature Field of the System of Figure 4.6.
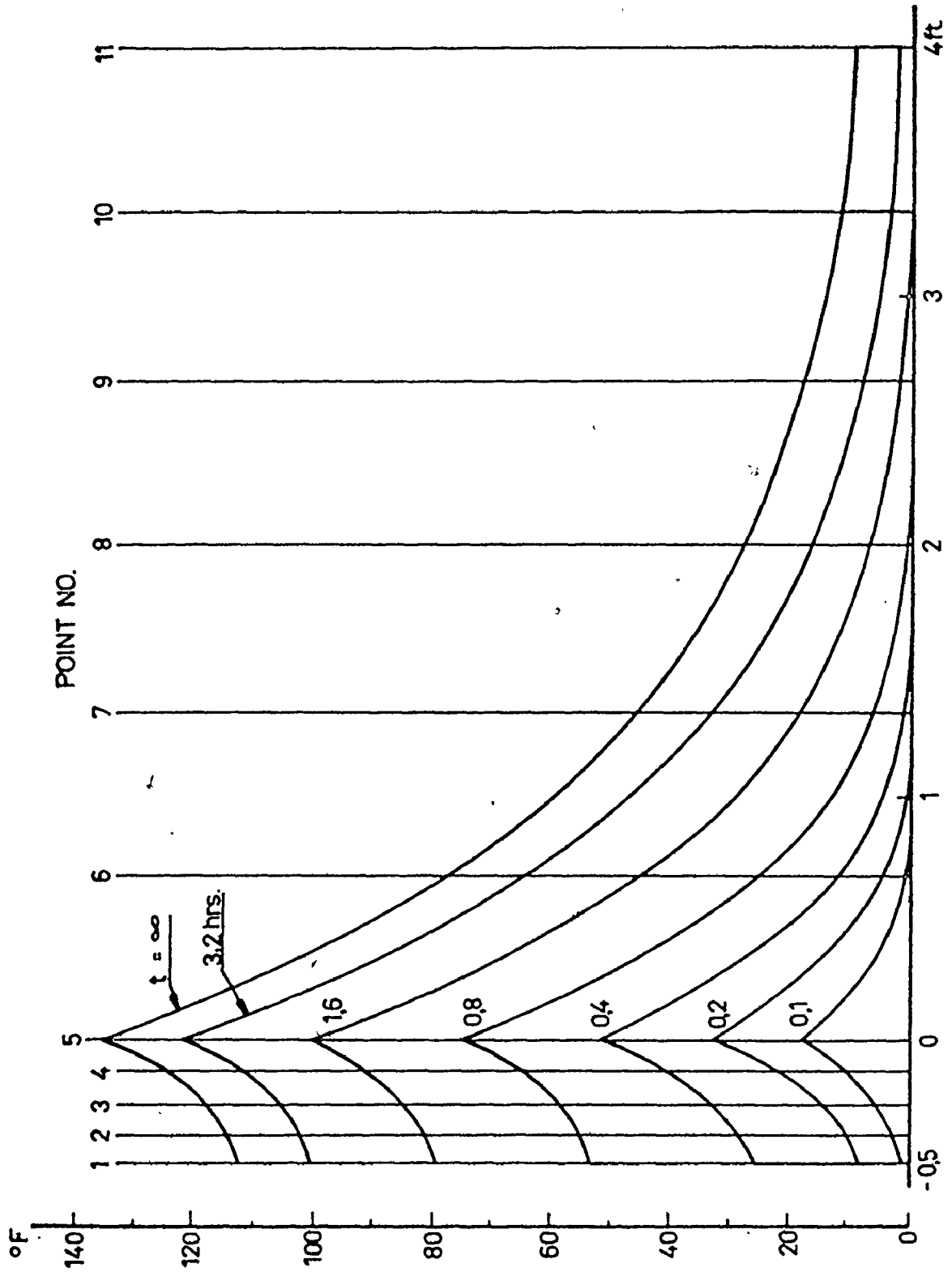
Figure 4.10 Transient Temperature Fields during the Heating-on Period for the System of Figure 4.5a.
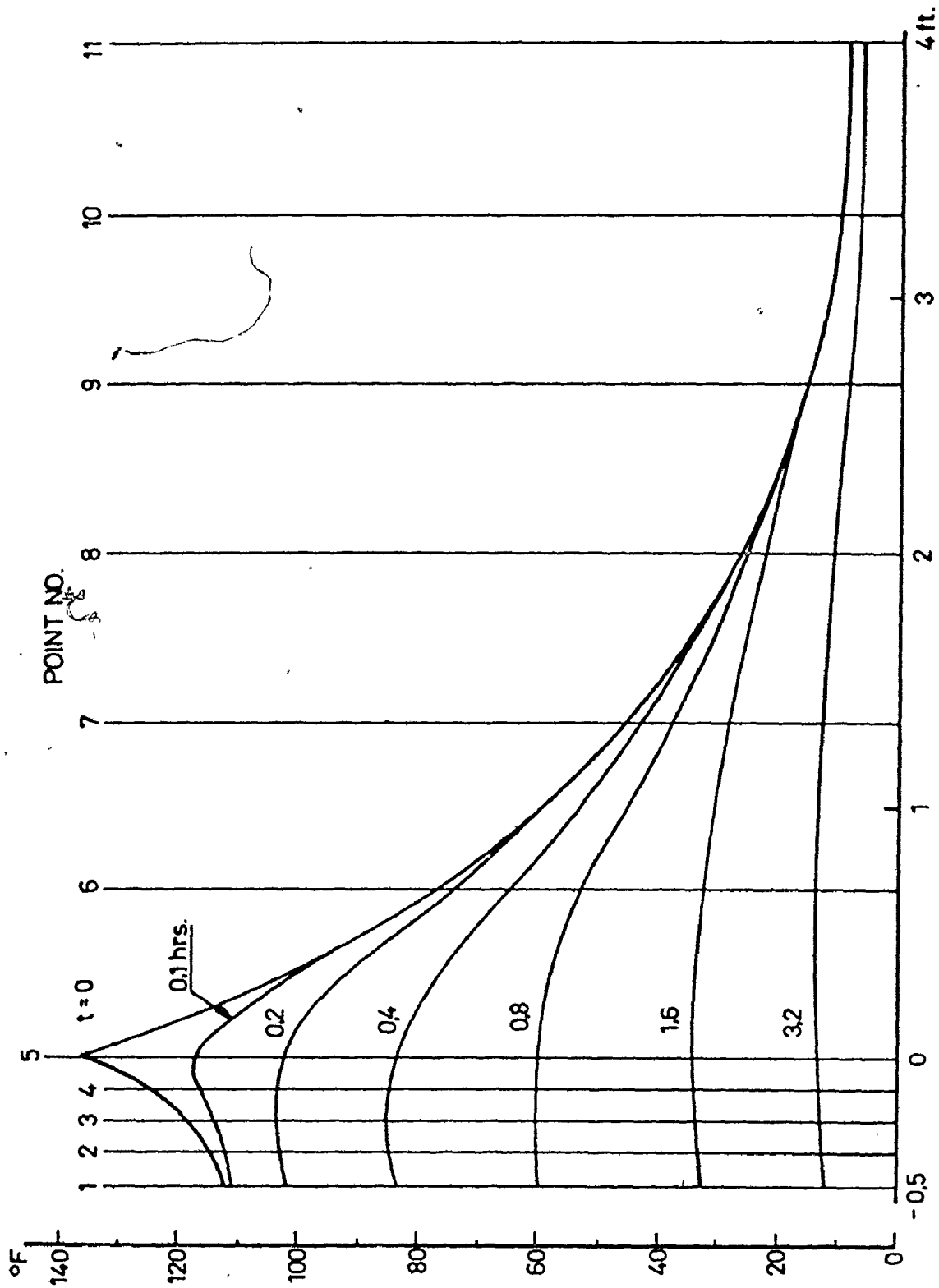
Figure 4.11 Transient Temperature Fields during the Heating-off Period
for the System of Figure 4.5a.
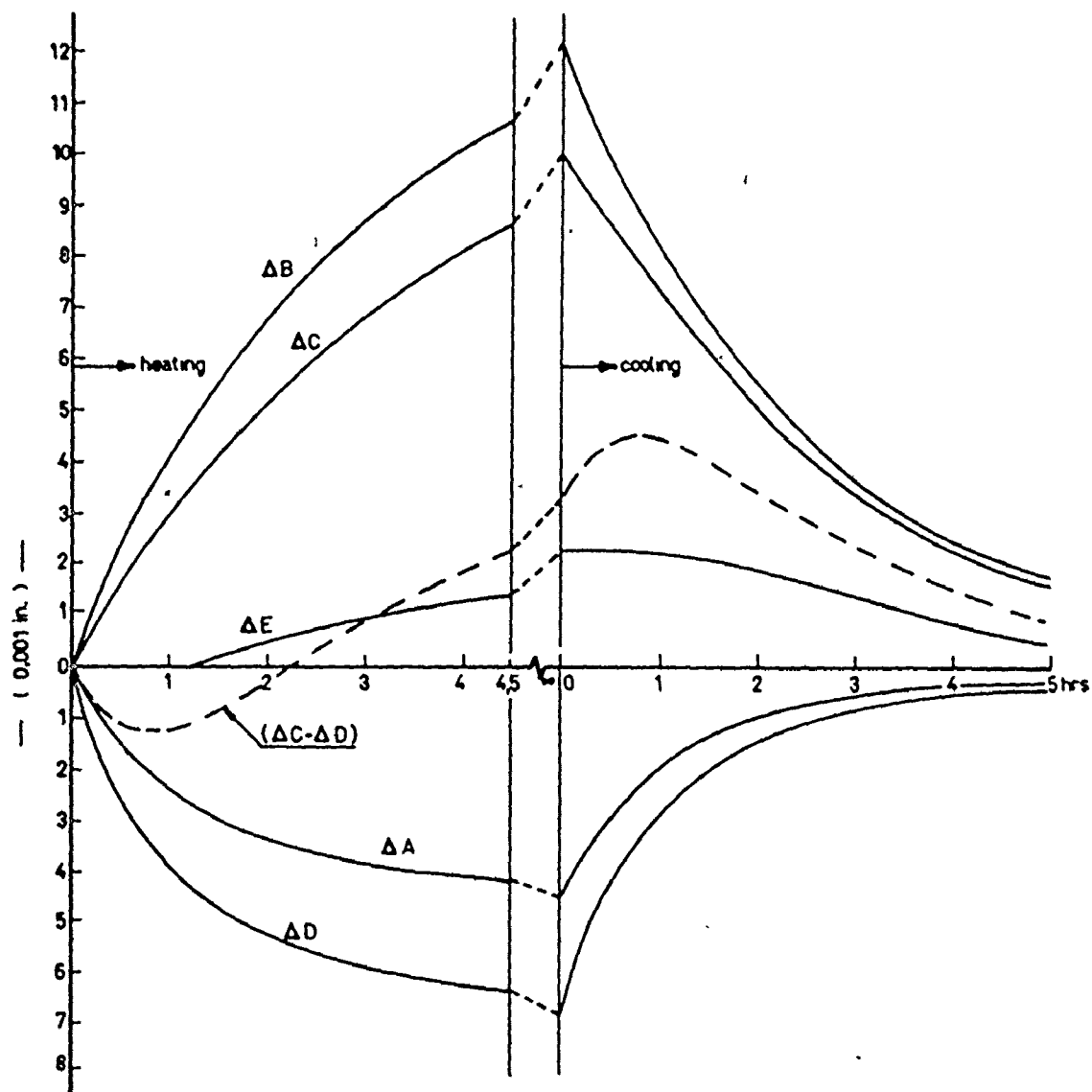
Figure 4.12   Transient Thermal Deformation in the System
of Figure 4.5a.
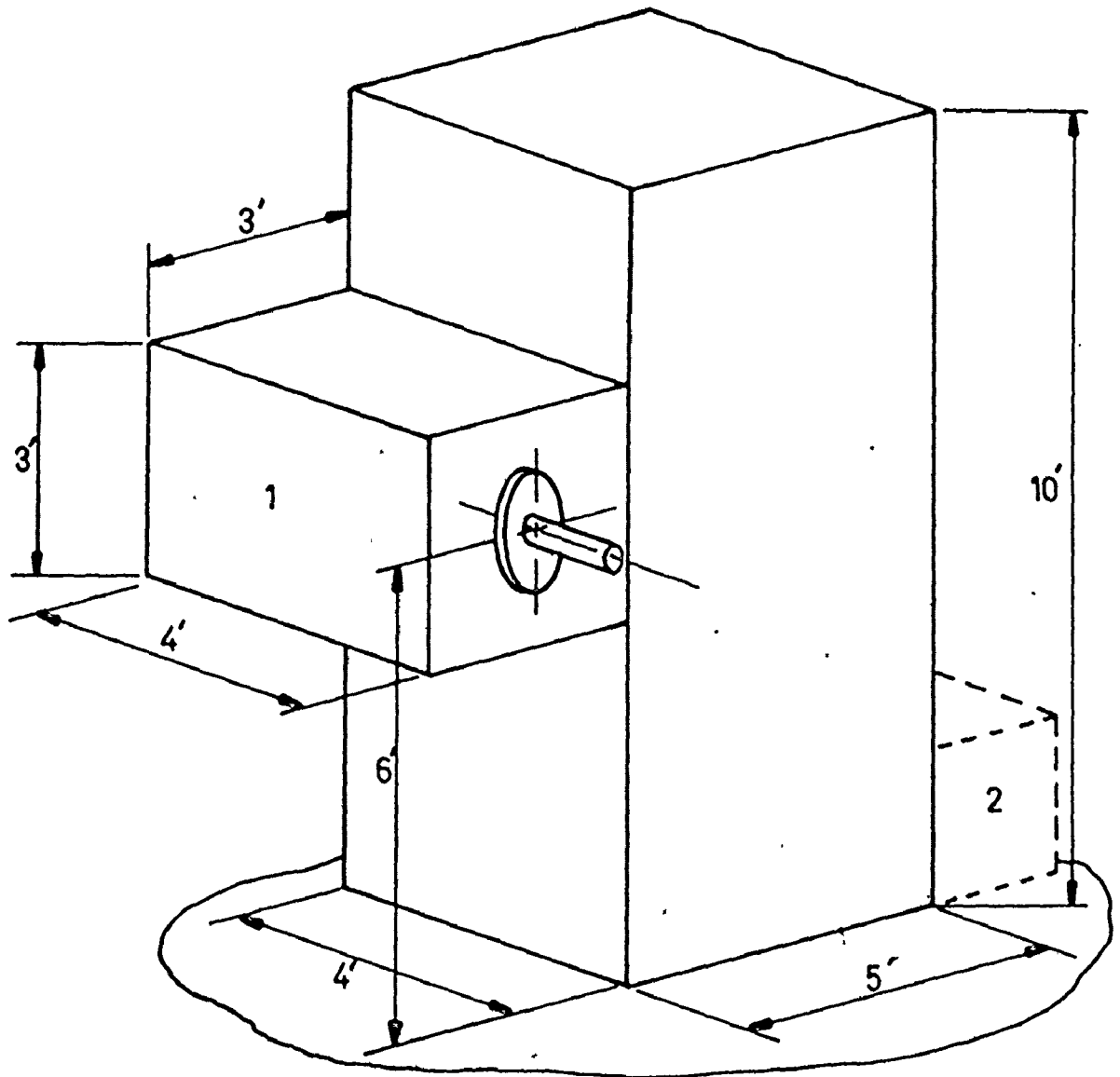
Figure 4.13   Configuration of a Horizontal Boring Machine
for Finite Element Analysis of Thermal
Deformations due to the indicated Heat Sources.
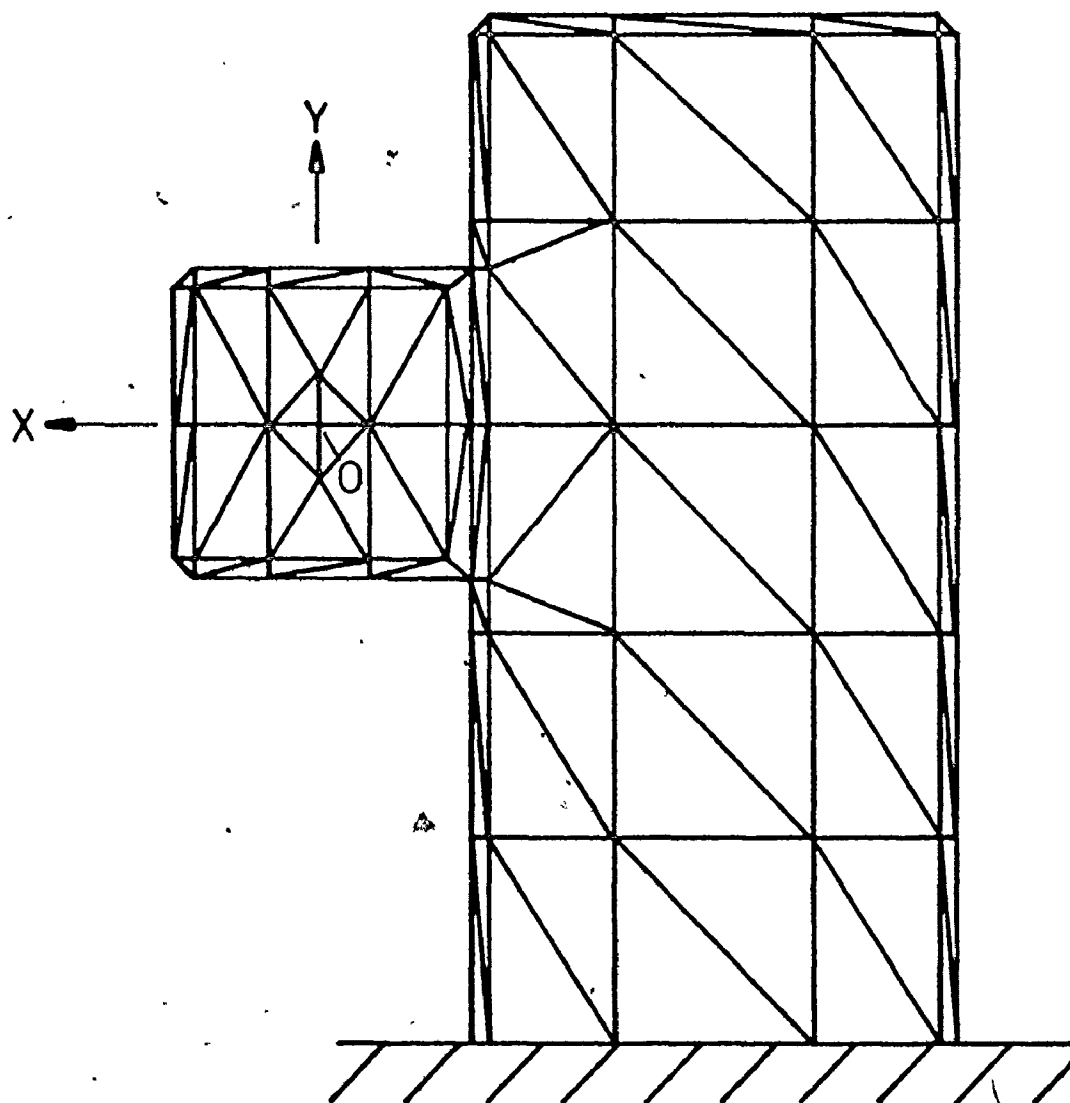
Figure 4.14 A Representative Finite Element Idealisation
of the Machine Depicted in Figure 4.13.
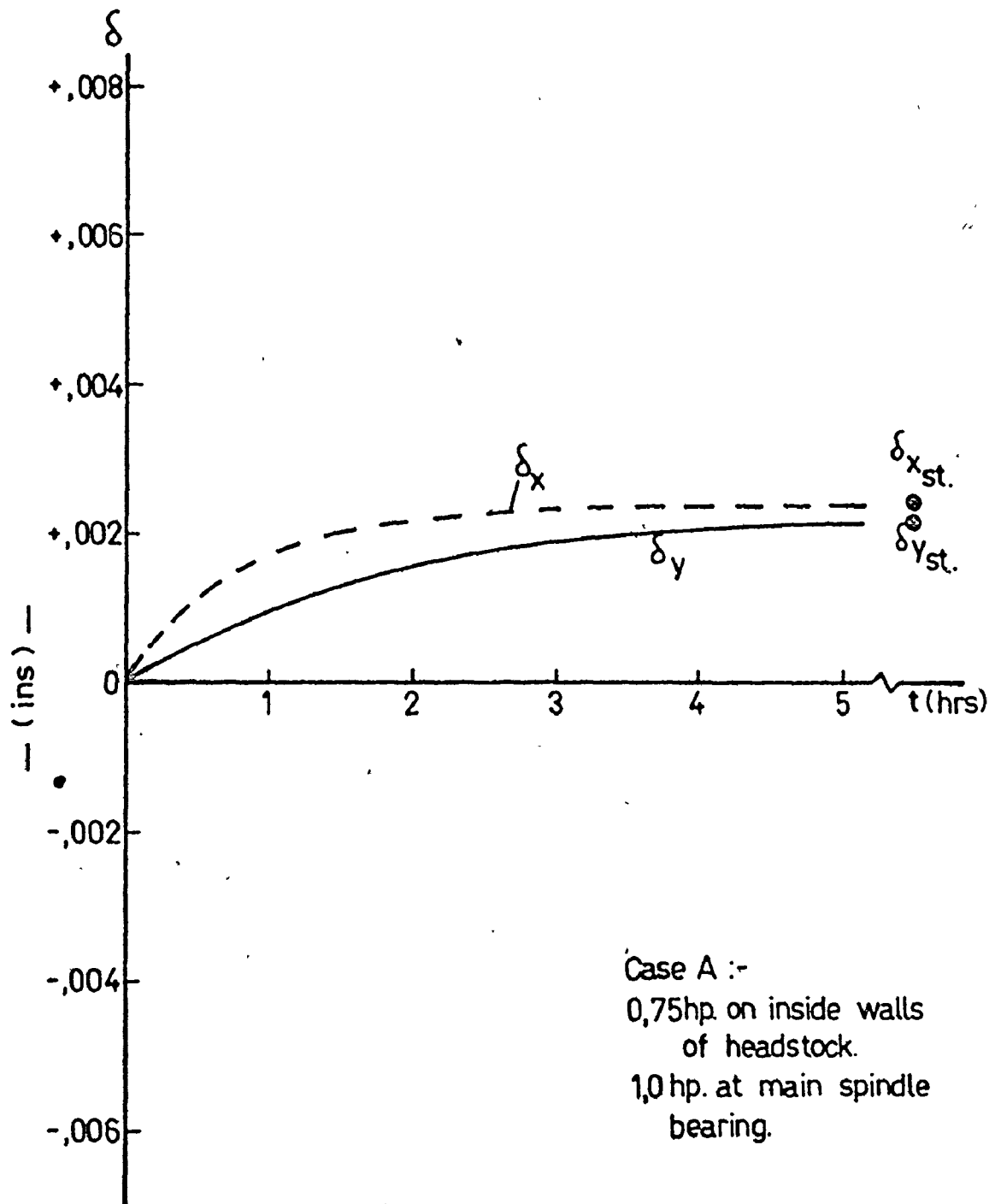
Figure 4.15 The δ_x and δ_y drifts of the "Spindle Nose" due to the Headstock Heat Source alone.
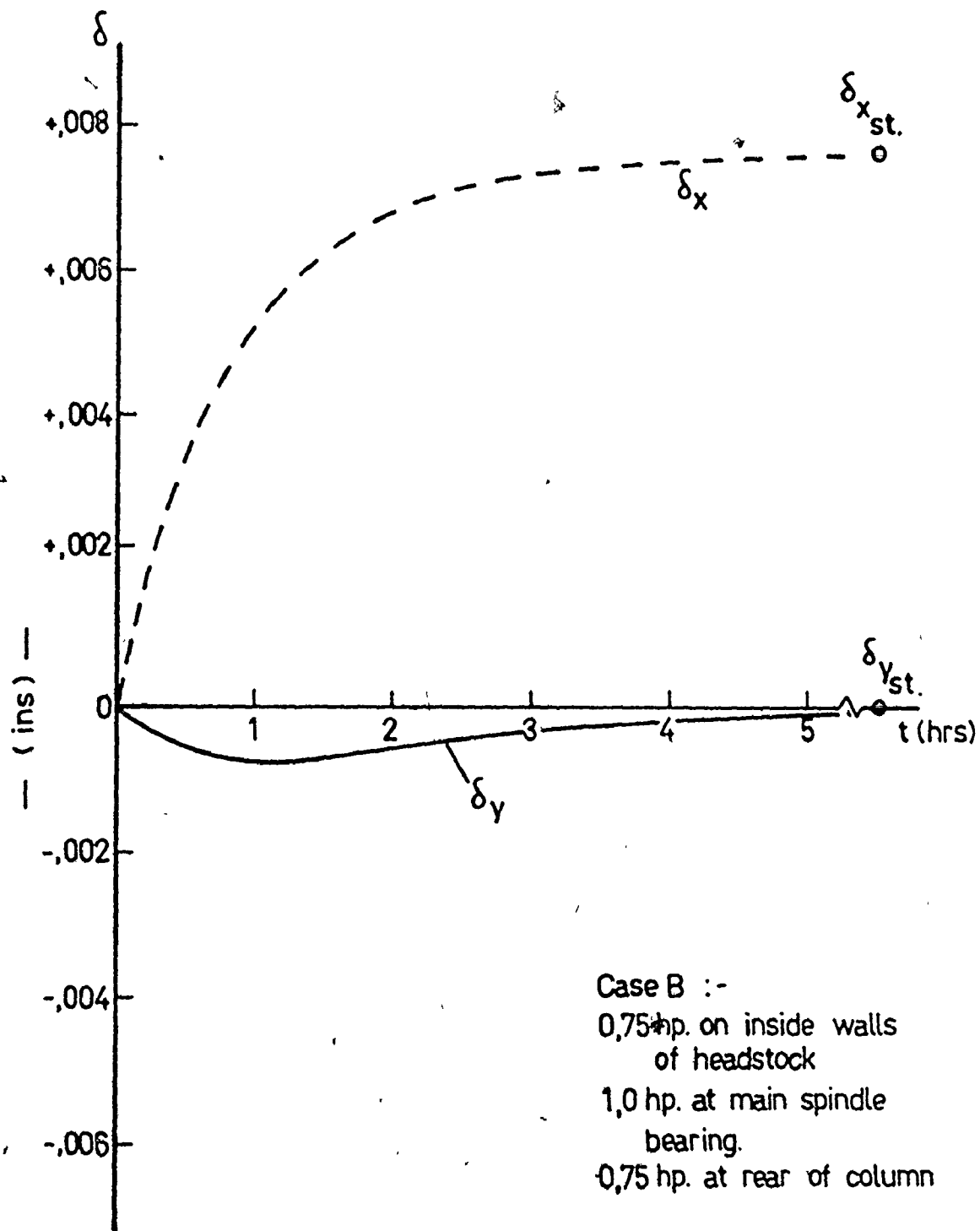
Figure 4.16   The δ_x and δ_y drifts of the "Spindle Nose"
due to the Headstock and Rear of Column
Hydraulic Heat Source.
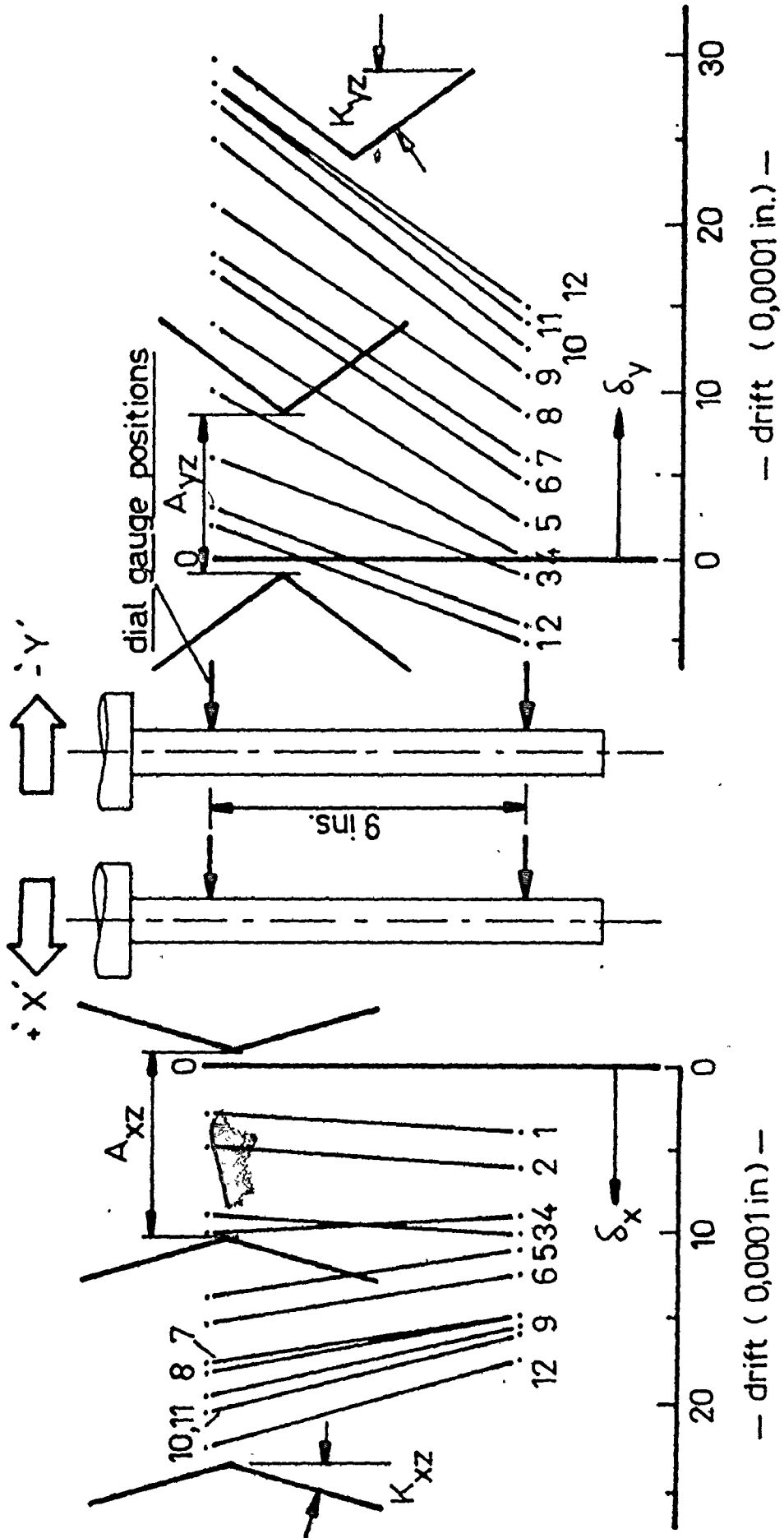
Figure 4.17 The $\delta_x(z)$ and $\delta_y(z)$ Drifts of the Machine
depicted in Figure 4.3: Evaluation.
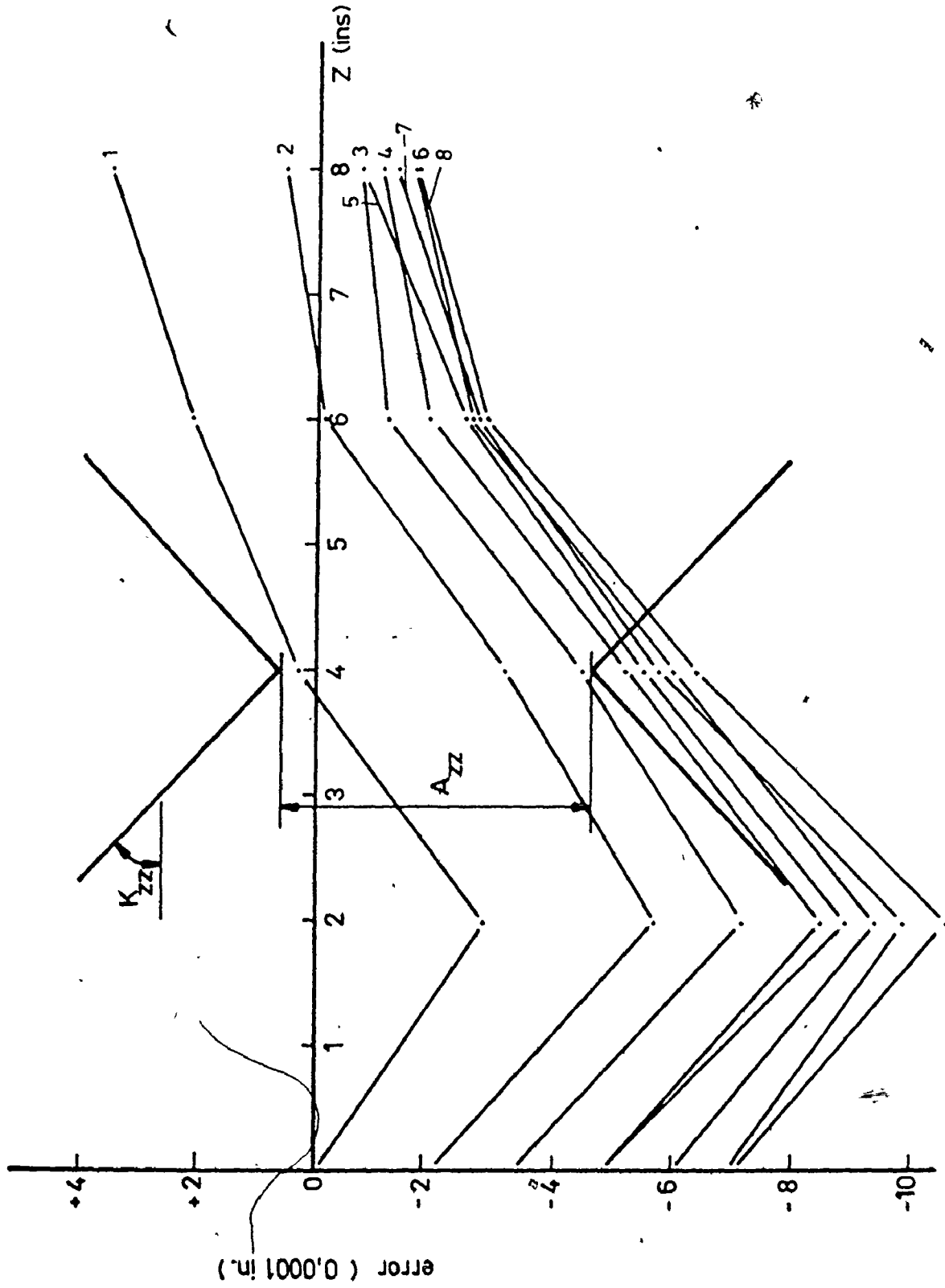
Figure 4.18 The Positioning Error of the Machine depicted
in Figure 4.3: Evaluation.
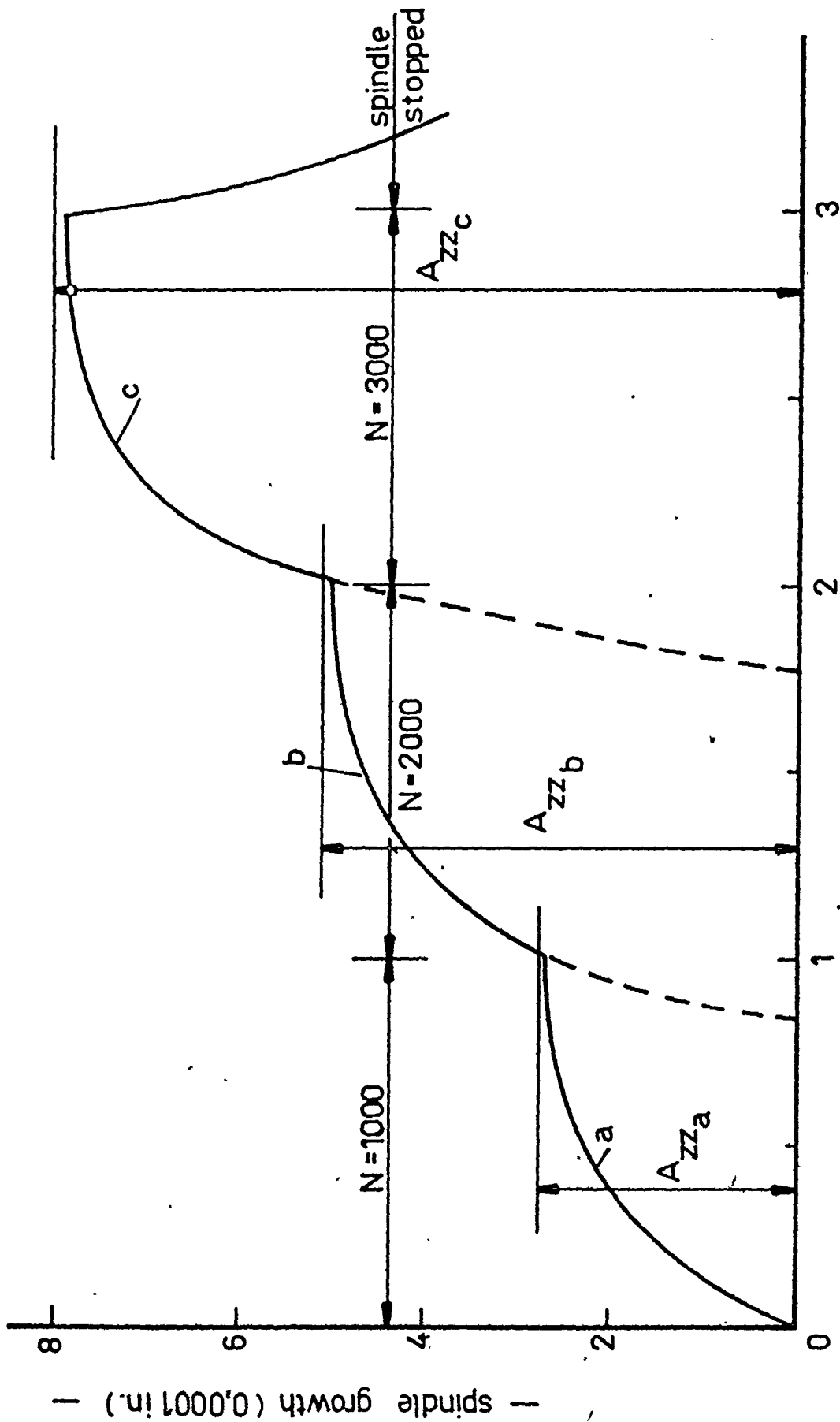
Figure 4.19   The Spindle "Growth" of the Machine depicted
in Figure 4.4:   Evaluation

238
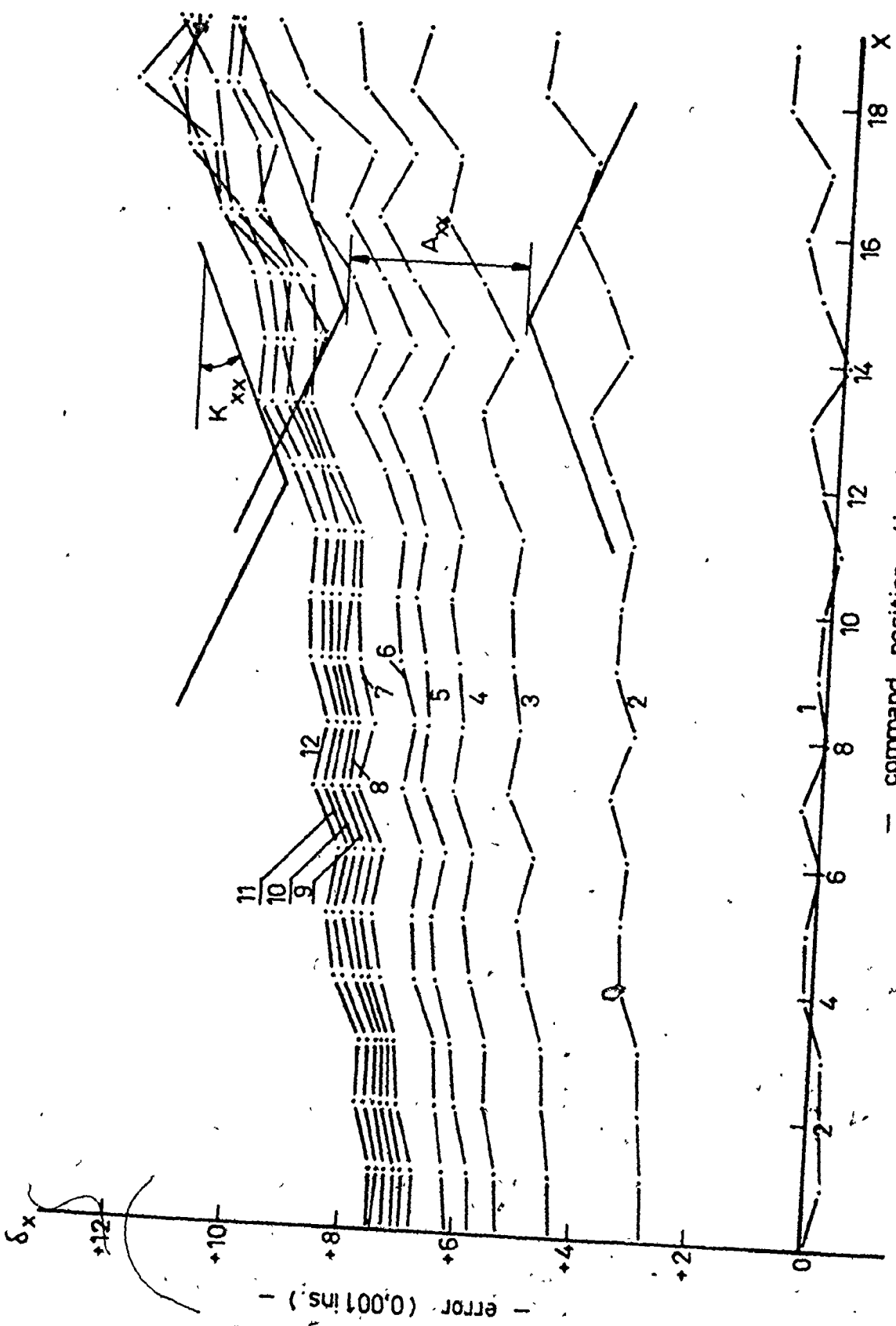
Figure 4.20   The Positioning Error of the Machine depicted
             in Figure 4.4:   Evaluation

(a)

Dial gauge

Mandrel

Table

(b)

M_1 M_2

c O 1 2 e

(c)

B R R_1 e O

(d)

e O D_{ref} r D

(e)

3 2 1 GW
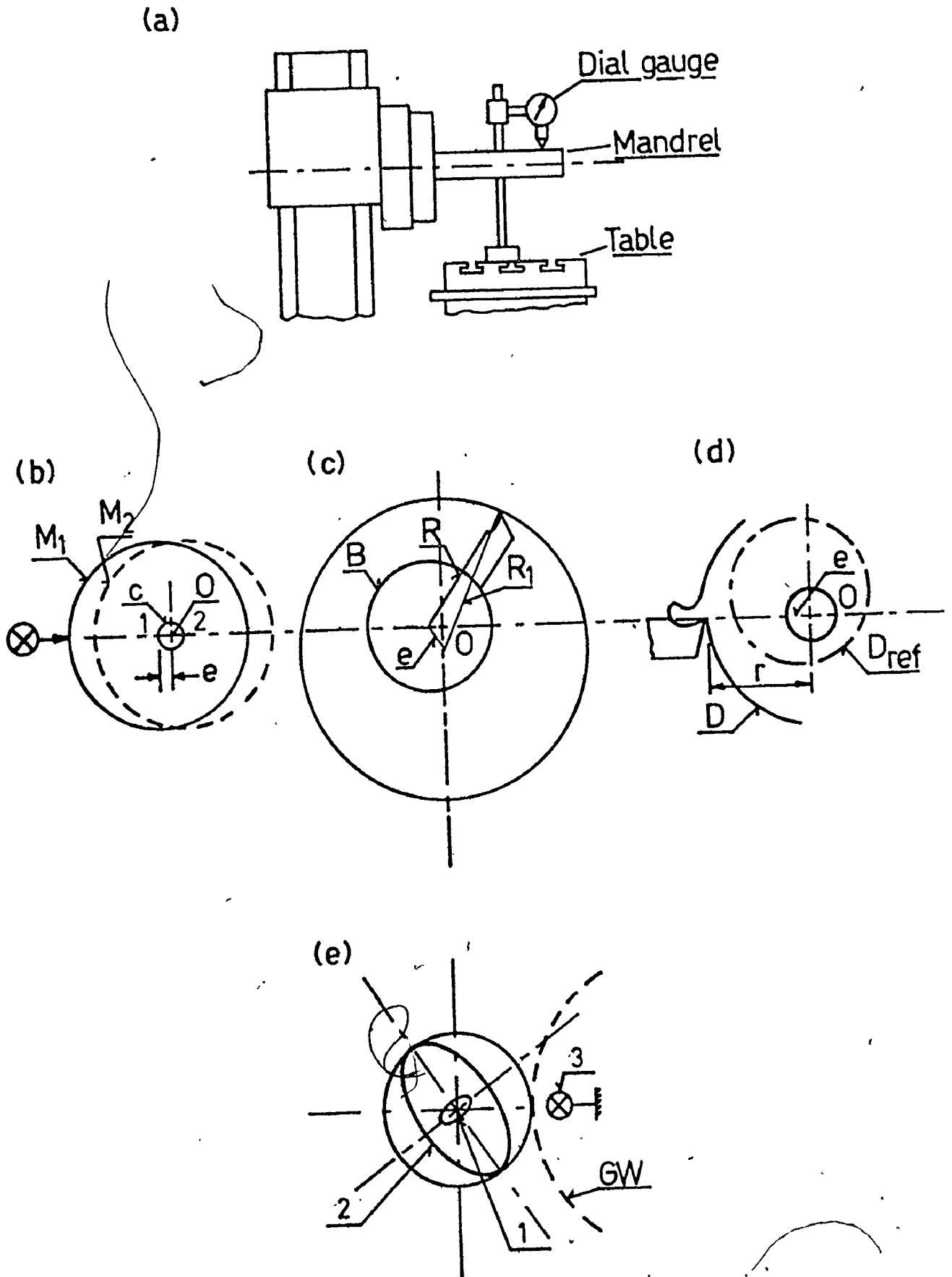
re 5.1   rams for the Discussion of the Short-
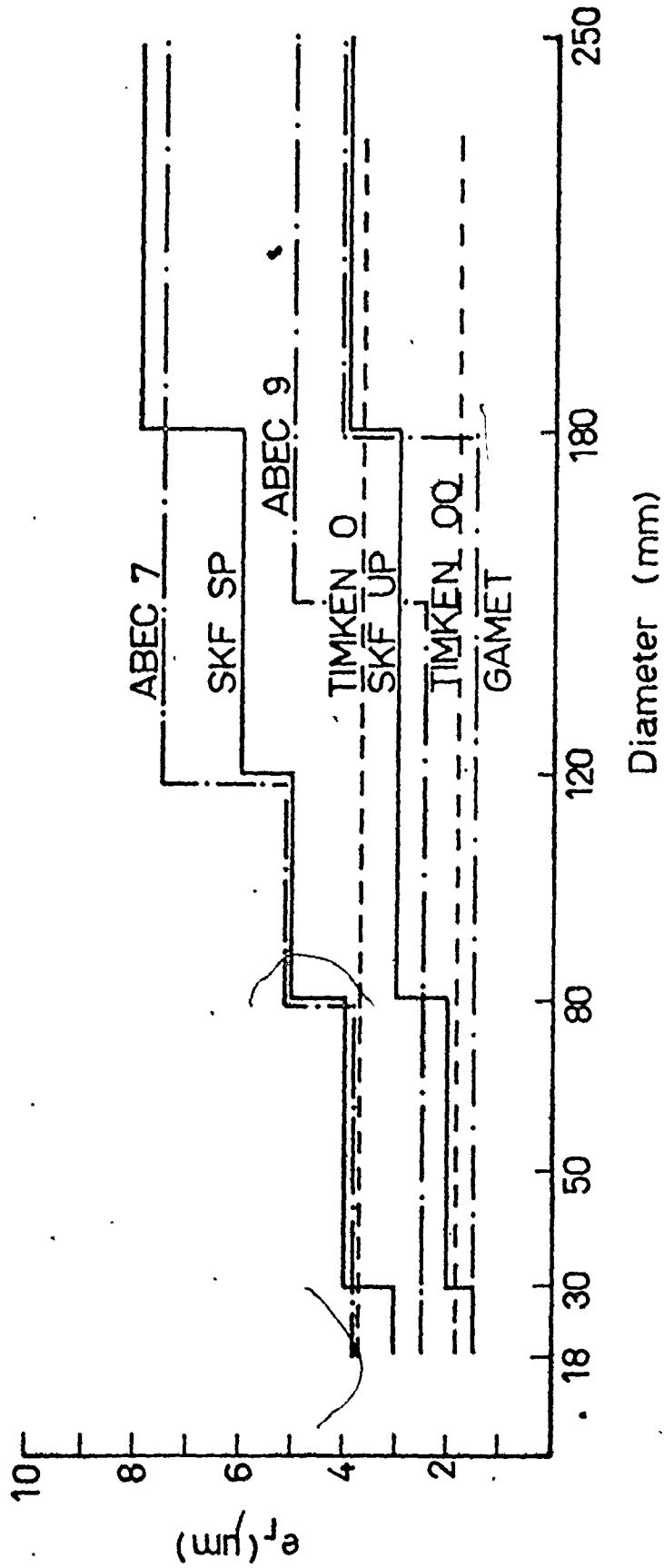
Figure 5.2   The Radial Run-out of the Inner Ring of Roller
Bearings.   The Tolerances of Various
Manufacturers [5].
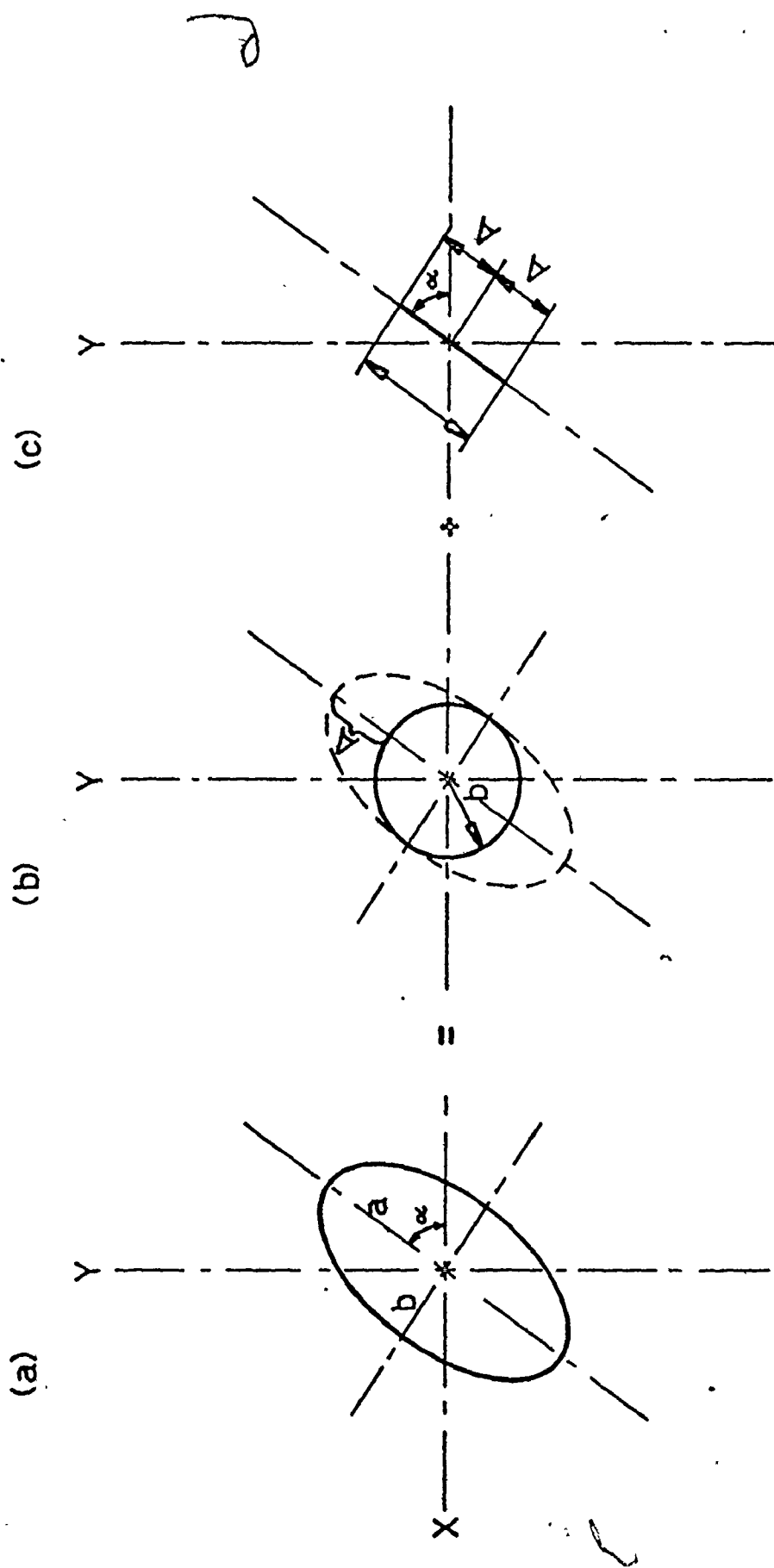
Figure 5.3   Defining the Axis of Rotation

(a)

$\overline{AB}$ Fixed relative to tool
$\overline{CD}$ Embedded in workpiece

Structural
Loop

$\overline{AB}$ Axis average line
$\overline{CD}$ Axis of rotation

(b)
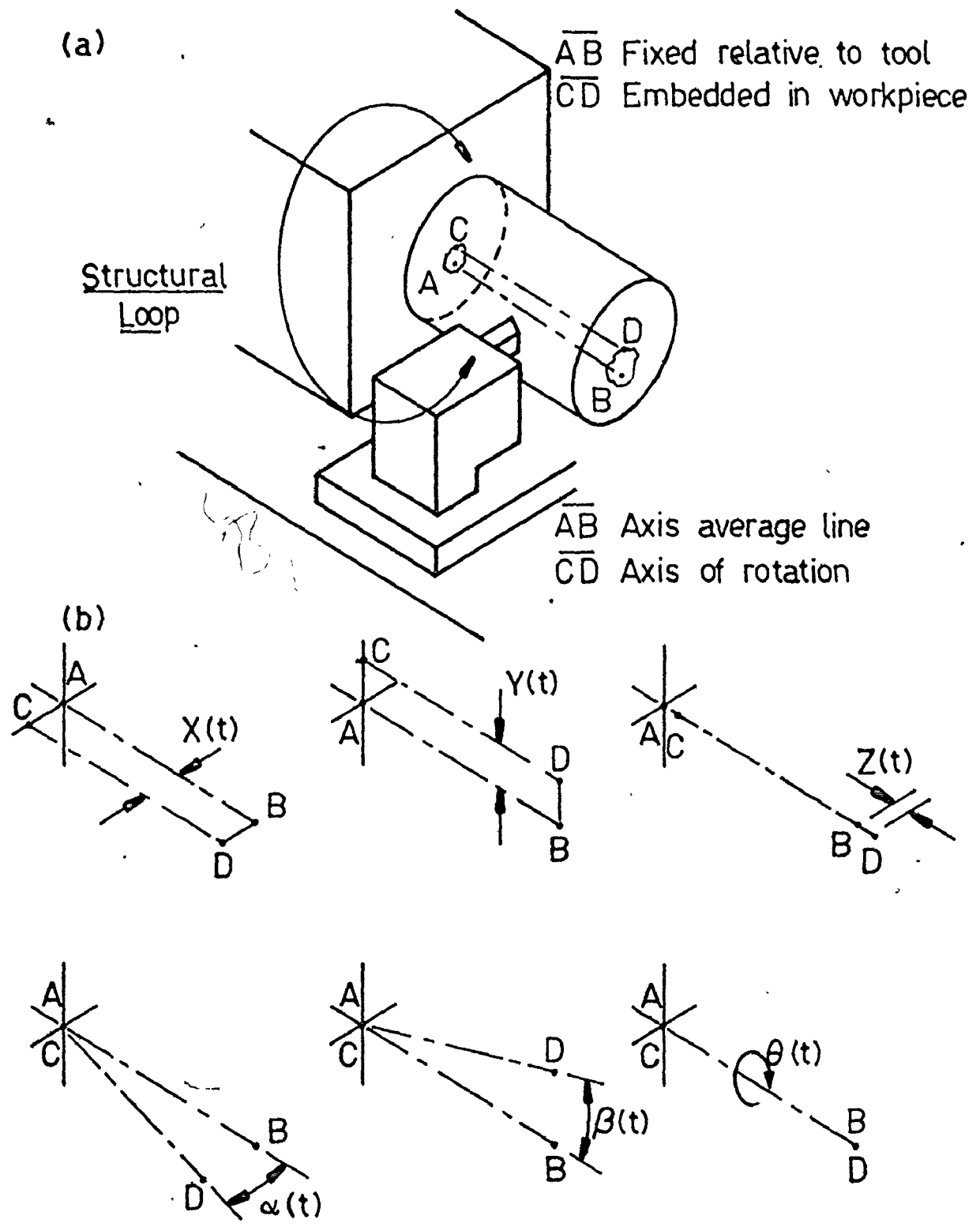
Figure 5.4   The 6 Degrees of Freedom Associated with
an Axis of Rotation.

Concepts of spindle rotation errors, rotating tool

Concepts of spindle rotation errors, rotating workpiece
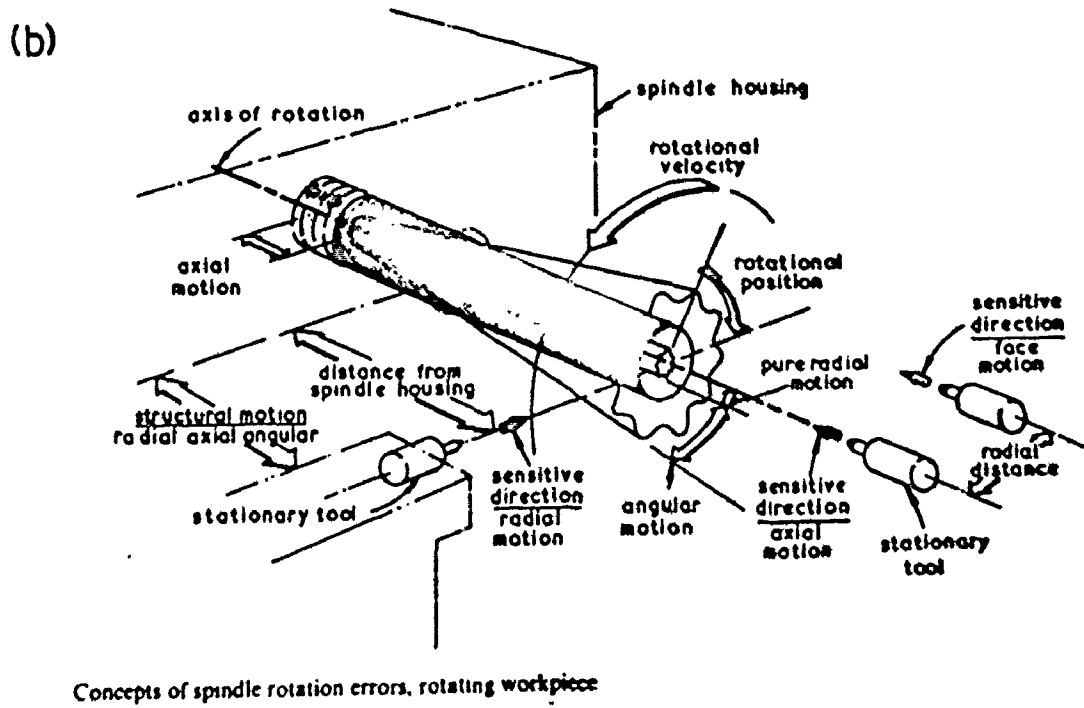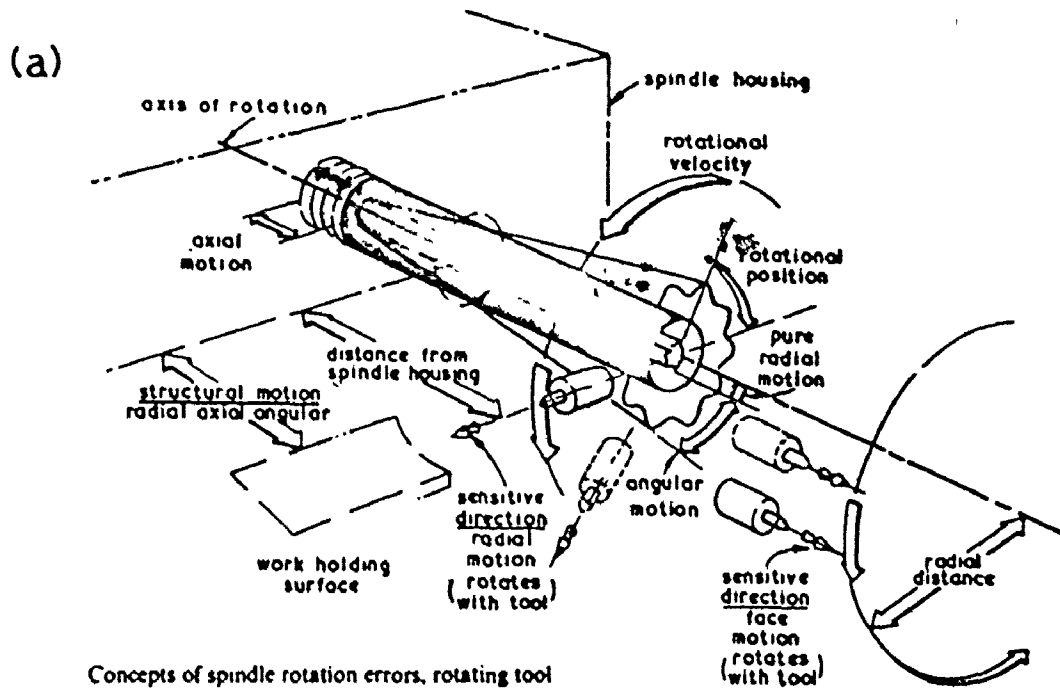
Figure 5.5   Concepts of Spindle Rotation Errors for
                   and Rotating Sensitive Directions
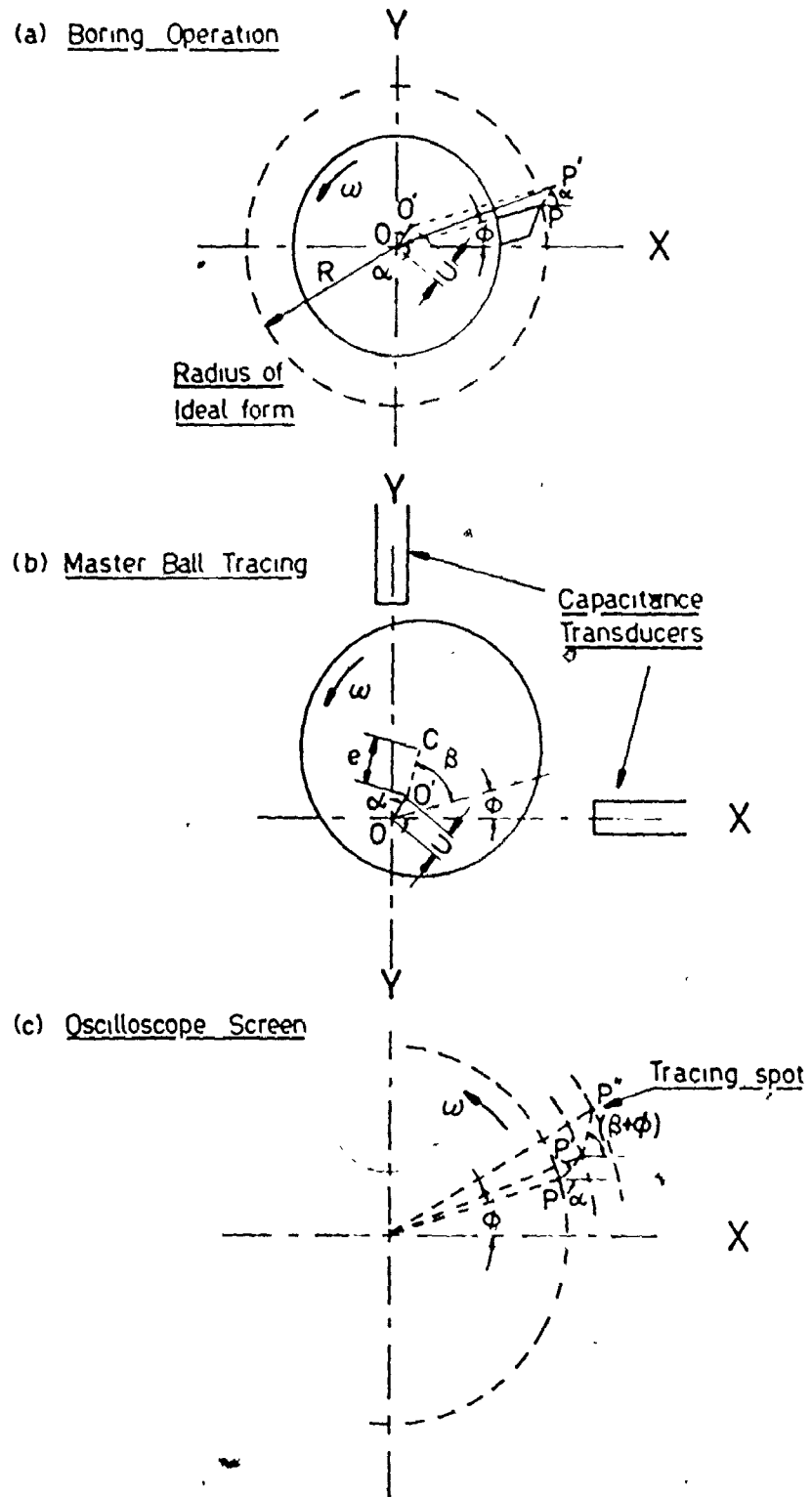
Figure 5.6   A Representation of the generation
of Errors in Boring, Decomposition
and Synthesis in the Master Ball
Trace Test.

(a) Turning Operation

(b) Master Ball Tracing

(c) Oscilloscope Screen
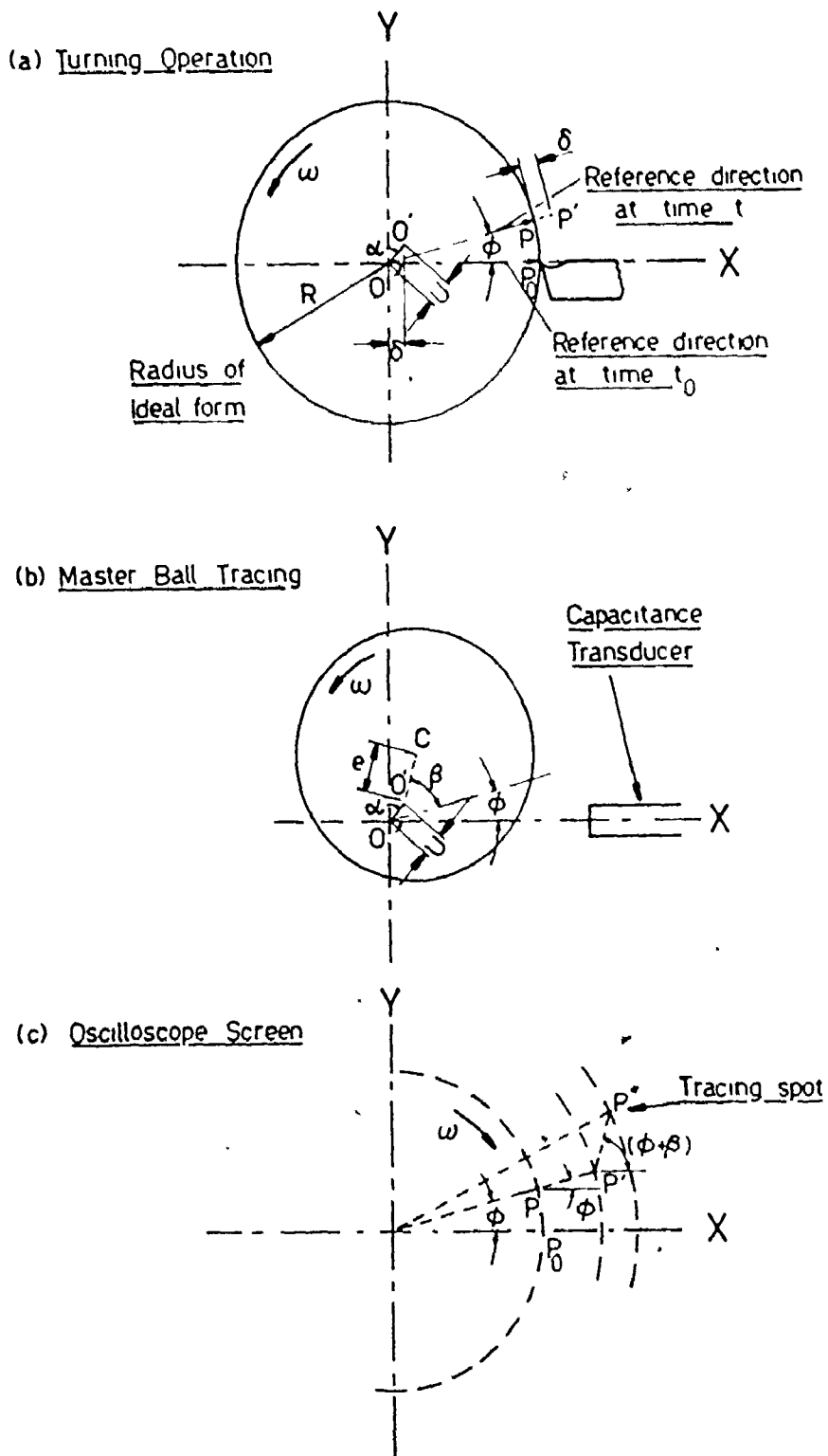
Figure 5.7 A Representation of the generation
of errors in Turning, their
Decomposition and Synthesis in the
Master Ball Trace Test.
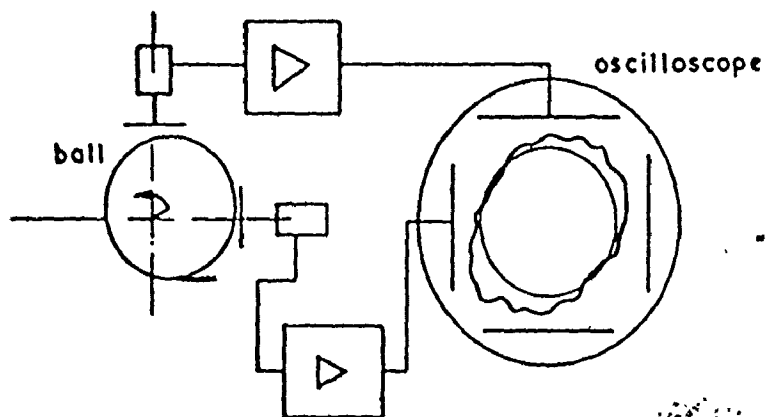
Figure 5.8 The Basic set-up for Measuring Radial Error
Motion: applicable to a rotating sensitive
direction (e.g. boring) [36].
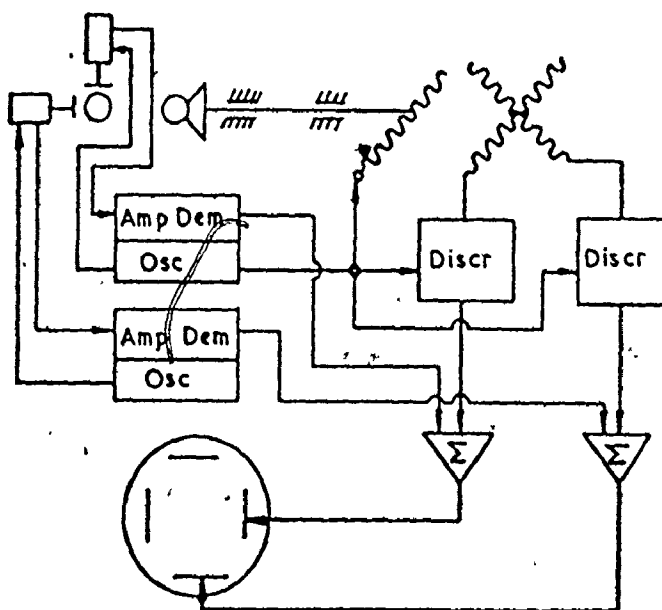
Figure 5.9 The Modified set-up for Measuring Radial
: a plicable to a rotating
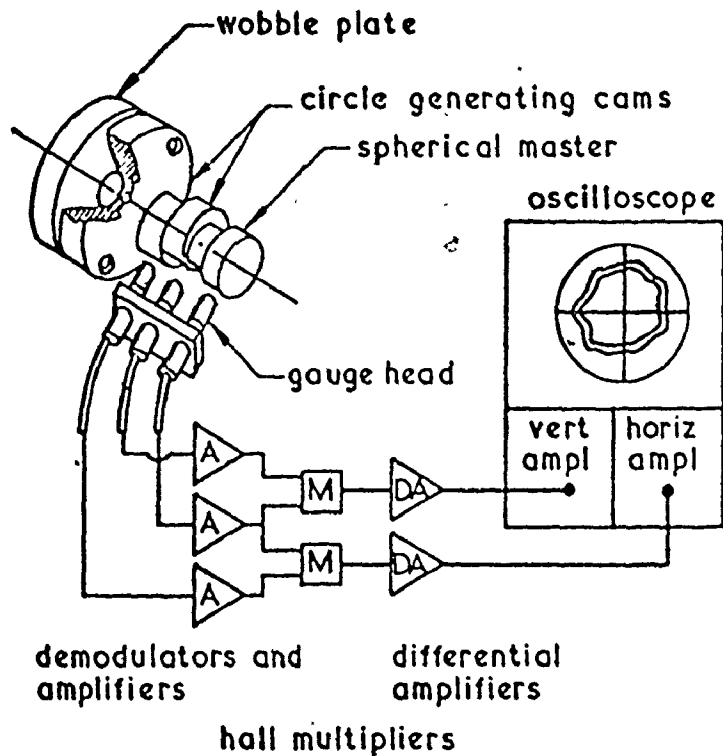
Figure 5.10   The Basic set-up for Measuring Radial
error motion: applicable to a fixed
sensitive direction (e.g. turning) [37].
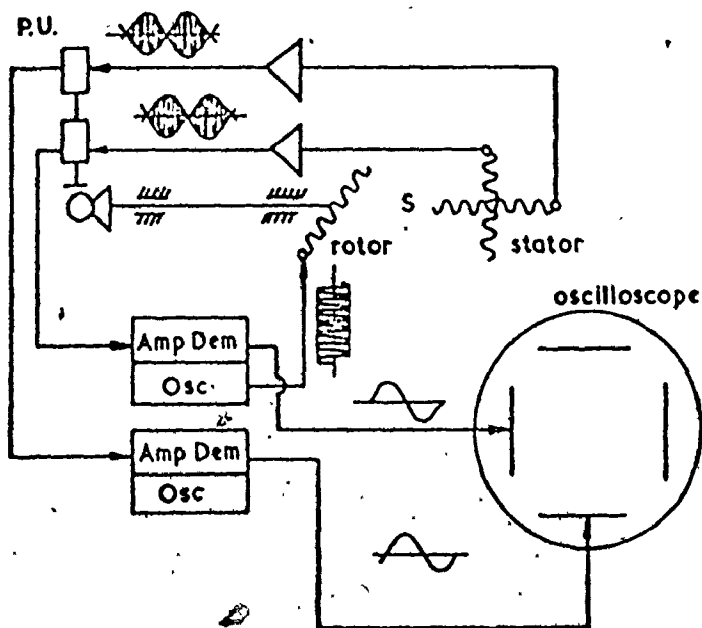
Figure 5.11   The Modified set-up for Measuring Radial
error Motion: applicable to a fixed
sensitive direction (e.g. turning) [5].
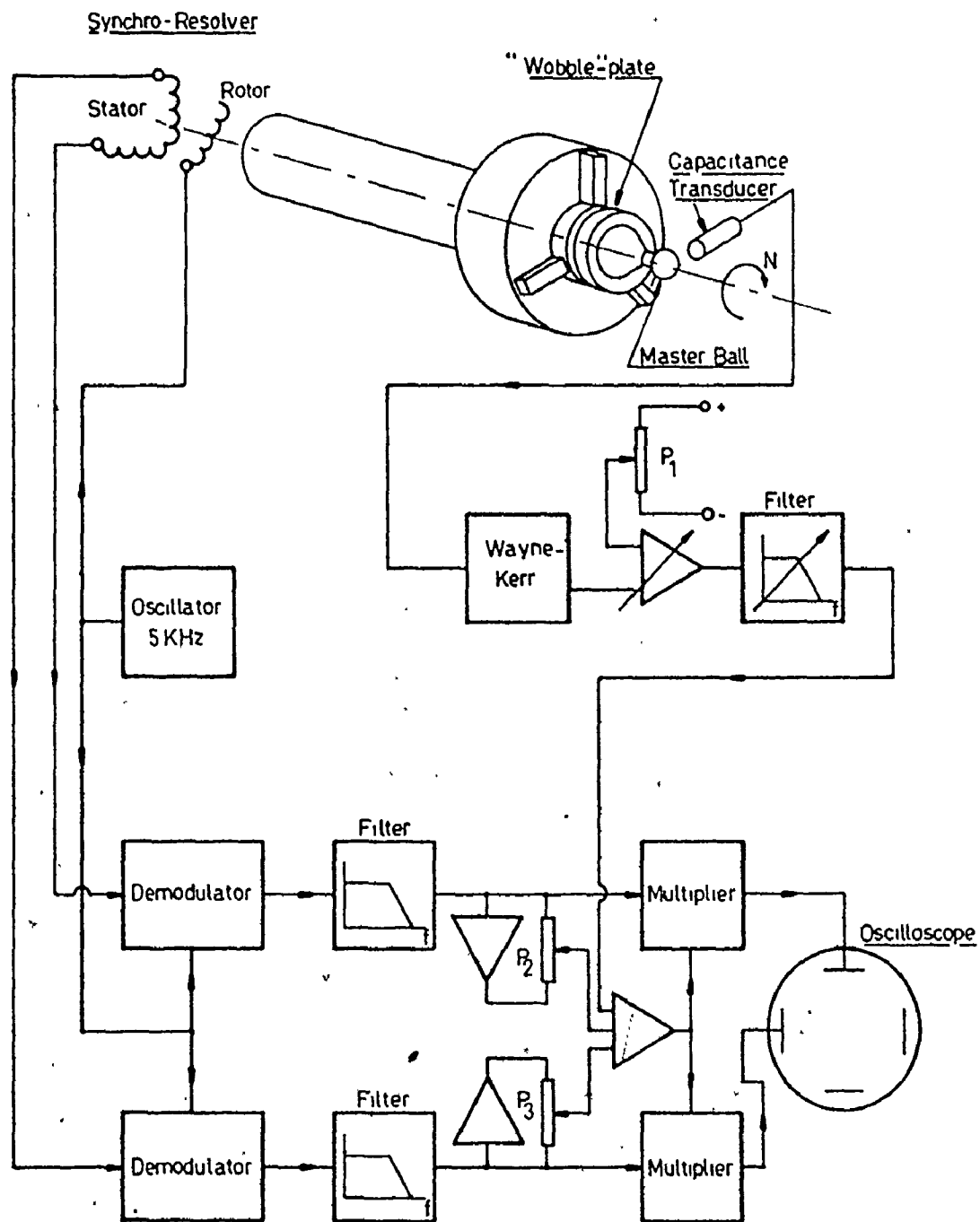
Figure 5.12 The Axis of Rotation Analyser: block
diagram of set-up for measuring radial
error motion in turning.
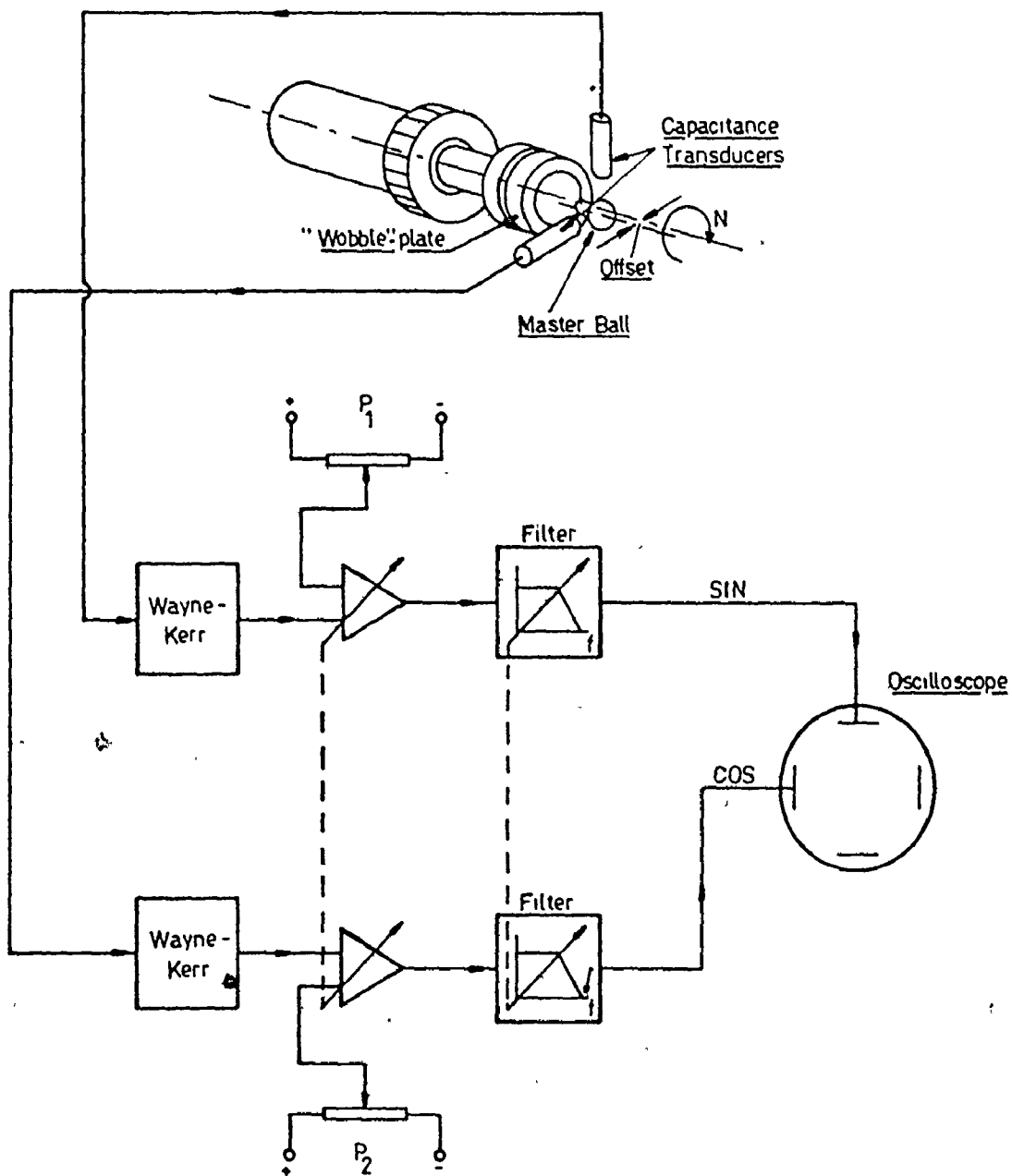
Figure 5.13 The Axis of Rotation Analyser: block
diagram of the basic set-up for measuring
radial error motion in boring. Reference
circle Generated by offset of the Master
Ball.
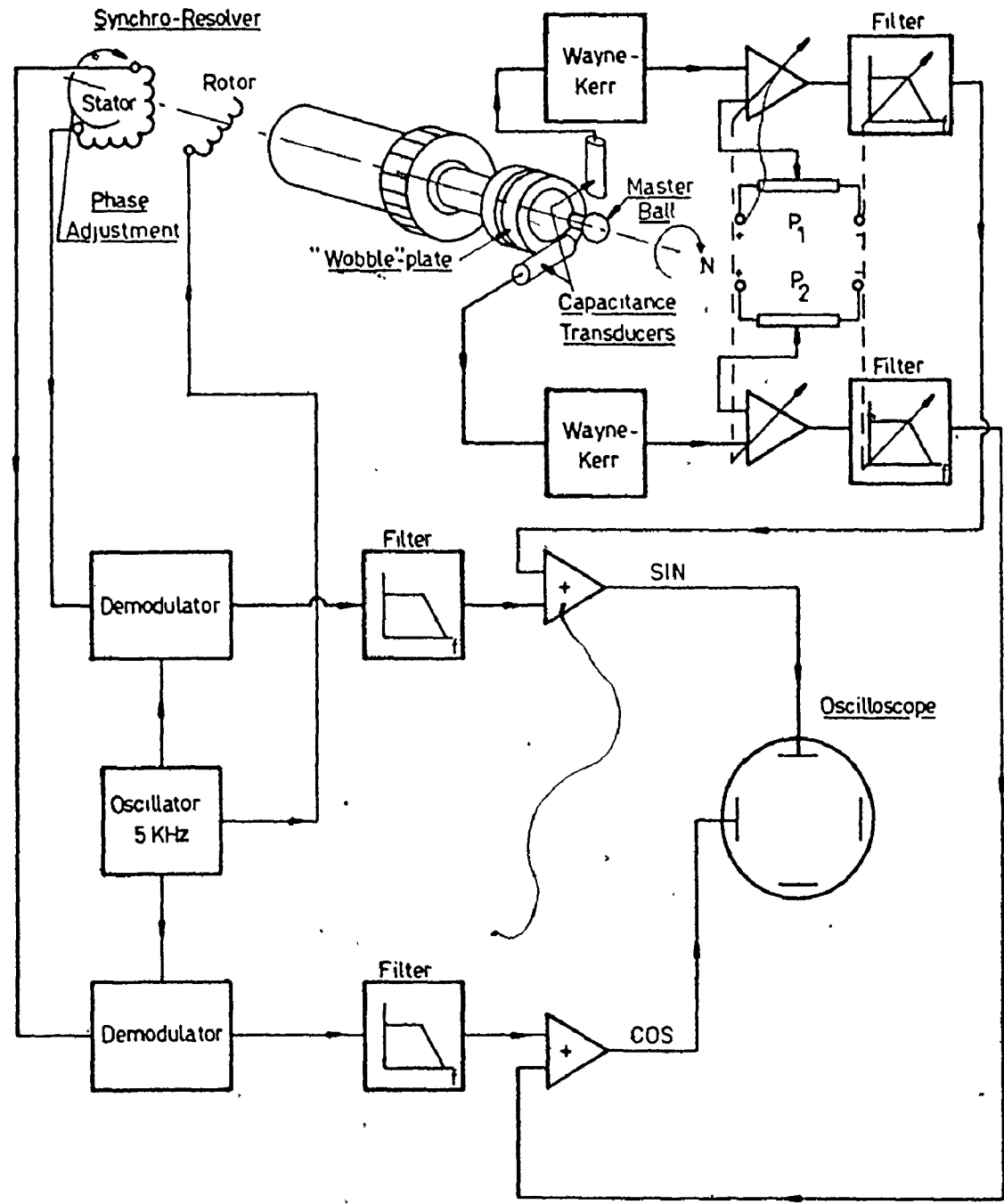
Figure 5.14 The Axis of Rotation Analyser: block
diagram of the Alternate Set-up for
measuring Radial error Motion in Boring.
Reference circle generated by Synchro-
Resolver.

(a)

(b)

To Z - Modulation
of Oscilloscope

(c)

(d)
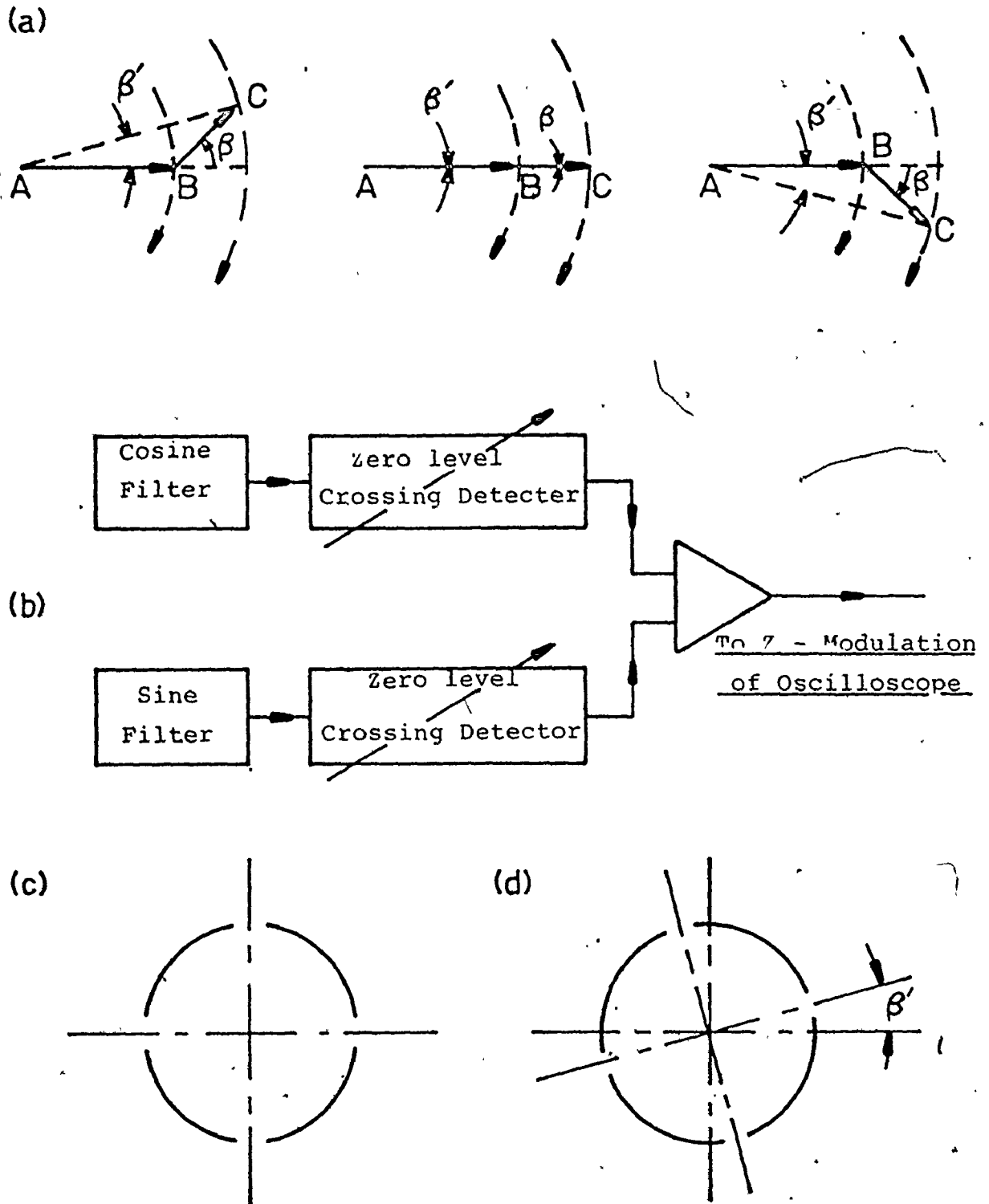
Figure 5.15   The Elimination of the effect of the
Residual Eccentricity of the Master Ball,
in the Measurement of Radial Error motion
in turning, by Z-modulation.

a) Minimum Circumscribed Circle   b) Maximum Inscribed Circle

$$R_{max} - R_{min} = 0.88 \text{ in.}$$
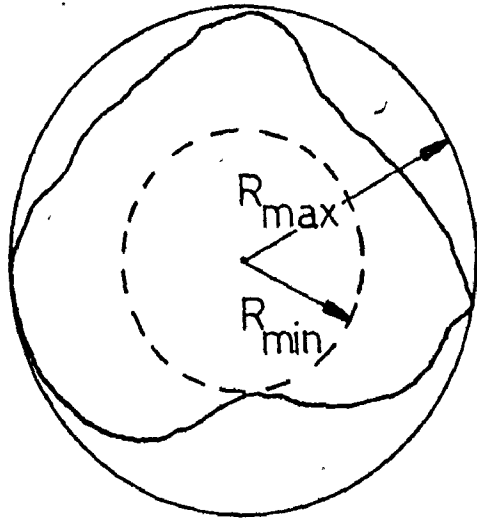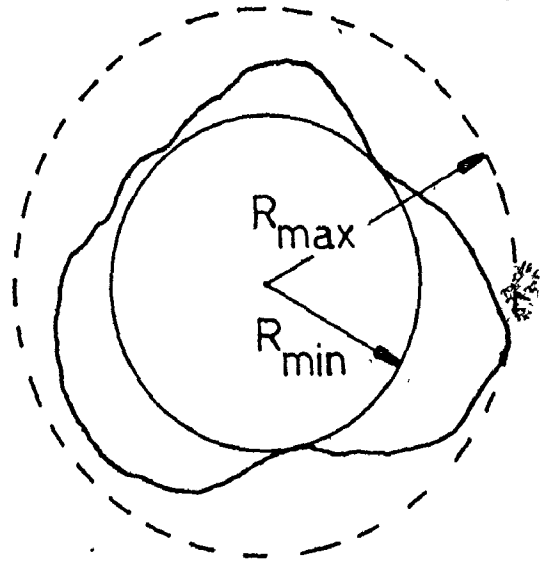
$$R_{max} - R_{min} = 0.76 \text{ in.}$$

c) Minimum Radial Separation   d) Least Squares Circle

$$R_{max} - R_{min} = 0.72 \text{ in.}$$
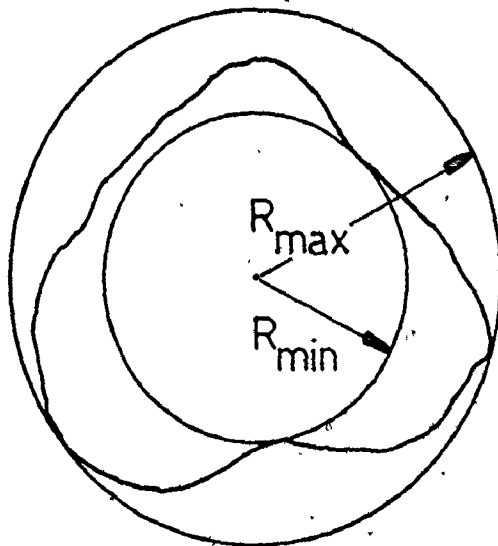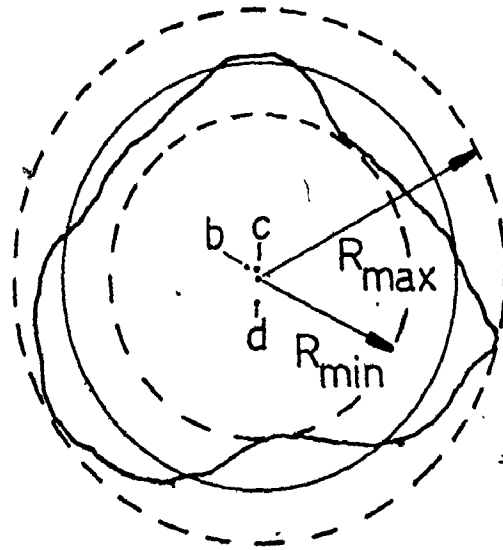
$$R_{max} - R_{min} = 0.75 \text{ in.}$$

Figure 5.16   Evaluation of Polar Graph of error
Various Techniques [43].

3730 : 1964

A3. Determination of the least squares centre and circle. The position of the centre of the least squares circle and the value of its radius, can be calculated from simple approximate formulae.

Referring to Fig. 10, the practical procedure is as follows:

The distances a and b of the least squares centre from the centre of the paper are calculated from the following approximate formulae:

$$a = \frac{2 \times \text{sum of } x \text{ values}}{\text{number of ordinates}} = \frac{2\Sigma x}{n}$$

$$b = \frac{2 \times \text{sum of } y \text{ values}}{\text{number of ordinates}} = \frac{2\Sigma y}{n}$$

The radius R of the least squares circle, if wanted, is calculated as the average radial distance of the points P from the centre, that is:

$$R = \frac{\text{sum of radial values}}{\text{number of ordinates}} = \frac{\Sigma r}{n}$$

In practice, if it is required to know only the radial width of the zone enclosing the curve, there is no point in finding R, and it is sufficient to draw the inscribing and circumscribing circles from the least squares centre.

A convenient method of laying out the work is to measure the positive and negative values of x and y sequentially and enter them in columns as shown below. They can then be quickly added up.

$+x$	$-x$		$+y$	$-y$
0·57	0·55		0·62	0·48
0·90	0·84		0·90	0·87
1·20	0·98		1·15	0·98
0·98	0·79		0·93	0·98
0·57	0·55		0·45	0·50
4·22	3·71		4·05	3·81

$$\Sigma x = +0·51 \qquad\qquad \Sigma y = +0·24$$

$$a = \frac{2 \times 0·51}{12} = +0·084 \qquad b = \frac{2 \times 0·24}{12} = +0·04$$

The accuracy of determination, both of the centre and of the width of the radial zone, depends on the number of ordinates taken.

For guidance, graphs exemplifying different types of profile have been evaluated using 12, 24, 48 and 96 ordinates, the latter being chosen as coming nearest to the absolute value.

Least squares circle

Least squares centre

From the centre of the chart, draw a sufficient even number of equally spaced radial ordinates. In the illustration they are shown, numbered 1-12. Two of these at right angles are selected to provide a system of rectangular co-ordinates XX, YY.

The distances of the points of intersection of the polar graph with these radial ordinates, P₁ to P₁₂, are measured from the axes XX and YY, taking positive and negative signs into account.

Fig. 10. Determination of least squares centre and circle

Figure 5.17 Determination of the Least Squares Center and Circle [44].

(a) MRSZ MRSC

(b) $\Delta_r TR$

(c) $\Delta_r TR, 4 revs$

(d) Δ_n / ER

(e) $\Delta_r TR = v_r$

(f) OE IE $\Delta_r TR$ v_r

$$\Delta IE = 0$$
$$\Delta OE = 0$$
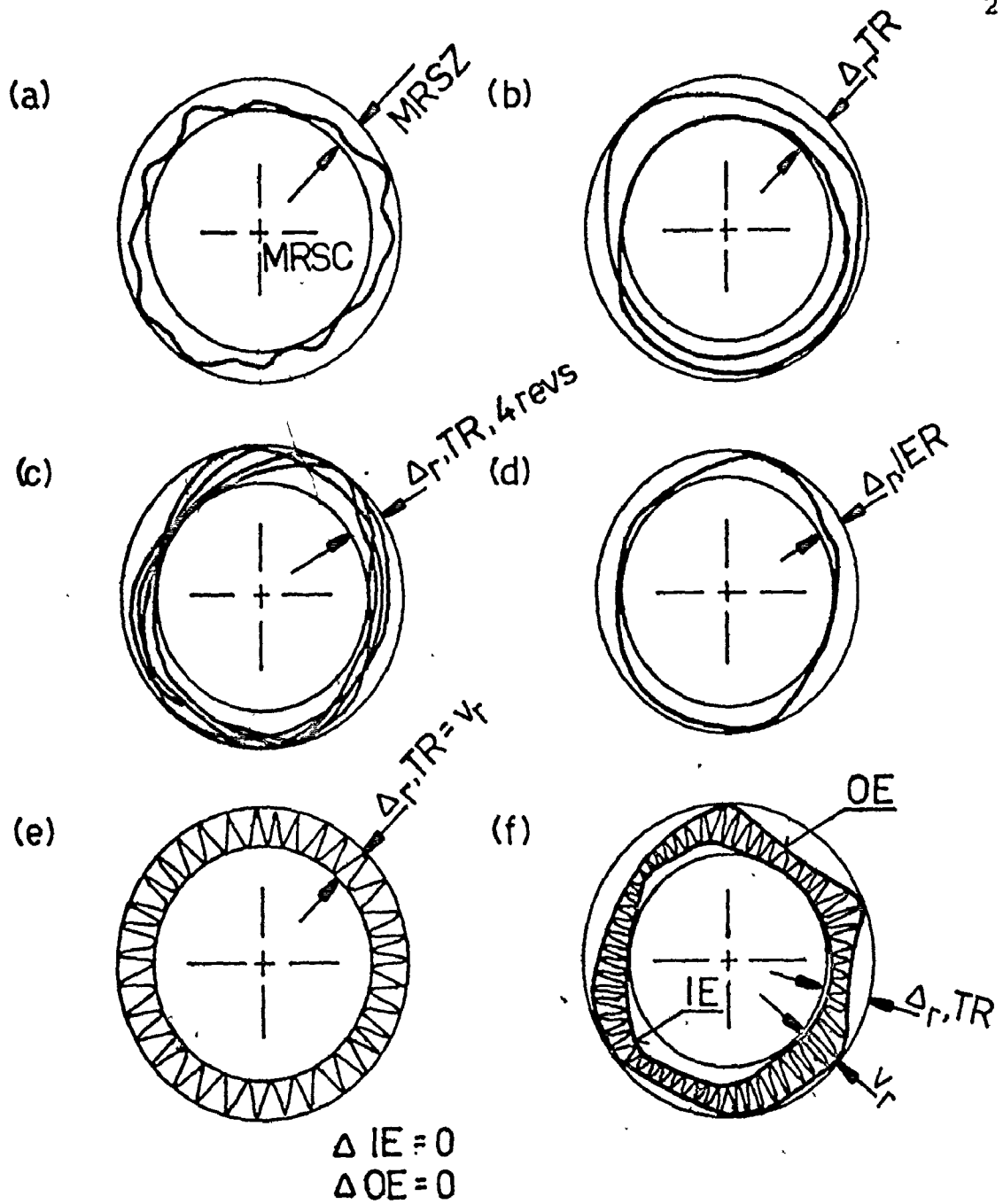
Figure 5.18   Evaluating Radial Error Motion

v_a

MRSC
PC

1

2
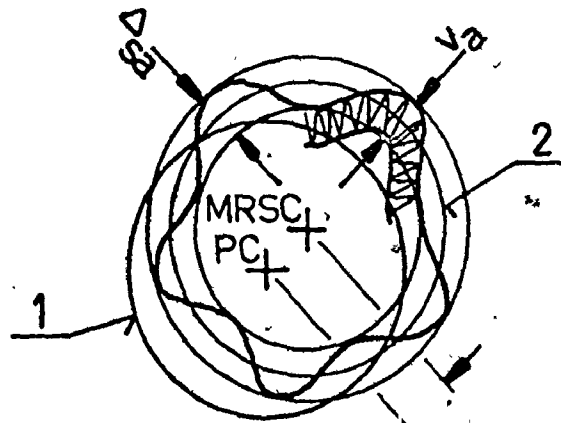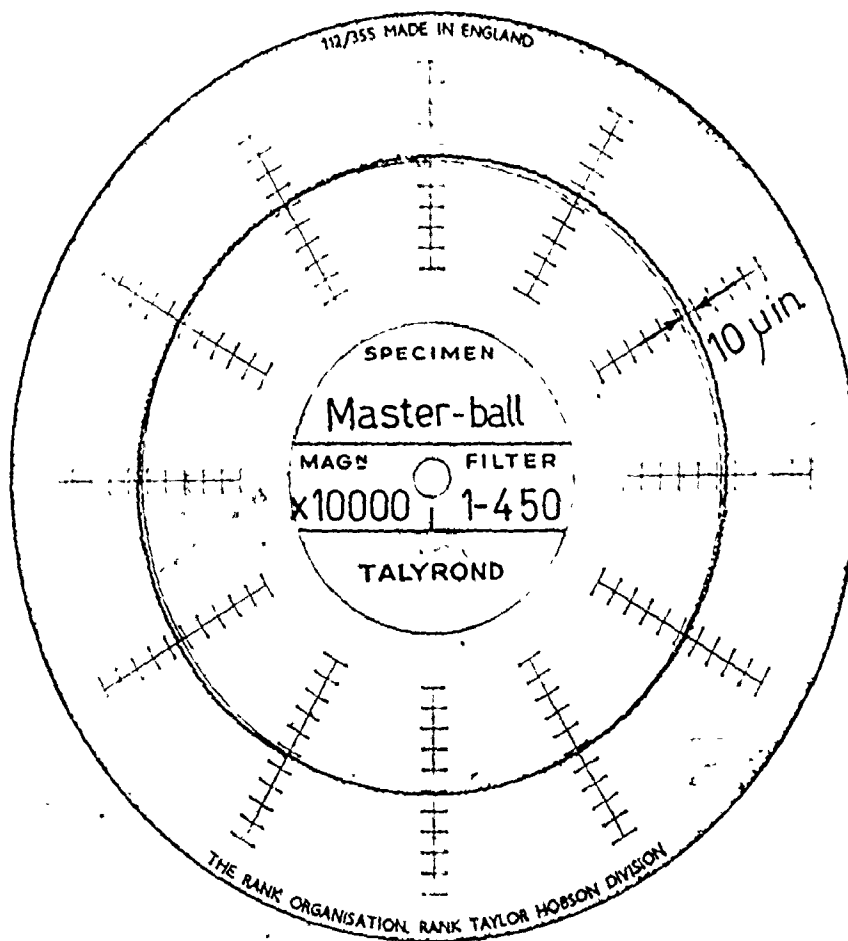
Figure 5.20   Talyrondgram showing the Roundness
of the Master Ball
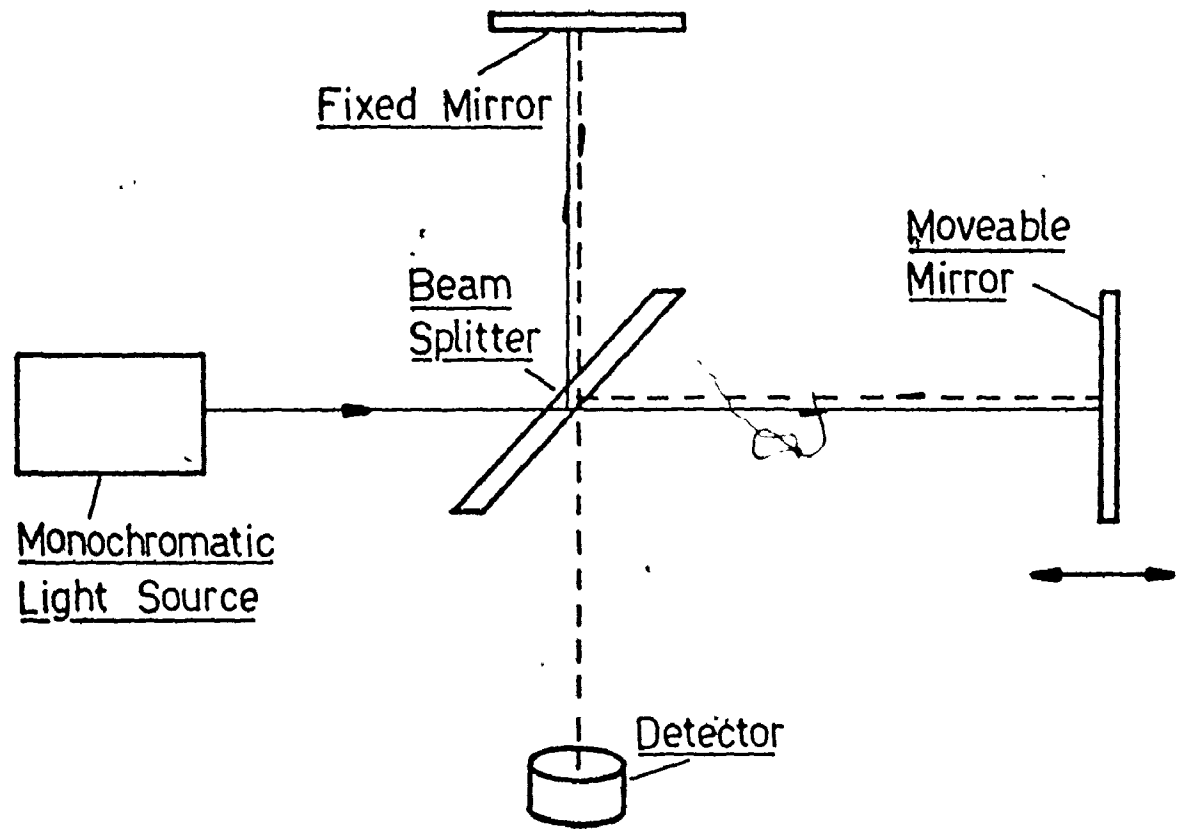
Figure 6.1 The Basic Michelson Interferometer
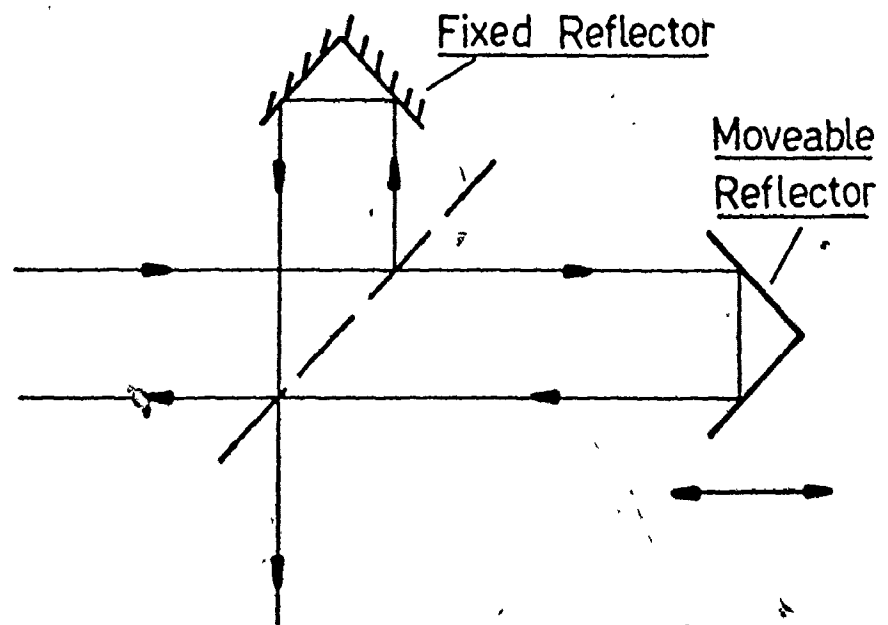
ıre 6.2 The Use of Cube-Corner Reflectors
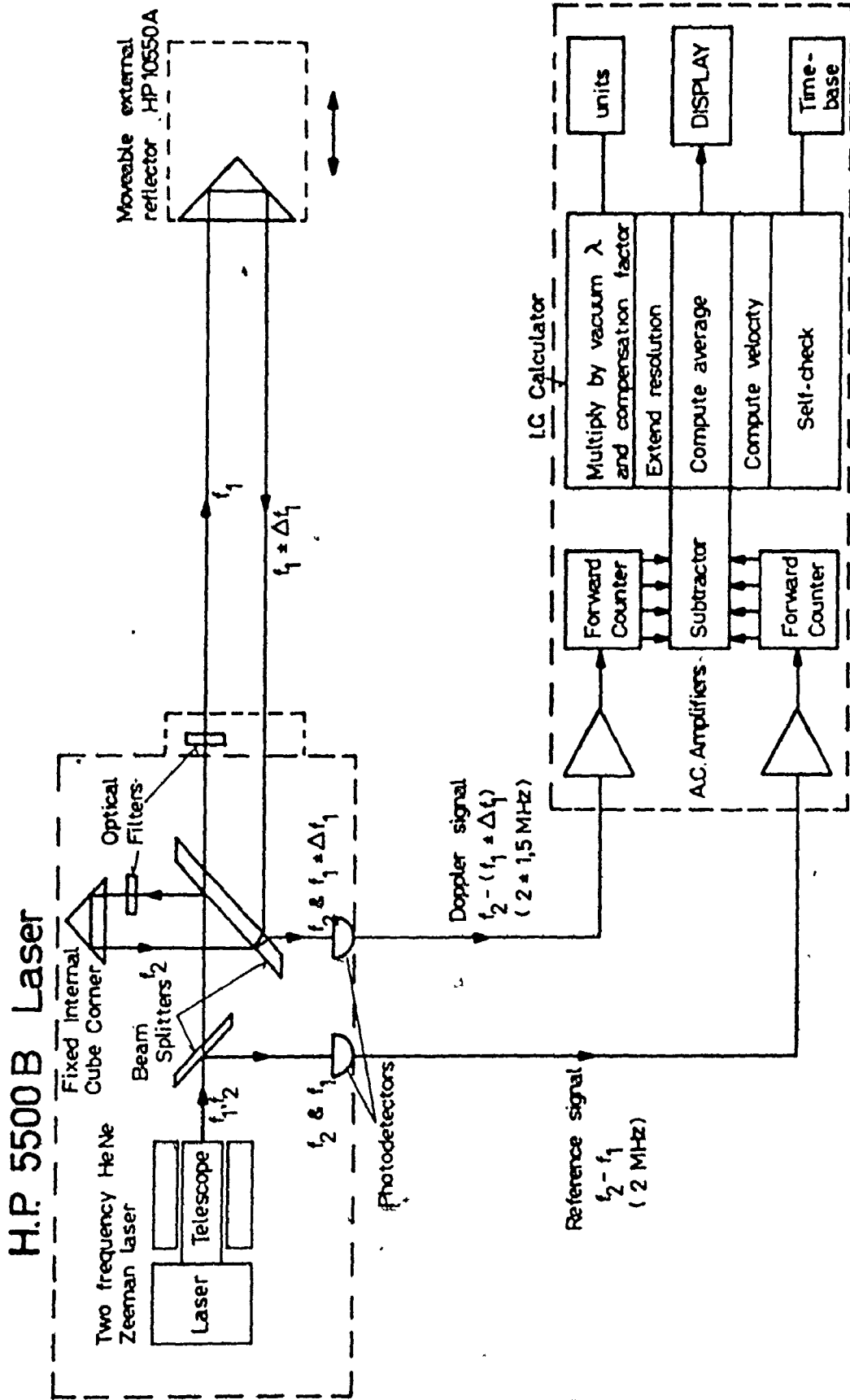
Figure 6.3   Block diagram of the HP5525B Laser Interferometer.
System [46].

HP 10565 A
Reference Reflector

f_1 f_2 f_2 f_1

$f_1 \pm \Delta f_1$

$f_1 \pm \Delta f_1$

HP 10565 A
Remote
Interferometer

HP 10550 A
Reflector
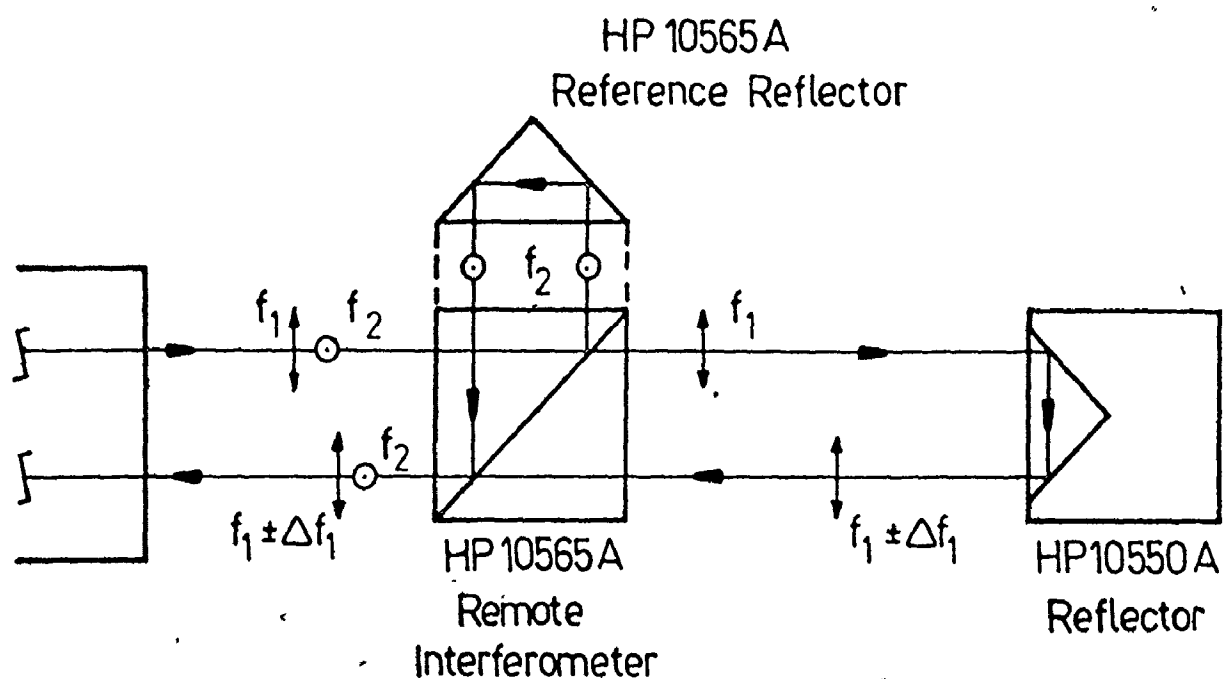
Figure 6.4   The Linear Interferometer [47]
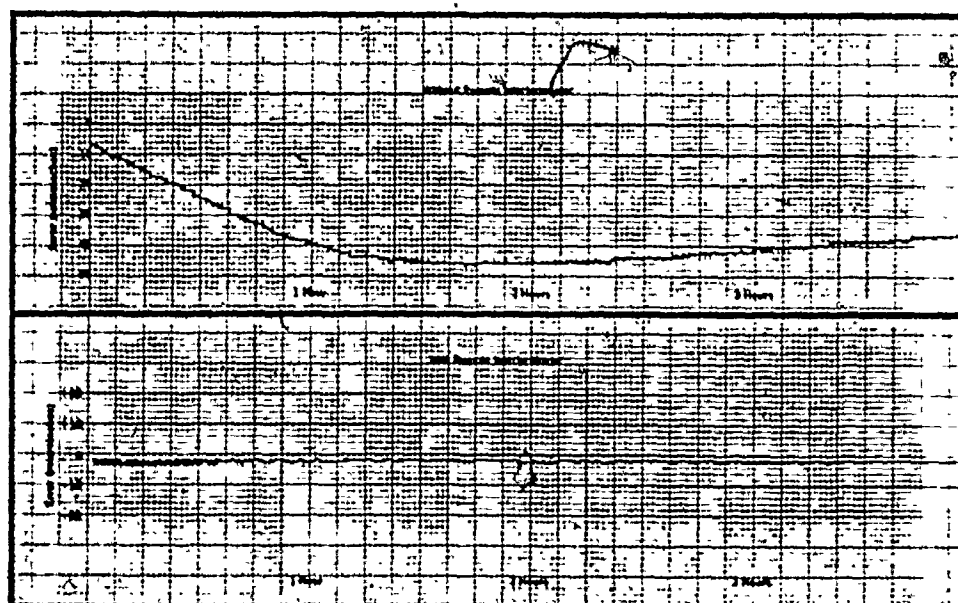
Figure 6.5   The Improved Zero (reference) Stability
when using the Linear Interferometer [46].
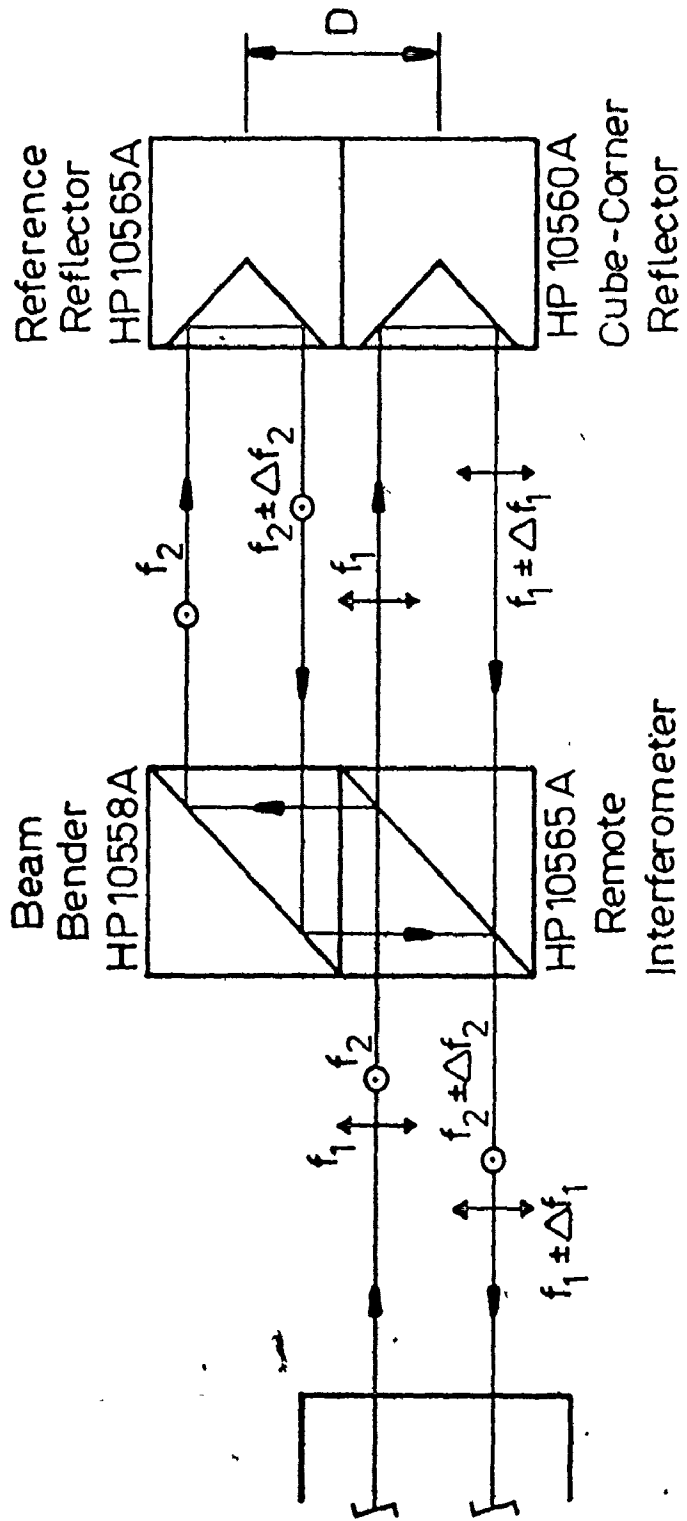
Figure 6.6 The Angular/Flatness Interferometer [47].
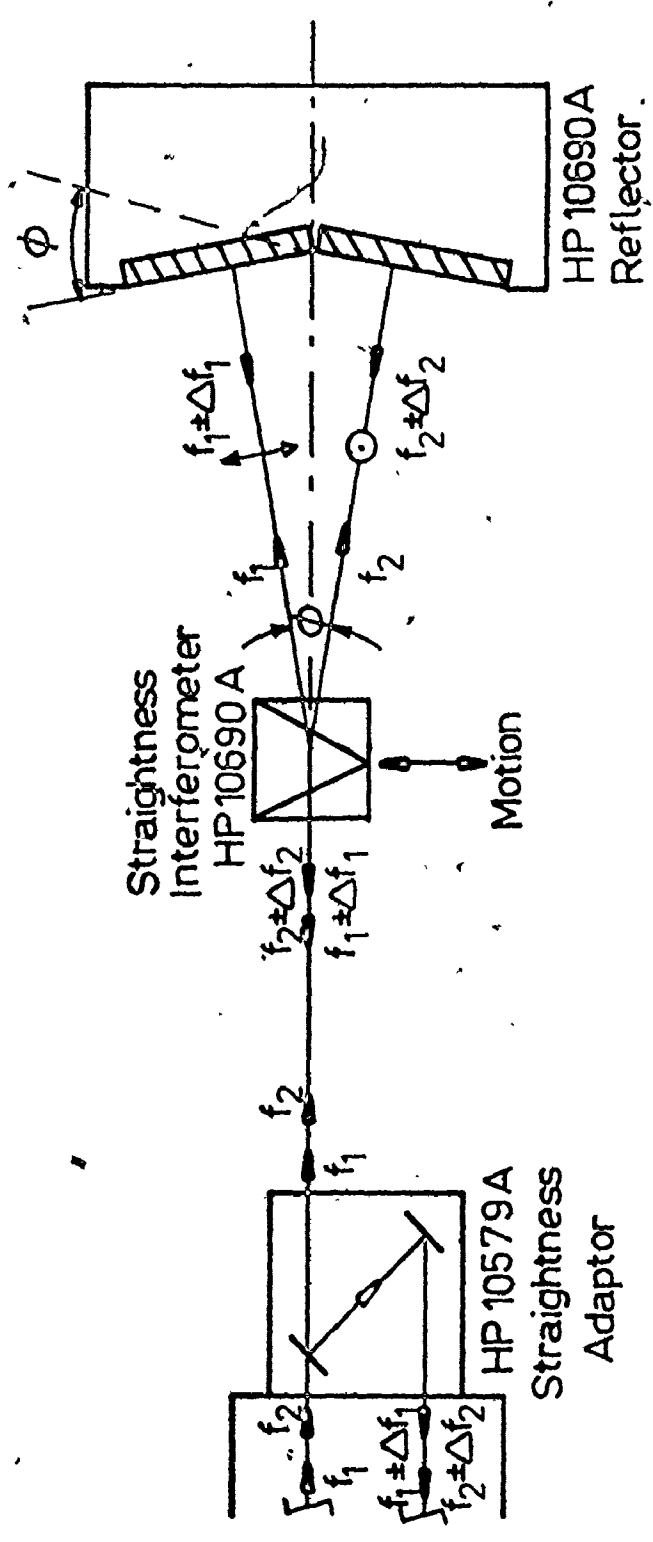
Figure 6.7 The Straightness Interferometer [48].
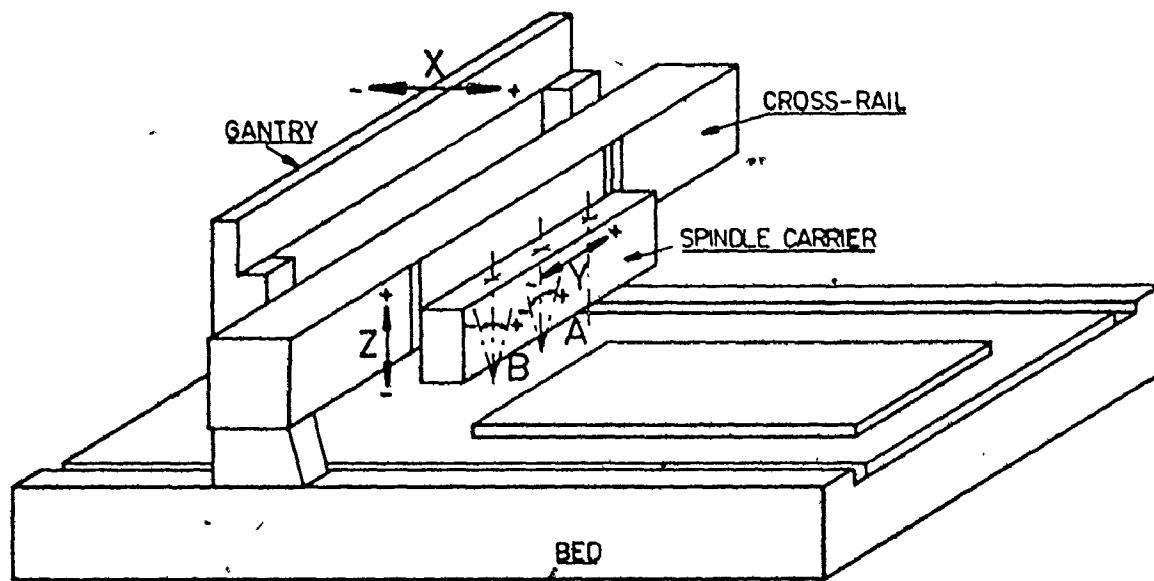
Figure 7.1   The Axis Nomenclature of a 5-Axis
              Aerospace Skin-Milling Machine.
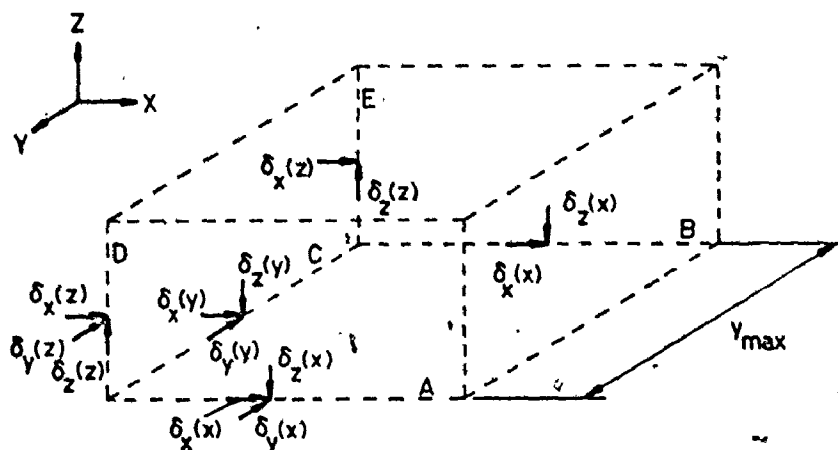
Figure 7.2   The Minimum number of Translative
              Deviations to be Measured on the Skin-
              Milling Machine, with a Limitation to
              Flat Workpieces.

(a)

(b)
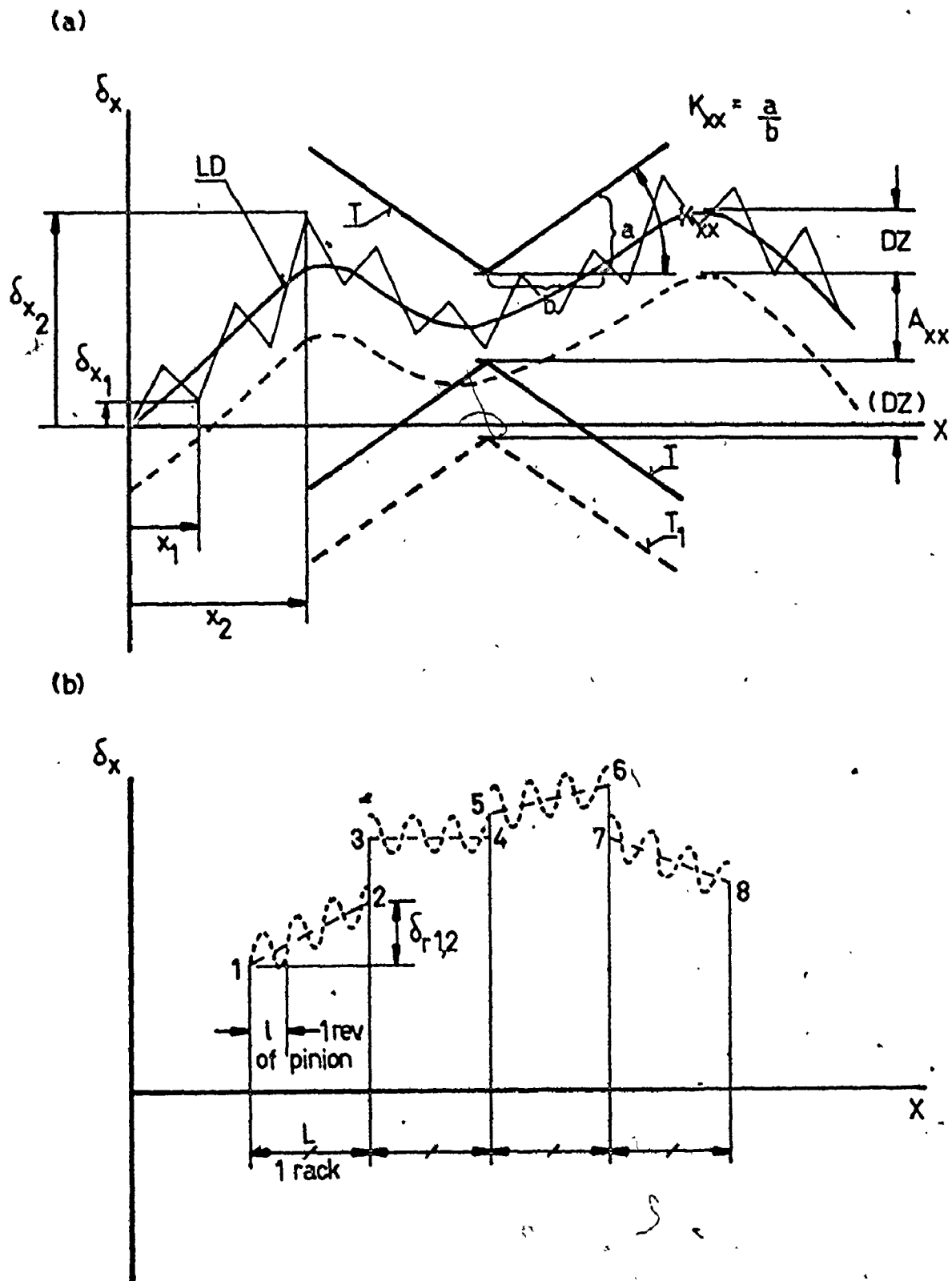
Figure 7.3 The Identification of short and long
           Distance error Deviations for a Rack and
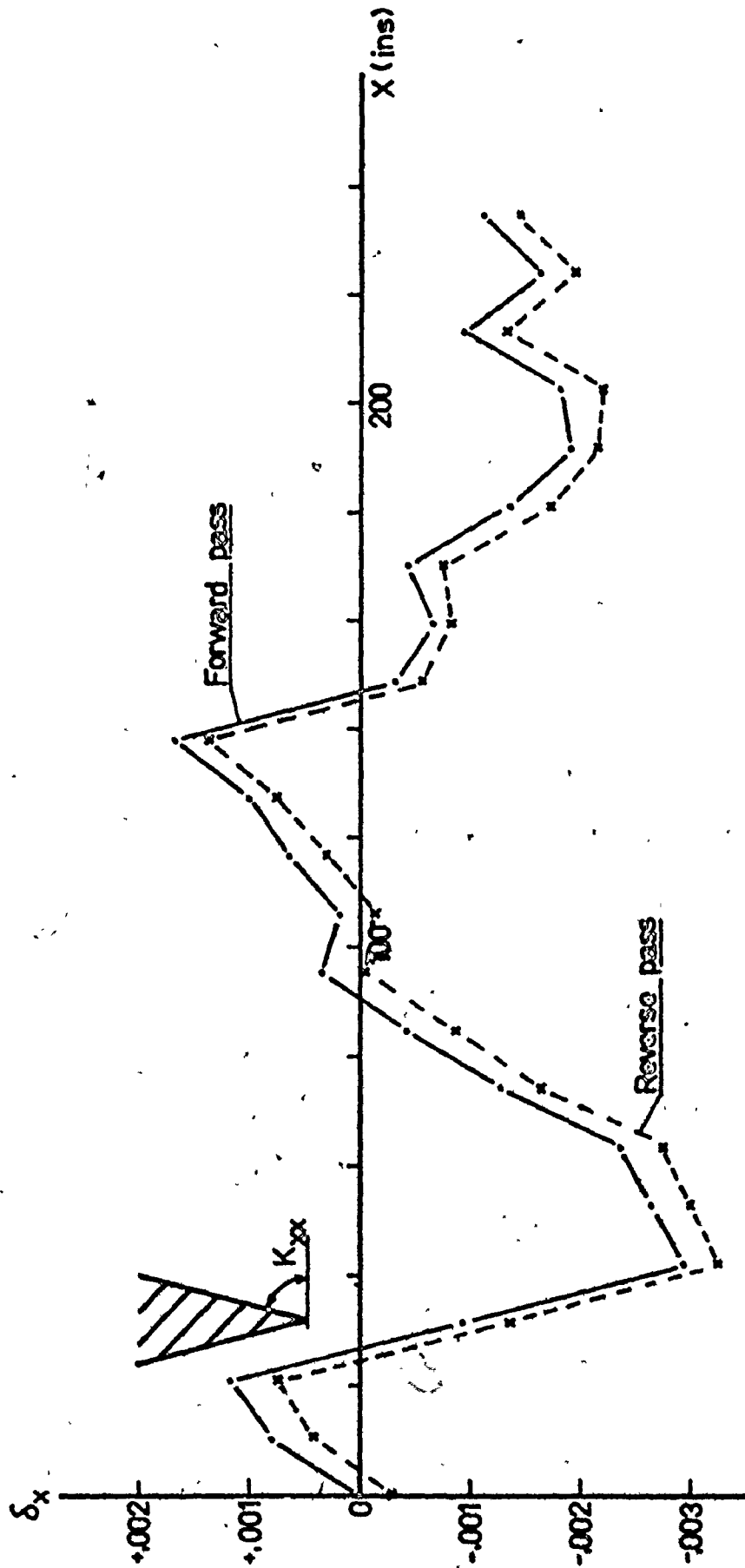
Figure 7.4 A Measurement of Positioning Accuracy on the Skin-Milling Machine: $\delta_x(x)_A$ of Figure 7.2.
(a) full traverse in steps of 10.5 in.
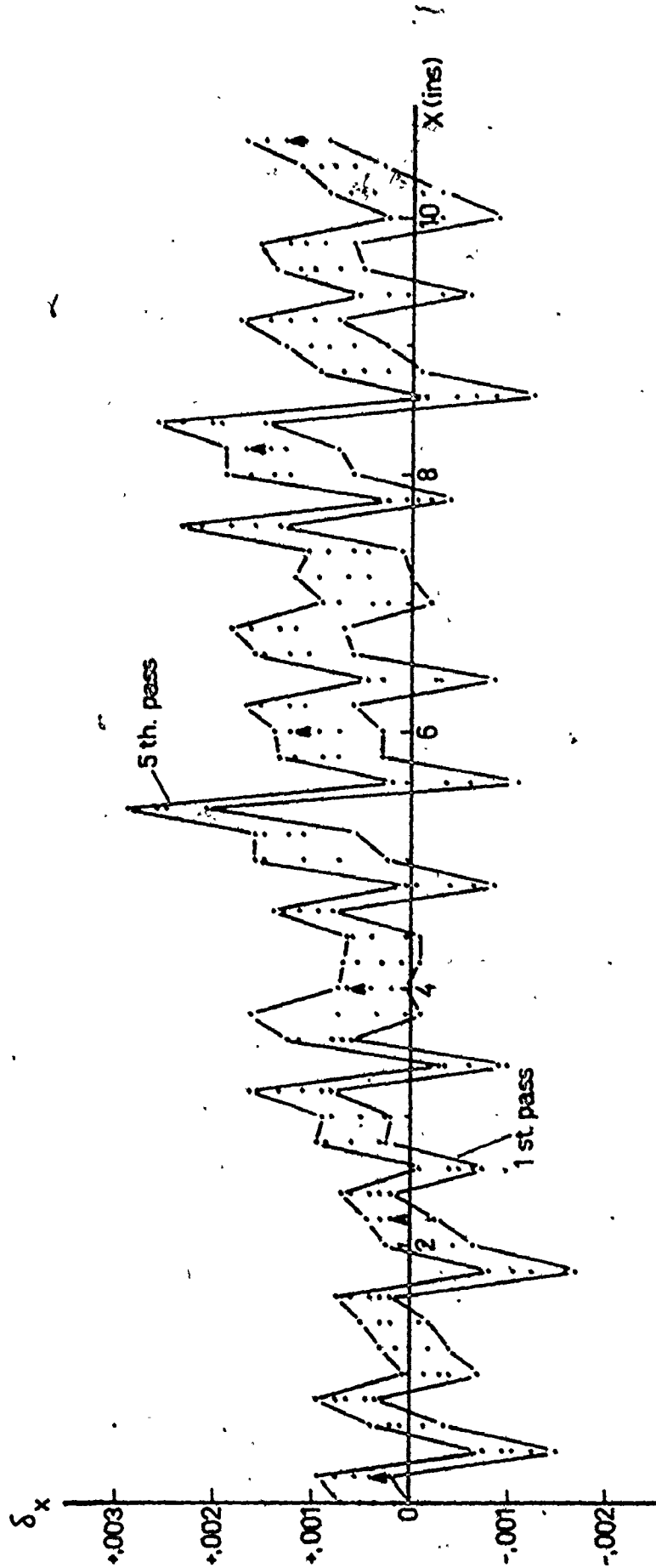
Figure 7.5 A measurement of Positioning Accuracy on the Skin-Milling Machine:
$\delta_x(x)_A$ of Figure 7.2
(b) 10.5 ins. in steps of 0.200 in.
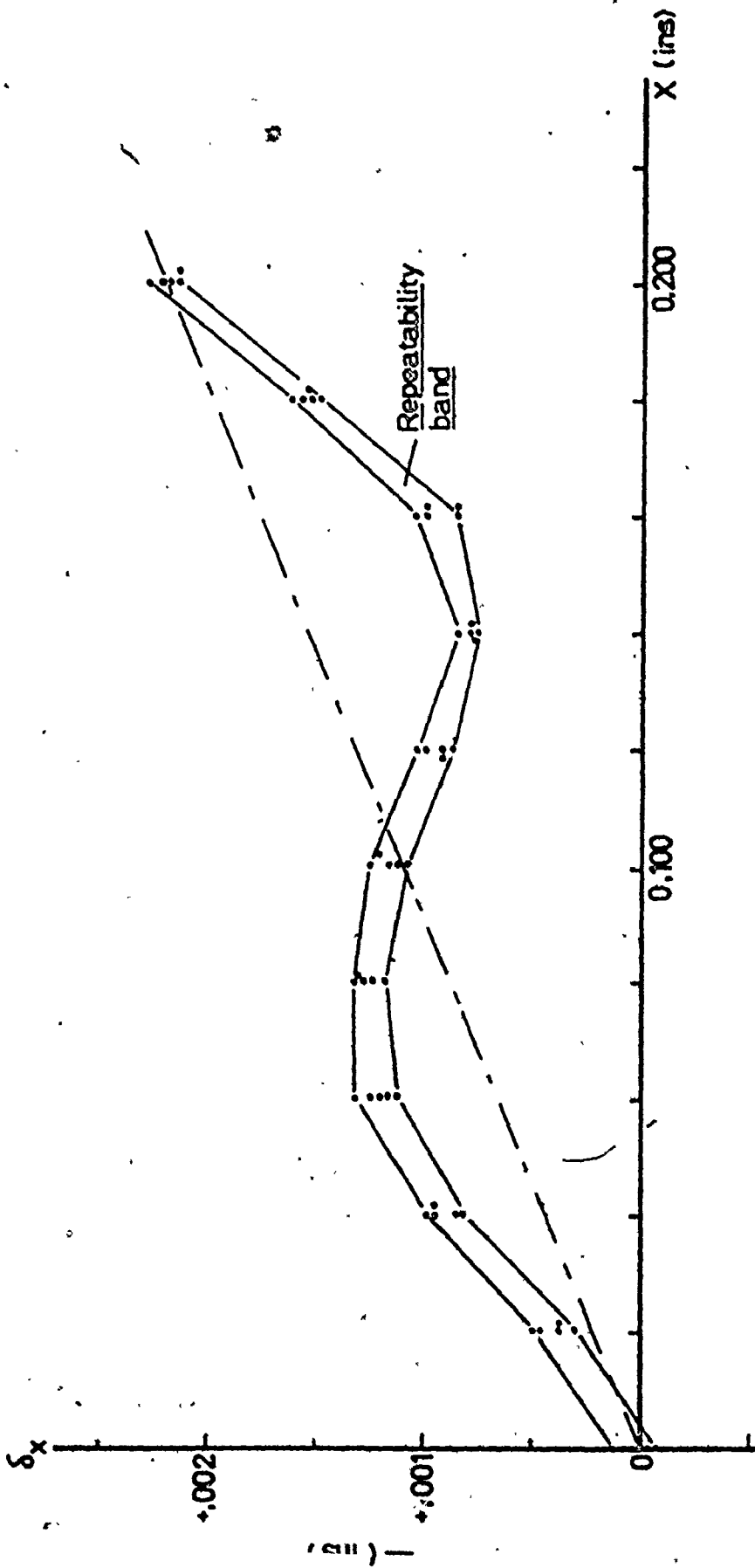
Figure 7.6 A Measurement of Positioning Accuracy on the Skin-Milling Machine:
$\delta_x(x)_A$ of Figure 7.2
(c) 0.200 ins. in steps of 0.020 in.
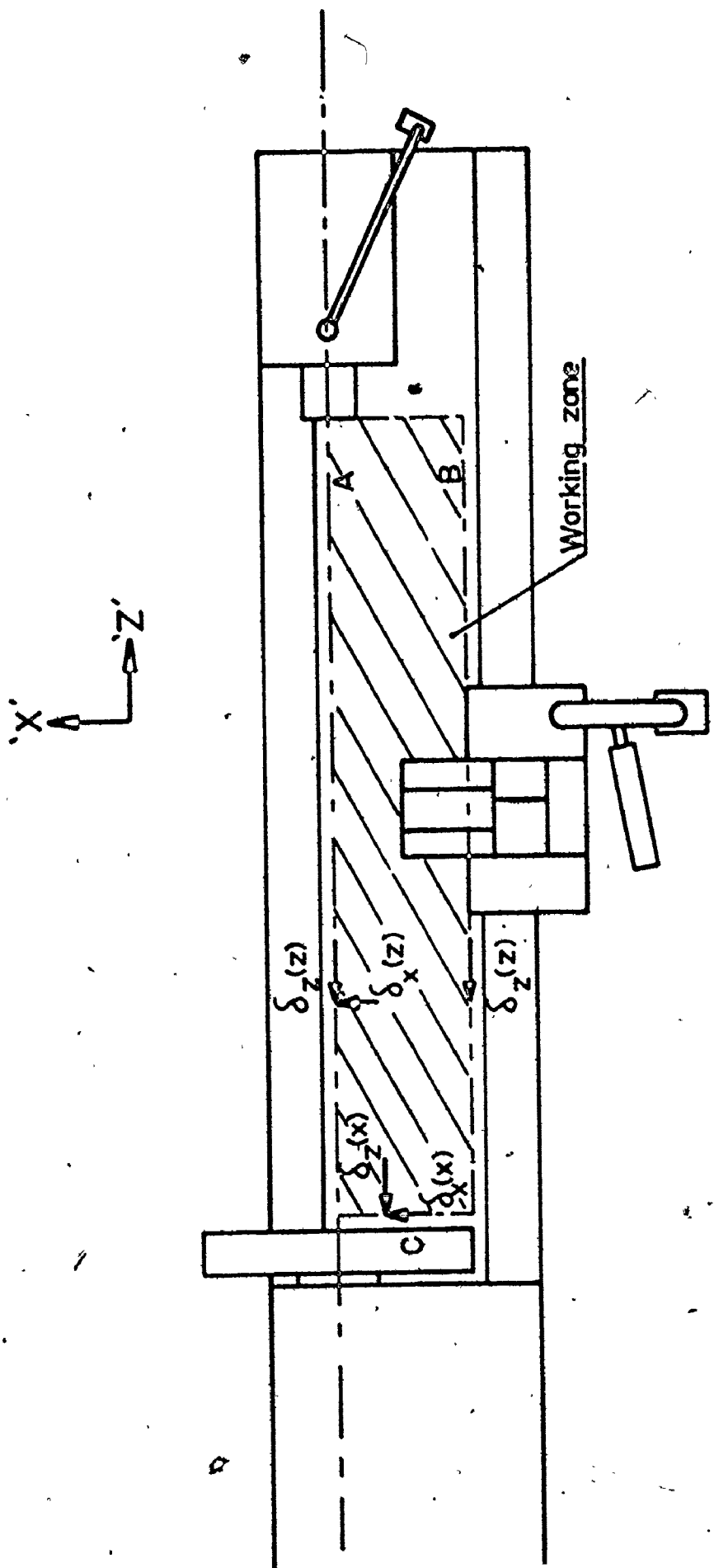
Figure 7.7 The Minimum required number of Translative Deviations to be measured on an N.C. Lathe.
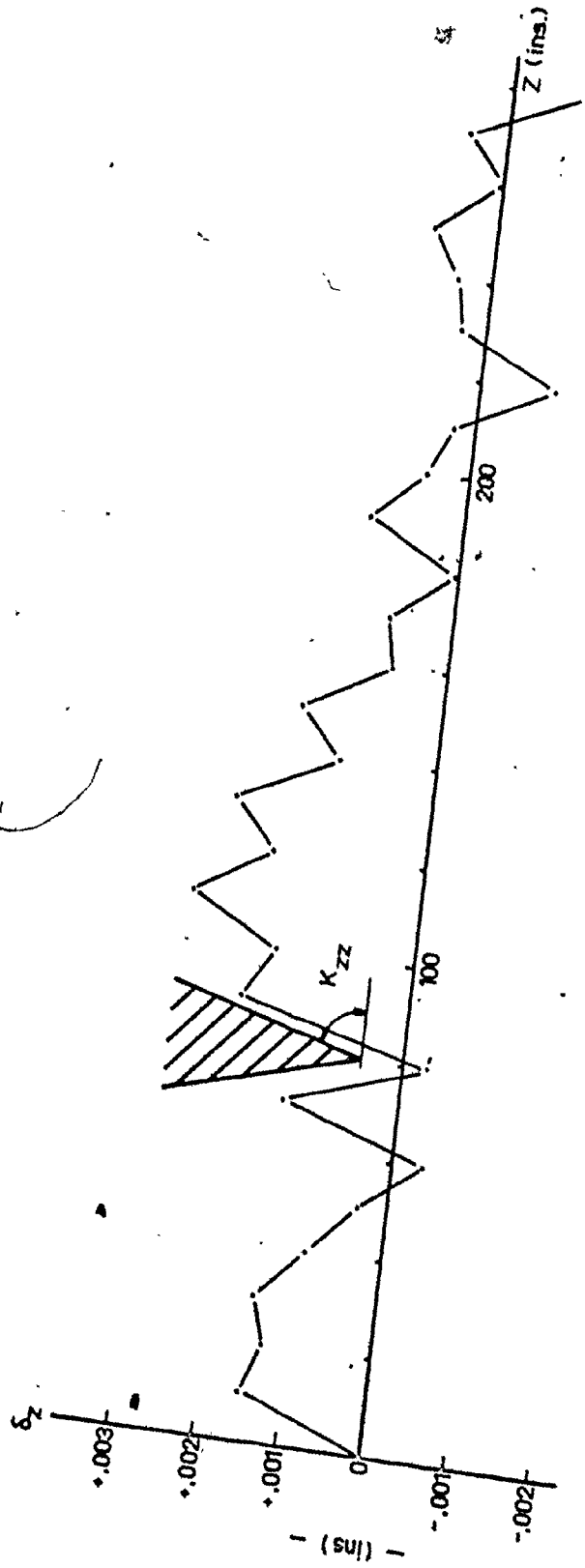
Figure 7.8 Positioning Accuracy of the N.C. Lathe before Adjustments of
Feedback Transducers; $\delta_z(z)_A$ of Figure 7.7 (280 ins. in
steps of 10 ins.).
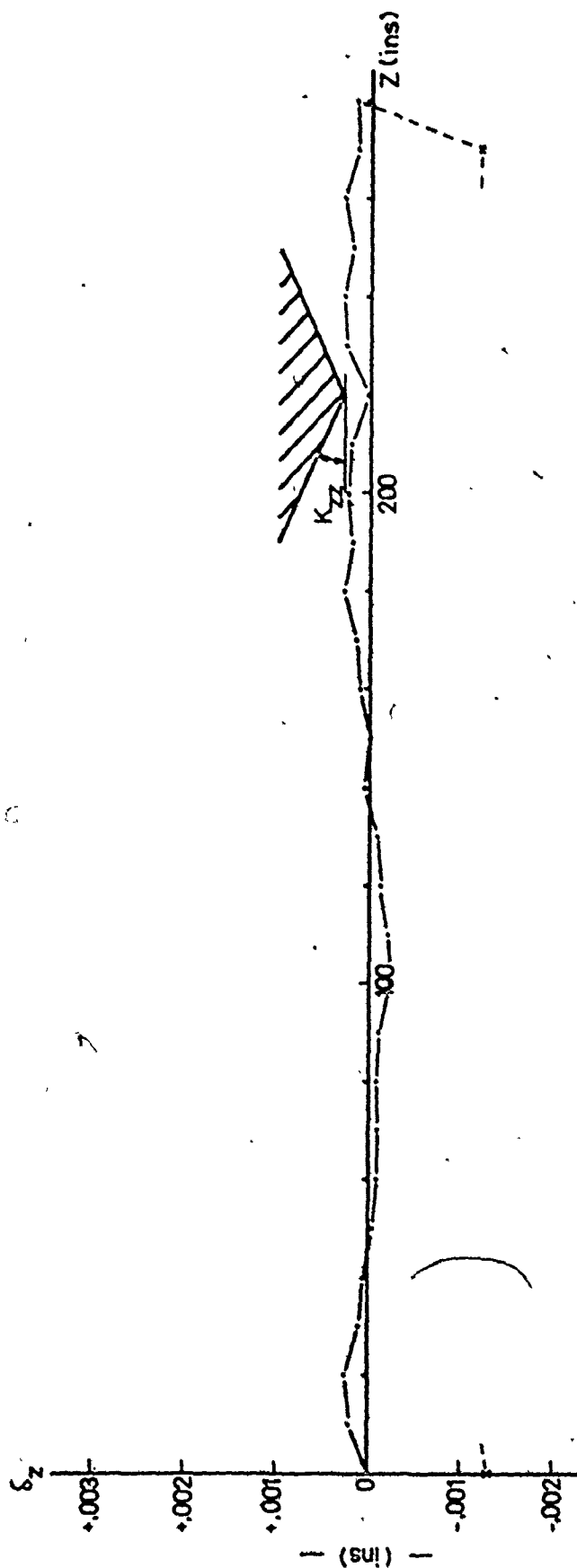
Figure 7.9   Positioning Accuracy of the N.C. Lathe after Adjustment of Feedback
Transducers: $\delta_z(z)_A$ of Figure 7.7 (280 ins. in steps of 10 in.).

269
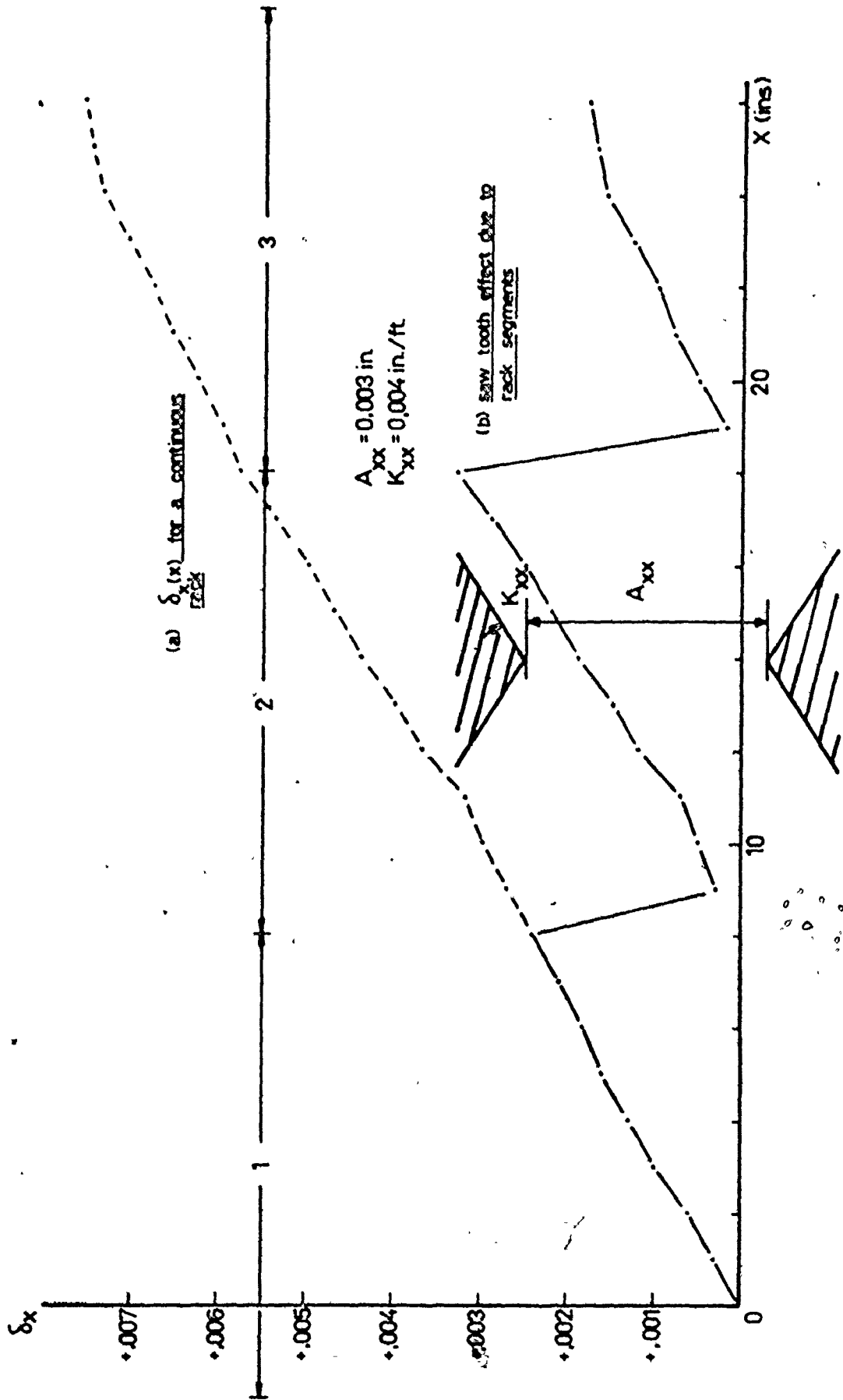
Figure 7.10 Positioning Accuracy of the N.C. Lathe $\delta_x(x)_C$ of Figure 7.7 (30 ins. in steps of 10 in.).
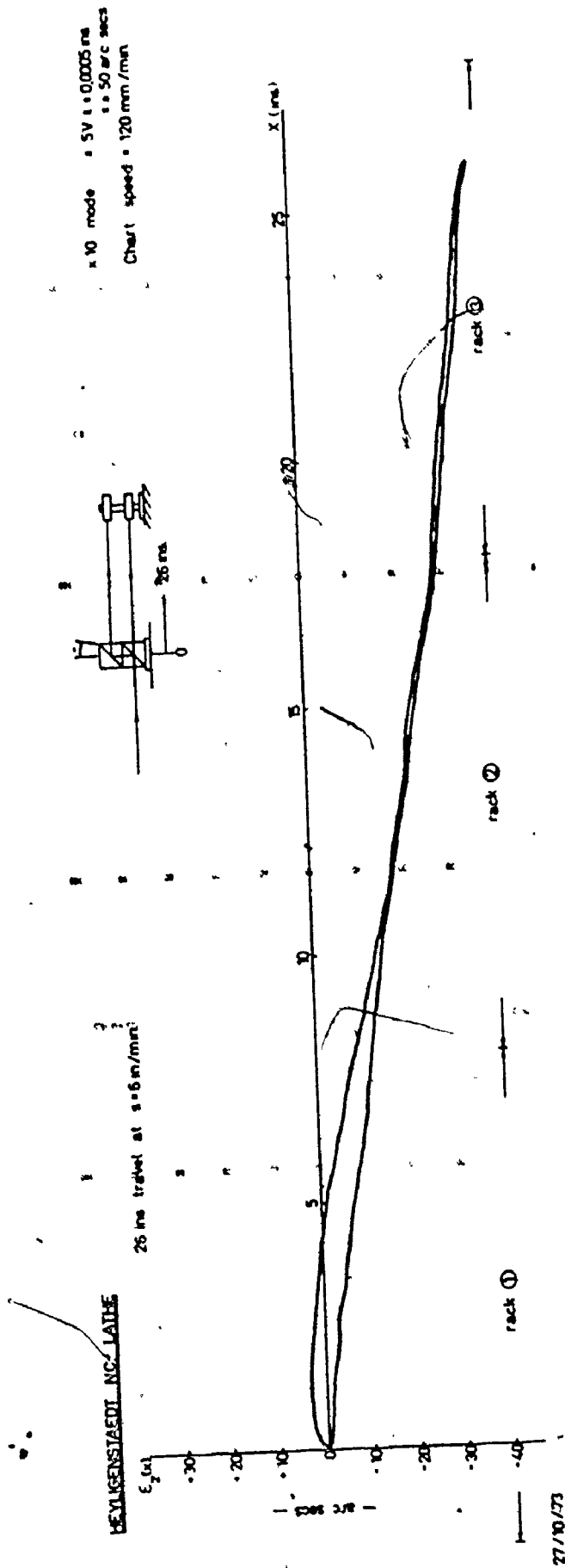
Figure 7.11 Pitch of N.C. Lathe cross-slide motion, $\varepsilon_{z}(x)$
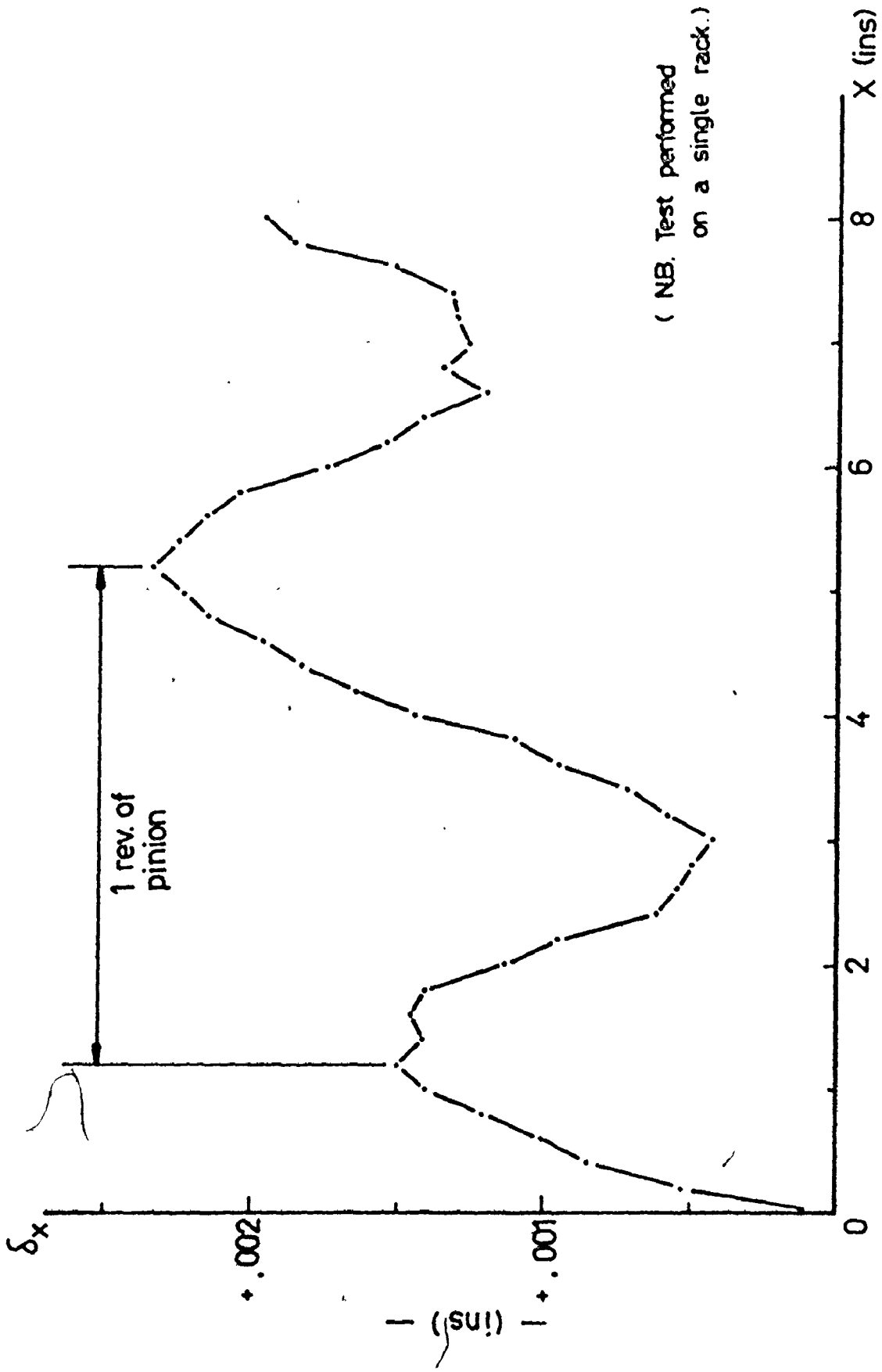
Figure 7.12 Positioning Accuracy of the N.C. Lathe:
$\delta_x(x)_C$ of Figure 7.7 (8 ins. in steps of 0.2 in.).

(NB. Test performed on a single rack.)
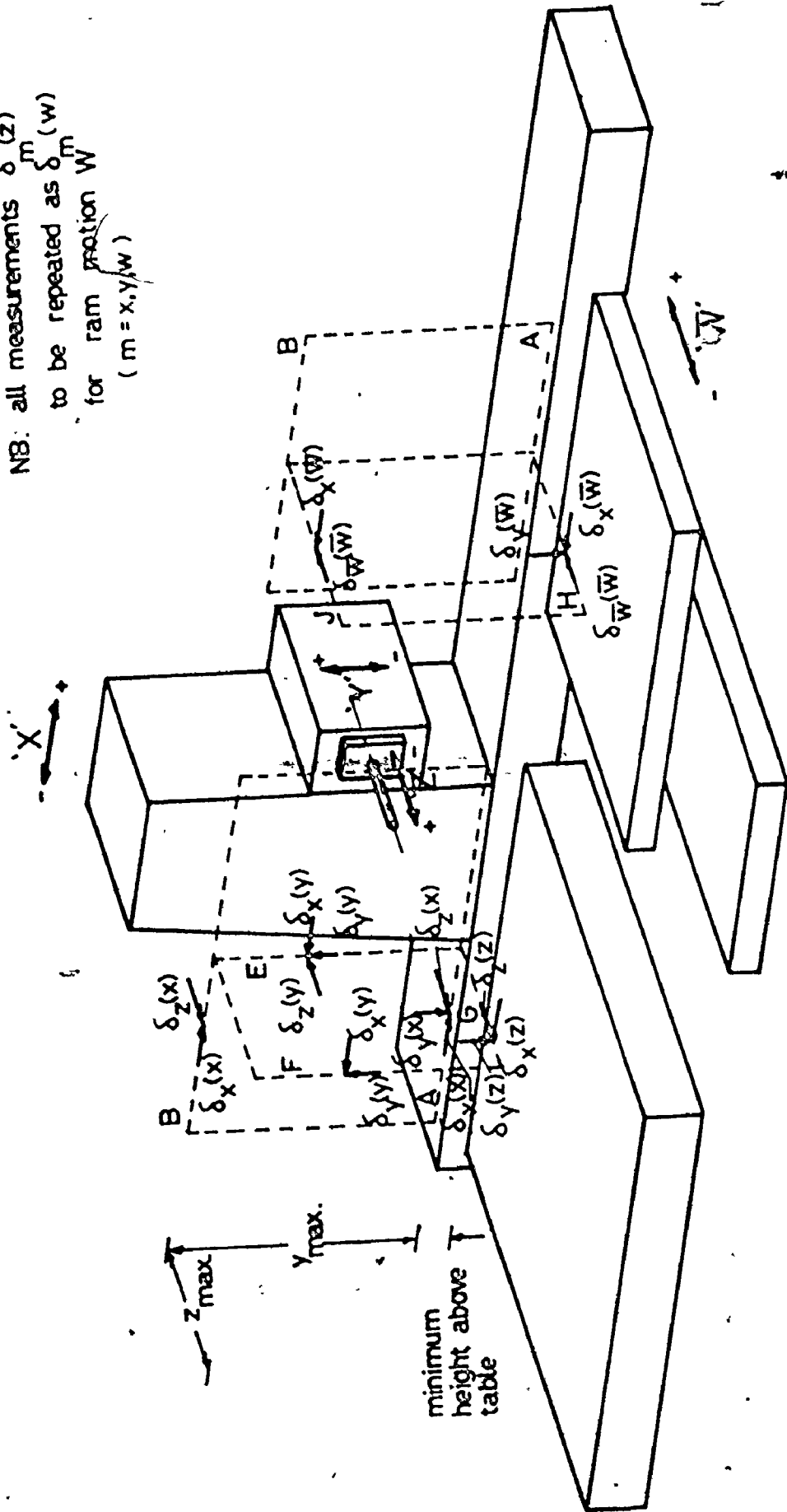
Figure 7.13   Minimum number of required Translative Deviation Measurements for a Floor-type Horizontal Boring and Milling Machine: limitation to working in a single (X,Y) Plane.
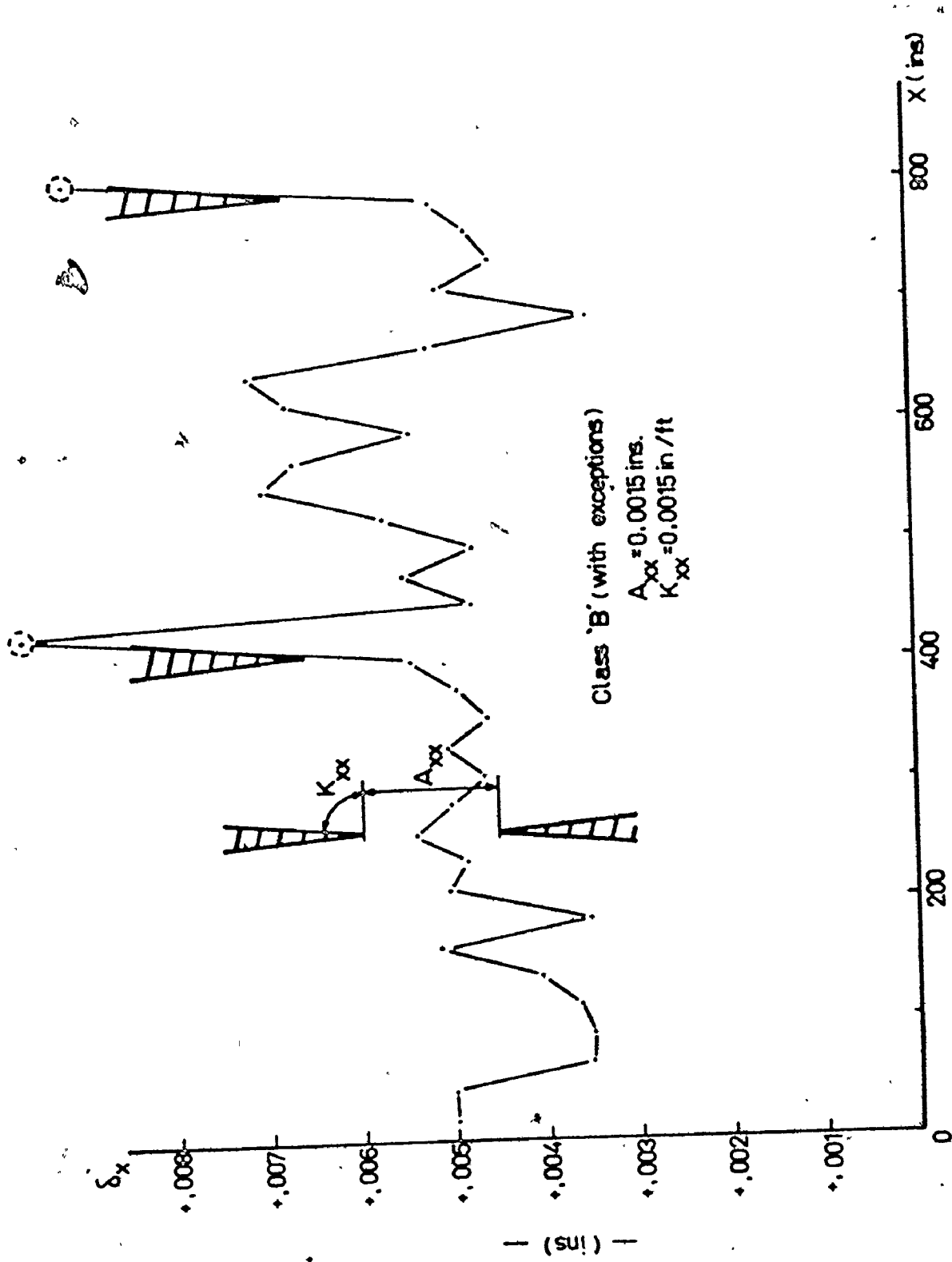
Figure 7.14 . Positioning Accuracy of the Boring and Milling Machine:
$\delta_x(x)_A$ of Figure 7.13.
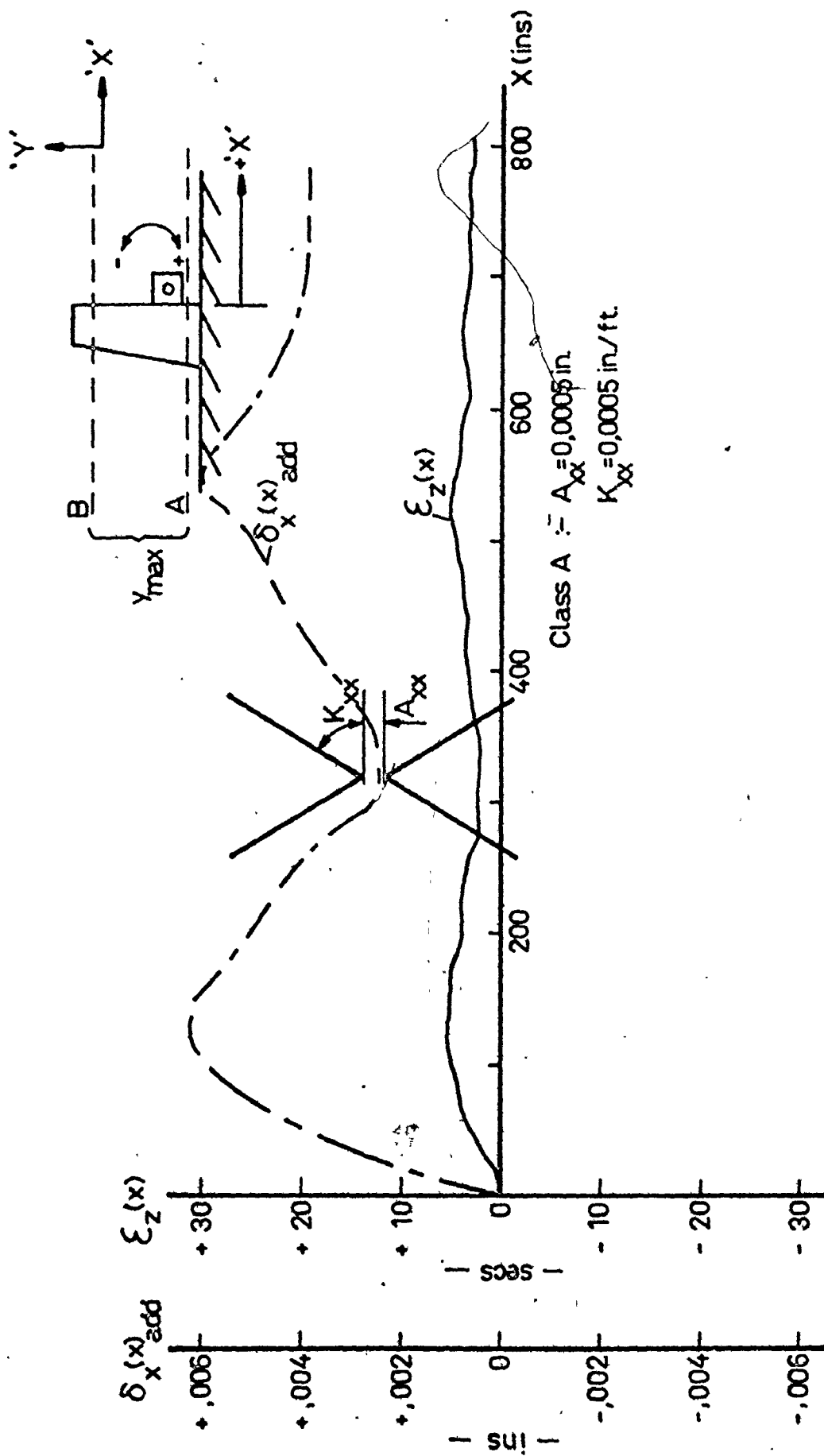
Figure 7.15 Pitch motion $\varepsilon_z(x)$ of the column and evaluation of the term $\delta_x(x)_{add}$. $(\delta_x(x)_B = \delta_x(x)_A + \delta_x(x)_{add}$.
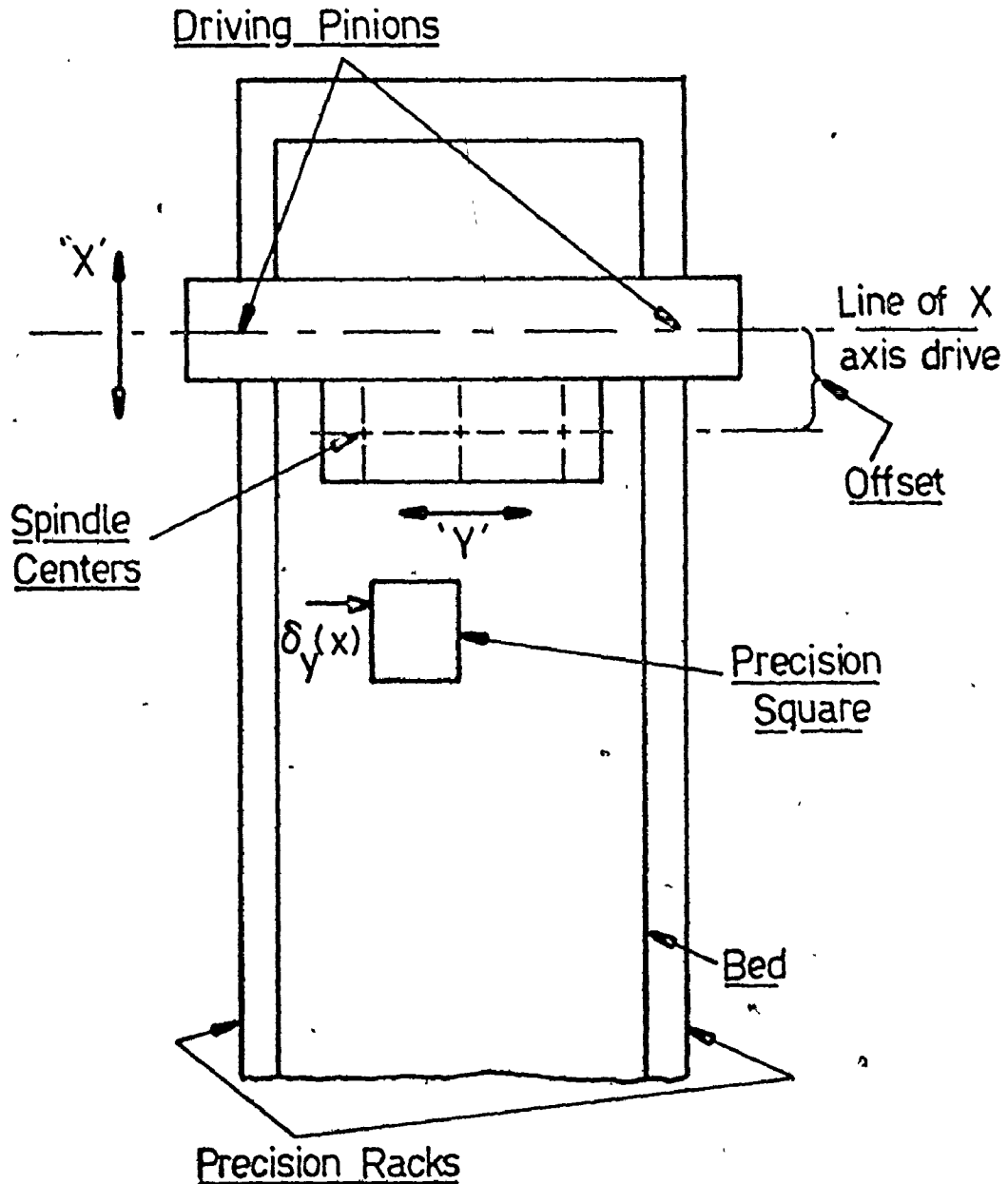
Figure 7.16   Configuration of the Skin Milling Machine:
angular deviations generated by the errors of
the driving pinion and the effect of the tool
offset.
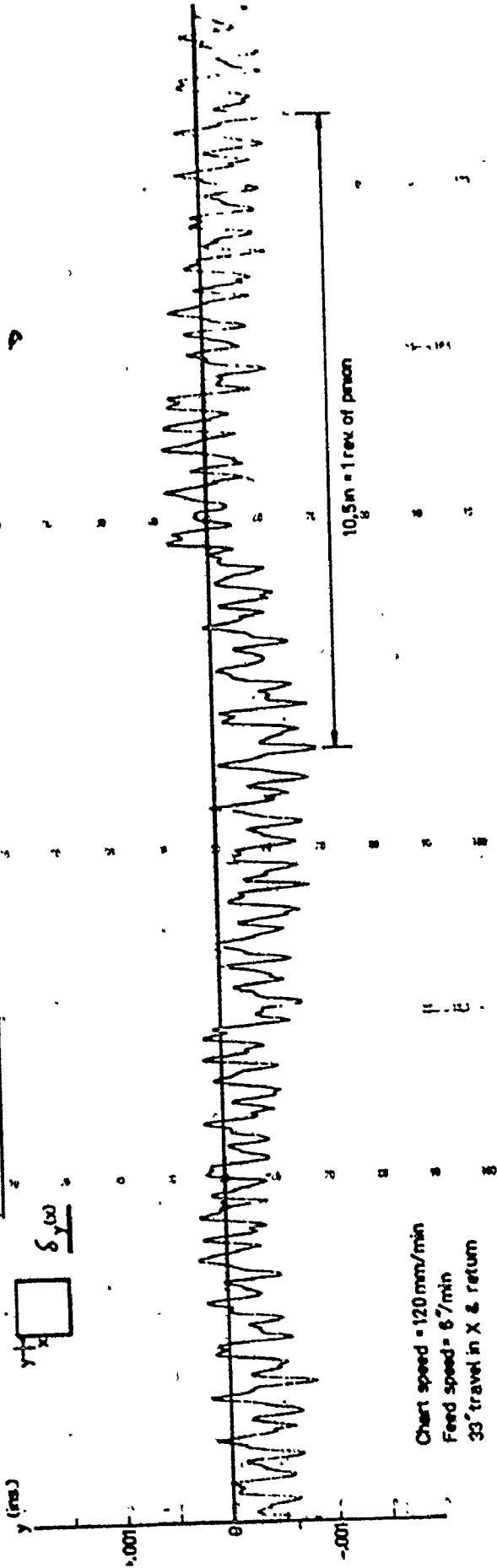
Figure 7.17 Measurements of Straightness of Motion on the Skin Milling
Machine: $\delta_y(x)$ of Figure 7.2. Effect of pinion errors.

KEARNEY & TRECKER MODEL 3 5-AXIS MACHINING CENTRE. (2708)

$\delta_x(y)$

δ_x (ins)

+.003
+.002
+.001
0
-.001
-.002
-.003

Y

33" travel in Y & return
Chart speed @ 120 mm/min
Feed speed 5 = 11"/min
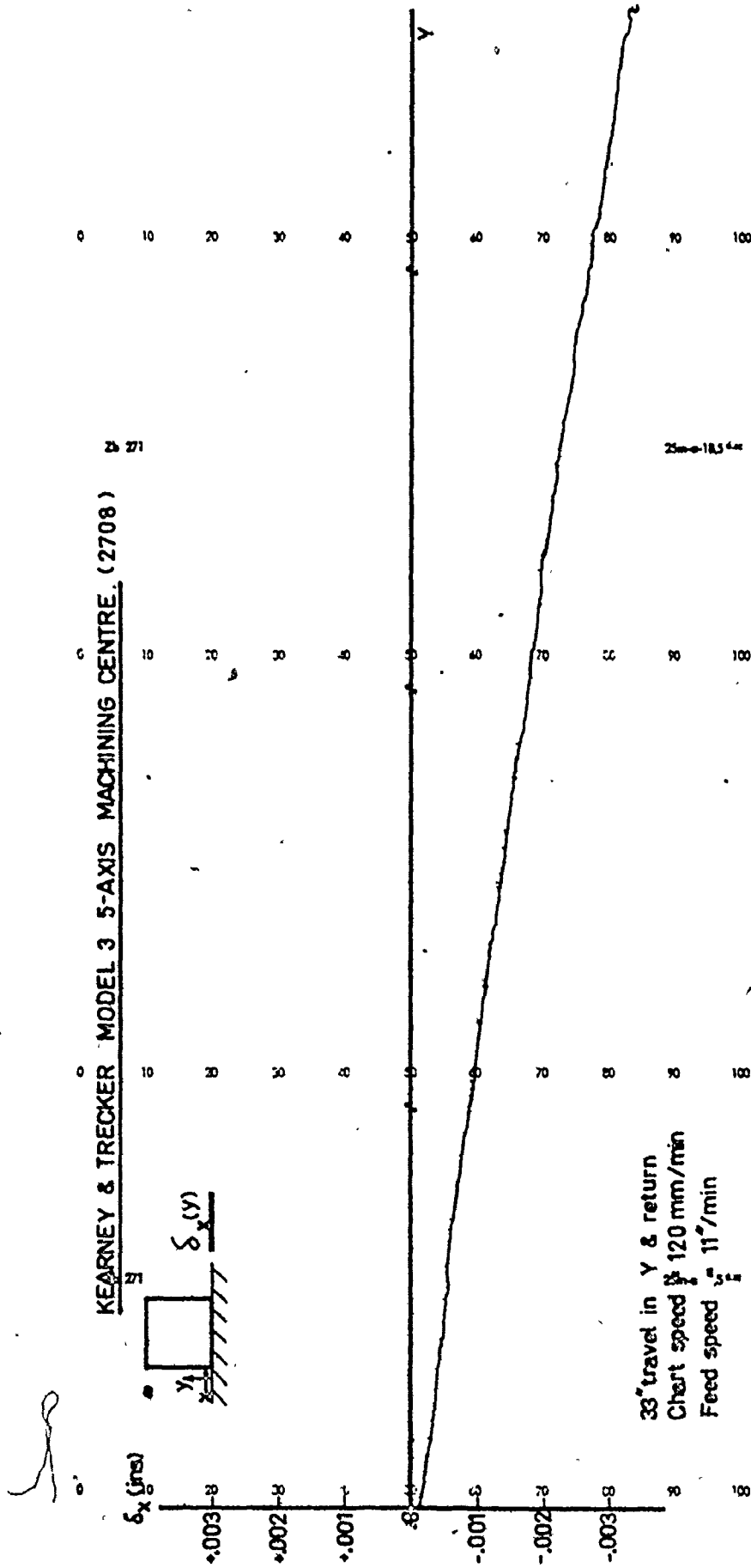
Figure 7.18   Straightness of Motion for a Machining Center:
$\delta_y(x)$ of Figure 4.2.
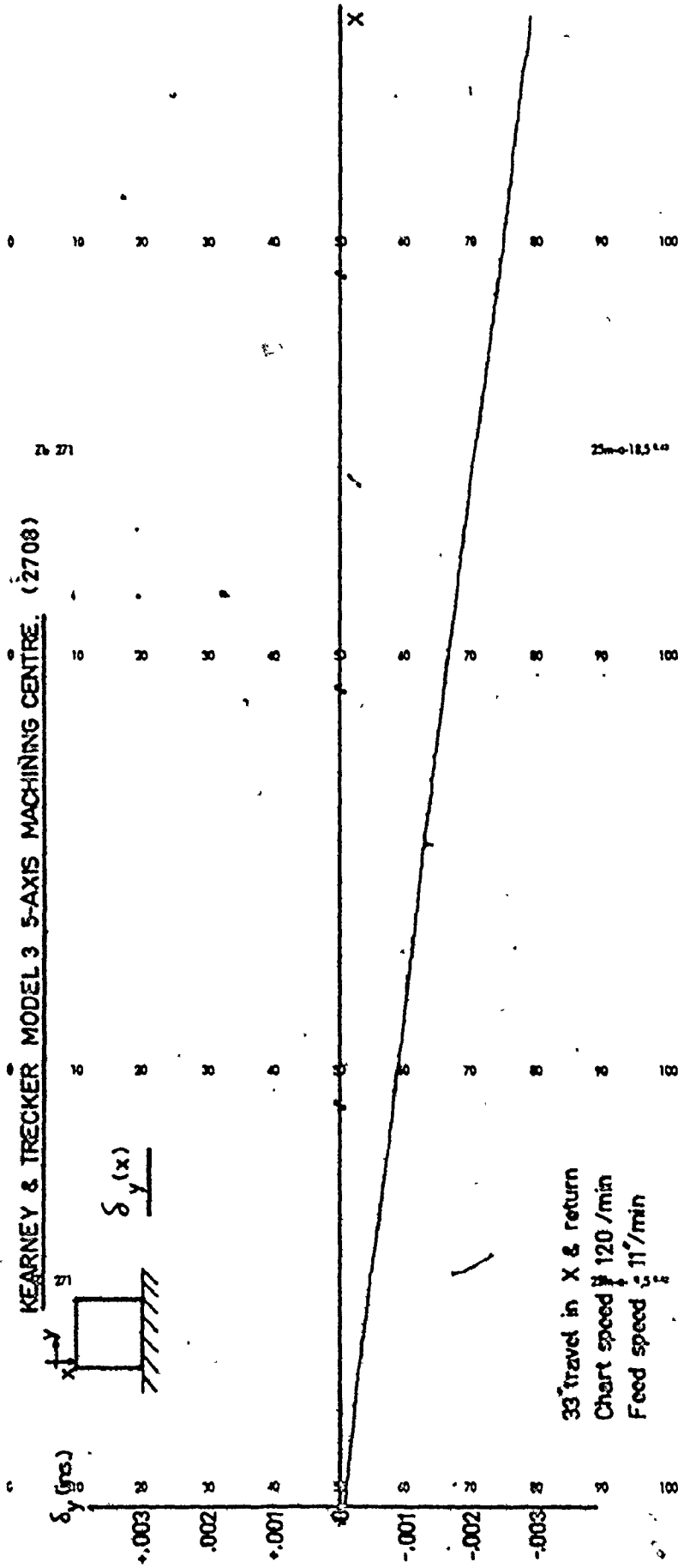
Figure 7.19 Straightness of Motion for a Machining Center: $\delta_x(y)$ of Figure 4.2.

APPENDICES

APPENDIX A

CALCULATION OF STEADY-STATE AND TRANSIENT TEMPERATURE
FIELDS AND THERMAL DISPLACEMENTS FOR SIMPLIFIED STRUCTURES

A 1   Steady-state temperature field in a simple structural
body with constant heat flux input and convection cool-
ing over the entire surface

The cast iron body of Figure 4.5a could be

approximated as a plate of thickness d and width B as

in Figure A.la. There is a steady heat input q at the

left hand end of the plate for which there is no cool-

ing on one side (corresponding to the inner wall of

the body of Figure 4.5a) and convection air cooling

on the other side. The problem is more easy to form-

ulate if a plate of thickness 2d is considered as in

Figure A.lb, with convective cooling on both sides

and with double the heat input. (For guidance in

solution see [33].)

In this case, the formulation of the problem in

terms of the co-ordinate system of Figure A.lb becomes

$$\frac{\partial^2 \theta}{\partial x^2} + \frac{\partial^2 \theta}{\partial y^2} = 0 \qquad (A.1)$$

where $\theta = (T - T_\infty)$

The boundary conditions are
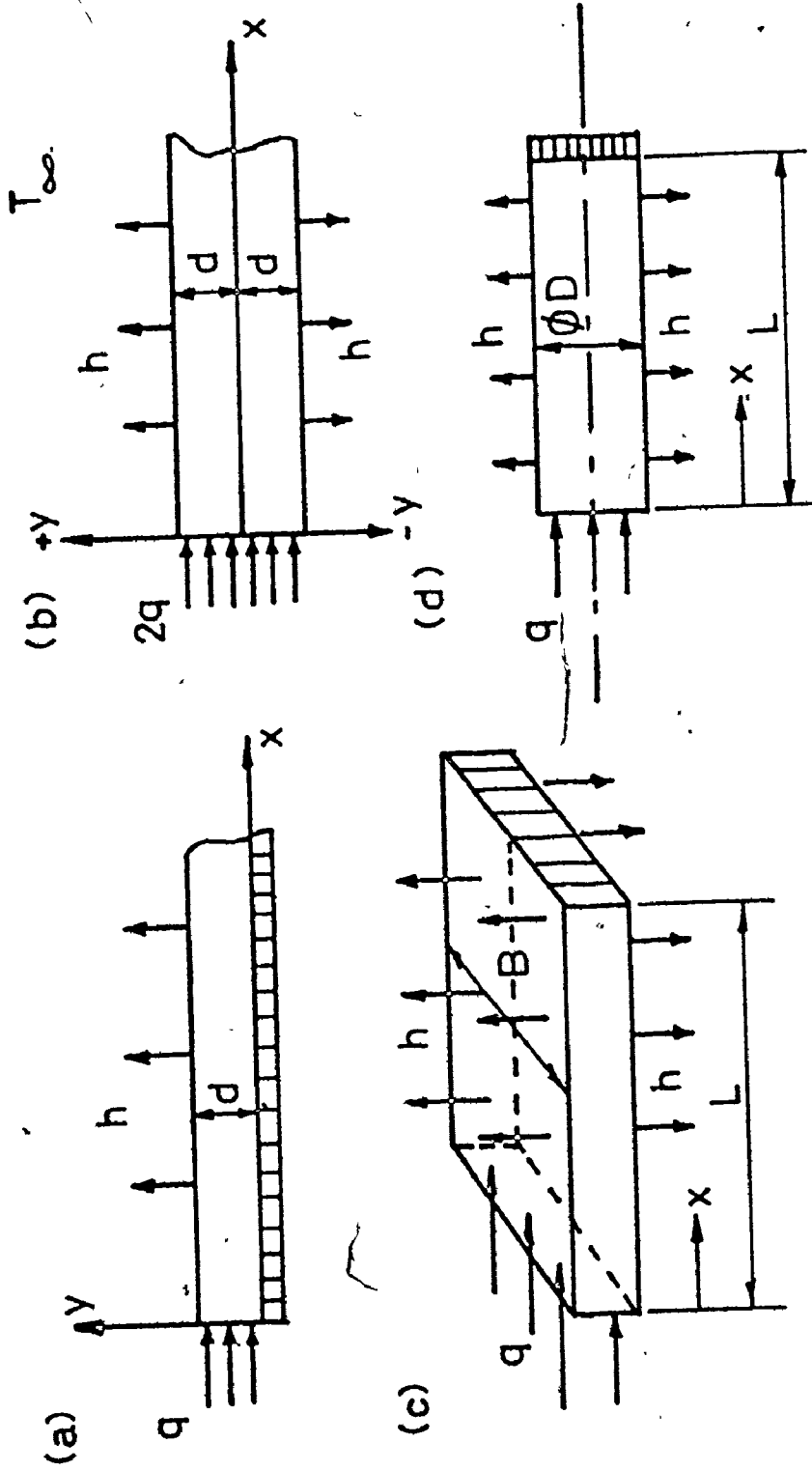
Figure A.1 Diagrams for the Thermal Calculations of Simple Bodies

$$-k \frac{\partial \theta}{\partial x} (0,y) = q'' \quad (A.2) \qquad \frac{\partial \theta}{\partial y} (x,0) = 0 \qquad (A.3)$$

$$\theta(\infty,y) = 0 \qquad (A.4) \qquad -k\frac{\partial \theta}{\partial y} (x,d) = h\theta (x,d) \qquad (A.5)$$

where the heat flux $q'' = \frac{q}{Bd}$

Here, we assume that there is no heat loss
from the edges of the plate which corresponds to the
fact that the plate represents an enclosed body.
This also leads to the consequence of no variation of
temperature along the width of the plate.

Assuming the existence of a product solution
of the form

$$\theta (x,y) = X(x) \, Y(y) \qquad (A.6)$$

and introducing equation (A.6) into equation (A.1),
dividing each term by XY, we obtain

$$\frac{1}{X} \frac{d^2X}{dx^2} = \frac{-1}{Y} \frac{d^2Y}{dy^2} = \pm \lambda^2 \qquad (A.7)$$

Choosing the sign of λ such that the homogen-
eous y-direction results in a characteristic-value
problem, the problem may be separately expressed in
the x and y directions as

$$\frac{d^2X}{dx^2} - \lambda^2 X = 0 \quad , \quad X(\infty) = 0 \tag{A.8}$$

$$\frac{d^2Y}{dy^2} + \lambda^2 Y = 0 \quad , \quad \frac{dY}{dy}(0) = 0, \quad -k \frac{dY}{dy}(d) = hY(d) \tag{A.9}$$

A general solution for Y is

$$Y = C_1 \cos \lambda y + C_2 \sin \lambda y$$

The characteristic-value problem of the y direction, equation (A.9), results in the solution

$$Y_n(y) = C_n \cos \lambda_n y \tag{A.10}$$

where the characteristic-values are the roots of the equation

$$k \lambda_n \sin \lambda_n d = h \cos \lambda_n d \tag{A.11}$$

The boundary-value problem of the x direction gives

$$X_n(x) = B_n e^{-\lambda_n x} \tag{A.12}$$

where B_n is an arbitrary constant.

The product solution of equation (A.6) results in

$$\theta(x,y) = \sum_{n=1}^{\infty} a_n e^{-\lambda_n x} \cos \lambda_n y \tag{A.13}$$

where the coefficients of a_n may be found, using the

non-homogeneous boundary condition that is equation

(A.2). We may obtain therefore,

$$\frac{q'}{k} = \sum_{n=1}^{\infty} \lambda_n \, a_n \cos \lambda_n y \qquad (A.14)$$

where

$$a_n = \frac{2 \frac{q''}{k \lambda_n} \sin \lambda_n d}{\lambda_n d + \sin \lambda_n d \cos \lambda_n d} \qquad (A.15)$$

Let us now calculate a typical case, choosing wall thickness $d = 0.96$ in. $= 0.08$ ft., thermal conductivity $k = 30$ Btu/hr. ft. $^{\circ}F$, heat input $q = 1260$ Btu/hr., plate width $B = 4$ ft. and a rather high value of the heat convection coefficient $h = 2$ Btu/hr. ft.^{2} $^{\circ}F$.

Thus, equation (A.11) becomes

$$\lambda_n \tan 0.08 \, \lambda_n = 0.0666 \qquad (A.16)$$

The first three characteristic-values of λ_n and of the corresponding values of $d\lambda_n$ and a_n are obtained as,

TABLE 1

n	λ_n	$d \lambda_n$	$\dfrac{ka_n}{2q''}$
1	0.908	0.07264	0.551145
2	39.290852	3.14326	-0.00001356
3	78.539816	6.283185	0.0000017

It is apparent that the distribution of temperature
in the direction y for any particular value of x, as
it is expressed by equation (A.13) is practically
given by the term for n = 1, while all a_n coeffi-
cients for n > 1 are negligibly small. Neglecting
them, equation (A.13) becomes

$$\theta(x,y) = 1.102 \frac{q''}{k} e^{-0.908x} \cos 0.908\, y$$

$$\theta(x,y) = X(x) \cos 0.908\, y \qquad (A.17)$$

where X(x) is the temperature in the center of the
thickness of the wall at y = 0. Towards the surface,
it falls to

$$\theta(x,d) = X(x) \cos 0.908\, d = 0.997X(x)$$

This calculation of a typical structure shows that
the temperature across the thickness of the wall may
be considered constant.

An analogous calculation for the cross section
of the "spindle" of Figure 4.5a revealed a temperature
variation of less than 2%.

A 2   <u>Transient temperature fields in simple bodies with
constant heat flux and convection cooling over the
entire surface</u>

The two typical bodies considered correspond to the "housing" and "spindle" of Figure 4.5a.

In this paragraph we consider them separately and for this purpose they may be simplified as shown in Figure A.1c and A.1d respectively.

In Figure A.1c the housing is considered as a plate of length L, width B and thickness 2d. (for the same reason as in Figure A.1b) which has a steady heat input at x = 0 and is insulated at the sides which corresponds to the housing being closed. Heat is convected from the surfaces of the plate.

Similarly, the spindle represented by a solid cylinder is considered insulated at the end x = L. This may be understood in such a way that the surface at the face is added to the circumference which is correspondingly lengthened.

With respect to the result of the calculations in the preceding paragraph, temperature is considered constant through each section for any particular value of x. Thus as regards geometry, the problem is single-dimensional in the co-ordinate x.

Considering transients, the other co-ordinate of the problem is the time t.

The formulation of the problem in terms of $\theta = (T-T_\infty)$ is

$$\frac{\partial^2 \theta}{\partial x^2} - m^2\theta = \frac{1}{\alpha}\frac{\partial \theta}{\partial t} \qquad (A.18)$$

where $\alpha = \dfrac{k}{\rho c_p}$ is the thermal diffusity, and

$$m^2 = \frac{hP}{kA}$$ where P is the periphery of the

section and A is its area.

The solution of equation (A.18) may be considered

as a superimposition of a steady-state temperature

Φ and the transient one ψ:

$$\theta(x,t) = \psi(x,t) + \Phi(x) \qquad (A.19)$$

For the transient, ψ no heat input is con-

sidered and it is assumed that its initial state is

the negative of the steady-state Φ so that $\theta(x)$ is

zero at time t=0 and, as ψ vanishes with time,

$\theta(x,\infty) = \Phi(x)$

Thus, we have

$$\frac{\partial^2 \psi}{\partial x^2} - m^2\psi = \frac{1}{\alpha}\frac{\partial \psi}{\partial t} \qquad (A.20)$$

and,

$$\frac{d^2 \Phi}{dx^2} - m^2\Phi = 0 \qquad (A.21)$$

with the initial condition,

$$\psi(x,0) = -\Phi(x) \tag{A.22}$$

and the boundary conditions,

$$\frac{\partial \psi}{\partial x}(0,t) = 0 \quad \text{(A.23)} \quad k\frac{d\Phi}{dx}(0) = -q'' \tag{A.25}$$

$$\frac{\partial \psi}{\partial x}(L,t) = 0 \quad \text{(A.24)} \quad k\frac{d\Phi}{dx}(L) = 0 \tag{A.26}$$

The transient function $\psi(x,t)$ is solved by the separation of variables

$$\psi(x,t) = X(x)\,F(t) \tag{A.27}$$

The solutions of the three functions have the following form:

$$X(x) = \sum_{n=0}^{\infty} A_n \cos \mu_n x \tag{A.28}$$

$$\text{where } \mu_n = \frac{n\pi}{L}, \ n=0, 1, 2 \ldots \tag{A.29}$$

$$F_n(t) = C_n \, e^{-\alpha \lambda_n^2 t} \tag{A.30}$$

$$\text{where } \lambda_n^2 = (m^2 + \mu_n^2) \tag{A.31}$$

$$\Phi(x) = B_1 e^{-mx} + B_2 e^{mx} \tag{A.32}$$

Using the boundary conditions,

$$\Phi(x) = \frac{q''}{km} \frac{\cosh m (L-x)}{\sinh mL} \qquad (A.33)$$

$$\text{and} \quad \psi(x,t) = \sum_{n=0}^{\infty} a_n e^{-\alpha \lambda_n^2 t} \cos \mu_n x \qquad (A.34)$$

Using the initial condition (A.22),

$$a_0 = -\frac{q''}{kLm^2} \quad , \quad a_n = \frac{-2q''}{kL\lambda_n^2} \quad , \quad n = 1,2,3 \cdots \qquad (A.35)$$

Equation (A.34) shows that the temperature field along x is obtained as a sum of "modes". These are functions of x. The n=0 ("zero" mode) is constant over the whole length of the body while all the other modes are functions of x: the first (n=1) extending over the interval $(0,\pi)$, the next one (n=2) over the interval $(0,2\pi)$ etc. The amplitude of these modes are equal to a_n for t = 0 and they decay exponentially with time with corresponding time constants

$$\tau_n = \frac{1}{\alpha \lambda_n^2} \qquad (A.36)$$

for each mode.

The thermal deformation between two points x_1 and x_2 is obtained as

$$\Delta_{1,2} = \alpha_s \int_{x_1}^{x_2} \theta dx = \alpha_s \int_{x_1}^{x_2} \phi dx + \alpha_s \int_{x_1}^{x_2} \psi dx$$

$$= \Delta_{(s)1,2} + \Delta_{(t)1,2} \qquad (A.37)$$

where α_s is the coefficient of thermal expansion and $\Delta_{(s)}$ denotes the steady-state $(t=\infty)$ deformation and $\Delta_{(t)}$ denotes the transient deformations.

Using (A.34) we obtain:

$$\Delta_{1,2} = \alpha_s \int_{x_1}^{x_2} \left(-\frac{q''}{kLm^2} - \frac{2q''}{kL} \sum_{n=1}^{\infty} \frac{\cos(\frac{n\pi}{L})x}{\lambda_n^2} \right) e^{-\alpha\lambda_n^2 t}$$

$$\Delta_{1,2} = \alpha_s \left[\frac{q''}{kLm^2} (x_1-x_2) e^{-\alpha m^2 t} + \frac{2q''}{kL} \cdot \right.$$

$$\left. \sum_{n=1}^{\infty} \frac{L(\sin(\frac{n\pi}{L})x_1 - \sin(\frac{n\pi}{L})x_2)}{n\pi\lambda_n^2} e^{-\alpha\lambda_n^2 t} \right]$$

$$\Delta_{1,2} = \alpha_s \left[D_0 e^{-\alpha m^2 t} + \sum_{n=1}^{\infty} D_n e^{-\alpha\lambda_n^2 t} \right] \qquad (A.38)$$

For any particular path (x_2-x_1) over which the integration (A.37) is carried out, the individual D_0, D_n terms are constants. In this way, a thermal deform-

ation is a sum of modal terms each one of which is an exponential function of time with a corresponding time constant. This is in agreement with what McClure has obtained [30].

Let us now evaluate the time constants in accord with our chosen parameters:

a) The "housing"

The parameters are: d=0.08 ft, B=4 ft, L=4 ft, h=1.666 Btu/hr.ft² °F, k=30 Btu/hr. ft. °F, α=0.666 ft²/ hr. The heat input q=1260 Btu/hr=0.5 hp.

According to the double wall thickness notation q" = $\frac{2q}{A}$ = 3940 Btu/ft²hr.

Using this data, m^2 = 0.69444 and the amplitudes and time constants for the first six individual modes are obtained as in TABLE 2.

TABLE 2

n	$-\psi_n$ °F	$\alpha\lambda_n^2$	τ hrs
0	47.28	0.463	2.16
1	50.078	0.874	1.14
2	20.77	2.1	0.474
3	10.51	4.164	0.24
4	6.22	7.043	0.14
5	4.08	10.743	0.043

b) The "spindle"

The parameters are: ϕD = 4in. = 0.3333 ft, L = 0.5 ft, h = 4 Btu/hr. ft^2°F, k = 30 Btu/hr. ft.°F, α = 0.570 ft^2/hr. and m^2= 1.6. In order to obtain the same temperature for x=0, t=0 as for the housing, the values of q" = 3383 Btu/ft^{2}hr. and q = 295 Btu/hr. are used.

The resulting modal parameters are given in TABLE 3.

TABLE 3

n	$-\psi_n$ °F	$\alpha\lambda_n^2$	τ hrs
0	140.7	0.912	1.1
1	10.96	23.4	0.04
2	2.82	90.9	0.01
3	1.26	203.4	0.005
4	0.71	361.0	0.0028
5	0.46	563.0	0.0018

It is apparent from TABLES 2,3 that only a small number of the lowest modes is sufficient to express the temperature field with sufficient accuracy. Indeed, for the spindle, only the first two or three modes are sufficient.

The variation of the temperature fields during

the heating up for the above given parameters is

shown in the Figure 4.7. Figure 4.7a applies to the

spindle and Figure 4.7b to the housing.   The Figures

are separated because only the steady-state temper-

atures are matching at point x=0 and not the transients,

this being expected with the given specification

of the situation.   The variation of temperature of

a number of points on the housing is given in

Figure 4.8.

APPENDIX B

VERIFICATION OF THE FINITE-ELEMENT PROGRAM

The formulation of the finite-element approach to the analysis of steady-state and transient temperature fields in a structure was verified by a comparison of computed results for a specific problem with the results derived from a classical solution to the same problem.

a) The problem chosen, Figure B.1a, was that of a plate of width 2ℓ, depth L and thickness δ for which there is a heat input q along one edge and convection cooling from both faces and all other edges.

The convection coefficient is h and the conduction coefficient is k.

Therefore, the formulation of the problem in terms of the co-ordinate system of Figure B.1a becomes,

$$\frac{1}{\alpha}\frac{\partial\theta}{\partial t} = \frac{\partial^2\theta}{\partial x^2} + \frac{\partial^2\theta}{\partial y^2} - m^2\theta \qquad (B.1)$$

where $\theta = (T - T_\infty)$ and $m^2 = \frac{2h}{k\delta}$

subject to boundary conditions,

$$\frac{\partial\theta}{\partial x}(0,y,t) = 0 \quad (B.2) \qquad -k\frac{\partial\theta}{\partial x}(\ell,y,t) = h\theta(\ell,y,t) \qquad (B.3)$$
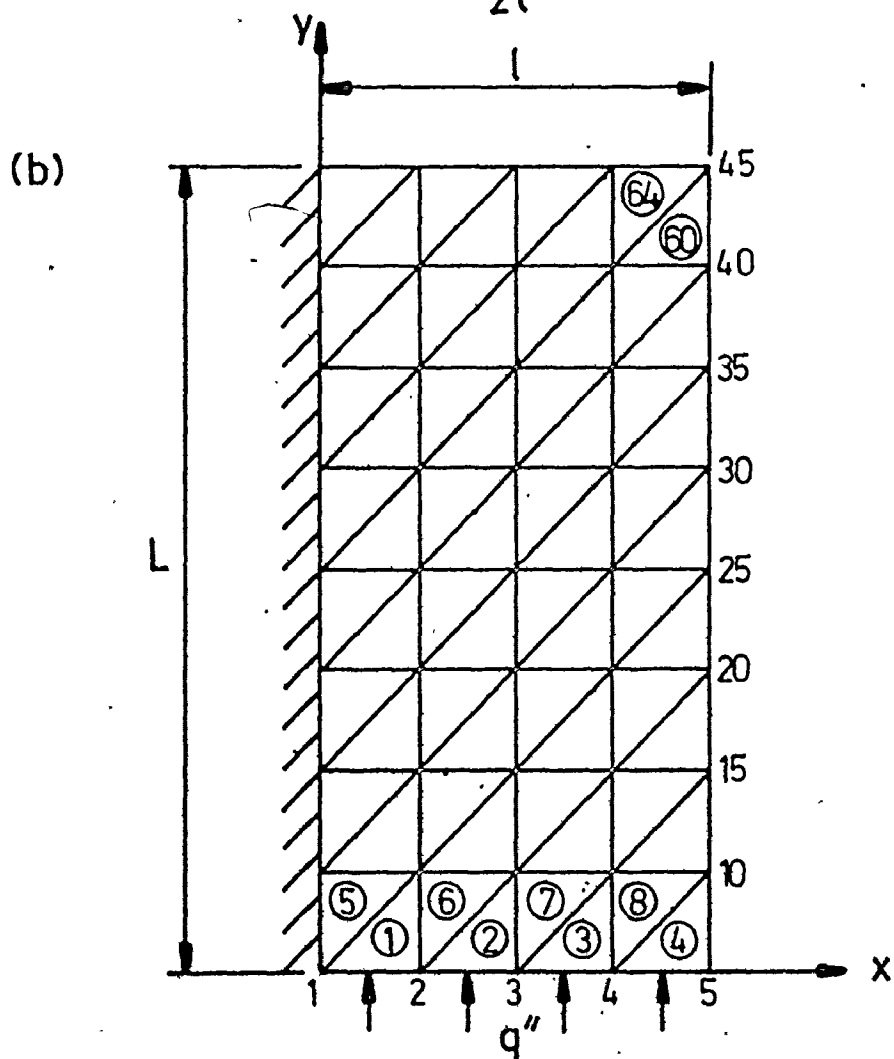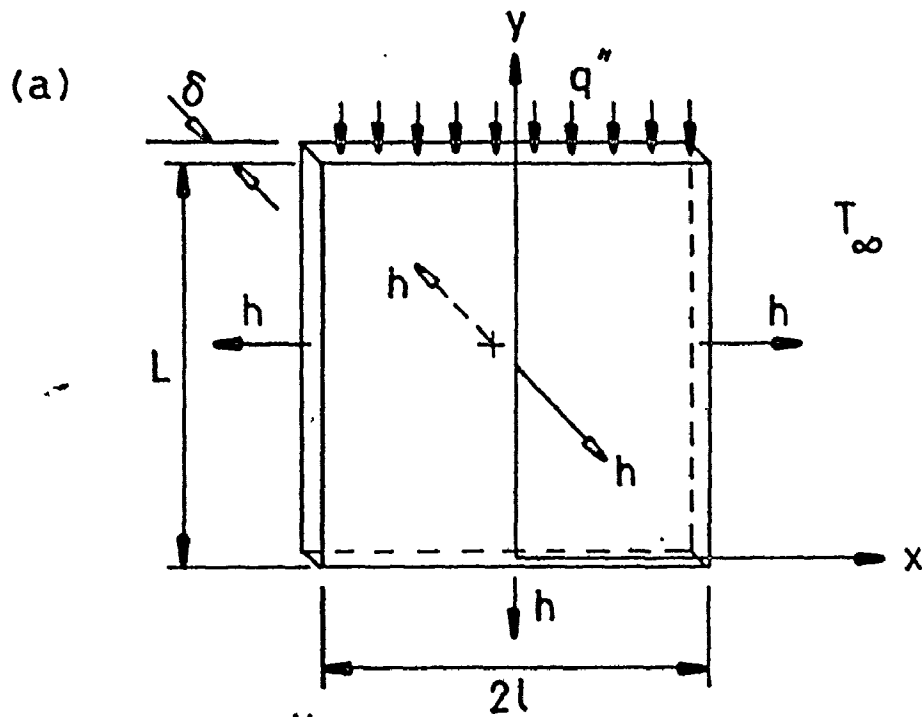
$$k\frac{\partial\theta}{\partial y}(x,L,t) = q" \quad \text{(B.4)}, \quad k\frac{\partial\theta}{\partial y}(x,0,t) = h\theta(x,0,t) \quad \text{(B.5)}$$

Assuming a product solution of form

$$\theta(x,y,t) = \psi(x,y,t) + \phi(x,y) \quad \text{(B.6)}$$

leads to the solution given by equation (B.7)

$$\theta(x,y,t) = \sum_{n=1}^{\infty}\sum_{k=1}^{\infty} a_n b_{nk}\, e^{-\alpha(\lambda_n^2 + \eta_k^2 + m^2)t}\cos\eta_k(L-y)\cos\lambda_n x$$

$$+ \sum_{n=1}^{\infty} a_n\left(\cosh\mu_n y + \frac{h}{k\bar{\mu}_n}\sinh\mu_n y\right)\cos\lambda_n x \quad \text{(B.7)}$$

where, $\mu_n^2 = (\lambda_n^2 + m^2)$, $m^2 = \dfrac{2h}{k\delta}$ $\qquad$ (B.8)

$$\tan\eta_k L = \frac{Bi_y}{\eta_k L} \quad , \quad Bi_y = \frac{hL}{k} \quad \text{(B.9)}$$

$$\tan\lambda_n \ell = \frac{Bi_x}{\lambda_n \ell} \quad , \quad Bi_x = \frac{h\ell}{k} \quad \text{(B.10)}$$

$$a_n = 2q"\left(\frac{\sin\lambda_n \ell}{\lambda_n \ell + \sin\lambda_n \ell \cos\lambda_n \ell}\right)\left(\frac{1}{\mu_n k \sinh\mu_n L + h\cosh\mu_n L}\right)$$

$$\text{(B.11)}$$

$$b_{nk} = - \frac{\left[\mu_n \sinh \mu_n L + \eta_k \sin \eta_k L + \frac{h}{k} (\cosh \mu_n L - \cos \eta_k L) \right]}{\left(\eta_k^2 + \mu_n^2 \right) \left(\frac{\sin 2\eta_k L}{4\eta_k} + \frac{L}{2} \right)} \qquad (B.12)$$

A computer program was written to evaluate the solution to equation (B.7) in accordance with the specified parameters of the plate: length L = 2 ft, width ℓ = 1 ft, thickness δ = 0.75 in. = 0.0625 ft, coefficient of conduction k = 30 Btu/hr ft °F, coefficient of convection h = 1.67 Btu/ hr ft^2 °F, thermal diffusity α = 0.666 ft^2/hr and the heat input q = 1/2 hp = 1271.5 Btu/hr (q" = $\frac{q}{2\ell\delta}$ = 10172 Btu/ft^{2}hr)

b) The finite-element solution was obtained after first dividing the half-plate into sixty-four equal sized tri-angular elements, Figure B.1b.

After preparing the appropriate data input for the program i.e. node co-ordinates, element numbering, boundary conditions, etc., the solution of steady-state temperatures and transient temperatures at the indicated node points was obtained.

The steady-state temperature calculations for selected node points are compared in TABLE B1 as resulting from the classical and finite-element approaches to the problem, Figure B2.

The transient temperature variation for node 1, Figure

Table B1

Node Number	Classical	Finite Element	Error (exact-approx)	Error (% exact)
1	253.601	251.934	1.667	0.68
5	248.994	247.816	1.178	0.42
23	68.938	68.435	0.403	0.58
41	32.408	32.392	0.016	0.05
45	31.531	31.457	0.074	0.23

Figure B.2   Steady State Temperature Comparison: Classical via Finite Element Solutions.

B.1, is shown in Figure B.3 as calculated in the finite element technique for two time intervals Δ (i.e. Δ = 0.1 hrs, Δ = 0.05 hrs) and compared with the exact solution.

It is apparent that large errors could occur in the technique if due attention is not given to the length of the time interval Δ at short time intervals, the error however diminishing with increasing time.
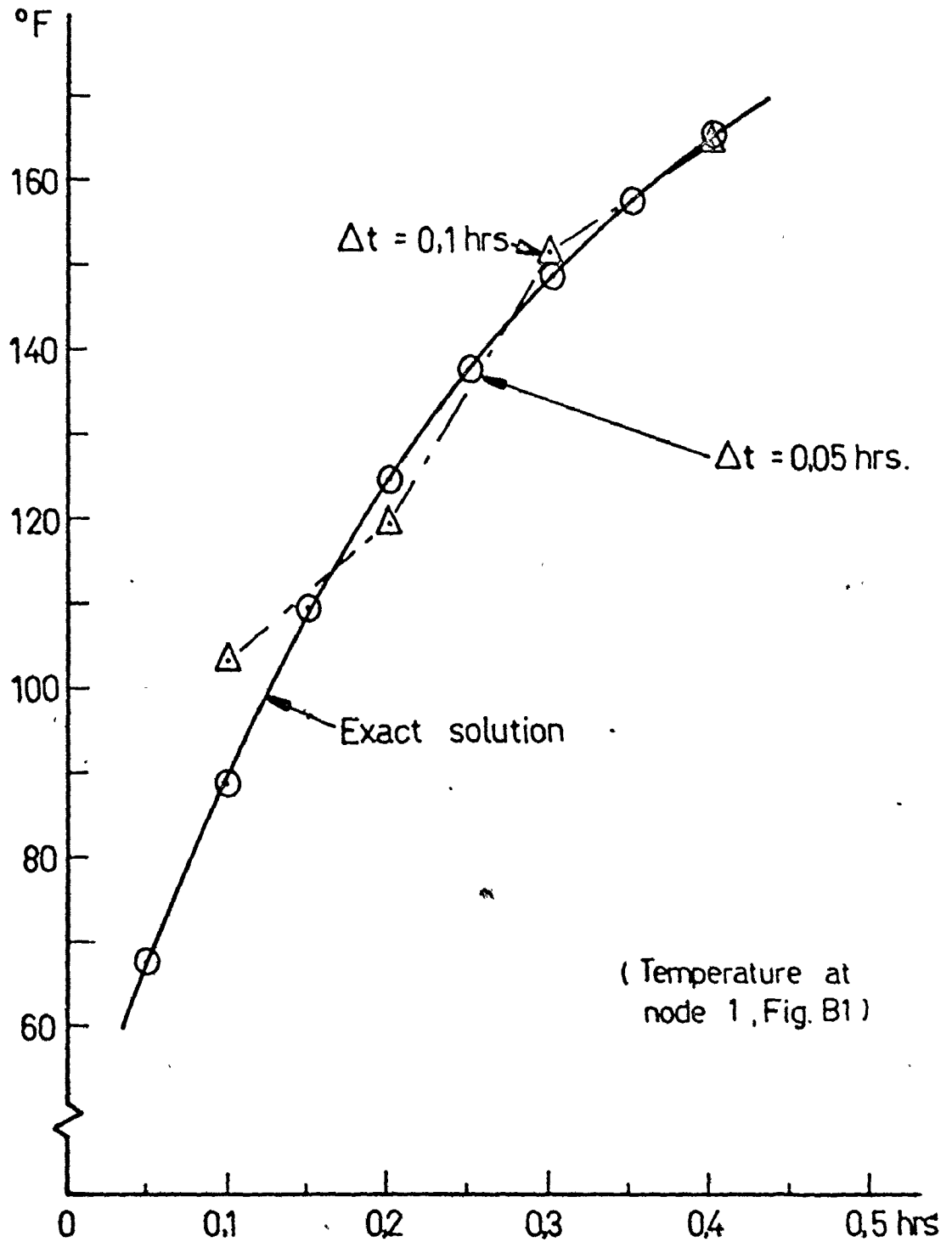
Figure B.3   Transient Temperature Comparison:
Classical via Finite Element Solutions.
The ˙ of   of time interval.

* APPENDIX C

A FINITE ELEMENT PROGRAM FOR THE ANALYSIS OF THERMAL DEFORMATIONS IN TWO-DIMENSIONAL BODIES DUE TO STEADY-STATE AND NON STEADY-STATE TEMPERATURE DISTRIBUTIONS

C 1   Program description

This appendix describes the method of setting-up a problem for solution using the Finite Element technique for the calculation of steady-state and transient temperature fields together with the result-ing thermal deformations. A listing is given of the FORTRAN IV program as used on the CDC 6400 computer at the Computing Center, McMaster University.

The program may be applied to the analysis of two-dimensional plane stress problems where the system to be analysed must first be represented by an array of triangular finite-elements. The corners of each element are the node points.

Boundary conditions may be specified as con-stant heat flux or convective conditions on the edges or faces of the elements which comprise the system, together with geometric constraints applied to defined node points.

The time interval between temperature calcula-

tions must be specified by the user.

The computer program solution involves solving a set of simultaneous algebraic equations. The coefficient matrix of this set is symmetric and has non-zero coefficients located in a band parallel to the main diagonal. The number of equations is equal to the number of node points while the band-width is equal to the maximum difference of any two node point numbers of the element array. The node point numbering arrangement should be such that the bandwidth is a minimum. The program as listed permits a maximum bandwidth of 35.

INPUT:

The input consists of eleven different groups of cards. Each group consists of one or more cards and the groups are placed behind each other sequentially as numbered below. The total number of input cards depends on the problem. Complete input decks may be stacked behind each other if more than one solution per run is required.

The card groups for each input deck are described as follows:

Group 1 : Number of problems'

Group 2 : Identification Card

Group 3 : Control Card

Group 4	:	Convection coefficient Card
Group 5	:	Material Cards
Group 6	:	Nodal point Cards
Group 7	:	Element Cards
Group 8	:	Cards for Convection from element edges
Group 9	:	Cards for Heat flux input to element edges
Group 10	:	Cards for Heat flux input to element faces
Group 11	:	Geometric constraint Cards

Group 1: FORMAT (I5) One card only

Field 1 : NPROB=number of complete input decks

Group 2: FORMAT (12A6) One card only

The contents of columns 1-72 are printed as an output heading and may be used for problem description.

Group 3: FORMAT (5I5, F10.4) One card only

Field 1 : NP= number of nodal points

Field 2 : NE= number of elements

Field 3 : NMAT= number of different materials

Field 4 : NDF= number of degrees of freedom

Field 5 : MAXIT= total number of time steps in a transient solution

If MAXIT=0, a steady-state solution only is outputed.

Field 6   :   DT = time interval

Group 4:   FORMAT (2F10.3) One card only

Field 1   :   HFO= convection coefficient on side 'A' of the element (Btu/hr ft^2 °F)

Field 2   :   HFI= convection coefficient on side 'B' of the element (Btu/hr ft^2 °F)

Group 5:   FORMAT (I5, 4F10.3, 2E10.2, F10.3) One card for each different material. Each material is identified in the program by a number and the materials are numbered sequentially starting with 1.

Field 1   :   N= the number of the material

Field 2   :   ORT(N,1)= the conduction coefficient, k, in Btu/hr ft °F.

Field 3   :   ORT(N,2)= density, ρ, in lb/ft^3

Field 4   :   ORT(N,3)= specific heat, c_p, in Btu/lb °F

Field 5   :   ORT (N,4)= Poisson's ratio ν

Field 6   :   ORT (N,5)= coefficient of thermal expansion, α, in ppm/°F

Field 7   :   ORT(N,6) = Young's modulus, E, in lbs/in^2

Field 8   :   ORT (N,7) = plate thickness, b, in inches.

GROUP 6: FORMAT (I5, 2F10.3) one card for each node

point where the node points are numbered
sequentially starting with 1

Field 1   :   N= the node point number

Field 2   :   COORD (N,1)= the x co-ordinate
of the node point N in inches.

Field 3   :   COORD (N,2)= the y co-ordinates
of the node point N in inches.

Group 7:   FORMAT (5I5) One card for each element where
the elements are numbered sequentially start-
ing with 1.

Field 1   :   N= the element number

Fields 2-4 :   NOP (N,1), NOP (N,2), NOP (N,3)
respectively.

These are the node point numbers
representing the corners of the
element, read as i,j,k, and
numbered anti-clockwise around
the element.

Field 5   :   IMAT= the number of the material
of which the element is composed.

Group 8:   FORMAT (I5) One card only

Field 1   :   NCB= the number of convection
cooled element edges. If none,
enter NCB=0 and proceed to
Group 9.

FORMAT (3I5, F10.3) One card for each
convection cooled element edge. Each edge is

numbered sequentially starting from 1.

(N.B. the numbering is independent of the
element numbering identified in Group 7).

Field 1   :   N= the edge number

Fields 2-3 :   CB1 (N), CB2 (N) respectively.
These are the node point
numbers the connection of
which defines the edge.

Field 4   :   HE (N)= the coefficient of
convection at the defined edge
in Btu/hr ft^2 $^\circ$F.

Group 9: FORMAT (I5) One card only

Field 1   :   NHB= the number of heated ele-
ment edges. If none, enter
NHB=0 and proceed to Group 10.

FORMAT (3I5, F10.3) One card for each heated

element edge. Each edge is numbered

sequentially, starting from 1. (N.B. the

numbering is independent of the element

numbering identified in Group 7)

Field 1   :   N= the edge number

Field 2-3 :   HB1 (N), HB2 (N) respectively.
These are the node point numbers
the connection of which defines
the edge.

Field 4   :   QB(N) = the heat flux at the
element edge in Btu/ft^2 hr.

Group 10: FORMAT (I5) One card only

Field 1   :   NHA= the number of heated
element faces. If none, enter
NHA=0 and proceed to Group 11.

FORMAT (I5, F10.3) One card for each heated
element face.

Field 1   :   HA= element number (as pre-
viously defined in Group 7)

Field 2   :   QA(N)=the heat flux on the element
face in Btu/ft^2 hr.

Group 11: FORMAT (I5) One card only

Field 1   :   NB= the number of geometrically
constrained node points.

FORMAT (2I5) One card for each constrained
node.

Field 1   :   NBC= node point number (as de-
fined previously in Group 6).

Field 2   :   NFIX, a code number defined as;
NFIX= 01, node constrained in Y
co-ordinate direction.

NFIX=10, node constrained in X
co-ordinate direction.

NFIX=11, node constrained in X
and Y co-ordinate directions.

OUTPUT:

All output is labelled. The following input
parameters are printed together with the solution;

(i)   the contents of the identification card

(ii)   NP, NE, NMAT, NDF, MAXIT, DT

(iii)   the coefficients of convection on the
        element faces, HFO and HFI

(iv)   a list of material properties

(v)   a list of all node points and their x
        and y co-ordinates

(vi)   a list of elements indicating the node
        points in i, j, k sequence, together
        with the NMAT identification

(vii)   a list of all input boundary conditions:

        (a)   convection cooled edges: node point
              connections and coefficient of con-
              vection, HE.

        (b)   heated element edges: node point
              connections and heat flux, Q_B

        (c)   heated element faces: element
              number and heat flux, Q_A

        (d)   geometrically constrained nodes and
              type of constraint.

The final solution is presented as lists of
node point and mean element temperatures and the
corresponding nodal displacements, together with the
equivalent nodal forces due to the computed temperature
fields. For the transient case, the time is printed
before each list of temperatures. The number of lists
of temperatures is MAXIT.

C 2   Program listing

The program has been written in a modular form as an aid to its versatility in use dependent on whether steady-state and/or transient temperature fields are required with or without the resulting thermal deformations.

The listing and flow diagrams for all subroutines follow a typical control program listing:

(N.B. Subroutines FORMK and SOLSYM are essentially as obtained from Zienkiewicz [35].

Flow chart - <u>PROGRAM MAIN</u>

```
                  ╭──────────────────────╮
                  │        Start         │
                  ╰──────────────────────╯
                             │
                             ▽
            ┌──────────────────────────────┐
            │    Read number of problems   │
            └──────────────────────────────┘
                             │
                             ▽
            ┌──────────────────────────────┐
      ┌────▶│   Loop on number of problems │
      │     └──────────────────────────────┘
      │                      │
      │                      ▽
      │     ┌──────────────────────────────┐
      │     │      Call for data input     │          Subroutine:
      │     └──────────────────────────────┘            DATA
      │                      │
      │                      ▽
      │     ┌──────────────────────────────┐
      │     │  Call for thermal stiffness  │          Subroutine:
      │     │ matrix and heat input vector │            STIFT 1
      │     └──────────────────────────────┘
      │                      │
      │                      ▽
      │     ┌──────────────────────────────┐
      │     │  Call for equation solver for│          Subroutine:
      │     │   steady-state temperatures  │            THETA
      │     └──────────────────────────────┘
      │                      │
      │                      ▽
      │     ┌──────────────────────────────┐
      │     │  Call for stiffness matrix   │          Subroutine:
      │     └──────────────────────────────┘       FORMK, STIFT 2(N)
      │                      │
      │                      ▽
      │     ┌──────────────────────────────┐
      │  ┌─▶│       Loop on load cases     │
      │  │  └──────────────────────────────┘
      │  │                   │
      │  │                   ▽
      │  │  ┌──────────────────────────────┐
      │  │  │  Call for thermal load vector│          Subroutine:
      │  │  └──────────────────────────────┘            LOAD
      │  │                   │
      │  │                   ▽
      │  │  ┌──────────────────────────────┐
      │  │  │   Call for equation solver   │          Subroutine:
      │  │  └──────────────────────────────┘            SOLSYM
      │  │                   │
      │  │                   ▽
```

```
                    ┌─────────────────────────────────┐         Subroutine:
                    │ Call for nodal displacements     │
                    └─────────────────────────────────┘           DISPL
                              ╱─────────────────╲
                             ╱ Is a transient solution ╲─────────
                             ╲      required           ╱
                              ╲─────────────────╱
                                   Yes                       No

                                                         Subroutines:
                    ┌─────────────────────────────────┐
                    │ Call for transient temperature   │   CAPT, TRANS
                    │           distribution           │
                    └─────────────────────────────────┘

                    ┌─────────────────────────────────┐
                    │       End loop on loads          │
                    └─────────────────────────────────┘

                    ┌─────────────────────────────────┐
                    │      End loop on problems        │
                    └─────────────────────────────────┘

                              ╭──────╮
                              │ Stop │
                              ╰──────╯
```

```
C
C      MAIN DRIVING PROGRAM
C
       COMMON/CONTR1/TITLE(12),NP,NE,NMAT,NDF,NSZF,NCN,
      1 COORD(68,2),NOP(100,3),ORT(10,7),IMAT(100)
       COMMON/CONTR2/NH(50),CB1(50),CB2(50),HF(50),NCB,NQ(50),
      1 HB1(50),HB2(50),QB(50),NHB,HA(50),QA(50),NHA,HFO,HFI
       COMMON/CONTR3/HK(68,68),GC(68,68),HQ(68),STEMP(100)
       COMMON/CONTR4/SK(136,35),F(136),EK(6,6),NB,NBC(25),
      1 NFIX(25)
       COMMON MAXIT,DT,ITER
C
       INTEGER CB1,CB2,HB1,HB2
       INTEGER TITLE
C
C      ****************************************************************
C      LET,
C           NPROB = NO.OF PROBLEMS
C           NP = NO.OF NODE POINTS
C           NE = NO.OF ELEMENTS
C           NMAT = NO.OF MATERIALS
C           NCB = NO.OF CONVECTION COOLED EDGES
C           NHB = NO.OF ELEMENT EDGES HEATED
C           NHA = NO.OF ELEMENT FACES HEATED
C           NB = NO. OF GEOMETRICALLY CONSTRAINED BOUNDARIES
C           NDF = NO.OF DEGREES OF FREEDOM
C           NCN = NO.OF NODES PER ELEMENT (3)
C           NSZF = NP*NDF
C           NBAND = MATRIX BANDWIDTH
C
C      THEN THE ABOVE STATEMENTS HAVE THIS FORM
C           COORD(NP,2)          NOP(NE,3)          ORT(NMAT,7)
C           IMAT(NE)             NBC(NB)            NFIX(NB)
C           NH(NCB)              CB1(NCB)           CB2(NCB)
C           HE(NCB)              NQ(NHB)            HB1(NHB)
C           HB2(NHB)             QB(NHB)            HA(NHA)
C           QA(NHA)              HK(NP,NP)          GC(NP,NP)
C           HQ(NP)               STEMP(NE)          SK(NSZF,NBAND)
C           F(NSZF)              EK(6,6)
C      ****************************************************************
C
       NCN = 3
C
C      ****************************************************************
C      LOOP ON NUMBER OF PROBLEMS
C      ****************************************************************
C
       READ (5,1) NPROB
     1 FORMAT (I5)
       DO 500 NPR = 1,NPROB
```

```
C
C
C
C     ***********************************************************
C     READ ALL INPUT GEOMETRY AND MATERIAL PROPERTIES
C     ***********************************************************
C
      CALL DATA
      NSZF = NP*NDF
C
C     ***********************************************************
C     FORM THERMAL STIFFNESS MATRIX (HK) AND HEAT INPUT
C     MATRIX (HQ)
C     ***********************************************************
C
      CALL STIFT1
C
C     ***********************************************************
C     SOLVE FOR STEADY STATE TEMPERATURE DISTRIBUTION
C     ***********************************************************
C
      CALL THETA
C
C     ***********************************************************
C     FORM SIMULTANEOUS EQUATIONS
C     ***********************************************************
C
      CALL FORMK
C
C     ***********************************************************
C     FORM FORCE VECTOR FROM ELEMENT INITIAL (THERMAL) STRAIN
C     VECTORS USING ELEMENT MEAN TEMPERATURE INCREASE
C     ***********************************************************
C
      ITER = 1
   50 CALL LOAD
C
C     ***********************************************************
C     SOLVE SIMULTANEOUS EQUATIONS
C     ***********************************************************
C
      CALL SOLSYM
C
C     ***********************************************************
C     CALCULATE NODAL DISPLACEMENTS
C     ***********************************************************
C
      CALL DISPL
C
      IF (ITER .GT. MAXIT) GO TO 20
C
C     ***********************************************************
C     SOLVE FOR TRANSIENT TEMPERATURE DISTRIBUTION
C     ***********************************************************
```

```
      IF (MAXIT .EQ. 0) GO TO 20
      CALL TRANS
C
      ITER = ITER + 1

      GO TO 50
C
  500 CONTINUE
C
   20 STOP
      END
```

Flow chart - subroutine <u>DATA</u>

```
                    ╭──────────────────────────────╮
                    │            Start             │
                    ╰──────────────────────────────╯
                                   │
                                   ▼
                    ┌──────────────────────────────┐
                    │   Read and print control data │
                    └──────────────────────────────┘
                                   │
                                   ▼
                    ┌──────────────────────────────┐
                    │Read and print material properties│
                    └──────────────────────────────┘
                                   │
                                   ▼
                    ┌──────────────────────────────┐
                    │    Read nodal co-ordinates    │
                    └──────────────────────────────┘
                                   │
                                   ▼
                    ┌──────────────────────────────┐
                    │    Read element connections and│
                    │         material types        │
                    └──────────────────────────────┘
                                   │
                                   ▼
                    ┌──────────────────────────────┐
                    │     Read boundary conditions: │
                    │ (a) Convection cooled edges and│
                    │     faces                     │
                    │ (b) Heated edges and faces    │
                    │ (c) Geometric constraints     │
                    └──────────────────────────────┘
                                   │
                                   ▼
                    ┌──────────────────────────────┐
                    │    Print nodal co-ordinates   │
                    └──────────────────────────────┘
                                   │
                                   ▼
```

```
┌─────────────────────────────┐
│   Print element connections  │
│     and material types       │
└─────────────────────────────┘
              │
              ▼
┌─────────────────────────────┐
│  Print boundary conditions   │
└─────────────────────────────┘
              │
              ▼
┌─────────────────────────────┐
│           Return             │
└─────────────────────────────┘
```
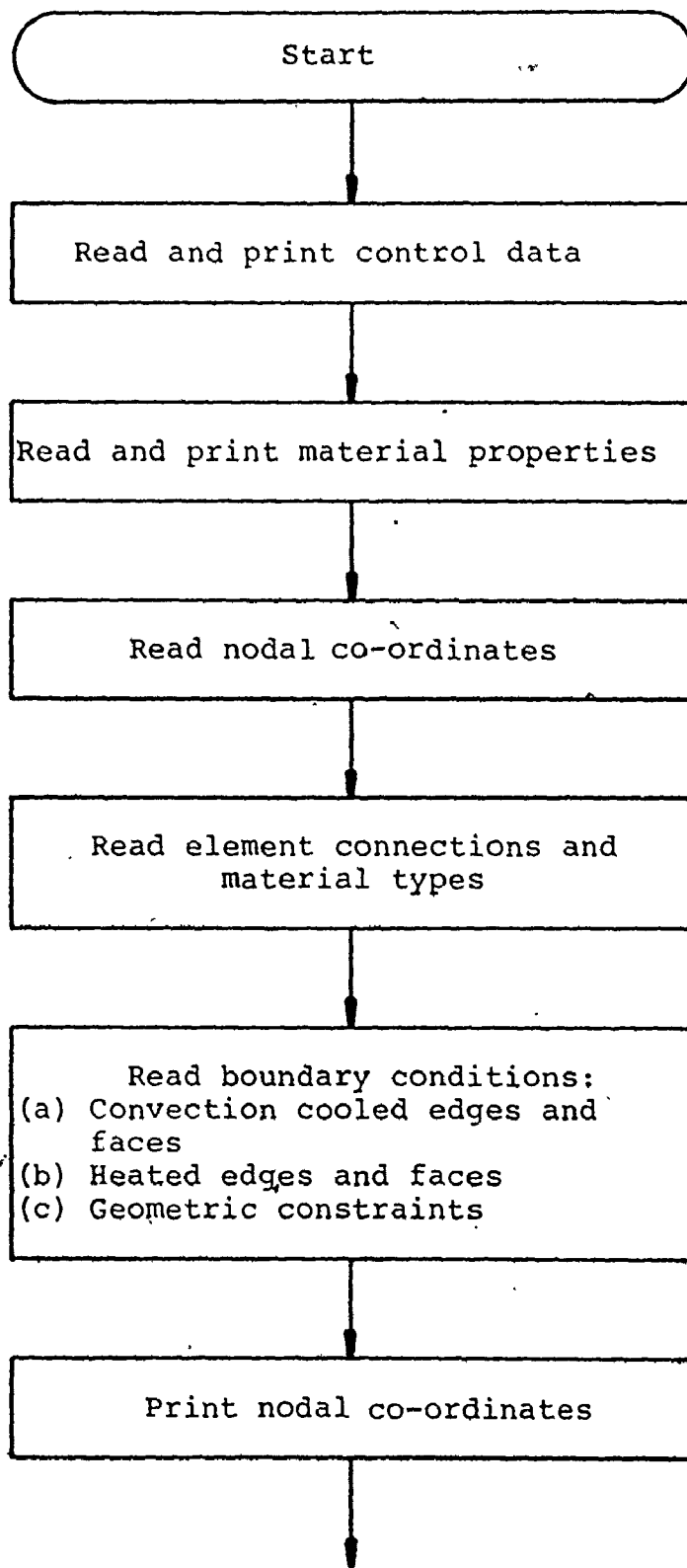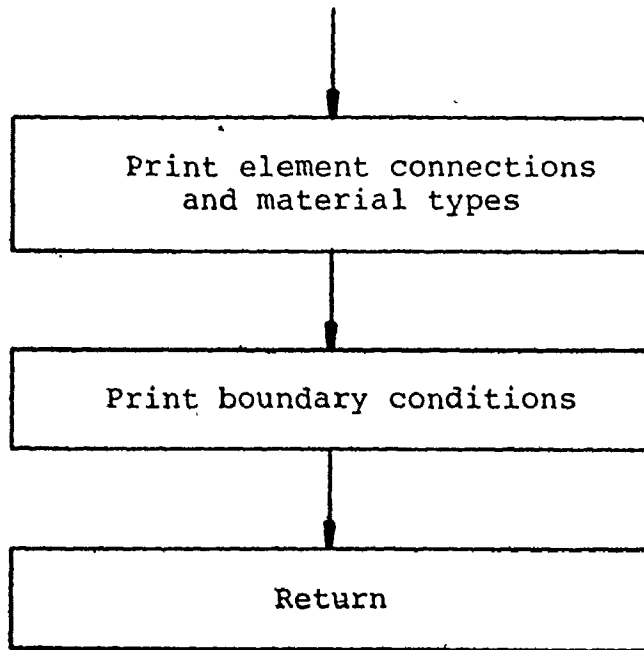
```
      SUBROUTINE DATA
C
      COMMON/CONTR1/TITLE(12),NP,NE,NMAT,NDF,NSZF,NCN,
     1 COORD(68,2),NOP(100,3),ORT(10,7),IMAT(100)
      COMMON/CONTR2/NH(50),CB1(50),CB2(50),HE(50),NCB,NQ(50),
     1 HB1(50),HB2(50),QB(50),NHB,HA(50),QA(50),NHA,HFO,HFI
      COMMON/CONTR4/SK(136,35),F(136),EK(6,6),NB,NBC(25),
     1 NFIX(25)
      COMMON MAXIT,DT,ITER
C
      DIMENSION NPN(68),NEN(100)
C
      INTEGER TITLE
      INTEGER CB1,CB2,HB1,HB2,HA
C
      READ (5,5) TITLE
    5 FORMAT (12A6)
      READ (5,10) NP,NE,NMAT,NDF,MAXIT,DT
   10 FORMAT (5I5,F10.4)
      WRITE (6,15) TITLE
   15 FORMAT (1H1,45X,12A6,/////)
      WRITE(6,20) NP,NE,NMAT,NDF,MAXIT,DT
   20 FORMAT (1H0,10X,* NUMBER OF NODAL POINTS = *,I5,//,11X,
     1 *NO.OF ELEMENTS = *,I5,//,11X,* NO.OF MATERIALS = *,
     2 I5,//,11X,* NUMBER OF DEGREES OF FREEDOM = *,I5,//,
     3 11X,* NO.OF TIME INCREMENTS = *,I5,//,11X,
     4 * TIME INTERVAL = *,F10.4,* HRS. *,//)
C
C     ********************************************************
C     IDENTIFY COEFFICIENTS OF HEAT CONVECTION FROM ELEMENT
C     FACES
C     ********************************************************
C
      READ (5,22) HFO,HFI
   22 FORMAT (2F10.3)
C
C     ********************************************************
C     READ AND PRINT MATERIAL PROPERTIES
C     ********************************************************
C
      READ (5,23) (N,(ORT(L,I),I=1,7),L=1,NMAT)
   23 FORMAT(I5,4F10.3,2E10.2,F10.3)
      WRITE (6,24)
   24 FORMAT(1H1,40X,* MATERIAL PROPERTIES *,////)
      WRITE (6,26) (N,(ORT(N,I),I=1,7),N=1,NMAT)
   26 FORMAT (1H0,//,10X,*MATERIAL NUMBER *,I5,///,
     1 10X,*CONDUCTION COEFFICIENT---- = *,F10.4,
     2 *BTU/HR.FT.DEG.F.*,//,
     3 10X,*DENSITY----------------- = *,F10.4,
     4 *LB/CUB.FT.*,//,
     5 10X,*SPECIFIC HEAT------------- = *,F10.4,
     6 *BTU/LB DEG.F.*,//,
```

```
      7 10X,*POISSONS'S RATIO---------- = *,F10.4,//,
      8 10X,*COEFFICIENT OF EXPANSION-- = *,E12.2,
      9 *PPM/DEG.F.*,//,
      0 10X,*YOUNG'S MODULUS---------- = *,E12.2,
      1 *LB/IN.SQ.*,////,
      2 10X,*THICKNESS---------------- = *,F10.3,*IN.*,//)
C
      DO 98 N = 1,NMAT
      ORT(N,6) = ORT(N,6)*144.0
      ORT(N,7) = ORT(N,7) / 12.0
   98 CONTINUE
C
C
      *********************************************************
      READ NODAL POINT DATA
      *********************************************************
C
      READ (5,25) (NPN(N),(COORD(N,M),M=1,2),N=1,NP)
   25 FORMAT (I5,2F10.3)
C
C
      *********************************************************
      READ ELEMENT DATA
      *********************************************************
C
      READ (5,30) (NEN(N),(NOP(N,M),M=1,3),IMAT(N),N=1,NE)
   30 FORMAT (5I5)
C
C
      *********************************************************
      PRINT OUT ALL NODE POINT AND ELEMENT DATA
      *********************************************************
C
      WRITE (6,35)
   35 FORMAT(1H1,10X,*NODE POINTS AND CO-ORDINATES *,///)
      WRITE (6,40)
   40 FORMAT (1H0,10X,* NODE NO. *, 7X,* X CO-ORDINATE *,10X,
      1 * Y CO-ORDINATE *,//)
      WRITE (6,45) (NPN(N),(COORD(N,M),M=1,2),N=1,NP)
   45 FORMAT (1H0,12X,I3,15X,F8.3,16X,F8.3,/)
C
      DO 99 N = 1,NP
      DO 99 M = 1,2
      COORD(N,M) = COORD(N,M) / 12.0
   99 CONTINUE
C
      WRITE (6,50)
   50 FORMAT (1H1,10X,* ELEMENT INFORMATION *,///)
      WRITE (6,55)
   55 FORMAT (1H0,10X,* ELEMENT NO. *,6X,* I *,8X,* J *,8X,
      1 * K *, 8X,* MATERIAL NO. *,//)
      WRITE (6,60) (NEN(N),(NOP(N,M),M=1,3),IMAT(N),N=1,NE)
   60 FORMAT (1H0,15X,I3,10X,I3,8X,I3,8X,I3,10X,I5,/)
      WRITE (6,61) HFO,HFI
```

```
   61 FORMAT (1H1,10X,*CONVECTION COEFFICIENT AT FACE 'A' = *,
      1 F10.3,2X,*BTU/HR.FT.DEG.F.*,//,11X,
      2*CONVECTION COEFFICIENT AT FACE 'B' = *,F10.3,2X,
      3 *BTU/HR.FT.DEG.F.*,///)
C
C     **************************************************************
C     BOUNDARY CONDITIONS  (A) CONVECTION COOLED EDGES
C
C     **************************************************************
C
      READ (5,70) NCB
   70 FORMAT (I5)
      IF (NCB .EQ. 0) GO TO 200
      WRITE (6,80) NCB
   80 FORMAT (1H1,* CONVECTION COOLED EDGES (*,I5,*)*,///)
      WRITE (6,85)
   85 FORMAT (1H0,10X,*  ELEMENT NO.*,10X,*NODE CONNECTIONS *,
      1 10X,* CONVECTION COEFFICIENT *,//)
      DO 95 N = 1,NCB
      READ (5,75) NH(N),CB1(N),CB2(N),HE(N)
   75 FORMAT (3I5,F10.3)
      WRITE (6,90) NH(N),CB1(N),CB2(N),HE(N)
   90 FORMAT (1H0,15X,I3,12X,I3,5X,*TO*,5X,I3,15X,F10.3,/)
   95 CONTINUE
  200 CONTINUE
C
C     **************************************************************
C     BOUNDARY CONDITIONS (B) APPLIED HEAT FLUX
C     **************************************************************
C
C
C                                        (1) TO EDGES
C
      READ (5,100) NHB
  100 FORMAT (I5)
      IF (NHB .EQ. 0) GO TO 205
      WRITE (6,110) NHB
  110 FORMAT (1H1,* HEATED EDGES (*,I5,*)*,///)
      WRITE (6,115)
  115 FORMAT (1H0,10X,* ELEMENT NO.*,10X,*NODE CONNECTIONS *,
      1 10X,* Q (BTU/FT.SQ.HR.)*,//)
      DO 125 N = 1,NHB
      READ (5,105) NQ(N),HB1(N),HB2(N),QB(N)
  105 FORMAT (3I5,F10.3)
      WRITE (6,120) NQ(N),HB1(N),HB2(N),QB(N)
  120 FORMAT (1H0,15X,I3,12X,I3,5X,*TO*,5X,I3,12X,F10.3,/)
  125 CONTINUE
  205 CONTINUE
C
C                                        (2) TO FACES
C
      READ (5,150) NHA
  150 FORMAT (I5)
```

```
      IF (NHA .EQ. 0) GO TO 210
      WRITE (6,155) NHA
155 FORMAT (1H1,* HEATED FACES (*,I5,*)*,///)
      WRITE (6,160)
160 FORMAT (1H0,10X,*  ELEMENT NO. *,10X,
    1* Q (BTU/FT.SQ.HR.) *,//)
      DO 175 I = 1,NHA
      READ (5,165) HA(I),QA(I)
165 FORMAT (I5,F10.3)
      WRITE (6,170) HA(I),QA(I)
170 FORMAT (1H0,15X,I5,10X,F10.4,/)
175 CONTINUE
210 CONTINUE
C
C     *********************************************************
C     BOUNDARY CONDITIONS (C) RESTRAINED BOUNDARIES
C     *********************************************************
C
      READ (5,130) NB
130 FORMAT(I5)
      READ (5,135) (NBC(I),NFIX(I),I = 1,NB)
135 FORMAT (2I5)
      WRITE (6,140)
140 FORMAT (1H1,* RESTRAINED BOUNDARIES *,///,5X,
    1 * 01 = FIXED IN 'Y' _    10 = FIXED IN 'X' *,
    2 5X,*11 = FIXED IN 'X' AND 'Y' *,////,
    3 10X,*NODE POINT *,10X,*CONDITION TYPE *,///)
      WRITE (6,145) (NBC(I),NFIX(I),I = 1,NB)
145 FORMAT (1H0,14X,I5,15X,I5,//)
C
      RETURN
      END
```

Flow chart - subroutine <u>STIFT 1</u>

```
                    ╭─────────────────────────────╮
                    │            Start            │
                    ╰─────────────────────────────╯
                                  │
                                  ▼
                    ┌─────────────────────────────┐
                    │ Zero thermal stiffness matrix│
                    └─────────────────────────────┘
                                  │
                                  ▼
                    ┌─────────────────────────────┐
                    │    Zero heat input vector    │
                    └─────────────────────────────┘
                                  │
                                  ▼
         ┌─────────▶ ┌─────────────────────────────┐
         │          │      Loop on elements        │
         │          └─────────────────────────────┘
         │                        │
         │                        ▼
         │          ┌─────────────────────────────┐
         │          │ Determine element connections│
         │          └─────────────────────────────┘
         │                        │
         │                        ▼
         │          ┌─────────────────────────────┐
         │          │    Form element conduction   │
         │          │            matrix            │
         │          └─────────────────────────────┘
         │                        │
         │                        ▼
         │          ┌─────────────────────────────┐
         │          │    Form element convection   │
         │          │            matrix            │
         │          └─────────────────────────────┘
         │                        │
         │                        ▼
         │          ┌─────────────────────────────┐
         │          │ Assemble thermal stiffness matrix│
         │          └─────────────────────────────┘
         │                        │
         │                        ▼
         │          ┌─────────────────────────────┐
         └──────────│    End loop on elements      │
                    └─────────────────────────────┘
                                  │
                                  ▼
```

```
┌─────────────────────────────────────┐
│   Loop on number of convection      │
│        cooled boundaries            │
└─────────────────────────────────────┘
                   │
                   ▼
┌─────────────────────────────────────┐
│  Form element convection boundary   │
│               matrix                │
└─────────────────────────────────────┘
                   │
                   ▼
┌─────────────────────────────────────┐
│   Assemble thermal stiffness matrix │
└─────────────────────────────────────┘
                   │
                   ▼
┌─────────────────────────────────────┐
│      End loop on number of          │
│   convection cooled boundaries      │
└─────────────────────────────────────┘
                   │
                   ▼
┌─────────────────────────────────────┐
│     Loop on number of heated        │
│               faces                 │
└─────────────────────────────────────┘
                   │
                   ▼
┌─────────────────────────────────────┐
│   Form element heat input matrix    │
└─────────────────────────────────────┘
                   │
                   ▼
┌─────────────────────────────────────┐
│     Assemble heat input matrix      │
└─────────────────────────────────────┘
                   │
                   ▼
```

```
┌─────────────────────────────┐
│   End loop on number of     │
│        heated faces         │
└─────────────────────────────┘

┌─────────────────────────────┐
│   Loop on number of heated  │
│         boundaries          │
└─────────────────────────────┘

┌─────────────────────────────┐
│  Form element heat input matrix  │
└─────────────────────────────┘

┌─────────────────────────────┐
│   Assemble heat input matrix   │
└─────────────────────────────┘

┌─────────────────────────────┐
│  End loop on number of heated  │
│         boundaries          │
└─────────────────────────────┘

┌─────────────────────────────┐
│  Print thermal stiffness matrix  │
└─────────────────────────────┘

┌─────────────────────────────┐
│   Print heat input vector   │
└─────────────────────────────┘

┌─────────────────────────────┐
│           Return            │
└─────────────────────────────┘
```

```
      SUBROUTINE STIFT1
C
      COMMON/CONTR1/TITLE(12),NP,NE,NMAT,NDF,NSZF,NCN,
     1 COORD(68,2),NOP(100,3),ORT(10,7),IMAT(100)
      COMMON/CONTR2/NH(50),CB1(50),CB2(50),HE(50),NCB,NQ(50),
     1 HB1(50),HB2(50),QB(50),NHB,HA(50),QA(50),NHA,HFO,HFI
      COMMON/CONTR3/HK(68,68),GC(68,68),HQ(68),STEMP(100)
      COMMON/CONTR4/SK(136,35),F(136),EK(6,6),NB,NBC(25),
     1 NFIX(25)
C
      DIMENSION HKE(3,3),HHAE(3,3),HHBE(2,2),HQBE(2),HQAE(3)
C
      INTEGER CB1,CB2,HB1,HB2,B1,B2,HA
      INTEGER TITLE
C
      DO 1 I = 1,NP
      DO 1 J = 1,NP
      HK(I,J) = 0.0
    1 CONTINUE
      DO 2 I = 1,NP
      HQ(I) = 0.0
    2 CONTINUE
C
      DO 50 N=1,NE
C
C     ****************************************************************
C     IDENTIFY ELEMENT NODE POINTS
C     ****************************************************************
C
      I = NOP(N,1)
      J = NOP(N,2)
      K = NOP (N,3)
C
      XIJ = COORD(J,1) - COORD(I,1)
      XIK = COORD(K,1) - COORD(I,1)
      XJK = COORD(K,1) - COORD(J,1)
      YIJ = COORD(J,2) - COORD(I,2)
      YIK = COORD(K,2) - COORD(I,2)
      YJK = COORD(K,2) - COORD(J,2)
C
C     ****************************************************************
C     CALCULATE THE AREA OF THE ELEMENT
C     ****************************************************************
C
      AREA = ABS((XIJ*YIK - XIK*YIJ)/2.0)
      L = IMAT(N)
      COND = ORT(L,1)
      T = ORT(L,7)
C
      CM = (COND*AREA*T) / ((XIJ*YJK - XJK*YIJ)**2)
C
C     ****************************************************************
C     FORM THE ELEMENT CONDUCTION MATRIX (HKE)
C     ****************************************************************
C
```

```
      DO 10 II = 1,3
      DO 10 JJ = 1,3
      HKE(II,JJ) = 0.0
   10 CONTINUE
C
      HKE(1,1) =  (XJK**2 + YJK**2)
      HKE(1,2) = -(XIK*XJK + YIK*YJK)
      HKE(1,3) =  (XIJ*XJK + YIJ*YJK)
      HKE(2,1) = HKE(1,2)
      HKE(2,2) =  (XIK**2 + YIK**2)
      HKE(2,3) =   -(XIJ*XIK + YIJ*YIK)
      HKE(3,1) = HKE(1,3)
      HKE(3,2) = HKE(2,3)
      HKE(3,3) =  (XIJ**2 + YIJ**2)
C
      DO 20 KK = 1,3
      DO 20 LL = 1,3
      HKE(KK,LL) = CM*HKE(KK,LL)
   20 CONTINUE
C
C     ********************************************************
C     ADD ELEMENT CONDUCTION MATRICES TO THERMAL
C     STIFFNESS MATRIX (HK)
C     ********************************************************
C
      HK(I,I) = HK(I,I) + HKE(1,1)
      HK(I,J) = HK(I,J) + HKE(1,2)
      HK(I,K) = HK(I,K) + HKE(1,3)
      HK(J,I) = HK(J,I) + HKE(2,1)
      HK(J,J) = HK(J,J) + HKE(2,2)
      HK(J,K) = HK(J,K) + HKE(2,3)
      HK(K,I) = HK(K,I) + HKE(3,1)
      HK(K,J) = HK(K,J) + HKE(3,2)
      HK(K,K) = HK(K,K) + HKE(3,3)
C
C     ********************************************************
C     FORM ELEMENT CONVECTION MATRIX (HHAE)
C     ********************************************************
C
      DO 30 II = 1,3
      DO 30 JJ = 1,3
      HHAE(II,JJ) = 0.0
   30 CONTINUE
C
      HHAE(1,2) = 1.0
      HHAE(1,3) = 1.0
      HHAE(2,1) = HHAE(1,2)
      HHAE(2,2) = 2.0
      HHAE(2,3) = 1.0
      HHAE(3,1) = HHAE(1,3)
      HHAE(3,2) = HHAE(2,3)
```

```
C
      DO 40 KK = 1,3
      DO 40 LL = 1,3
      HHAE(KK,LL) = (HFO + HFI)*(AREA/12.0)*HHAE(KK,LL)
   40 CONTINUE
C
C     ***********************************************************
C     ADD ELEMENT CONVECTION MATRICES TO THERMAL
C     STIFFNESS MATRIX (HK)
C     ***********************************************************
C
      HK(I,I)  =  HK(I,I)  +  HHAE(1,1)
      HK(I,J)  =  HK(I,J)  +  HHAE(1,2)
      HK(I,K)  =  HK(I,K)  +  HHAE(1,3)
      HK(J,I)  =  HK(J,I)  +  HHAE(2,1)
      HK(J,J)  =  HK(J,J)  +  HHAE(2,2)
      HK(J,K)  =  HK(J,K)  +  HHAE(2,3)
      HK(K,I)  =  HK(K,I)  +  HHAE(3,1)
      HK(K,J)  =  HK(K,J)  +  HHAE(3,2)
      HK(K,K)  =  HK(K,K)  +  HHAE(3,3)
C
   50 CONTINUE
C
      IF (NCB .EQ. 0) GO TO 160
C
C     ***********************************************************
C     BOUNDARY CONDITIONS (A) CONVECTION FROM PLATE EDGES
C     ***********************************************************
C
      DO 80 N = 1,NCB
C
C     ***********************************************************
C     CALCULATE THE LENGTH OF THE ELEMENT BOUNDARY
C     ***********************************************************
C
      I = NH(N)
      B1 = CB1(N)
      B2 = CB2(N)
      SIJ = SQRT((COORD(B1,2) - COORD(B2,2))**2 +
     1 (COORD(B1,1) - COORD(B2,1))**2)
      L = IMAT(I)
      T = ORT(L,7)
      H = HE(N)
      CM = (H*SIJ*T) / 6.0
C
C     ***********************************************************
C     FORM ELEMENT CONVECTION MATRIX (HHBE)
C     ***********************************************************
C
      DO 60 II = 1,2
      DO 60 JJ = 1,2
      HHBE(II,JJ) = 0.0
   60 CONTINUE
C
```

```
      HHBE(1,1) = 2.0
      HHBF(1,2) = 1.0
      HHBE(2,1) = HHBF(1,2)
      HHBE(2,2) = 2.0
C
      DO 70 LL = 1,2
      DO 70 MM = 1,2
      HHBE(LL,MM) = CM*HHBE(LL,MM)
   70 CONTINUE
C
C     ****************************************************************
C     ADD FDGE FLEMENT CONVECTION MATRICES TO THERMAL
C     STIFFNESS MATRIX (HK)
C     ****************************************************************
C
      HK(B1,B1) = HK(B1,B1) + HHBE(1,1)
      HK(B1,B2) = HK(B1,B2) + HHBE(1,2)
      HK(B2,B1) = HK(B2,B1) + HHBE(2,1)
      HK(B2,B2) = HK(B2,B2) + HHBE(2,2)
C
   80 CONTINUE
C
  160 IF (NHB .EQ. 0) GO TO 190
C
C     ****************************************************************
C     BOUNDARY CONDITIONS (B) HEAT INPUT AT EDGE
C     ****************************************************************
C
      DO 110 N = 1,NHB
C
C     ****************************************************************
C     CALCULATE THE LENGTH OF THE ELEMENT BOUNDARY
C     ****************************************************************
C
      I = NQ(N)
      B1 = HB1(N)
      B2 = HB2(N)
      SIJ = SQRT((COORD(B1,2) - COORD(B2,2))**2 + (COORD(B1,1)
     1 - COORD(B2,1))**2)
      L = IMAT(I)
      T = ORT(L,7)
      QDD = QB(N)
      CM = (QDD*SIJ*T) / 2.0
C
C     ****************************************************************
C     FORM ELEMENT HEAT FLUX MATRIX
C     ****************************************************************
C
      DO 90 II = 1,2
      HQBE (II) = 0.0
   90 CONTINUE
      HQBE(1) = 1.0
```

```
      HQBE(2) = 1.0
C
      DO 100 M = 1,2
      HQBE(M) = CM*HQBE(M)
  100 CONTINUE
C
C     ********************************************************
C     ADD EDGE ELEMENT HEAT INPUT MATRICES TO TOTAL HEAT
C     INPUT MATRIX (HQ)
C     ********************************************************
C
      HQ(B1) = HQ(B1) + HQBE(1)
      HQ(B2) = HQ(B2) + HQBE(2)
  110 CONTINUE
C
  190 IF (NHA .EQ. 0) GO TO 200
C
C     ********************************************************
C     BOUNDARY CONDITIONS (C) HEAT INPUT TO FACE
C     ********************************************************
C
      DO 140 N = 1,NHA
C
C     ********************************************************
C     IDENTIFY ELEMENT NODE POINTS
C     ********************************************************
C
      I = NOP(HA(N),1)
      J = NOP(HA(N),2)
      K = NOP(HA(N),3)
C
      XIJ = COORD(J,1) - COORD(I,1)
      XIK = COORD(K,1) - COORD(I,1)
      YIJ = COORD(J,2) - COORD(I,2)
      YIK = COORD(K,2) - COORD(I,2)
C
C     ********************************************************
C     CALCULATE ELEMENT AREA
C     ********************************************************
C
      AREA = ABS((XIJ*YIK - XIK*YIJ) / 2.0)
      QDD = QA(N)
      CM = (QDD*AREA) / 3.0
C
C     ********************************************************
C     FORM ELEMENT HEAT FLUX MATRIX
C     ********************************************************
C
      HQAE(1) = 1.0
      HQAE(2) = 1.0
      HQAE(3) = 1.0
C
```

```
      DO 145 M = 1,3
      HQAE(M) = CM*HQAE(M)
  145 CONTINUE
C
C     **********************************************************
C     ADD FACE ELEMENT HEAT INPUT MATRICES TO TOTAL
C     HEAT INPUT MATRIX (HQ)
C     **********************************************************
C
      HQ(I) = HQ(I) + HQAE(1)
      HQ(J) = HQ(J) + HQAE(2)
      HQ(K) = HQ(K) + HQAE(3)
C
  140 CONTINUE
C
  200 CONTINUE
C
C     **********************************************************
C     PRINT THERMAL STIFFNESS MATRIX AND HEAT INPUT MATRIX
C     **********************************************************
C
C
      WRITE (6,131)
  131 FORMAT (1H1,* HEAT STIFFNESS MATRIX *,////)
      DO 133 I = 1,NP
      WRITE (6,134) (HK(I,J),J = 1,NP)
  134 FORMAT (1H0,5X,10F10.4,//)
  133 CONTINUE
      WRITE (6,129)
  129 FORMAT (1H1,* HEAT INPUT MATRIX *,////)
      WRITE (6,132) (HQ(I),I = 1,NP)
  132 FORMAT (1H0,5X,10F10.4,//)
C
      RETURN
      END
```

Flow chart - subroutine <u>THETA</u>

```
          ╭─────────────────────╮
          │        Start         │
          ╰─────────────────────╯
                     │
                     ▼
          ┌─────────────────────┐
          │ Call equation solver │
          └─────────────────────┘
                     │
                     ▼
          ┌─────────────────────┐
          │ Print nodal temperatures │
          └─────────────────────┘
                     │
                     ▼
          ┌─────────────────────┐
     ┌───▶│   Loop on elements   │
     │    └─────────────────────┘
     │               │
     │               ▼
     │    ┌─────────────────────┐
     │    │      Determine       │
     │    │  element connections │
     │    └─────────────────────┘
     │               │
     │               ▼
     │    ┌─────────────────────┐
     │    │ Calculate mean element │
     │    │     temperatures     │
     │    └─────────────────────┘
     │               │
     │               ▼
     │    ┌─────────────────────┐
     └────│  End loop on elements │
          └─────────────────────┘
                     │
                     ▼
          ┌─────────────────────┐
          │  Print mean element  │
          │     temperatures     │
          └─────────────────────┘
                     │
                     ▼
          ┌─────────────────────┐
          │        Return        │
          └─────────────────────┘
```
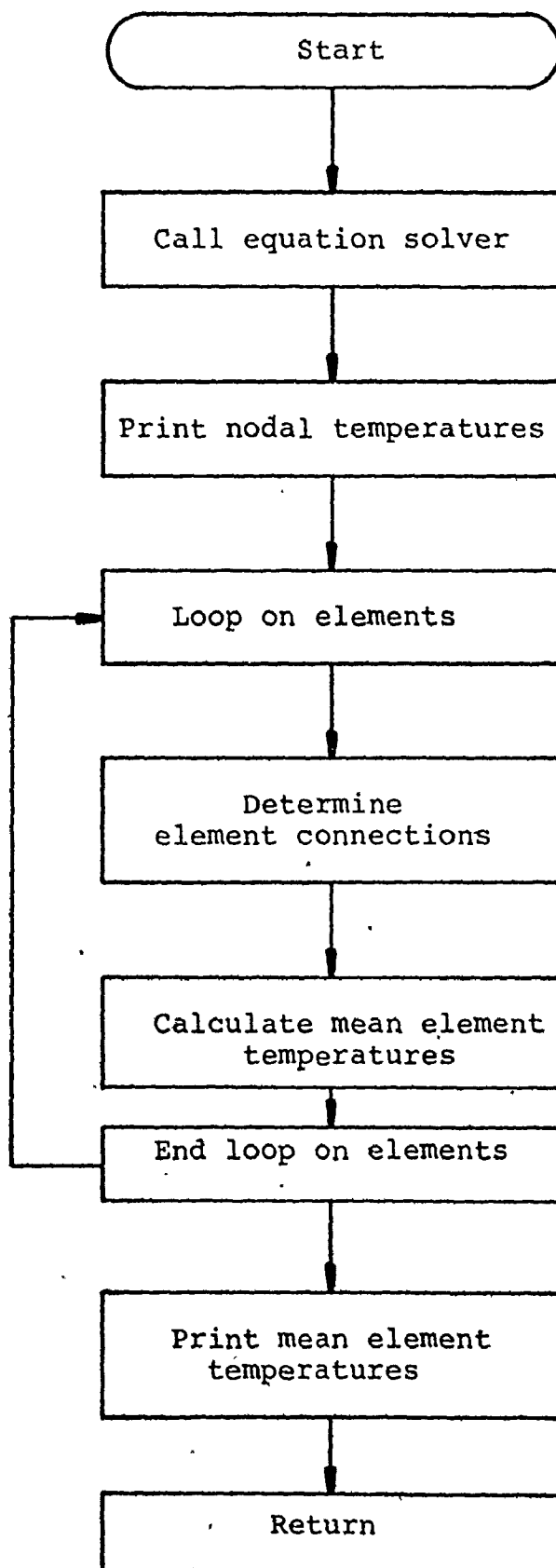
```
      SUBROUTINE THETA
C
      COMMON/CONTR1/TITLE(12),NP,NE,NMAT,NDF,NSZF,NCN,
     1 COORD(68,2),NOP(100,3),ORT(10,7),IMAT(100)
      COMMON/CONTR3/HK(68,68),GC(68,68),HQ(68),STEMP(100)
C
      DIMENSION HQW(68),HKW(68,68)
C
      INTEGER TITLE
      WRITE (6,5)
    5 FORMAT (1H1,50X,* RESULTS *,///,10X,*STEADY-STATE*,
     1* TEMPERATURE DISTRIBUTION *,///,10X,* NODE NO. *,10X,
     2* TEMPERATURE (DEG.F.) *,//)
C
      DO 10 I = 1,NP
      HQW(I) = HQ(I)
   10 CONTINUE
      DO 35 I = 1,NP
      DO 35 J = 1,NP
      HKW(I,J) = HK(I,J)
   35 CONTINUE
C
      CALL SOLVE (HKW,HQW,ID,NP,NP)
      DO 20 I = 1,NP
      WRITE (6,15) I,HQW(I)
   15 FORMAT (1H0,12X,I3,11X,F15.4,//)
   20 CONTINUE
C
      WRITE (6,25) ID
   25 FORMAT (1H1,26H DETERMINANT IS APPROX 2**,I3,//)
C
C     ***********************************************************
C     CALCULATE THE MEAN TEMPERATURE OF EACH ELEMENT
C     ***********************************************************
C
      WRITE (6,30)
   30 FORMAT(1H0,* ELEMENT (MEAN) TEMPERATURES *,////)
      DO 50 N = 1,NE
C
      I = NOP(N,1)
      J = NOP(N,2)
      K = NOP(N,3)
C
      STEMP(N) = (HQW(I) + HQW(J) + HQW(K)) / 3.0
C
   50 CONTINUE
      WRITE (6,40) (STEMP(N),N = 1,NE)
   40 FORMAT (1H0,10X,10F10.4,//)
C
      RETURN
      END
```

Flow chart - subroutine FORMK

```
                    ┌─────────────────────┐
                    │       Start         │
                    └─────────────────────┘
                               │
                               ▼
              ┌──────────────────────────────┐
              │    Zero stiffness matrix      │
              └──────────────────────────────┘
                               │
                               ▼
              ┌──────────────────────────────┐
    ┌────────▶│     Loop on elements          │
    │         └──────────────────────────────┘
    │                        │
    │                        ▼
    │         ┌──────────────────────────────┐
    │         │    Call element stiffness     │
    │         └──────────────────────────────┘
    │                        │
    │                        ▼
    │         ┌──────────────────────────────┐
    │         │  Store element stiffness      │
    │         │  in rectangular matrix        │
    │         └──────────────────────────────┘
    │                        │
    │                        ▼
    │         ┌──────────────────────────────┐
    └─────────│    End loop on elements       │
              └──────────────────────────────┘
                               │
                               ▼
              ┌──────────────────────────────┐
              │  Insert boundary conditions   │
              └──────────────────────────────┘
                               │
                               ▼
              ┌──────────────────────────────┐
              │          Return               │
              └──────────────────────────────┘
```
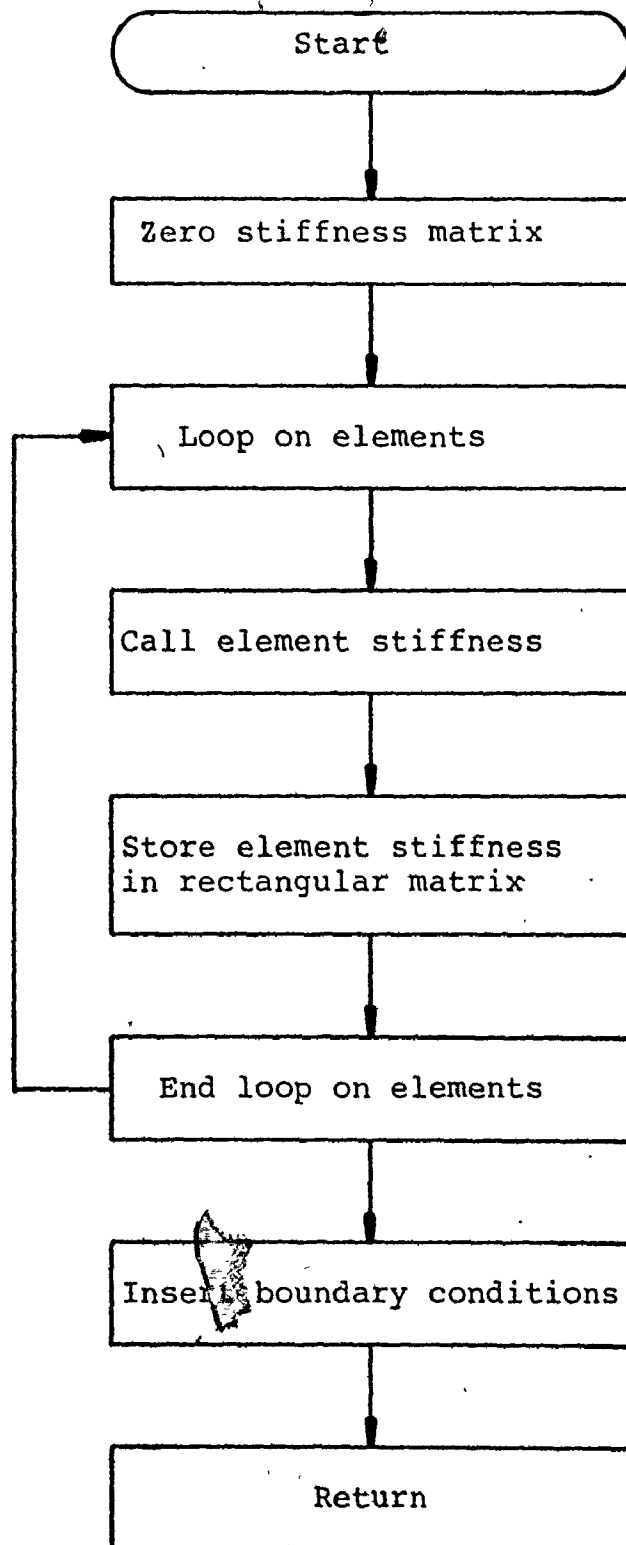
```
      SUBROUTINE FORMK
C
C     ****************************************************************
C     FORMS STIFFNESS MATRIX IN UPPER TRIANGULAR FORM
C     ****************************************************************
C
      COMMON/CONTR1/TITLE(12),NP,NE,NMAT,NDF,NSZF,NCN,
     1 COORD(68,2),NOP(100,3),ORT(10,7),IMAT(100)
      COMMON/CONTR4/SK(136,35),F(136),EK(6,6),NB,NBC(25),
     1 NFIX(25)
C
      INTEGER TITLE
C
      NBAND = 25
C
C     ****************************************************************
C     ZERO TERMS OF STIFFNESS MATRIX
C     ****************************************************************
C
      DO 5 N = 1,NSZF
      DO 5 M = 1,NBAND
      SK(N,M) = 0.0
    5 CONTINUE
C
C     SCAN ELEMENTS
C
      DO 100 N = 1,NE
      CALL STIFT2(N)
C
C     ****************************************************************
C     (EK) IS RETURNED AS ELEMENT STIFFNESS MATRIX AND STORED
C     IN (SK) , FIRST,
C                                        ROWS
C     ****************************************************************
C
      DO 50 JJ = 1,NCN
      NROWB = (NOP(N,JJ) - 1)*NDF
      DO 50 J = 1,NDF
      NROWB = NROWB + 1
      I = (JJ - 1)*NDF + J
C
C                          THEN COLUMNS
C
      DO 60 KK = 1,NCN
      NCOLB = (NOP(N,KK) - 1)*NDF
      DO 70 K = 1,NDF
      NCOL = NCOLB + K + 1 - NROWB
      L = (KK - 1)*NDF + K
C
C     SKIP STORING IF BELOW BAND
C
      IF        70,70,80
```

```
   80 SK(NROWB,NCOL) = SK(NROWB,NCOL) + EK(I,L)
C
   70 CONTINUE
C
C     END LOOP ON COLUMNS
C
   60 CONTINUE
C
C     END LOOP ON ROWS
C
   50 CONTINUE
C
C     END LOOP ON ELEMENTS
C
  100 CONTINUE
C
C     ****************************************************************
C     INSERT BOUNDARY CONDITIONS
C     ****************************************************************
C
      DO 200 N = 1,NB
      NX = 10**(NDF - 1)
      I = NBC(N)
      NROWB = (I - 1)*NDF
C
C     ****************************************************************
C     EXAMINE EACH DEGREE OF FREEDOM
C     ****************************************************************
C
      DO 190 M = 1,NDF
      NROWB = NROWB + 1
      ICON = NFIX(N) / NX
      IF (ICON) 180,180,150
  150 SK(NROWB,1) = 1.0
      DO 160 J = 2,NBAND
      SK(NROWB,J) = 0.0
      NR = NROWB + 1 - J
      IF (NR) 160,160,155
  155 SK(NR,J) = 0.0
  160 CONTINUE
      NFIX(N) = NFIX(N) - NX*ICON
  180 NX = NX / 10
  190 CONTINUE
  200 CONTINUE
C
      WRITE (6,250)
  250 FORMAT (1H1,10X,* STIFFNESS MATRIX (IN BAND FORM)
     1 LBS/FT.*,///)
      DO 310 I = 1,NSZF
      WRITE (6,300) (SK(I,J),J = 1,NBAND)
  300 FORMAT (1H0,10EI2.5,//)
  310 CONTINUE
C
      RETURN
```

Flow chart - subroutine <u>STIFT 2(N)</u>

```
                    ╭────────────────────╮
                    │       Start        │
                    ╰────────────────────╯
                              │
                              ▼
               ┌──────────────────────────────┐
               │   Locate nodal connections    │
               └──────────────────────────────┘
                              │
                              ▼
               ┌──────────────────────────────┐
               │  Calculate element dimensions │
               └──────────────────────────────┘
                              │
                              ▼
               ┌──────────────────────────────┐                      False
               │     Check for consistent      │──────────────────────►
               │         numbering             │                      │
               └──────────────────────────────┘                      ▼
                              │                              ┌─────────────┐
                           True                             │    Error    │
                              │                             │   message   │
                              ▼                             └─────────────┘
               ┌──────────────────────────────┐                      │
               │     Generate strain -         │                      ▼
               │     displacement matrix       │                  ╭───────╮
               └──────────────────────────────┘                  │ Stop  │
                              │                                   ╰───────╯
                              ▼
               ┌──────────────────────────────┐
               │     Generate stress -         │
               │       strain matrix           │
               └──────────────────────────────┘
                              │
                              ▼
               ┌──────────────────────────────┐
               │     Calculate element         │
               │     stiffness matrix          │
               └──────────────────────────────┘
                              │
                              ▼
               ┌──────────────────────────────┐
               │          Return               │
               └──────────────────────────────┘
```
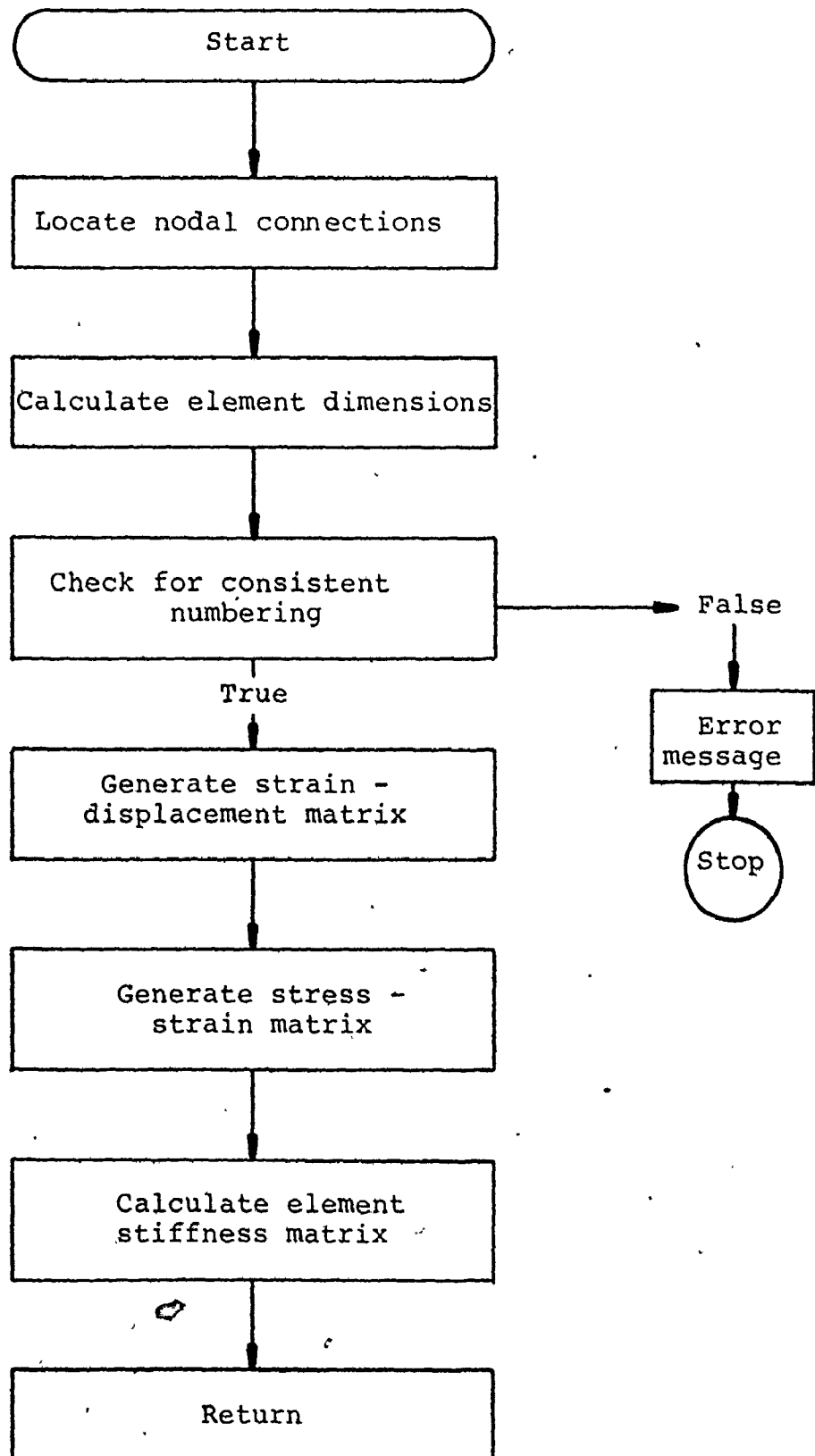
```fortran
      SUBROUTINE STIFT2(N)
C
      COMMON/CONTR1/TITLE(12),NP,NE,NMAT,NDF,NSZF,NCN,
     1 COORD(68,2),NOP(100,3),ORT(10,7),IMAT(100)
      COMMON/CONTR4/SK(136,35),F(136),EK(6,6),NB,NBC(25),
     1 NFIX(25)
C
      DIMENSION B(3,6),D(3,3),BT(6,3),BTD(6,3)
C
      INTEGER TITLE
C
C     *********************************************************************
C     IDENTIFY NODE POINTS
C     *********************************************************************
C
      I = NOP(N,1)
      J = NOP(N,2)
      K = NOP(N,3)
      L = IMAT(N)
C
C     *********************************************************************
C     SET UP LOCAL COORDINATE SYSTEM
C     *********************************************************************
C
      XIJ = COORD(J,1) - COORD(I,1)
      XIK = COORD(K,1) - COORD(I,1)
      YIJ = COORD(J,2) - COORD(I,2)
      YIK = COORD(K,2) - COORD(I,2)
C
      AREA = (XIJ*YIK - XIK*YIJ) / 2.0
      IF (AREA .LE. 0.0) GO TO 100
C
C     *********************************************************************
C     FORM ELEMENT STRAIN-DISPLACEMENT MATRIX
C     *********************************************************************
C
      B(1,1) = YIJ - YIK
      B(1,2) = 0.0
      B(1,3) = YIK
      B(1,4) = 0.0
      B(1,5) = -YIJ
      B(1,6) = 0.0
      B(2,1) = 0.0
      B(2,2) = XIK - XIJ
      B(2,3) = 0.0
      B(2,4) = -XIK
      B(2,5) = 0.0
      B(2,6) = XIJ
      B(3,1) = XIK - XIJ
      B(3,2) = YIJ - YIK
      B(3,3) = -XIK
      B(3,4) = YIK
      B(3,5) = XIJ
      B(3,6) = -YIJ
```

```
C
      DO 5 II = 1,3
      DO 5 JJ = 1,6
      B(II,JJ) = (1.0/(2.0*AREA))*B(II,JJ)
    5 CONTINUE
C
C     ******************************************************************
C     FORM STRESS-STRAIN MATRIX (PLANE STRESS)
C     ******************************************************************
C
      D(1,1) = 1.0
      D(1,2) = ORT(L,4)
      D(1,3) = 0.0
      D(2,1) = D(1,2)
      D(2,2) = D(1,1)
      D(2,3) = 0.0
      D(3,1) = 0.0
      D(3,2) = 0.0
      D(3,3) = (1.0 -ORT(L,4)) / 2.0
C
      CM = ORT(L,6) / (1.0 - ORT(L,4)**2)
C
      DO 10 II = 1,3
      DO 10 JJ = 1,3
      D(II,JJ) = CM*D(II,JJ)
   10 CONTINUE
C
C     ******************************************************************
C     FORM THE ELEMENT STIFFNESS MATRIX (EK)
C     ******************************************************************
C
      CALL MTRA (B,BT,3,6,0)
C
      CALL MPRD (BT,D,BTD,6,3,0,0,3)
      CALL MPRD (BTD,B,EK,6,3,0,0,6)
C
      T = ORT(L,7)
      DO 15 II = 1,6
      DO 15 JJ = 1,6
      EK(II,JJ) = T*AREA*EK(II,JJ)
   15 CONTINUE
C
      RETURN
C
  100 WRITE (6,125) N
  125 FORMAT (1H1,* ZERO OR NEGATIVE AREA ELEMENT NO. *,I4,//,
     1 40X,* EXECUTION TERMINATED *,//)
      STOP
      END
```

Flow chart - subroutine LOAD
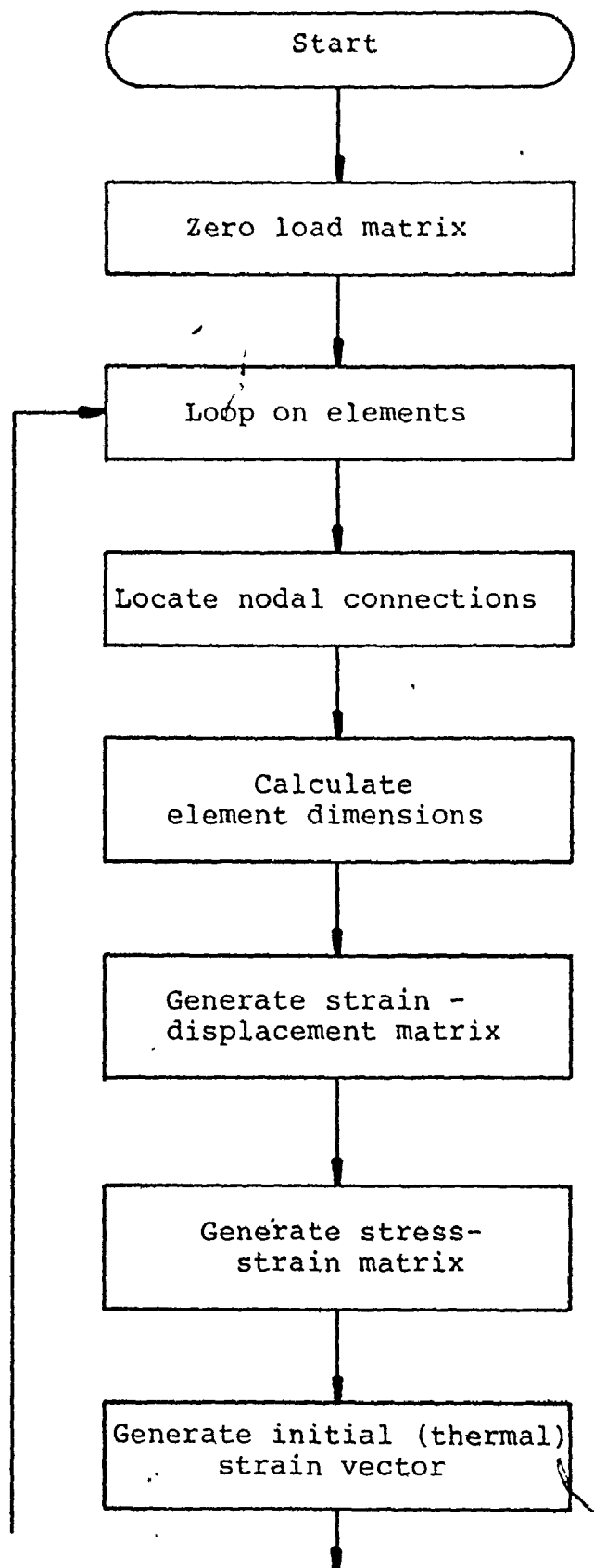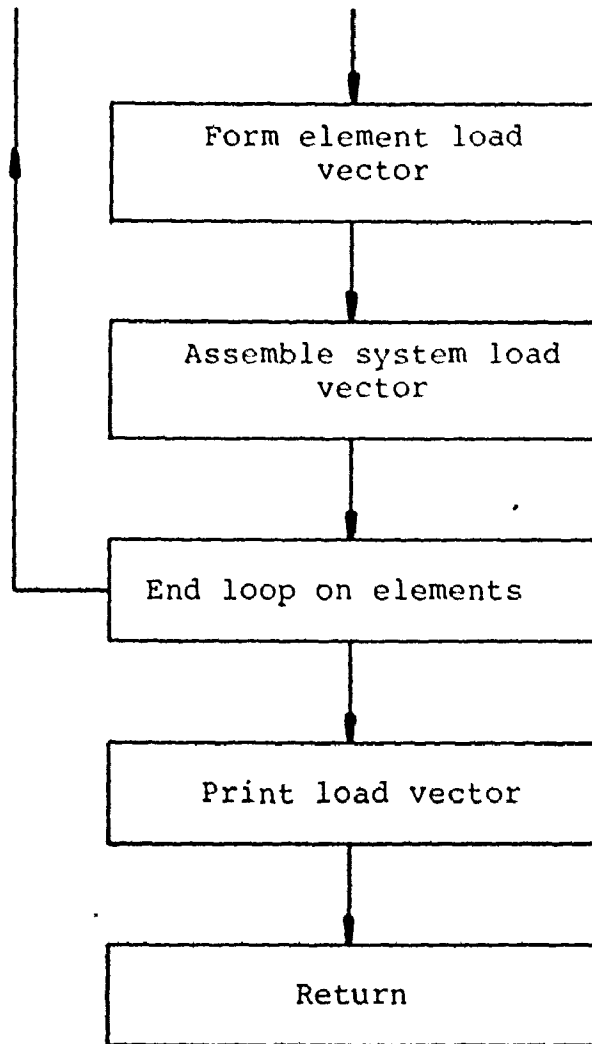
```
                    ╭────────────────────╮
                    │       Start        │
                    ╰────────────────────╯
                              │
                              ▼
                    ┌────────────────────┐
                    │  Zero load matrix  │
                    └────────────────────┘
                              │
                              ▼
          ┌───────▶┌────────────────────┐
          │        │  Loop on elements  │
          │        └────────────────────┘
          │                   │
          │                   ▼
          │        ┌────────────────────────┐
          │        │Locate nodal connections│
          │        └────────────────────────┘
          │                   │
          │                   ▼
          │        ┌────────────────────┐
          │        │     Calculate      │
          │        │ element dimensions │
          │        └────────────────────┘
          │                   │
          │                   ▼
          │        ┌────────────────────┐
          │        │  Generate strain - │
          │        │ displacement matrix│
          │        └────────────────────┘
          │                   │
          │                   ▼
          │        ┌────────────────────┐
          │        │  Generate stress-  │
          │        │   strain matrix    │
          │        └────────────────────┘
          │                   │
          │                   ▼
          │        ┌────────────────────────────┐
          │        │Generate initial (thermal)  │
          │        │      strain vector         │
          │        └────────────────────────────┘
          │                   │
          │                   ▼
```

```
        ┌─────────────────────────┐
        │   Form element load     │
        │        vector           │
        └─────────────────────────┘
                    │
                    ▼
        ┌─────────────────────────┐
        │  Assemble system load   │
        │        vector           │
        └─────────────────────────┘
                    │
                    ▼
        ┌─────────────────────────┐
        │  End loop on elements   │
        └─────────────────────────┘
                    │
                    ▼
        ┌─────────────────────────┐
        │   Print load vector     │
        └─────────────────────────┘
                    │
                    ▼
        ┌─────────────────────────┐
        │        Return           │
        └─────────────────────────┘
```

```
      SUBROUTINE LOAD
C
      COMMON/CONTR1/TITLE(12),NP,NE,NMAT,NDF,NSZF,NCN,
     1 COORD(68,2),NOP(100,3),ORT(10,7),IMAT(100)
      COMMON/CONTR3/HK(68,68),CC(68,68),HQ(68),STEMP(100)
      COMMON/CONTR4/SK(136,25),F(136),FK(6,6),NB,NBC(25),
     1 NFIX(25)
C
      DIMENSION B(3,6),D(3,3),BT(6,3),BTD(6,3),FE(6),E(3)
C
      INTEGER TITLE
C
      NSZF = NDF*NP
C
C     ***********************************************************
C     ZERO LOAD ARRAY
C     ***********************************************************
C
      DO 50 J = 1,NSZF
      F(J) = 0.0
   50 CONTINUE
C
      DO 100 N = 1,NE
C
C     ***********************************************************
C     IDENTIFY ELEMENT NODES
C     ***********************************************************
C
      I = NOP(N,1)
      J = NOP(N,2)
      K = NOP(N,3)
C
      L = IMAT(N)
C
C     ***********************************************************
C     SET UP LOCAL COORDINATE SYSTEM
C     ***********************************************************
C
      XIJ = COORD(J,1) - COORD(I,1)
      XIK = COORD(K,1) - COORD(I,1)
      YIJ = COORD(J,2) - COORD(I,2)
      YIK = COORD(K,2) - COORD(I,2)
C
      AREA = ABS((XIJ*YIK - XIK*YIJ) / 2.0)
C
C     ***********************************************************
C     FORM ELEMENT STRAIN-DISPLACEMENT MATRIX
C     ***********************************************************
```

```fortran
C
      B(1,1) = YIJ - YIK
      B(1,2) = 0.0
      B(1,3) = YIK
      B(1,4) = 0.0
      B(1,5) = -YIJ
      B(1,6) = 0.0
      B(2,1) = 0.0
      B(2,2) = XIK - XIJ
      B(2,3) = 0.0
      B(2,4) = -XIK
      B(2,5) = 0.0
      B(2,6) = XIJ
      B(3,1) = XIK - XIJ
      B(3,2) = YIJ - YIK
      B(3,3) = -XIK
      B(3,4) = YIK
      B(3,5) = XIJ
      B(3,6) = -YIJ
C
      DO 5 II = 1,3
      DO 5 JJ = 1,6
      B(II,JJ) = (1.0/(2.0*AREA))*B(II,JJ)
    5 CONTINUE
C
C     ************************************************************
C     FORM STRESS-STRAIN MATRIX
C     ************************************************************
C
      D(1,1) = 1.0
      D(1,2) = ORT(L,4)
      D(1,3) = 0.0
      D(2,1) = D(1,2)
      D(2,2) = D(1,1)
      D(2,3) = 0.0
      D(3,1) = 0.0
      D(3,2) = 0.0
      D(3,3) = (1.0 - ORT(L,4)) / 2.0
C
      CM = ORT(L,6) / (1.0 - ORT(L,4)**2)
C
      DO 10 II = 1,3
      DO 10 JJ = 1,3
      D(II,JJ) = CM*D(II,JJ)
   10 CONTINUE
C
C     ************************************************************
C     FORM ELEMENT INITIAL (I.E. THERMAL ) STRAIN VECTOR
C     ************************************************************
C
```

```
      ALPHA = ORT(L,5)
C
      E(1) = STEMP(N)*ALPHA
  F   E(2) = STEMP(N)*ALPHA
      E(3) = 0.0
C
C     ****************************************************************
C     FORM TRANSPOSE OF (B) I.E. (BT)
C
C     ****************************************************************
C
      CALL MTRA(B,BT,3,6,0)                      .
C
C     ****************************************************************
C     FORM MATRIX PRODUCT (BT)*(D) = (BTD)
C     ****************************************************************
C
      CALL MPRD(BT,D,BTD,6,3,0,0,3)
C
C     ****************************************************************
C     FORM ELEMENT FORCE VECTOR
C     ****************************************************************
C
      CALL MPRD(BTD,E,FE,6,3,0,0,1)
      T = ORT(L,7)
      DO 20 II = 1,6
      FE(II) =   FE(II)*T*AREA
   20 CONTINUE
C
C     ****************************************************************
C     ASSEMBLE GLOBAL FORCE VECTOR
C     ****************************************************************
C
      IU = 2*I - 1
      IV = IU + 1
      JU = 2*J - 1
      JV = JU + 1
      KU = 2*K - 1
      KV = KU + 1
C
      F(IU) = F(IU) + FE(1)
      F(IV) = F(IV) + FE(2)
      F(JU) = F(JU) + FE(3)
      F(JV) = F(JV) + FE(4)
      F(KU) = F(KU) + FE(5)
      F(KV) = F(KV) + FE(6)
C
  100 CONTINUE
C
      WRITE (6,120)
  120 FORMAT (1H0,10X,* THERMAL FORCE VECTOR (LBS)*,//A/)
      WRITE (6,125) (F(N),N = 1,NSZF)
  125 FORMAT (1H0,10E12.5,//)
C
      RETURN
```

Flow chart - subroutine <u>SOLSYM</u>

```
                    ┌──────────────────────────┐
                    │          Start           │
                    └──────────────────────────┘
                                 │
                                 ▼
     ┌──────────────────────────────────────────────────┐
  ┌─▶│            Loop on each equation                  │
  │  └──────────────────────────────────────────────────┘
  │                              │
  │                              ▼
  │  ┌──────────────────────────────────────────────────┐
  │  │   Compute modifications to stiffness              │
  │  │          matrix and reduce                        │
  │  └──────────────────────────────────────────────────┘
  │                              │
  │                              ▼
  │  ┌──────────────────────────────────────────────────┐
  └──│           End loop on equations                   │
     └──────────────────────────────────────────────────┘
                                 │
                                 ▼
     ┌──────────────────────────────────────────────────┐
  ┌─▶│            Loop on each equation                  │
  │  └──────────────────────────────────────────────────┘
  │                              │
  │                              ▼
  │  ┌──────────────────────────────────────────────────┐
  │  │            Modify load vector                     │
  │  └──────────────────────────────────────────────────┘
  │                              │
  │                              ▼
  │  ┌──────────────────────────────────────────────────┐
  └──│           End loop on equations                   │
     └──────────────────────────────────────────────────┘
                                 │
                                 ▼
  ┌─▶┌──────────────────────────────────────────────────┐
  │  │      Loop backwards on each equation              │
  │  └──────────────────────────────────────────────────┘
  │                              │
  │                              ▼
```

```
┌─────────────────────────────────────────┐
│  Back substitution for equation solution │
└─────────────────────────────────────────┘

┌─────────────────────────────────────────┐
│         End loop on equations            │
└─────────────────────────────────────────┘

┌─────────────────────────────────────────┐
│                 Return                   │
└─────────────────────────────────────────┘
```
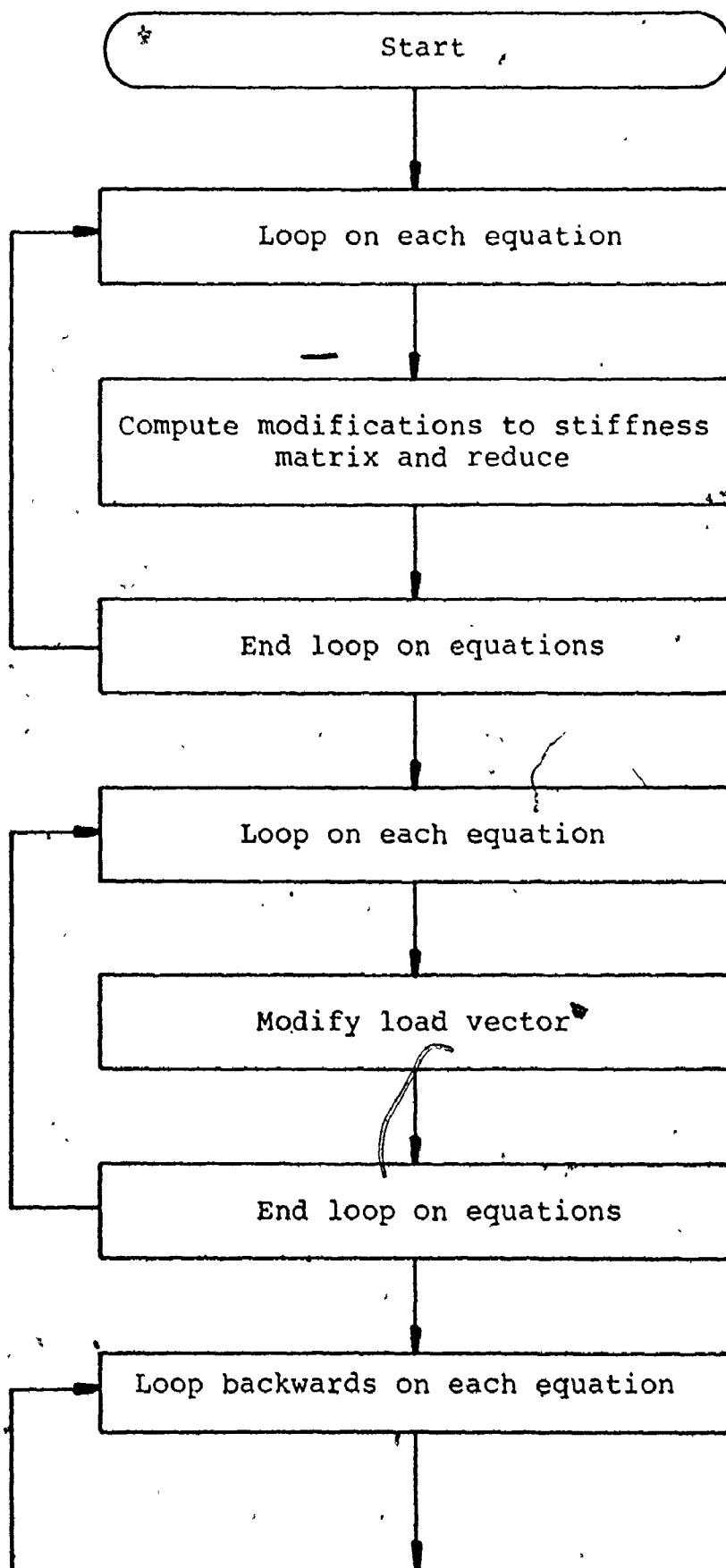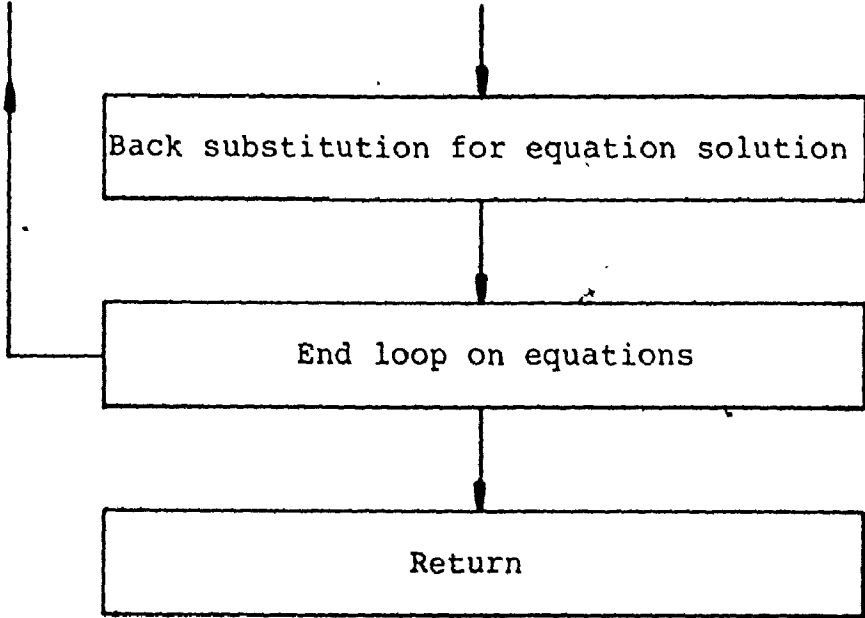
```
      SUBROUTINE SOLSYM
C
      COMMON/CONTR1/TITLE(12),NP,NE,NMAT,NDF,NSZF,NCN,
     1 COORD(68,2),NOP(100,3),ORT(10,7),IMAT(100)
      COMMON/CONTR4/SK(136,35),F(136),EK(6,6),NB,NBC(25),
     1 NFIX(25)
C
      DIMENSION SKW(136,35)
C
      INTEGER TITLE
C
      NBAND = 25
C
      DO 100 I = 1,NSZF
      DO 100 J = 1,NBAND
      SKW(I,J) = SK(I,J)
  100 CONTINUE
C
C     ****************************************************************
C     REDUCE MATRIX
C     ****************************************************************
C
      DO 280 N = 1,NSZF
      DO 270 L = 2,NBAND
      IF (SKW(N,L) .EQ. 0.0) GO TO 270
      C = SKW(N,L) / SKW(N,1)
      I = N + L - 1
      IF (NSZF - I) 260,240,240
  240 J = 0
      DO 250 K = L,NBAND
      J = J + 1
  250 SKW(I,J) = SKW(I,J) - C*SKW(N,K)
  260 SKW(N,L) = C
  270 CONTINUE
  280 CONTINUE
C
C     ****************************************************************
C     REDUCE LOAD VECTOR FOR EACH EQUATION
C     ****************************************************************
C
      DO 290 N = 1,NSZF
      DO 285 L = 2,NBAND
      I = N + L - 1
      IF (NSZF - I) 290,285,285
  285 F(I) = F(I) - SKW(N,L)*F(N)
  290 F(N) = F(N) / SKW(N,1)
C
C     ****************************************************************
C     BACK SUBSTITUTION
C     N.B. LOAD VECTOR (F) BECOMES FINALLY THE SOLN. VECTOR
C     ****************************************************************
```

```
      N = NSZF
  300 N = N - 1
      IF (N) 350,500,350
  350 DO 400 K = 2,NBAND
      L = N + K - 1
      IF (NSZF - L) 400,370,370
  370 F(N) = F(N) - SKW(N,K)*F(L)
  400 CONTINUE
      GO TO 300
C
  500 RETURN
      END
```

Flow chart - subroutine <u>DISPL</u>

```
      ╭─────────────────────────╮
      │          Start          │
      ╰─────────────────────────╯
                   │
                   ▼
      ┌─────────────────────────┐
      │ Print nodal displacements│
      └─────────────────────────┘
                   │
                   ▼
      ┌─────────────────────────┐
      │         Return          │
      └─────────────────────────┘
```

```
      SUBROUTINE DISPL
C
      COMMON/CONTR1/TITLE(12),NP,NE,NMAT,NDF,NSZF,NCN,
     1 COORD(68,2),NOP(100,3),ORT(10,7),IMAT(100)
      COMMON/CONTR4/SK(136,35),F(136),EK(6,6),NB,NBC(25),
     1 NFIX(25)
C
      DIMENSION DIS(2,68)
C
      INTEGER TITLE
C
      EQUIVALENCE (DIS(1),F(1))
C
C     ************************************************************
C     PRINT DISPLACEMENTS
C     ************************************************************
C
      WRITE (6,10)
   10 FORMAT (1H1,40X,* NODE NO. *,20X,
     1 * DISPLACEMENTS (INS) ,///,70X,* X *,11X,* Y *,///)
     1 70X,* X *,11X,* Y *,///)
      DO 15 M = 1,NP
      DO 15 J = 1,NDF
      DIS(J,M) = DIS(J,M) * 12.0
   15 CONTINUE
C
      DO 30 I = 1,NSZF
      EPS = ABS(DIS(I))
      IF (EPS .LT. 1.0E-06) GO TO 25
      GO TO 30
   25 DIS(I) = 0.0
   30 CONTINUE
C
      WRITE (6,20) (M,(DIS(J,M),J = 1,NDF),M = 1,NP)
   20 FORMAT (1H0,41X,I5,18X,F10.6,2X,F10.6,//)
C
      RETURN
      END
```

Flow chart - Subroutine <u>TRANS</u>

```
                    ┌──────────────────────────┐
                    │          Start           │
                    └──────────────────────────┘
                                 │
                                 ▼
                        ╱─────────────────╲
                       ╱    IS ITER > 1    ╲──────────────┐
                       ╲                   ╱              │
                        ╲─────────────────╱               │
                                 │ No                     │ Yes
                                 ▼                        │
                    ┌──────────────────────────┐          │
                    │  Call for  capacity matrix│         │
                    └──────────────────────────┘          │
                                 │                        │
                                 ▼                        │
                    ┌──────────────────────────┐          │
                    │ Zero nodal temperature array│◄──────┘
                    └──────────────────────────┘
                                 │
                                 ▼
                    ┌──────────────────────────┐
                    │ Zero element temperature array│
                    └──────────────────────────┘
                                 │
                                 ▼
                    ┌──────────────────────────┐
                    │Modify thermal stiffness matrix│
                    └──────────────────────────┘
                                 │
                                 ▼
                    ┌──────────────────────────┐
                    │ Modify heat input matrix for │
                    │      time increment          │
                    └──────────────────────────┘
                                 │
                                 ▼
                    ┌──────────────────────────┐
                    │   Call equation solver    │
                    └──────────────────────────┘
                                 │
                                 ▼
```

```
         ┌─────────────────────────────┐
         │      Loop on elements       │
         └─────────────────────────────┘
                       │
                       ▼
         ┌─────────────────────────────┐
         │     Determine element       │
         │        connections          │
         └─────────────────────────────┘
                       │
                       ▼
         ┌─────────────────────────────┐
         │     Determine element       │
         │     mean temperatures       │
         └─────────────────────────────┘
                       │
                       ▼
         ┌─────────────────────────────┐
         │     End loop on elements    │
         └─────────────────────────────┘
                       │
                       ▼
         ┌─────────────────────────────┐
         │   Print mean temperatures   │
         └─────────────────────────────┘
                       │
                       ▼
         ┌─────────────────────────────┐
         │           Return            │
         └─────────────────────────────┘
```

```
      SUBROUTINE TRANS
C
C     ****************************************************************
C     TO SOLVE FOR TRANSIENT TEMPERATURES USING THE
C     CRANK - NICOLSON METHOD
C     ****************************************************************
C
      COMMON/CONTR1/TITLE(12),NP,NE,NMAT,NDF,NSZF,NCN,
     1 COORD(68,2),NOP(100,3),ORT(10,7),IMAT(100)
      COMMON/CONTR3/HK(68,68),GC(68,68),HQ(68),STEMP(100)
      COMMON MAXIT,DT,ITER
C
      DIMENSION HKBR(68,68),HQI(68),GCTV(68),TV(68),TVP1(68)
      DIMENSION TI(68),HQV(68),HQV1(68)
C
      INTEGER TITLE
C
      IF (ITER .GT. 1) GO TO 30
C
C     ****************************************************************
C     FORM GLOBAL CAPACITANCE MATRIX (GC)
C     ****************************************************************
C
      CALL CAPT
      WRITE (6,5)
    5 FORMAT (1H1,30X,* TRANSIENT TEMPERATURE   (DEG.F.)*,/////)
C
C     ZERO NODAL TEMPERATURE ARRAY FOR INITIAL CONDITIONS
C
      DO 10 I = 1,NP
      TV(I) = 0.0
   10 CONTINUE
C
C     ZERO ELEMENT TEMPERATURE ARRAY FOR INITIAL CONDITIONS
C
      DO 15 I = 1,NE
      STEMP(I) = 0.0
   15 CONTINUE
C
      TM = DT
      TIME = TM
C
      DO 12 I = 1,NP
      HQV1(I) = HQ(I)
      HQV(I) = HQ(I)
   12 CONTINUE
C
   30 CONTINUE
      CALL MPRD(GC,TV,GCTV,NP,NP,0,0,1)
      DO 25 I = 1,NP
              0 =      I)          V1(I) + (2.0/TM)*GCTV(I)
```
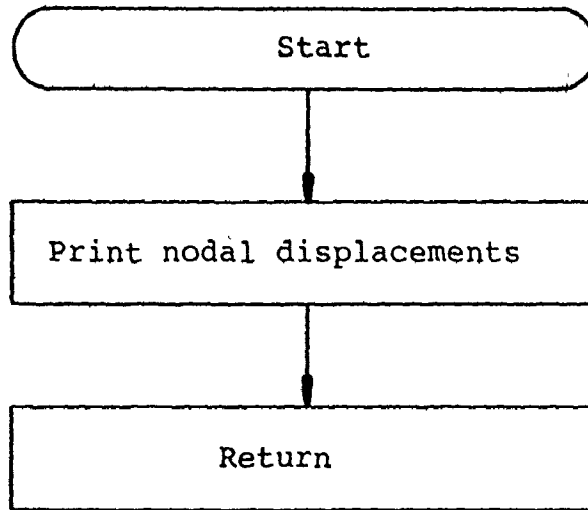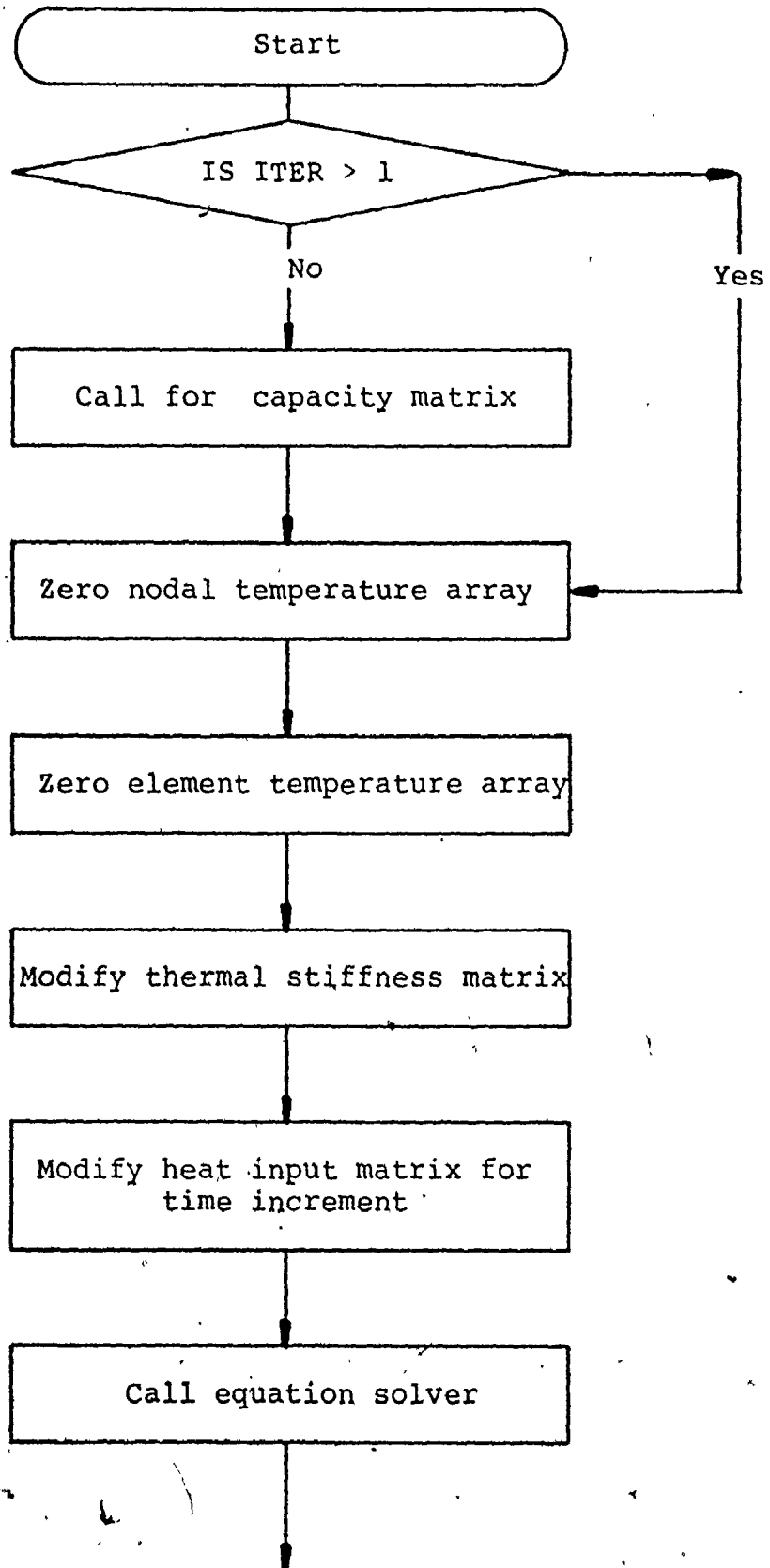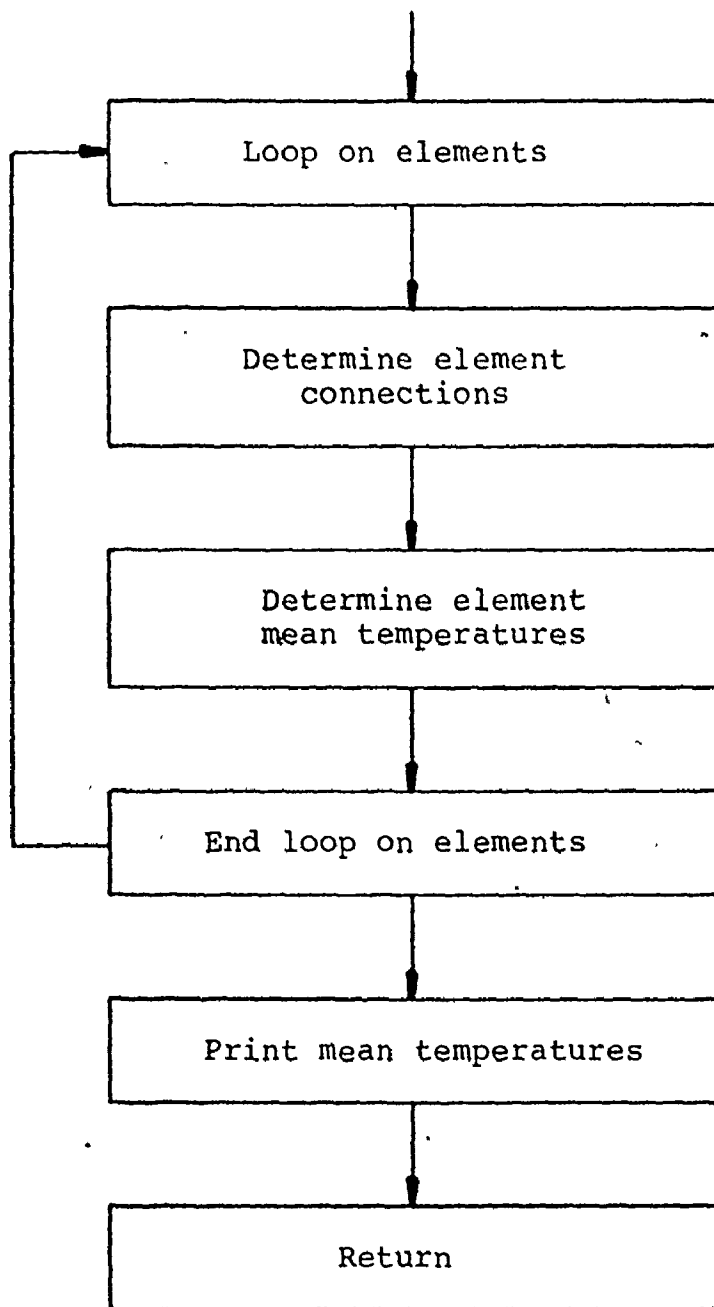
```
C
      DO 20 I = 1,NP
      DO 20 J = 1,NP
      HKBR(I,J) = HK(I,J) + (2.0/TM)*(GC(I,J))
   20 CONTINUE
C
      DO 70 I = 1,NP
      HQV(I) = HQV1(I)
   70 CONTINUE
C
C     ****************************************************************
C     SOLVE FOR TEMPERATURES AT TIME 'T'  N.B.  (HQI) IS
C     FINALLY THE SOLUTION VECTOR
C     ****************************************************************
C
      CALL SOLVE (HKBR ,HQI,ID,NP,NP)
C
      WRITE (6,45) ID
   45 FORMAT (1H0,26H DETERMINANT IS APPROX 2**,I5,/////)
      DO 50 I = 1,NP
      TI(I) = HQI(I)
   50 CONTINUE
C
      DO 35 I = 1,NP
      TVP1(I) = 2.0*TI(I) - TV(I)
   35 CONTINUE
      DO 40 I = 1,NP
      TV(I) = TVP1(I)
   40 CONTINUE
C
      WRITE (6,80) TIME
   80 FORMAT (1H0,* NODE TEMPERATURES AT TIME = *,F10.2,//)
      WRITE(6,65) (TV(I),I = 1,NP)
C
      DO 55 N = 1,NE
C
      I = NOP(N,1)
      J = NOP(N,2)
      K = NOP(N,3)
C
      STEMP(N) = (TV(I) + TV(J) + TV(K)) / 3.0
C
   55 CONTINUE
      WRITE (6,60) TIME
   60 FORMAT (1H0,* ELEMENT MEAN TEMPERATURES AT TIME = *,
     1 F10.2,//)
      WRITE (6,65) (STEMP(N),N = 1,NE)
   65 FORMAT (1H0,10X,10F10.4,//)
C
      TIME = TIME + TM
C
```

Flow chart - subroutine CAPT

```
                    ┌──────────────────────┐
                    │        Start         │
                    └──────────────────────┘
                               │
            ┌─────────────►┌──────────────────────┐
            │              │   Loop on elements   │
            │              └──────────────────────┘
            │                       │
            │              ┌──────────────────────┐
            │              │ Locate nodal connections │
            │              └──────────────────────┘
            │                       │
            │              ┌──────────────────────┐
            │              │     Form element     │
            │              │  capacitance matrix  │
            │              └──────────────────────┘
            │                       │
            │              ┌──────────────────────┐
            │              │   Generate global    │
            │              │  capacitance matrix  │
            │              └──────────────────────┘
            │                       │
            │              ┌──────────────────────┐
            └──────────────│ End loop on elements │
                           └──────────────────────┘
                                    │
                           ┌──────────────────────┐
                           │        Return        │
                           └──────────────────────┘
```
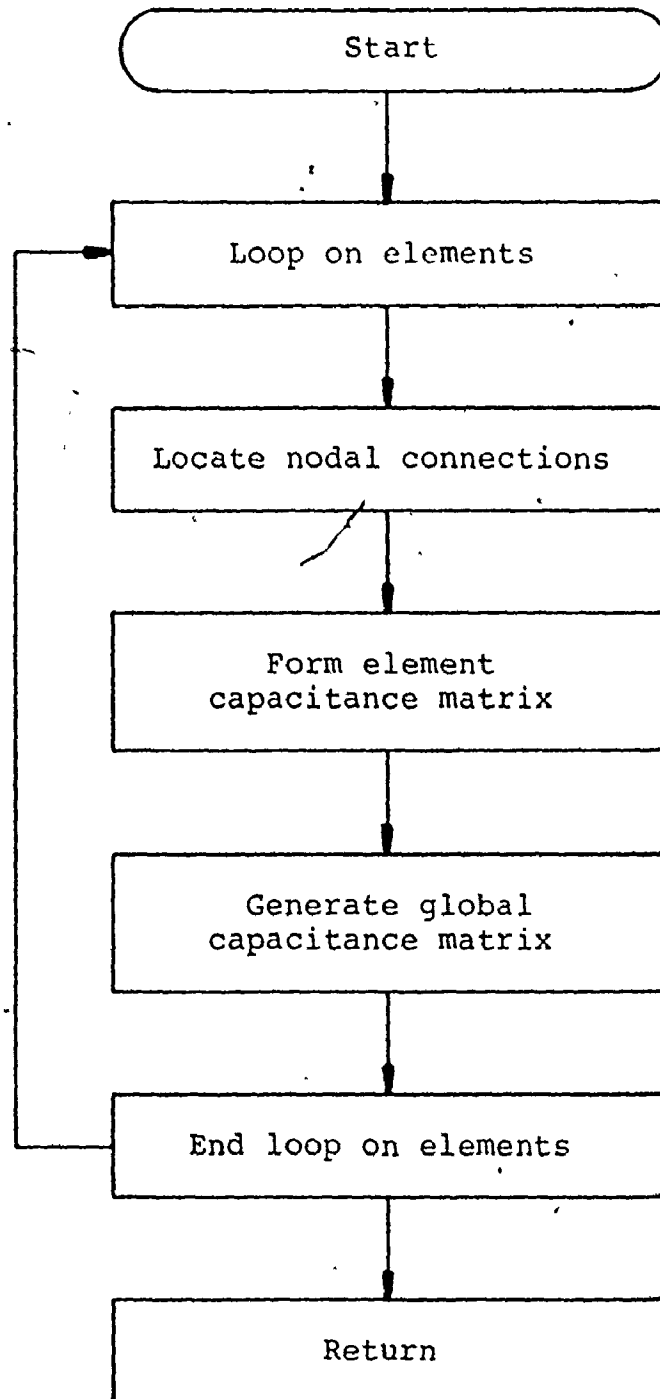
```
      SUBROUTINE CAPT
C
      COMMON/CONTR1/TITLE(12),NP,NE,NMAT,NDF,NSZF,NCN,
     1 COORD(68,2),NOP(100,3),ORT(10,7),IMAT(100)
      COMMON/CONTR3/HK(68,68),GC(68,68),HQ(68),STFMP(100)
C
      DIMENSION EC(3,3)
C
      INTEGER TITLE
C
      DO 1 I = 1,NP
      DO 1 J = 1,NP
      GC(I,J) = 0.0
    1 CONTINUE
C
      DO 20 N = 1,NE
C
C     ****************************************************************
C     IDENTIFY NODE POINTS
C     ****************************************************************
C
      I = NOP(N,1)
      J = NOP(N,2)
      K = NOP(N,3)
C
      L = IMAT(N)
C
      XIJ = COORD(J,1) - COORD(I,1)
      XIK = COORD(K,1) - COORD(I,1)
      YIJ = COORD(J,2) - COORD(I,2)
      YIK = COORD(K,2) - COORD(I,2)
C
C     ****************************************************************
C     CALCULATE THE AREA OF THE ELEMENT
C     ****************************************************************
C
      AREA = ABS((XIJ*YIK - XIK*YIJ) / 2.0)
      RHO = ORT(L,2)
      CP = ORT(L,3)
      T = ORT(L,7)
C
      CM = (RHO*CP*AREA*T) / 12.0
C
C     ****************************************************************
C     FORM THE ELEMENT CAPACITANCE MATRIX (EC)
C     ****************************************************************
C
      DO 5 II = 1,3
      DO 5 JJ = 1,3
      EC(II,JJ) = 0.0
    5
```

APPENDIX D

AN AXIS OF ROTATION ANALYSER

D 1   Design of the Master Ball Holder

The master ball is attached by epoxy to the
end of the Master Ball Holder as seen in Plate XI- A,
pg. 360. The "wobble-plate" design permits the cen-
tering of the ball to be achieved by the adjustment
of the two sets of diametrically opposed fine-thread
screws. It is practically possible to minimise the
eccentricity of the ball to approximately 0.0001 in.,
the effect of this residual eccentricity being removed
by the use of the compensating circuitry incorporated
in the instrument design.

D 2   Design of the Pick-up and Synchro Resolver Holder

A view of this combined unit is seen in Plate
XI -B, pg. 360 .

While the rotor of the synchro may be attached
to the rear of the spindle utilising some suitable
fixture, since the rear of the spindle is not always
accessible and also since the design of a versatile
and quite general fixture would be difficult to
achieve, it has been found practical to incorporate

provision for the synchro resolver in a common
rigid fixture together with the capacitance pick-ups,
the rotor of the synchro now being directly coupled
to the rotating master ball. It is necessary to
devise a linkage however such that the influence of
noise is minimal. Naturally, this set-up excludes the
possibility of measuring and depicting axial error
motion on a polar form of graph, however an alternative
procedure here may be to record the error on a time
base record if we still wish to avoid connecting the
rotor of the synchro to the rear of the spindle.

The resolver type and primary characteristics
are as follows:

Vector Resolver: CVH-10-AS-1

(available from Clifton Precision,

Litton Industries).

length: 1.24 ins.

weight: 2 oz.

rotor moment of inertia: 1.2 gm - cm^2
[N.B. while the resolver is manufactured for primary
voltage excitation at 400 Hz, there is no problem to
its functioning at the 5KHz excitation frequency, as
in its application in the Axis of Rotation Analyser]

D 3   Axis of Rotation Analyser - Circuit Diagrams

Detail of the required instrument front panel

controls and an interior view of the instrument are shown in Plate X, pg 359.

The circuit diagrams are as follows:

(i)   Card Interconnections (1 of 2)

(ii)   Card Interconnections (2 of 2)

(iii)   Cards 1,2 : Post Wayne - Kerr

(iv)   Card 3   : Special Board

(v)   Card 4   : Z - Modulation

(vi)   Cards 5,6 : Filters

(vii)   Card 7   : Multiplier

(viii) Card 8,9   : Demodulators

(ix)   Card 10   : Vector Resolver

(x)   Card 11   : Oscillator

(xi)   ± 15V Power Supply

NOTES   1) If a measurement of radial error motion in boring is required where the circle is to be generated by the offset of the master ball, Special Card 3' (see 'Card Interconnection 2 of 2) is to be substituted for the standard Card 3.

2) The filter on the left hand side of the Post Wayne - Kerr Card circuitry is equivalent to the Wayne Kerr F731A Filter and this portion of circuitry is therefore optional.
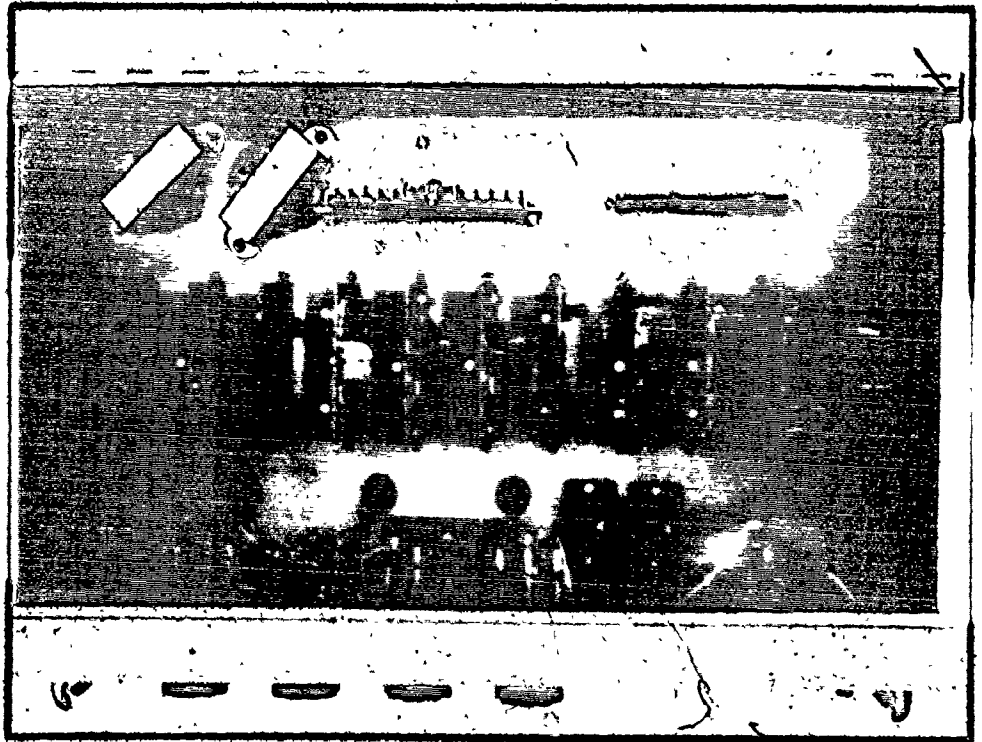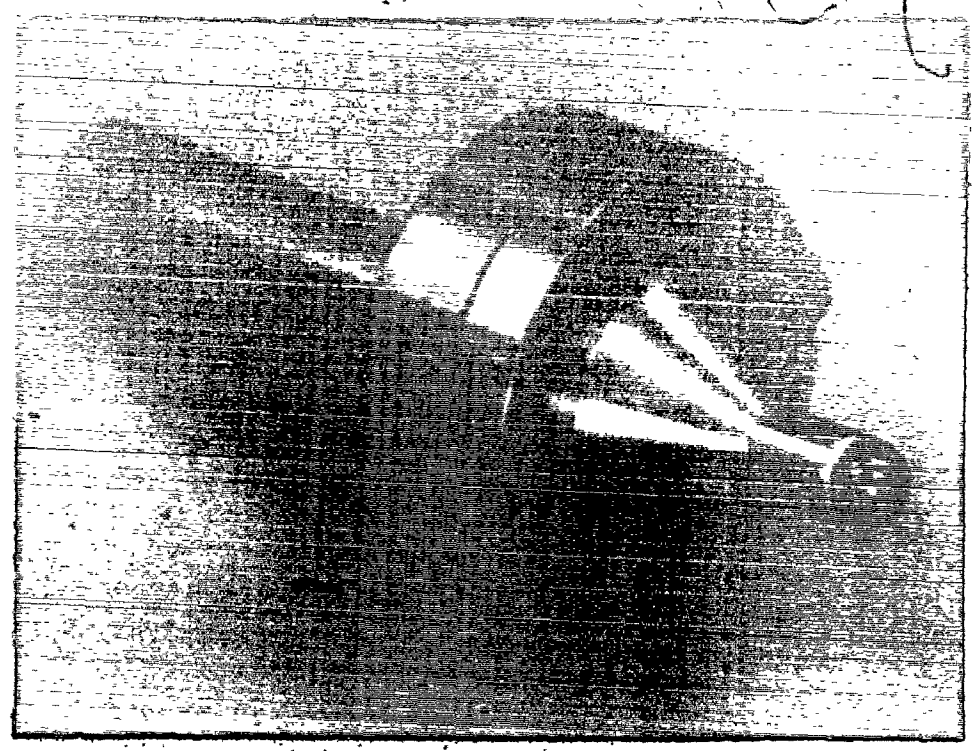
A
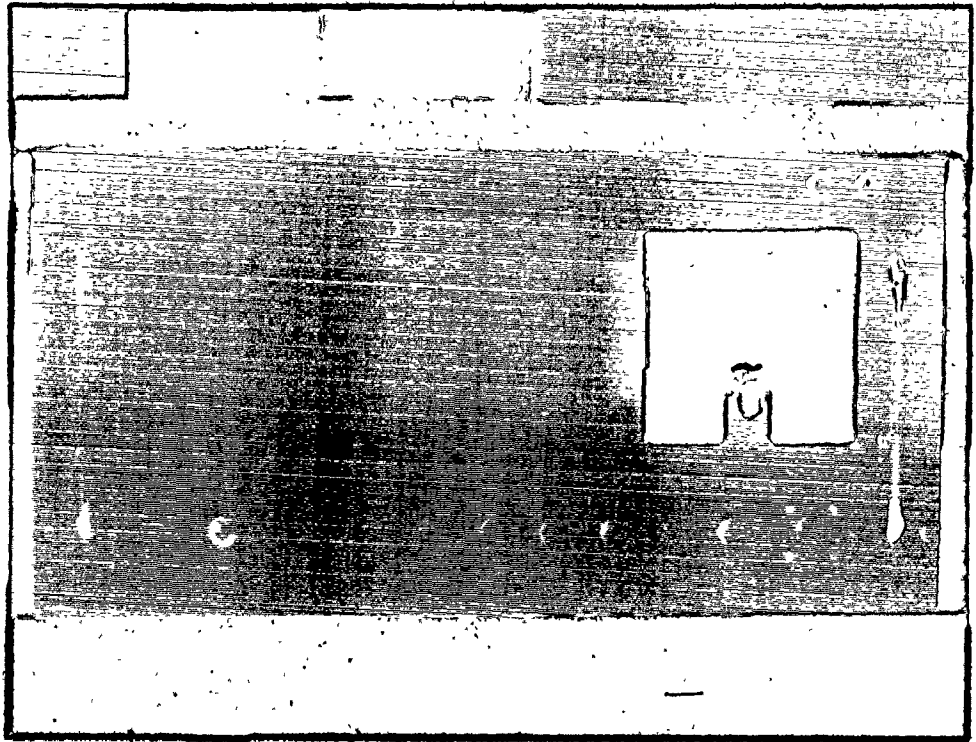
B.

Plate X   THE AXIS OF ROTATION ANALYSER
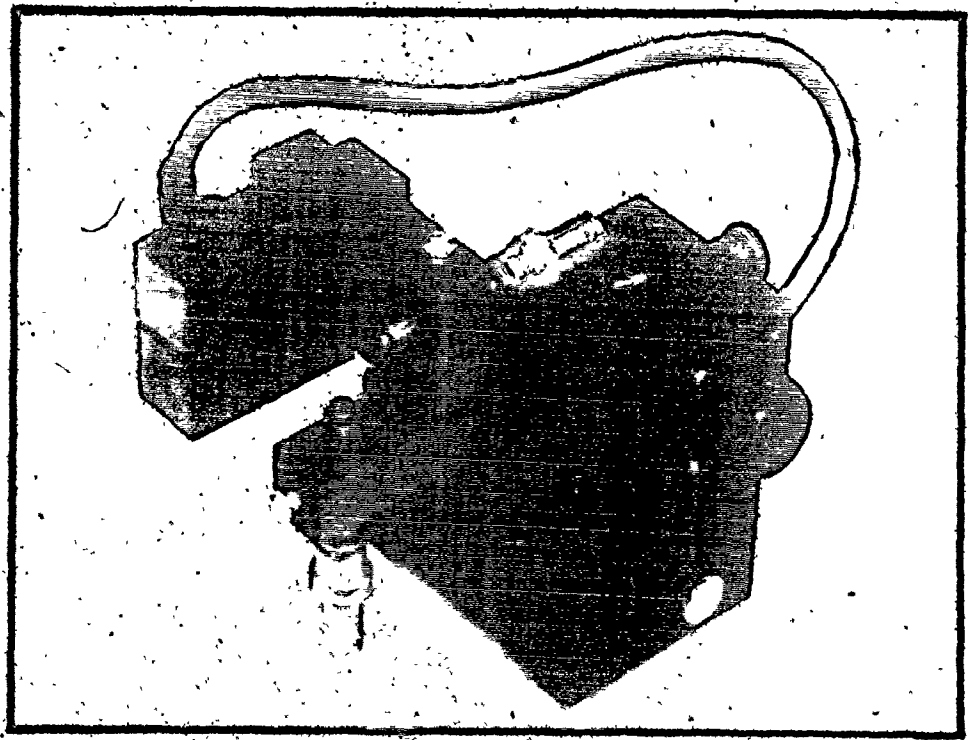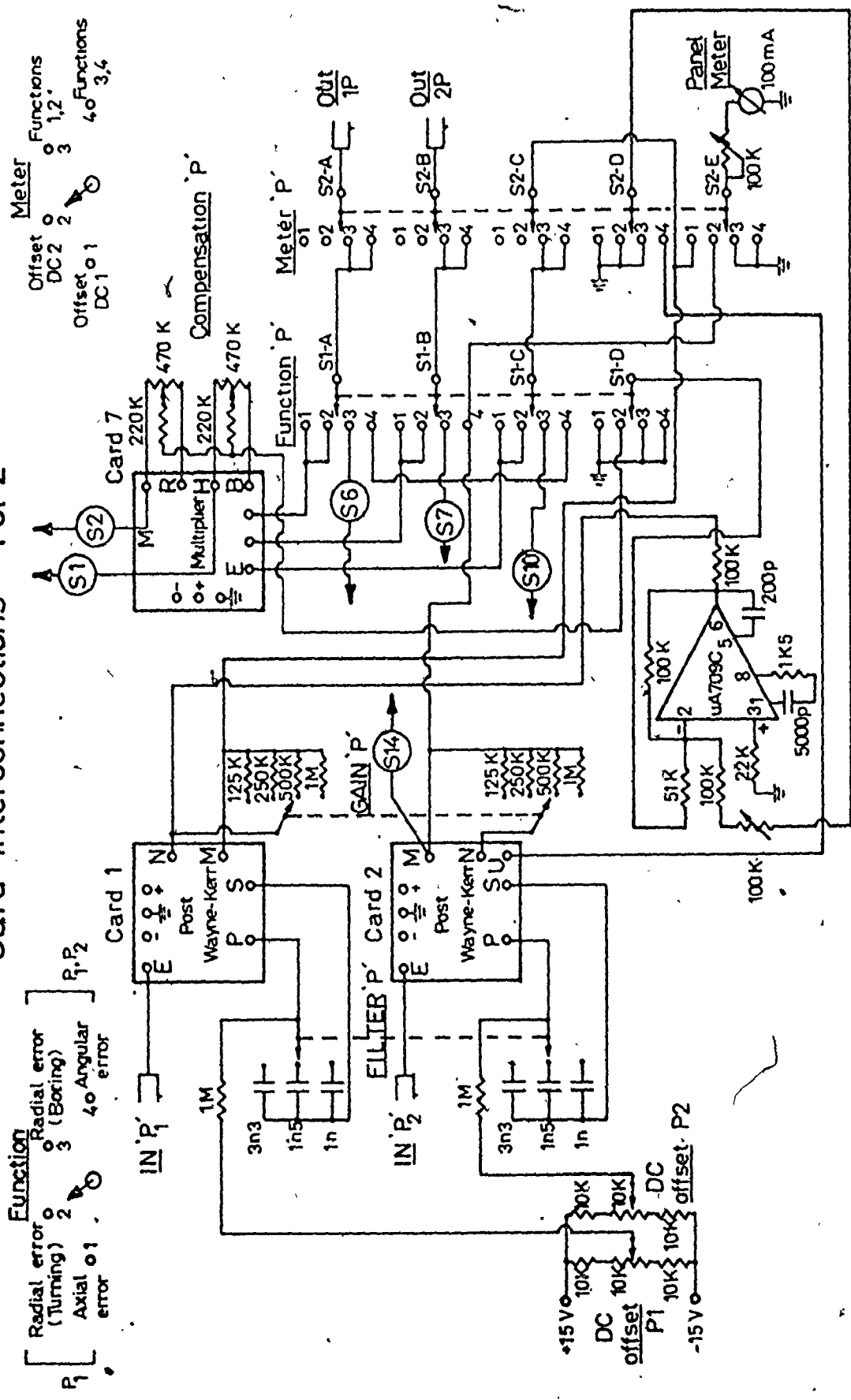
A.   Front panel layout
B.   Interior design

Plate XI   THE AXIS OF ROTATION ANALYSER

A.   Close up of the master-ball holder
B.   Close up of the pick-up and synchro-resolver holder

Card Interconnections 1 of 2

Card Interconnections 2 of 2
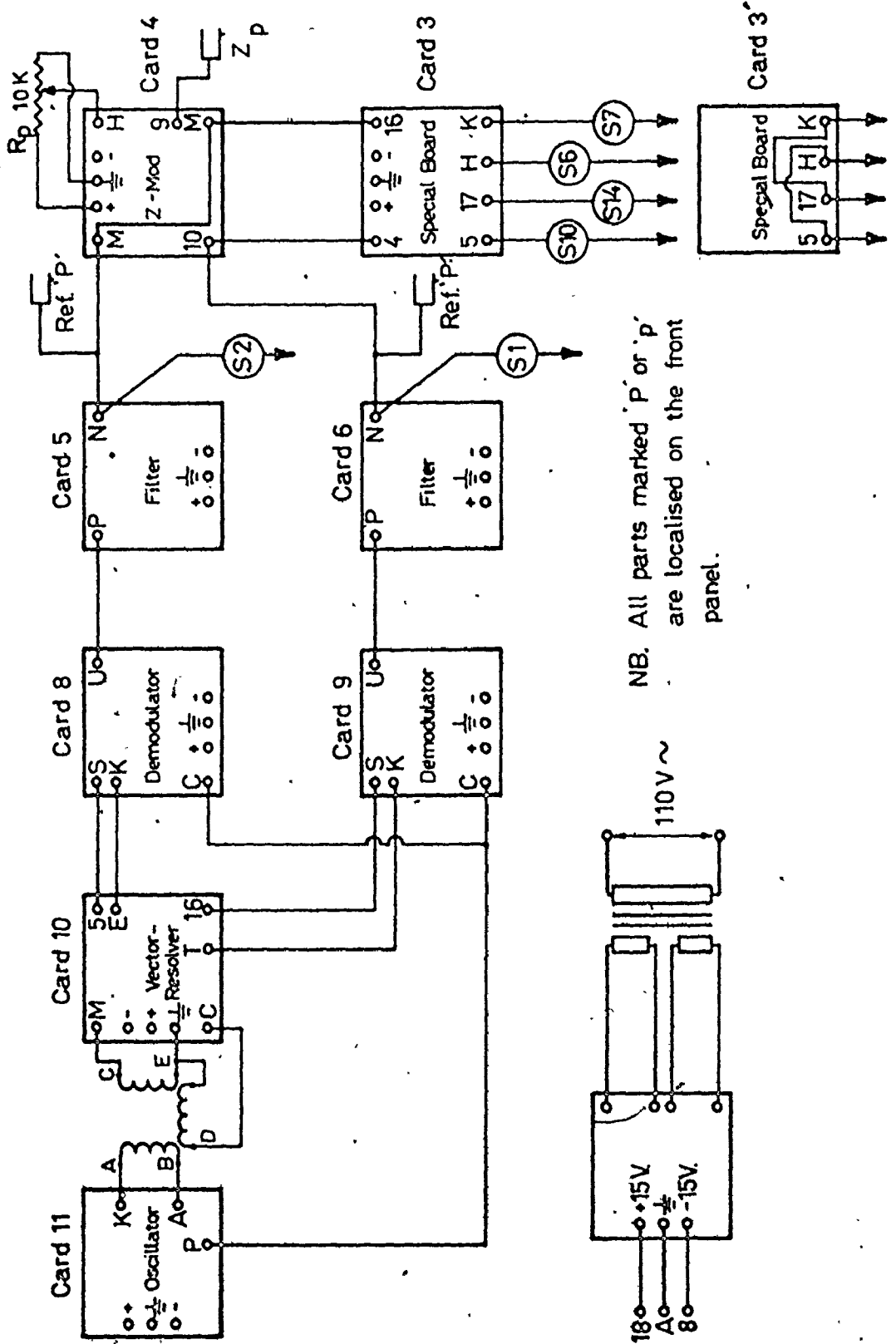
NB. All parts marked 'P' or 'p' are localised on the front panel.

Post Wayne-Kerr (CARDS 1,(2))
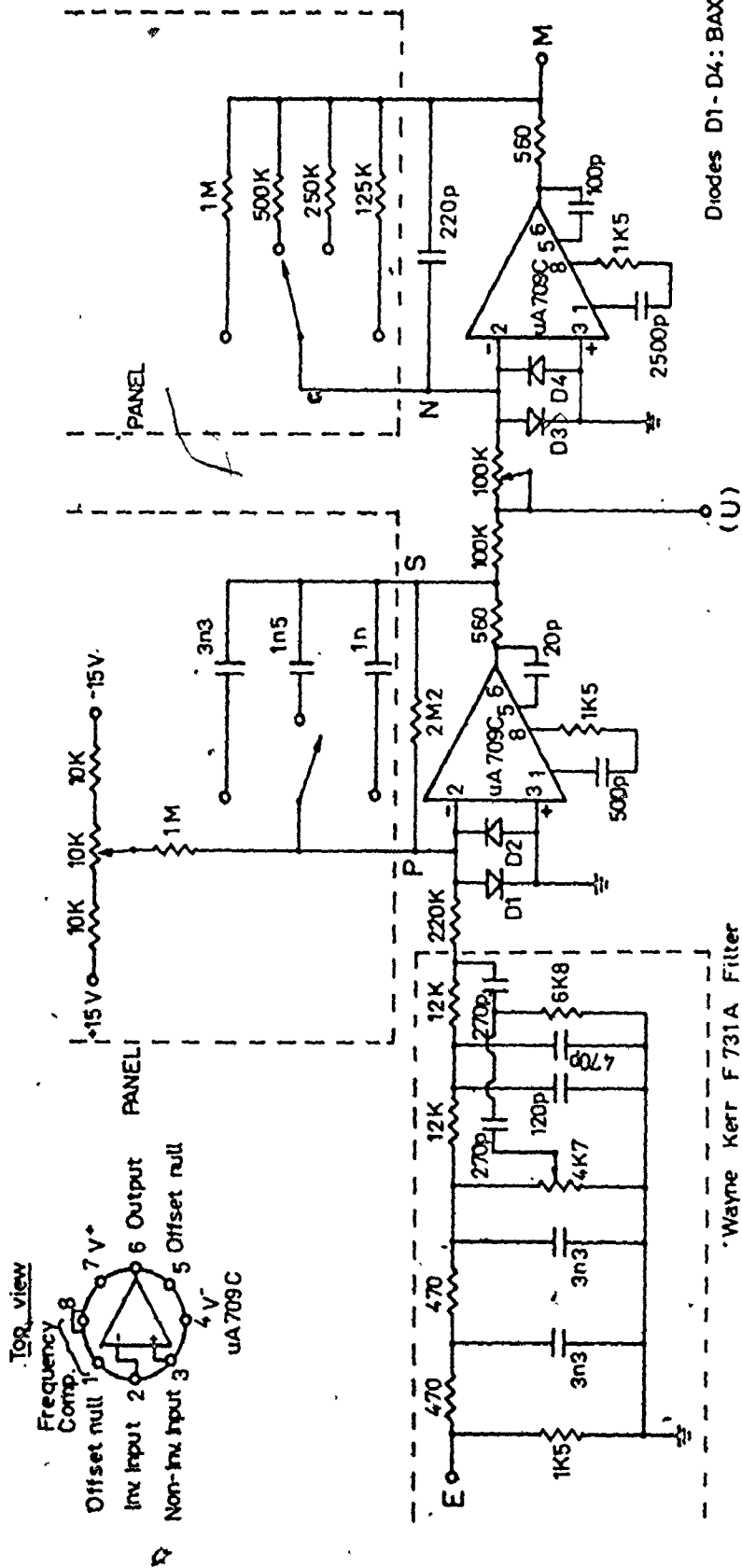
Diodes D1-D4: BAX 13

Wayne Kerr F731A Filter

Top view
uA709C

1 Frequency Comp.
8 Offset null
2 Inv Input
7 V+
3 Non-Inv Input
6 Output
4 V-
5 Offset null
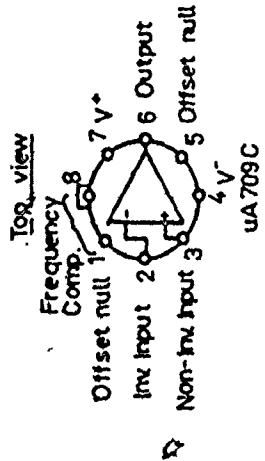
Special Board (CARD 3)
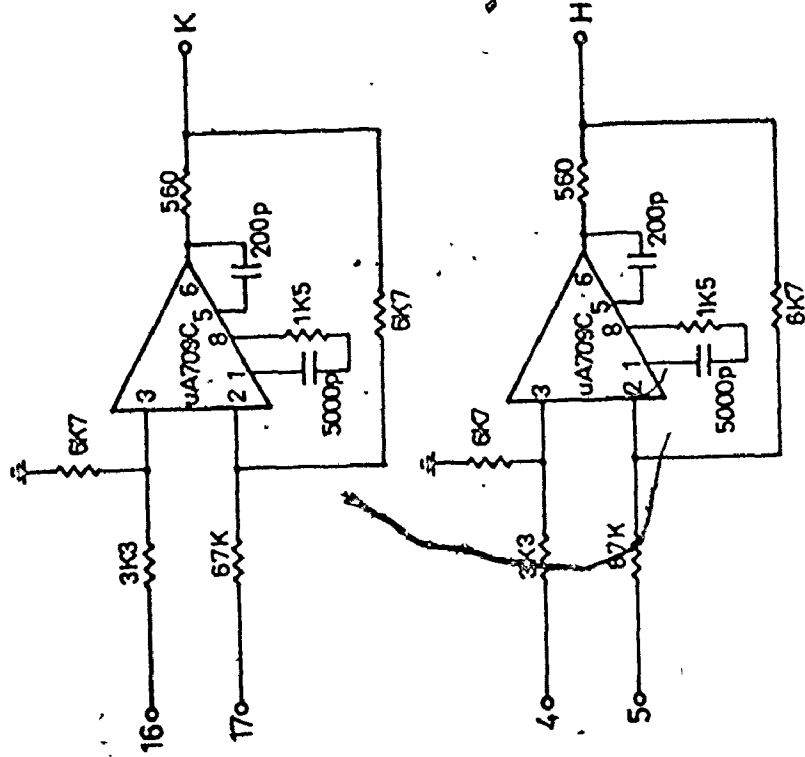
Z - Modulation (CARD 4)

Diodes D1-D8 : BAX 13

Filters (CARDS 5.6)
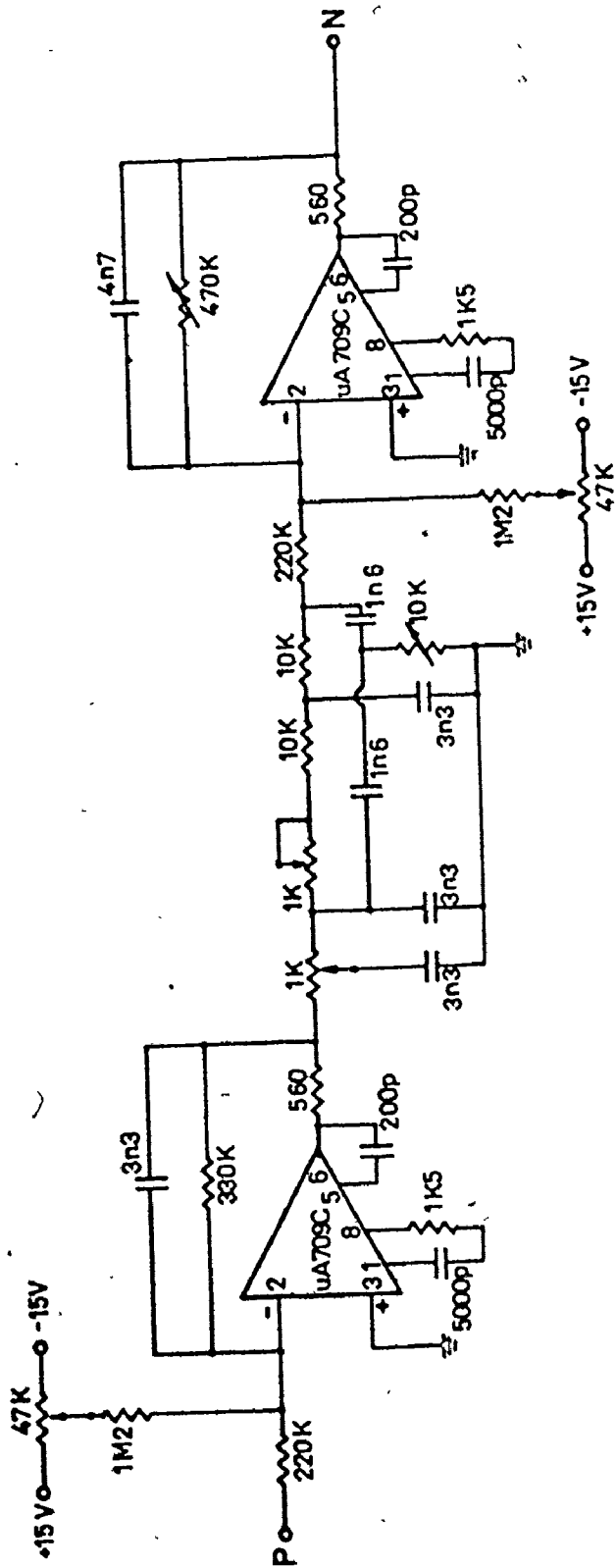
Multiplier (CARD 7)
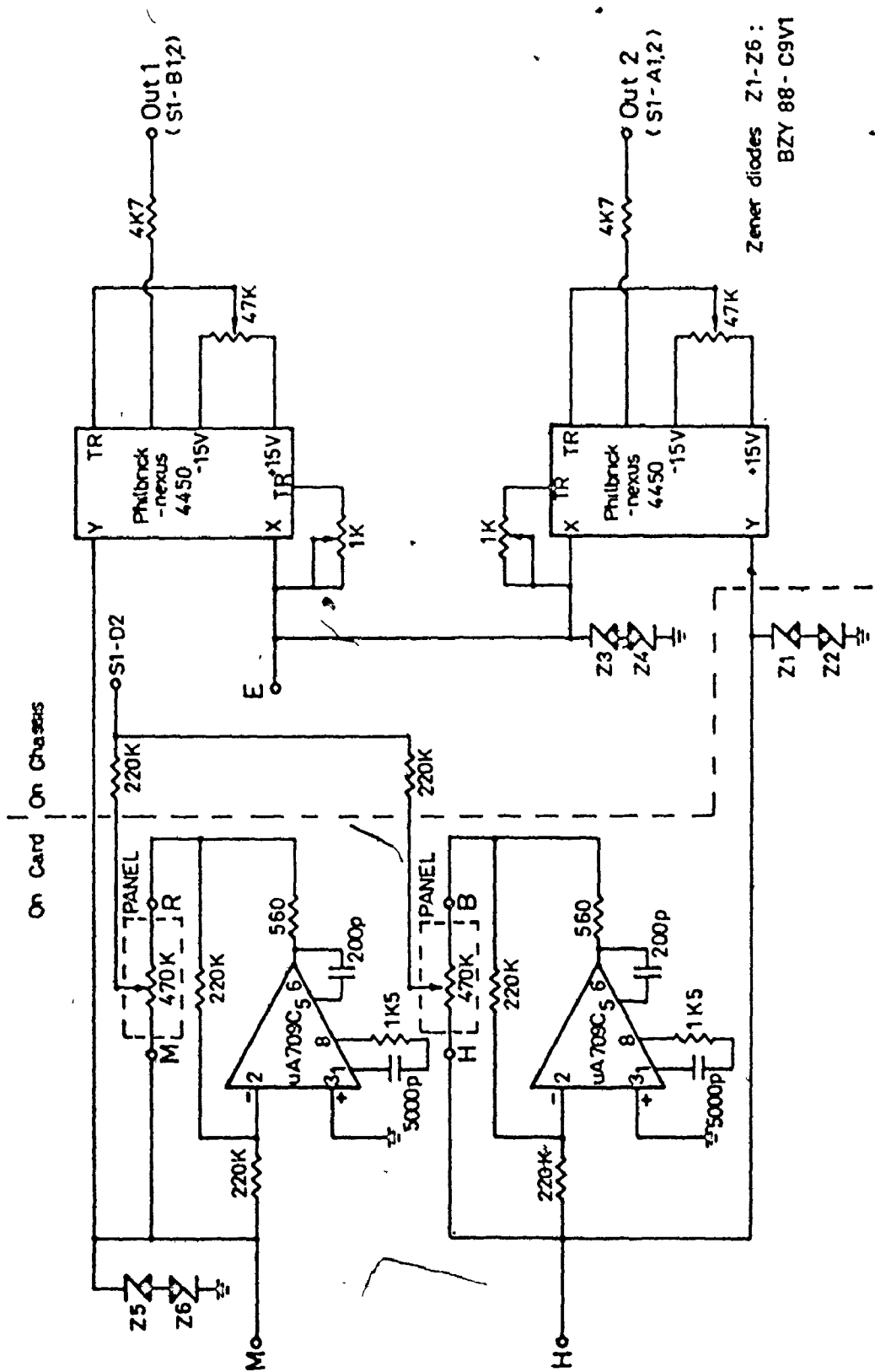
Zener diodes Z1-Z6:
BZY 88 - C9V1

Demodulators (CARDS 8.9)
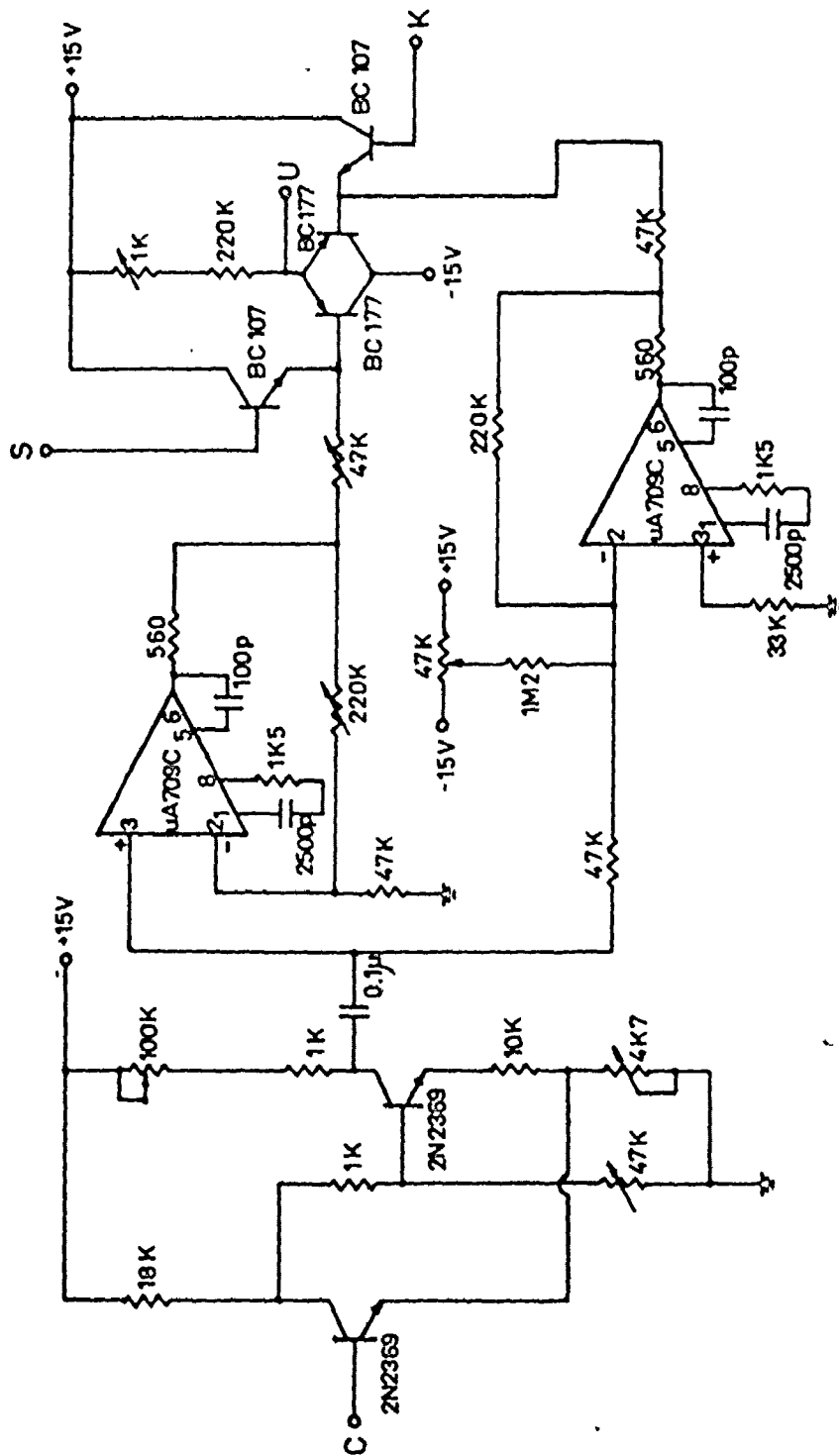
Vector Resolver (CARD 10)
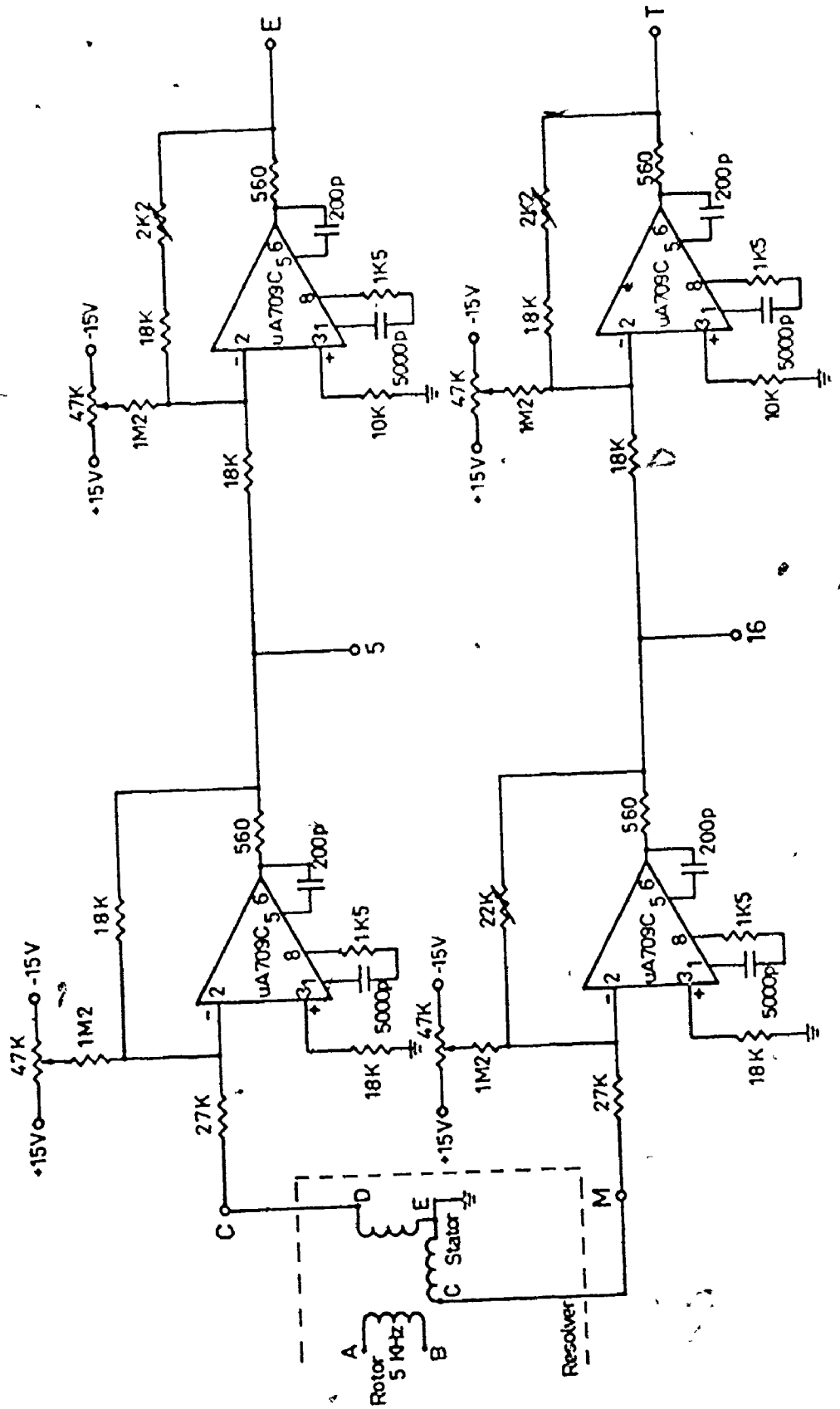
Oscillator (CARD 11)
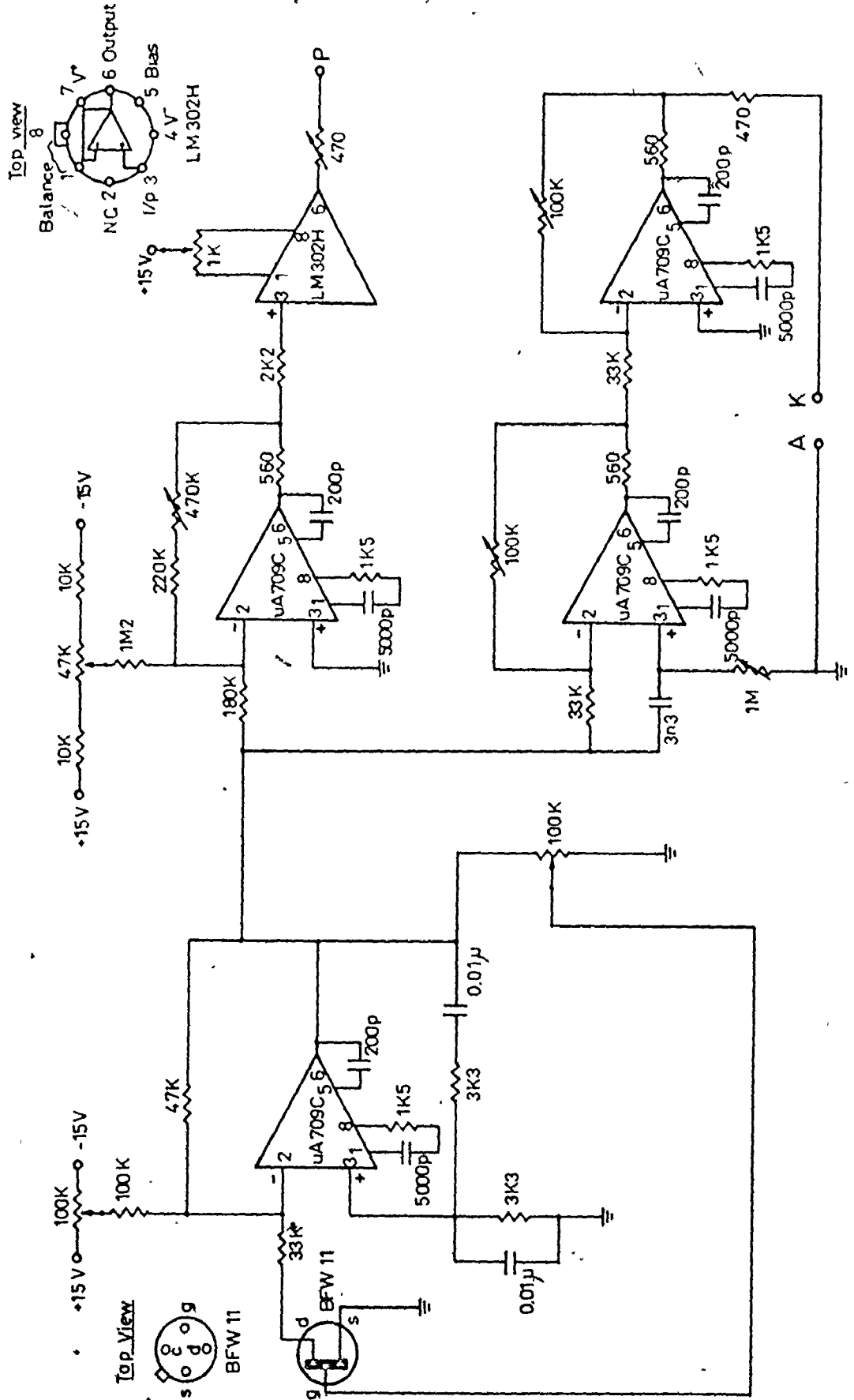
Power Supply
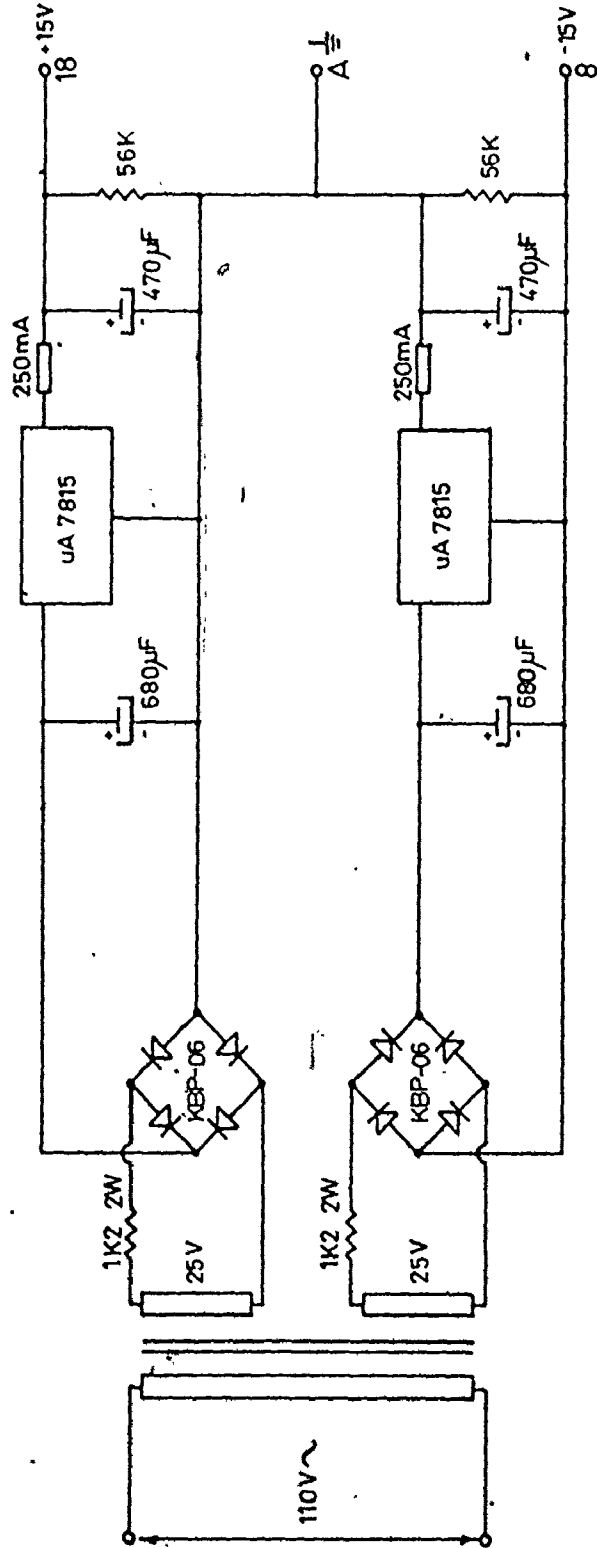
APPENDIX E

INSTRUMENTATION SPECIFICATIONS

E 1   The Laser and its Accessories (Plate VI pg 152)

All positioning, straightness, yaw and pitch deviation measurements were performed using the versatile capabilities of the HP5525B Laser Interferometer System together with its accessories.

The units comprising the total system and an abbreviated specification may be given as:

E.1.1 The Basic system

(i)   HP5505A Laser Display Unit

(ii)   HP5500A Laser Head

(iii) HP10550A Laser Reflector .

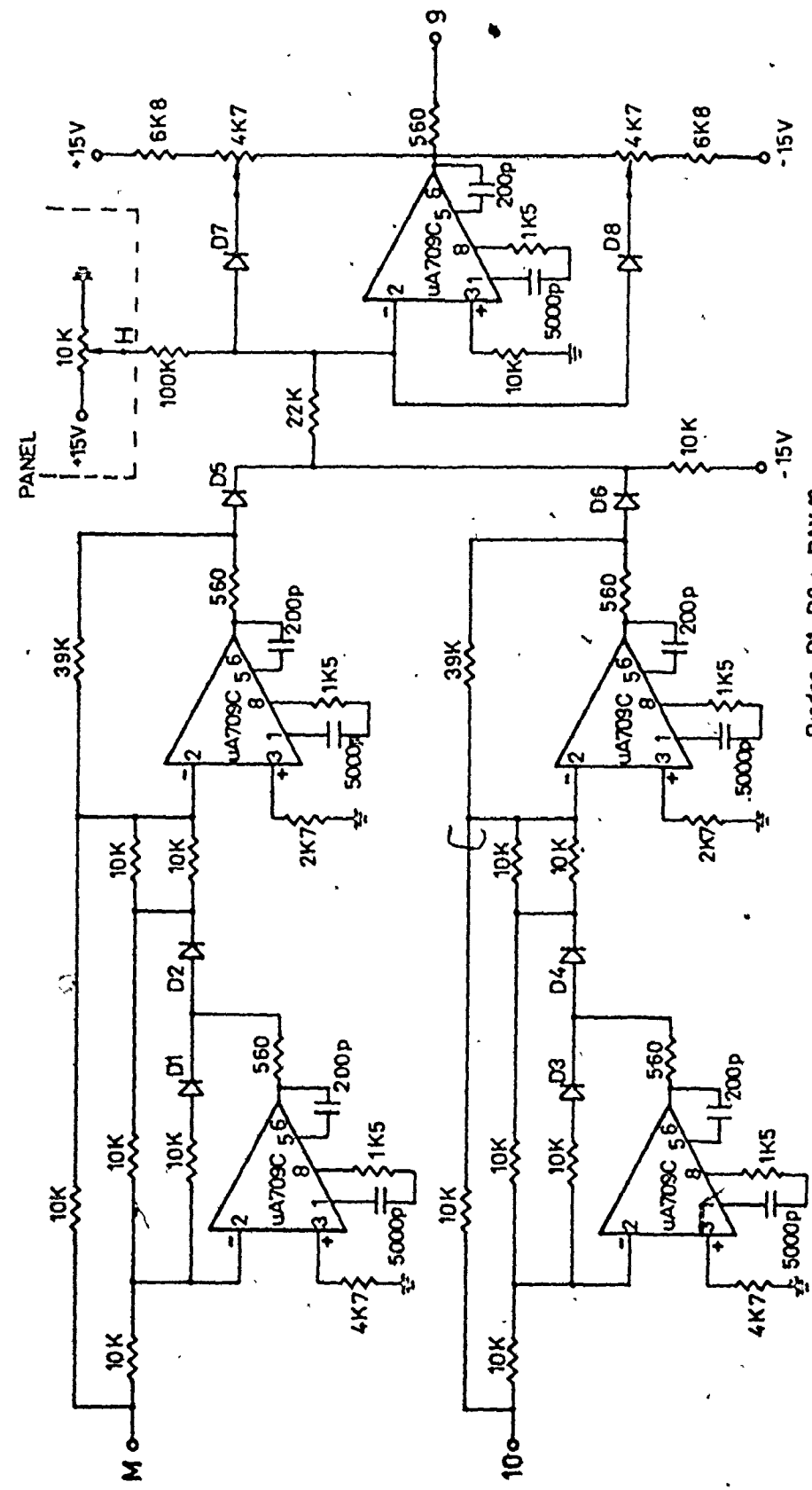ACCURACY: Inch units $\pm$ 0.5 µin $\pm$ 1 count in
last digit
Metric units $\pm$ 0.5 µm $\pm$ 2 counts in
last digit

RESOLUTION: Normal and smooth modes;

Inch: 0.000,01 inch

Metric: 0.1 µm

Angular: 1 arc-second

X10 mode;

Inch: 0.000,001 inch

Metric: 0.01 µm

Angular: 0.1 arc-second

MAXIMUM MEASURING VELOCITY: 720 in/min

(0.3 m/sec)

VELOCITY MEASUREMENT 'ACCURACY: $\pm$ 0.01 in/min

($\pm$ 4 µm/sec)

E.1.2   Remote Interferometers

(iv) Linear Interferometer (HP 10565A)

The specifications of the basic HP5525B system

apply

(v) Angular/Flatness Interferometer

(HP10565A + HP10558A)

ACCURACY: $\pm$ 0.1 arc-second $\pm$ 1 count up to

$\pm$ 100 arc-seconds,

$\pm$ 1 arc-second $\pm$ 1 count up to

$\pm$ 1000 arc-seconds,

$\pm$ 4 arc-seconds $\pm$ 1 count up to

$\pm$ 10 degrees,

RESOLUTION: (X 10 Mode, Inch units selected)

0.1 arc-second

(vi) Straightness Interferometer (Option 30)

ACCURACY: Straightness reference,

Inch: $\pm$ 5 µin./ft. $\pm$ 1 count in last

digit

Metric: $\pm$ 0.4 µm/meter $\pm$ 2 counts in

last digit

(N.B. The accuracy can be improved to the value

of last digit uncertainty by rotating the

Straightness Reflector through 180° and making

a second pass)

RESOLUTION: As for 5525B system

LATERAL RANGE: ± 0.1 inch (± 2.5 mm)

AXIAL RANGE: 10 ft (3m)

(N.B. a 100 ft model is available)

E.1.3　Miscellaneous Accessories

(vii) Error plotting option (Option 10)

ACCURACY:

Digital: ± 5 parts in 10^7 ± 1 count in

last digit

Analog: linearity ± 0.5%

Analog time constants: X-axis: 450 m sec

Y-axis: 34 m sec

RESOLUTION:

Normal mode: 0.000,01 in (0.000,1 mm)

X 10 mode: 0.000,001 in (0.000,01 mm)

RANGE:

X-Axis (distance travelled):

Normal mode: 100 in (1000 mm)

x 10 mode: 10 in (100 mm)

(N.B. traverses in excess of these distances

are made in stages)

Y-Axis (error amplitude):

      Normal mode $\pm$ 0.005 in ($\pm$ 0.05 mm)

      X 10 mode $\pm$ 0.0005 in ($\pm$ 0.005 mm)

CALIBRATION INTERVAL:

Any integral multiple of,

      Normal mode: 0.010 in (0.1 mm)

      X 10 mode: 0.001 in (0.01 mm)

OUTPUT:

Full scale voltages:

      X-axis: 10V

      Y-axis: $\pm$ 5V

PLOTTING ACTUATION:

1) Manual: actuate front panel switch on
          display unit

2) Automatic: external actuation

3) Internal Timing: rate set by front panel
   switch

RECORDING: HP7035B X-Y Recorder

(viii) Barometer/Thermometer Kit (HP10560A)

(ix) Beam Bender/Alignment Mirror (HP10551A)

An invaluable accessory for aligning and

deflecting the laser beam.

      ACCURACY:

        Mirror alignment:

          Perpendicular and parallel to

          base and sides within $\pm$ 1 minute

Alignment surfaces:

$\pm$ 1 minute

E 2   Instrumentation associated with the use of the Axis
       of Rotation Analyser

E.2.1   Error sensing

The B731B Wayne-Kerr Vibration/Distance Meter
is a portable instrument for accurate measurements
of distance and vibration amplitude from 30μin (0.75 μin)
to 0.100 in (2.5 mm) over the frequency range 1 Hz to
10 KHz utilising a range of associated capacitance
transducers.

The range and accuracy of these transducers
are as follows:

Probe	Full scale range	Measurement accuracy
MA1	0.001 in. (25 μm)	30 μin (0.75 μm)
MB1	0.005 in. (125 μm)	100μin (2.5 μm)
MC1	0.010 in. (250 μm)	200μin (5 μm)
MD1	0.050 in. (1.25 mm)	0.001 in (25 μm)
ME1	0.100 in. (2.50 mm)	0.002 in (50 μm)

METER CHARACTERISTICS:

Meter output: 0-1 mA from meter circuits at
                1000 Ω

Discrimination: $\leqslant$ 0.5% F.S.D.

E.2.2   Polar trace recording

The processed error outputs from the Axis of
Rotation Analyser are taken to a Tektronix D13/5103N
Dual-Beam Storage Oscilloscope for display. The con-
ventional time-base module in the X plate compartment
being removed, two high-gain amplifier modules
(5A22N) are inserted in the X and Y plate compartments
respectively for X-Y operation.

These particular units have characteristics
especially suited to our purpose and among these, we
may list the following;

(a) D13/5103N Dual Beam Storage Oscilloscope features:

(i) Storage display: writing speed: 20 divi-
                                      sions/millisecond

                                      storage time: 1 hr (at

                                      normal brightness)

(ii) Large screen: 4 in. x 5 in.

                                      (8 divs x 10 divs)

(iii) Z-Axis (beam intensity) modulation:

                                      +5V turns display on to a

                                      normal brightness level from

                                      an off level

                                      -5V turns display off from a

                                      normal brightness level

(b) Differential Amplifier 5A22N

(i)   High gain: 10µV/div. to 5V/div. in 18 steps

(1-2-5 sequence)

(ii)   D.C. offset: Range ± 0.5V from 10µV/div. to

50 mV/div.

± 50V from 100mV/div. to 5V/div.

(iii)   High and Low   -3dB Frequencies:

HF   -3dB: Selectable from

0.1 KHz to 1MHz in 7 steps

(1-3-10 sequence)

LF   -3dB: Selectable from

DC to 10kHz in 7 steps

(1-10-100 sequence)

This latter feature enables a reduction of the upper

frequency bandwidth and an increase of the lower

frequency bandwidth to be made in the interest of

obtaining a better signal-to-noise ratio.

A permanent record of the recorded polar

record can be obtained by using a Tektronix C-5 Camera

which incorporates a Polaroid Land Camera, flash unit

and camera/oscilloscope adapter.

E 3   <u>Straightness measurements - an alternative procedure</u>

Long distance continuous straightness measure-

ments may now be obtained for the entire traverse length

of the largest machine tools using the laser straight-·

ness interferometer accessory to the laser system. However, valuable information will be obtained by tracing an accurately lapped granite straight-edge or square with an electronic (LVDT-type) contacting pick-up held in the machine spindle nose and recording the sensed deviations on a chart recorder.

For machine tools with smaller working zones, this procedure is preferable due to a reduced set-up time.

An assembly of equipment is shown in Plate XII, pg.380 and the relevant specifications are as follows:

(a) Sheffield Model 51 Accutron Amplifier and
     Electrojet (0.010 in. range) Gauging Cartridge

Amplifier Range	Resolution
A ± 0.004 in.	0.000,2 in.
B ± 0.002 in.	0.000,1 in.
C ± 0.000,4 in.	0.000,02 in.
D ± 0.000,2 in.	0.000,01 in.

AMPLIFIER RECORDER OUTPUT: ± 10mV (i.e. 20 mV

DC F.S.D.)

(b) Simpson Model 2741 Single pen Chart Recorder

RANGE: Fixed: 2mV DC FSD to 20V DC FSD in

11 calibrated steps (2-5-10) sequence
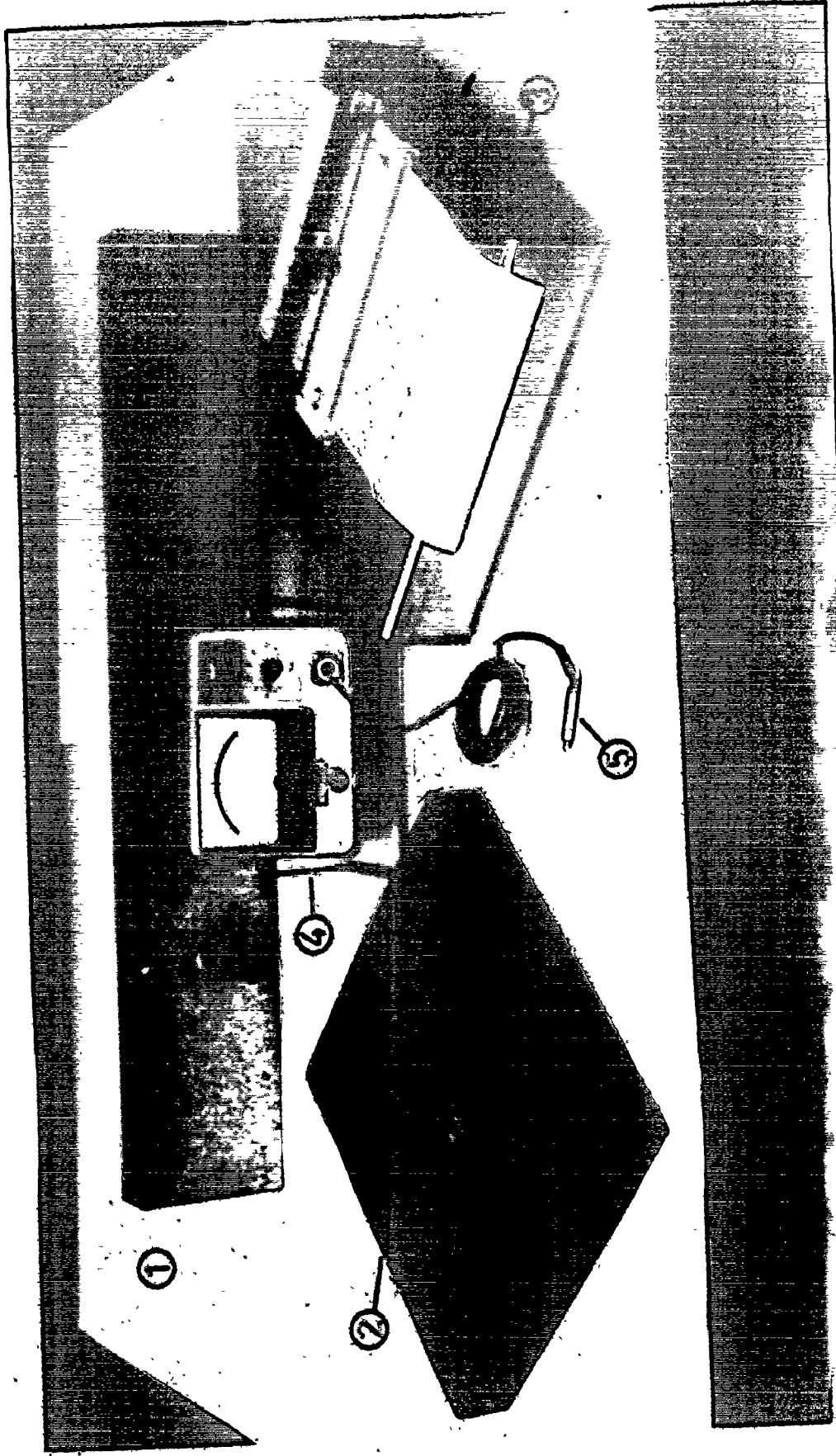
FIG. : AN ASSEMBLY OF MISCELLANEOUS METROLOGY EQUIPMENT

1. 36 in granite straight edge)
2. 36 in granite master square)
3. Surgeon Model 2741 chart recorder
4. Sheffield Model 51 Accutron Arm
5. Electrojet gauging cartridge

Variable: a continuously variable gain
             between calibrated steps is
             selectable

ACCURACY: ± 0.5% of reading (± 20 µV for
             readings of less than 400 µV)

RESOLUTION: ± 0.2% of full scale or ± 10 µV,
             whichever is greater

MAXIMUM WRITING SPEED: 20 cm/sec.

RESPONSE TIME: Normal environmental conditions:
                 1 sec. for a 100% change

CHART SPEEDS: 30, 120, 600 mm/min
                 30, 120, 600, mm/hr

N.B. A reverse chart feed facility is standard which is

a useful feature for obtaining forward and reverse

straightness deviations on the same portion of graph.

(c)   Starret (36 in. x 2 in. x 6 in) Granite Straight-
      edge   .

      Maximum surface Deviation: ± 0.000,05 in.

(d)   Rahn (14 in. x 14 in. x 2 in) 5-sided Granite
      Master Square

      Maximum Squareness and Straightness Deviation:

      0.000,025 in./6in.   .

E 4   A Simple Electronic Level

        It is not possible to measure the angular
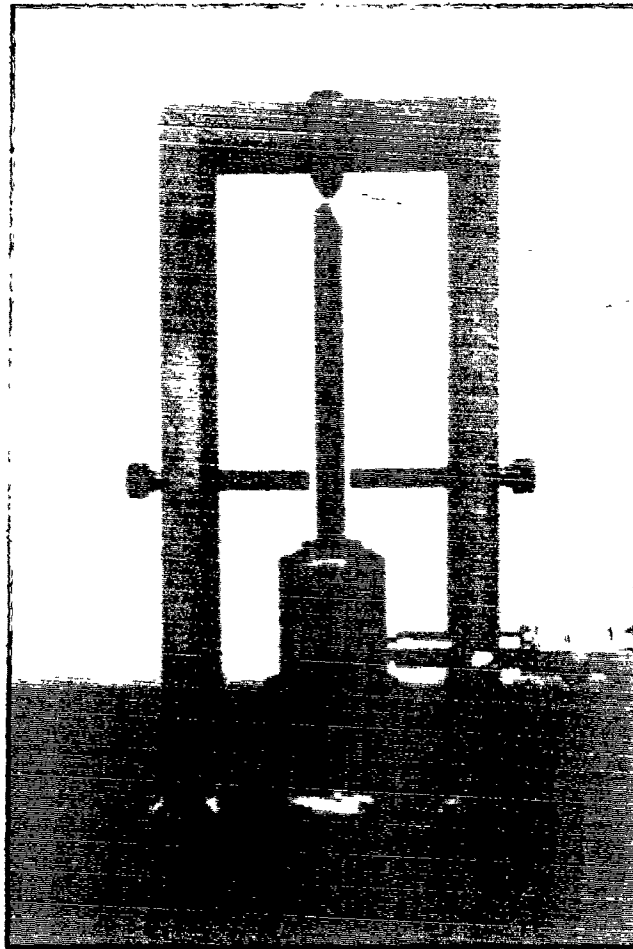
Plate XIII   A SIMPLE ELECTRONIC LEVEL

deviation of roll with any existing interferometer available as an accessory to the laser system. The only practical way of measuring this deviation is by utilising an electronic level. Several commercial instruments are available e.g. TALYVELL (Rank Industries).

However, both as an economy measure, and since a recorder output was desired, the simple pendulum type instrument as shown in Plate XIII, pg. 382 was devised, featuring a frictionless cross-strip hinge from which the pendulum is suspended.

Here the damped motions of a pendulum, the bob of which is partially submerged in an oil dashpot, are sensed by a capacitance probe and the analogue output of the Wayne Kerr B731B Vibration/Distance Meter is available for plotting on a chart recorder.

TRANSDUCER: Wayne-Kerr Capacitance Probe MA1, 0.001 in.
range.

PROBE RESOLUTION: 0.000,03 in.

PENDULUM LENGTH: 6 ins.

LEVEL RESOLUTION: 1 arc-second

REFERENCES

1. Anon.   "Survey of Turning Requirements in Industry"
                    Production Engineering Research Association
                    of Great Britain, 1969.

2. Anon.   "Survey of Machining Requirements in In-
                    dustry", Production Engineering Research
                    Association of Great Britain, 1969.

3. Anon.   "ISO System of Limits and Fits", ISO (Inter-
                    national Organisation for Standardisation)
                    Recommendation R286, 1st. Ed., December 1962.

4. Erickson, O., Fagerkist, A. and Rasch, F.O., "Testing of
                    Machine Tools", (Swedish) Machine Tool In-
                    dustry Research Association, Translation
                    T320, Macclesfield, Cheshire, England.

5. Tlusty, J. and Koenigsberger, F., "Specifications and
                    Tests of Metal Cutting Machine Tools",
                    University of Manchester Institute of Science
                    and Technology, 1970.

6. Anon.   "Improvements Required in Machine Tools",
                    Report of the Research and Technical
                    Committee, Institution of Production
                    Engineers, May 1968.

7. Thompson, J.R. et al., "Machine Tools - what the user
                    wants", The Chartered Mechanical Engineer,
                    September 1969, pp 335-342.

8. Weller, J.A., "Where Canada Stands in Metalworking
                    Production Engineering", Engineering Journal,
                    December 1971, pp 19-26.

9. Anon.   "Canada's N.C. Installations", Canadian
                    Machinery and Metalworking, March 1974,
                    pp 60-69.

10. Tlusty, J., "Survey Investigation of Problems of
                    Accuracy of Numerically Controlled Machine
                    Tools", McMaster Univ. Department of
                    Mechanical Engineering, April 1971.

11.   Ausgten, G.,   "Test Procedures to Characterise the
                Accuracy Performance of Position Con-
                trolled Machine Tools", Institute of
                Steuring der Werkzeugmaschinen, University
                of Stuttgart, 1971.

12.   Anon.   "Specification for ISO Limits and Fits",
                British Standard BS 4500: 1969, British
                Standards Institute.

13.   Schlesinger, G., "Prufbuch für Werkzeugmaschinen (Die
                Arbeitsgenauigkeit der Werkzeugmaschinen)",
                Julius Springer, Berlin 1927.

14.   Schlesinger, G., "Testing Machine Tools", The Machinery
                Publishing Co. Ltd., 7th ed., 1970.

15.   Salmon, P., "Machines-Outils, Réception, Vérification",
                1st Ed., 1937, Henri Francois, Paris.

16.   Anon.   "Machine Tool Test Code", ISO Recommenda-
                tion R230, 1st ed., December 1961.

17.   Anon.   "Test Conditions for General Purpose Para-
                llel Lathes", ISO Recommendation R1708,
                1st Ed, April 1970, I.S.O.

18.   Anon.   "Test Conditions for Milling Machines", ISO
                Recommendation R1701, 1st. Ed., April 1970,
                I.S.O.

19.   Anon.   "Dixi Horizontal Optical Jig-Borer Test
                Chart", Dixi S.A., Le Locle, Switzerland.

20.   Erickson, C., "Machine Alignment - the First step to-
                wards Product Accuracy", Technical Paper
                MM66-171, ASTME, 1966.

21.   Anon.   "Mean Work Zone Alignment Procedure for the
                OM-2 Omnimill Machining Centre", Sundstrand
                Machine Tool, Belvidere, Illinois.

22.   Anon.   "Mean Work Zone Alignment Philosophy",
                Sundstrand Machine Tool, Belvidere, Illinois.

23.   Bryan, J.B., and Pearson, J.W., "Machine Tool
                Metrology" Lawrence Radiation Laboratory,
                University of California, UCRL-71164 July
                1968.

24. Kirkham, E.E., "Identifying sources of errors in Machine Tools", A.S.M.E. Conference New York, May 15-17, 1967.

25. Anon. "Genauigkeitsangaben bei numerische gesteuerten Werkzeugmaschinen (Begriffe and Kenngrößen)" Verein Deutscher Ingenieur (V.D.I.) 3254, April 1965. (Statement of Accuracy of Numerically Controlled Machine Tools, Terms and Characteristics - Translation, UMIST 1970)

26. Anon. "Numerischgesteuerte Werkzeugmaschinen Genauigkeitsangaben VDI 3254 Blatt 1, March 1971.

27. Anon. "Definition and Evaluation of Accuracy and Repeatability for Numerically Controlled Machine Tools", 2nd ed., August 1972, National Machine Tool Builders Association.

28. Tlusty, J., "A System of Testing Accuracy of N.C. Machine Tools", Proceedings 12th Int. MTDR Conference, Manchester 1971.

29. Bryan, J.B., "International Status of Thermal Error Research", Annals of the C.I.R.P. Vol. 16 1968, pp203-215.

30. McClure, E.R., "Manufacturing Accuracy through the Control of Thermal Effects", D. Eng. Thesis, University of California, Lawrence Radiation Laboratory, U.C.R.L. 50636, Livermore, California, 1969.

31. Spur, G. and Fischer H.,"Thermal behaviour of Machine Tools", Proceedings 10th Inst. M.T.D.R. Conference, U.M.I.S.T., 1969.

32. Spur, G., Fischer H. and'de Hass, P., "Thermisches Verhalten von Werkzeugmaschinen", presented to C.I.R.P., Stockholm, August 1972.

33. Arpaci, V.S., "Conduction Heat Transfer", Addison-Wesley Co., 1966, Library of Congress Catalog. Card no: 66-25602.

34. Myers, G.E., "Analytical Methods in Conduction Heat Transfer", McGraw-Hill, 1971, Library of Congress Catalog. Card no: 76-141299.

48. Anon.   "Calibration of a Surface Plate", Laser
                   Measurement System Application Note 156-2
                   Hewlett Packard.

49. Baldwin, R.R., Grote, B.E. and Harland, D.A., "A
                   Laser Interferometer that measures Straight-
                   ness of Travel", Hewlett-Packard Journal,
                   January 1974, Vol 25, No. 5, pp 10-20.

50. Tlusty, J. and Mutch, G.F. "Analysis of accuracy of
                   N.C. Machine Tools at Canadair", MWRG No.1,July
                   1972, McMaster University, Department of
                   Mechanical Engineering.

51. Tlusty, J. and Mutch, G.F. "An assessment of the accuracy
                   of the Cincinnati 30 in. N.C. multi-spindle
                   Hydrotel", MWRG No. 7, April 1973, McMaster
                   University, Department of Mechanical Engin-
                   eering.

52. Mutch, G.F. and Tlusty J., "Accuracy of the Sundstrand
                   OM-1 Omnimill Machining Center", MWRG No. 16,
                   October 1973, McMaster University, Depart-
                   ment of Mechanical Engineering.

53. Mutch, G.F. and Tlusty, J., "An assessment of the
                   accuracy of a Mitsubishi-Innocenti FAF95
                   Horizontal (floor-type) Milling and Boring
                   Machine", MWRG No. 27, November 1973,
                   McMaster University, Department of Mech-
                   anical Engineering.

54. Mutch, G.F. and Tlusty J., "Measurements of Geometric
                   Accuracy errors and setting of feedback
                   transducers of an N.C. Lathe at Westinghouse
                   Turbine and Generator Division (Hamilton)",
                   MWRG No. 28, November 1973, McMaster
                   University, Department of Mechanical Engin-
                   eering.

55. Mutch, G.F. and Tlusty J., "An Accuracy evaluation of
                   Innocenti Horizontal (floor-type) Milling
                   and Boring Machines at Canadian General
                   Electric Co. Ltd., Scarborough, Ontario",
                   MWRG No. 49, September 1974, McMaster
                   University, Department of Mechanical Engin-
                   eering.